DEVELOPMENT OF CONTROL STRATEGIES FOR ENHANCED NUTRIENT REMOVAL IN BIOLOGICAL WASTEWATER TREATMENT PLANTS

Submitted in partial fulfillment of the requirement for the award of the degree of

DOCTOR OF PHILOSOPHY

in

CHEMICAL ENGINEERING

by

SHEIK ABDUL GAFFAR

Roll No: 716164

Under the supervision of

Dr. MURALI MOHAN SEEPANA

Assistant Professor

(Supervisor)

Dr. SESHAGIRI RAO AMBATI

Associate Professor

(Co-Supervisor)

DEPARTMENT OF CHEMICAL ENGINEERING

NATIONAL INSTITUTE OF TECHNOLOGY WARANGAL

TELANGANA – 506004, INDIA.

NOVEMBER 2021

NATIONAL INSTITUTE OF TECHNOLOGY

Warangal – 506004, Telangana, INDIA.

CERTIFICATE

This is to certify that the thesis entitled **"Development of Control Strategies for Enhanced Nutrient Removal in Biological Wastewater Treatment Plants"** being submitted by **Mr. Sheik Abdul Gaffar** for the award of the degree of Doctor of Philosophy (Ph.D) in Chemical Engineering, National Institute of Technology, Warangal, India, is a record of the bonafide research work carried out by him under my supervision. The thesis has fulfilled the requirements according to the regulations of this Institute and in my opinion, has reached the standards for submission. The results embodied in the thesis have not been submitted to any other University or Institute for the award of any degree or diploma.

Dr. Seshagiri Rao Ambati
Thesis Co-Supervisor
Associate Professor
Department of Chemical Engineering

Dr. Murali Mohan Seepana
Thesis Supervisor
Assistant Professor
Department of Chemical Engineering

Date: November 12, 2021
National Institute of Technology, Warangal, India.

DECLARATION

This is to certify that the work presented in the thesis entitled "**Development of Control Strategies for Enhanced Nutrient Removal in Biological Wastewater Treatment Plants**" is a bonafide work done by me under the supervision of Dr. Murali Mohan Seepana and Dr. Seshagiri Rao Ambati and is not submitted elsewhere for the award of any degree.

I declare that this written submission represents my ideas in my own words and where others' ideas or words have been included, I have adequately cited and referenced the original source. I also declare that I have adhered to all principles of academic honesty and integrity and have not misrepresented or fabricated or falsified any idea/data/fact/source in my submission.

I understand that any violation of the above will be a cause for disciplinary action by the Institute and can also evoke penal action from the sources which have thus not been properly cited or from whom proper permission has not been taken when needed.

SHEIK ABDUL GAFFAR

Roll No.716164

ACKNOWLEDGMENTS

It gives me immense pleasure to express my heartiest and sincere gratitude, indebtedness to my supervisors and mentors **Dr. Murali Mohan Seepana and Dr. Seshagiri Rao Ambati** for their patient guidance, timely appreciation, extraordinary support enormous enlightening discussion with constructive criticism, and sustain inputs during the research work and preparation of the thesis.

I owe a deep sense of gratitude to **Prof. M. Chidambaram,** Emeritus Professor, Department of Chemical Engineering, NIT Warangal, for his keen interest in me at every stage of my research.

I am very much thankful to **Dr. S. Srinath**, Head of the Department of Chemical Engineering for their advice and encouragement.

I take this privilege to thank all my Doctoral Committee members, **Dr. P. V. Suresh**, Associate Professor, Department of Chemical Engineering, **Dr. V. Ramasagar**, Assistant Professor, Department of Chemical Engineering and **Dr. P. Hari Prasad Reddy**, Associate Professor, Department of Civil Engineering for their detailed review, constructive suggestions and excellent advice during the progress of this research work.

I also appreciate the encouragement from teaching, non-teaching members, and the fraternity of the Department of Chemical Engineering of NIT Warangal. They have always been encouraging and supportive.

I wish to express my sincere thanks to **Prof. N. V. Ramana Rao**, Director, NIT Warangal for his official support and encouragement.

There is no way to express how much it meant to me to have been a scholar in NIT Warangal. These brilliant friends and colleagues inspired me over the many years: I convey my special thanks to Research Scholars Dr. Patan Ameer Khan, Dr. Vinay Raj, Dr. M.S. Sekhar, Dr. E. Chandra Mohan Goud, Dr. G. Maruthi Prasad, Mr. Suresh Kumar Chiluka, Dr. B. Anil Kumar Naik, Dr. Y. Sasidhar, Dr. Abdullah Sheikh, Dr. P. Aruna, Dr. H. Upendra, Mr. Mullapudi Siva, Mr. Basanth Kumar Pillai, Mr. G. Ramakanth, Mr. P. Karthik, Mr. Vamshi Krishna, Mr. Indranil dey, Mr. A. Aditya, and M. Tech students, Mr. V.S.M. Raghu Kumar, Ms. P. Soniya, and Ms. P. Maheshwari all the other current and former NIT Warangal students and visitors that I know. I cannot forget

my friends Mr. Tony Jayakar, Mr. K. Teja Krishna, Mr. Anand, and Ms. Hamsa Sheik for their support.

I acknowledge my gratitude to Dr. Kimberly Solon and Dr. Xavier Flores-Alsina for supporting my research work and all teachers and colleagues at various places for supporting and cooperating with me to complete the work.

My heartfelt gratitude and indebtedness are due to my parents Shri. Meera Mohiddin & Smt. Ahmadunnisha Begum and younger brother Abdul Rahim. I am very blessed to have uncles like Mr. Sheik Basha, Mr. Sheik Alisha, Mr. Ahmed Meeravali, and their wives and children for their sincere prayers, blessings, constant encouragement, shouldering the responsibilities, and moral support rendered to me throughout my life. I heartily acknowledge all my relatives for their love and affection towards me.

Above all, I express my deepest regards and gratitude to “ALMIGHTY” whose divine light and warmth showered upon me the perseverance, inspiration, faith, and enough strength to keep the momentum of work high even at tough moments of research work.

ABSTRACT

The treatment of polluted wastewater using biological processes has been widely adopted, from traditional domestic wastewater to industrial wastewaters for simultaneous removal of nutrients. The reduction of nutrients (carbon, nitrogen, and phosphorus) released to the surface water as per the regulatory bodies guidelines is mandatory in accordance with the municipal water directive (91/271/EC). There is a growing interest to improve the effluent quality (EQ) of sewage wastewater treatment operations. Controlling anaerobic, anoxic and aerobic environment allows the growth of microbial communities, which are accountable for removing of organic materials and nutrients.

Wastewater treatment plants are highly complex, nonlinear and slow processes. Lack of proper instrumentation and stern environmental legislations along with demand for cost effective plants have made automation of wastewater treatment process an important priority. But the intricate nature of the process poses a barrier to the successful implementation of the control system. The challenge lies in the design of a control strategy to reduce operational costs (OC) and improve EQ simultaneously. This research addresses the development of different control strategies to address these challenges. Benchmark Simulation Model No. 1-P (BSM1-P) and Benchmark Simulation Model No. 2-P (BSM2) are considered as working platforms to assess the control strategies. The objective is to avoid the violations in the effluent ammonia, total nitrogen, and total phosphorus, simultaneously to minimize OC, and to improve EQ. The proposed control strategies are based on proportional integral (PI), Fuzzy logic controller (FLC), and model predictive control (MPC).

BSM1-P (ASM3bioP is a bioprocess) platform is used to design PI, MPC and FLC for both lower and supervisory level. In the lower level two control loops are considered, such as, controlling the dissolved oxygen (DO) in tank 7 ($S_{O,7}$), and nitrate concentrations in reactor 4 ($S_{NO,4}$) by manipulating the oxygen mass transfer coefficient (K_La_7), and the internal recycle flow rate (Q_{intr}). For supervisory level, manipulate the DO controller's set-points based on the ammonia concentration in a particular tank. At a lower level, default PI and MPC controllers are used and at a higher level, MPC and fuzzy controllers are designed. A novel control strategy is implemented by the design of cascade control with a pair of PI feedback controllers and integrated with override control to inhibit the overflow of S_{NO} (Nitrate) in the discharge. In the lower (PI) and supervisory

(Fuzzy/PI) level cases, $S_{NO,4}$ orthophosphates ($S_{PO,7}$) is controlled by regulating the internal recycle and $S_{NO,7}$ and override control is placed based on the concentration of $S_{NO,7}$. Additionally, last three aerobic tanks are controlled by using DO set points.

BSM2-P (ASM2d is a bioprocess) platform is used to design PI, MPC and FLC for both lower and supervisory level. A lower-level control framework is implemented to DO in the sixth reactor by regulating the K_La of fifth, sixth, and seventh reactors in the biological treatment process. Here PI is used at the lower level, whereas FLC and MPC are used at the supervisory level. Based on the literature, three different biological wastewater treatment processes are considered such as A^2O process (anaerobic, anoxic, and aerobic reactors with internal and external recycles), Reverse R-A^2O process (anoxic, anaerobic, and aerobic reactors with external recycle), and Inverted I-A^2O process (anoxic, anaerobic, and aerobic with internal and external recycles) are modelled in the simulation platform. Additionally, DO is maintained in the respective aerobic reactors using a PI controller. Furthermore, metal and carbon addition is done at BSM1-P (ASM2d) platform.

The effect of temperature on the phosphorous, nitrogen, and organic matter removal in an activated sludge system (ASS) is assessed. Benchmark Simulation Model No.1 (BSM1-P) with an ASS (ASM3bioP) is used and the temperature is chosen between 10°C to 35°C. The kinetic expressions for the maximum growth rate of heterotrophic biomass, autotrophic, and phosphate accumulating organisms and their decay rate are considered. Additionally, lower level FLC is designed to monitor the effluent quality index (EQI) and operational cost index (OCI) in Wastewater treatment plants. For the plant-wide model of the ASS, benchmark Simulation model (BSM2-P) with an ASS (ASM2d) is used and the temperature is selected between 10 to 35°C covering different seasons. A steady-state simulations are carried out to evaluate the effluent concentrations by changing kinetic and physio chemical parameters of ASS and anaerobic digestion model.

Keywords: Activated sludge system, Benchmark simulation model, Effluent quality index, Feedback controllers, Kinetic and physio chemical parameters, Operational cost index.

CONTENTS

List of Figures

List of Tables

Nomenclature

AE	Aeration energy rate (Kwh/d)
ASM1	Activated sludge model No.1
ASM2	Activated sludge model No.2
ASM2d	Activated sludge model No.2d
ASM3	Activated sludge model No.3
BOD_5	Biological oxygen demand
COD	Chemical oxygen demand
CE	Consumed energy
DO	Dissolved oxygen
EQI	Effluent quality index
IQI	Influent quality index
K	Proportional gain
K_La	Oxygen transfer coefficient
TN	Total nitrogen
NO	Nitrate
TP	Total phosphorus
PE	Pumping energy consumption (kWh/d)
HU_k	Pollutant load corresponding to the component
Q_o	Influent flow rate (m^3/d)
Q_{intr}	Internal recycle flow rate (m^3/d)
Q_r	Return sludge flow rate (m^3/d)
Q_w	Waste sludge flow rate (m^3/d)
RGA	Relative gain array
S_A	Fermentation products (g COD/m^3)
S_F	Readily biodegradable organic substrate

S_{HCO}	Alkalinity of the waste water (HCO_3/m^3)
S_I	Inert soluble organic material (g COD/m^3)
S_{NH}	Ammonium and ammonia nitrogen (g N/m^3)
S_{NO}	Nitrate and nitrite nitrogen (g N/m^3)
S_{N2}	Dinitrogen (g N/m^3)
S_{PO4}	Inorganic soluble phosphate (g P/m^3)
S_S	Readily biodegradable organic substrate (g COD/m^3)
t_o	Start time
t_f	End time
T_{BOD}	Total BOD concentration
T_{COD}	Total COD concentration
T_{NO}	Nitrate concentration
T_{Ntot}	Total N concentration
T_{Ptot}	Total phosphorous concentration
T_{TKN}	Total organic N concentration
T_{TSS}	Total suspended solids concentration
WWTP	Waste water treatment plant
X_A	Nitrifying organisms (g COD/m^3)
X_H	Heterotrophic organisms (g COD/m^3)
X_I	Inert particulate organic material (g COD/m^3)
X_S	Slowly biodegradable substrates (g COD/m^3)
X_{PAO}	Phosphate accumulating organisms (g COD/m^3)
X_{PHA}	Cell internal storage product of PAO's (g COD/m^3)
X_{PP}	Polyphosphate (g P/m^3)
X_{STO}	Cell inner storage product of heterotopy
X_{TSS}	Suspended solids (g SS/m^3)
α_j	Cost factor for components j (j= EQI, AE, PE, and SP)
β_k	Weighting factor for components K (T_k = T_{BOD}, T_{COD}, T_{TKN}, T_{NO3},T_{Ptot}, and T_{TSS})

Chapter 1

Introduction

Chapter 1

Introduction

1.1 Wastewater treatment

Water is indispensable for all forms of survival. Modern humanity evolves swiftly, and the increased demand for water resources plays a key role in the civil activity and industrial fabrication. At the beginning of the twenty-first century, the world may face water quality crises because of poor water use practices and wastewater (WW) management strategies. It is immensely predominant to get the desired treatment of the water for healthy living. More than 80% of global water is released into the environment without adequate treatment. However, environmental protection has become increasingly important in recent decades, with strict effluent discharge limits for eutrophication substances like organic matter, priority substances, and other contaminants for wastewater treatment plants (WWTP). Wastewater treatment aims to protect public health as well as the environment. Controlling the wastewater treatment plant is generally difficult due to the multiple and numerous biological, chemical, and physical factors influencing wastewater treatment systems such as fluctuations, dynamics, disturbances, and uncertainties in the influent.

The intensification of the demand for clean water with deficient water resources has eventually resulted in a growing interest in resource recovery during the treatment of wastewater according to Puyol et al. (2017). It is perceived that valuable resources, like clean water, energy and nutrients can be recovered from wastewater. This leads to the progression of WWTP into a water resource recovery facility (WRRF) (Alex et al. (1999)). Nowadays, this approach takes more attention towards the research community to do the optimized treatment techniques can include either redesigning the process structure or it can be enhanced with advanced process control strategies of Van Der Hoek et al. (2016).

The rise in global population and urbanization has eventuated in an increase in water consumption and, as a result, wastewater production. It is necessary to maintain a balance between enabling technology advancements and the environment. There is a large number of publications towards the enhancement of wastewater treatment processes that are the result of comprehensive studies by the scientific community around the world (Blackall et al. (2002); Ledakowicz et al. (2001)). In recent times, the interest has shifted to the water-energy-food-health-nexus to better understand their interdependence and explore the requirements of one for the other.

1.1.1 Wastewater treatment process

The method of removing pollutants from wastewater or sewage and converting it into an effluent that can be added to the water cycle is known as the wastewater treatment process. Once returned to the water cycle, the effluent has a low environmental effect or can be reused for several usages. Chemical or physical and biological WWTP's are the two types of wastewater treatment plants. WWTP breaks down waste matter (organic matter) using biological bacteria. On the other hand, physical waste treatment plants handle WW by chemical reactions as well as physical processes. Physical wastewater treatment plants are often used to treat wastewater from industries, factories, and industrial companies, while biological treatment facilities are suitable for handling wastewater from municipal and businesses sectors.

The treatment of wastewater entails the following steps starting from the wastewater collection, grit, screening, primary, secondary and tertiary treatment, disinfection, and sludge treatment. Mainly WW treatment process targets minimizing water pollution, preventing water infection diseases and adequate water treatment applies to irrigation purposes. In WW treatment process is classified into three categories like physical, chemical, and biological treatment methods. Predominantly and precisely, the physical method deals with the process of primary treatment like grit, screening, primary sedimentation, and filtration. Whereas, biological and chemical methods deal in biological treatment. The biological method is accountable for the removal of organic matter and contaminants through microbial activity. The chemical method deals with the removal of contaminants by the addition of chemical dosages.

Fig 1.1 depicts the treatment process of wastewater. WWTP's are intricate because of chemical and biological interactions in between the process, peculiar nature of microbes, very slow process, and disorder of concentrations and dynamic rates of flow. Aside from that, it's a very energy-intensive operation. All these characteristics cause the controlling of WWTP's task to make more complex and challenging. However, recent research suggests that apart from water treatment it acquired resources on its own. It is widely acknowledged that value-added products such as clean water, clean energy, and nutrients would be recovered from the WW.

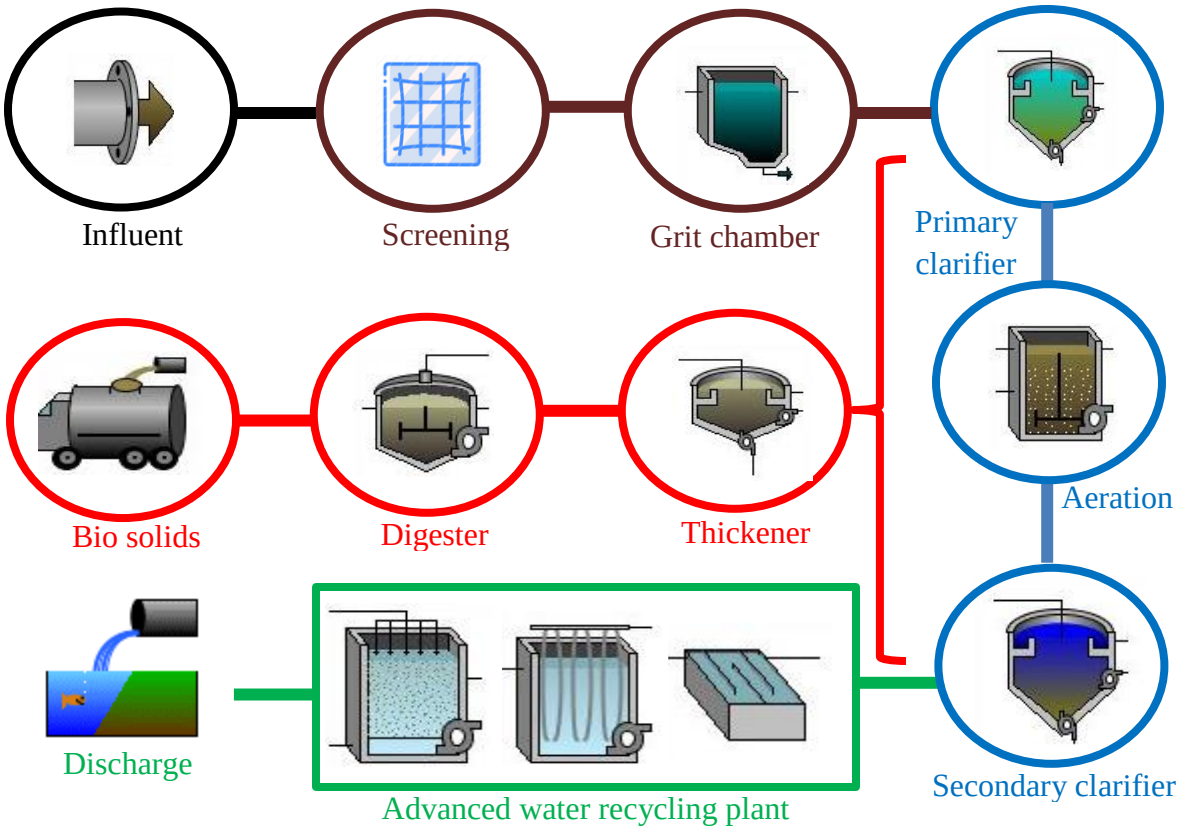

Figure 1.1 Wastewater treatment process

Mathematical models for WWTP

International Association on Water Pollution Research and Control (IAWPRC) task group has propounded diverse mathematical models, for instance, ASM1, ASM2, ASM2d, and ASM3. The activated sludge process is a complex process that contains a mix of bacterial activity for conversion and transport processes. The contaminants present in wastewater die according to the corresponding kinetics, stoichiometry, and transport processes Henze et al. (2000). The benchmark simulation model (BSM1) has become a standard framework for the comparison of various control approaches from Copp (2002). Benchmark Simulation Model No. 1-P (BSM1-P) and Benchmark Simulation Model No. 2-P (BSM2-P), established by the IAWPRC, are used to evaluate and compare various control strategies in this study.

BSM is a platform with a defined plant layout, bioprocess models (ASM), influent loads, sensors, and actuator as well as a set of evaluation criteria. BSM1-P framework deals with the biological treatment of WWTP. Here the WWTP is executed using activated sludge bioreactors (anaerobic, anoxic, and oxic). The performance evaluation is based on the last seven days of the plant process

Gernaey and Jørgensen (2004); Henze et al. (1999). BSM2-P is extended to a whole plant-wide simulation of a WWTP, which includes primary sedimentation, anaerobic digester, thickener unit, dewatering unit, and other related sub-processes Solon et al. 2017; Flores-Alsina et al. (2016). In BSM2-P, the evaluation criteria are based on the last 365 days of plant operation. IWA developed ASM's to evaluate WWTP. Optimization and control are balanced to meet stringent regulations of EQI with optimal cost. As for WWTP framework models, it can explore different aspects by analyzing them, for instance:

- ✓ Effluent quality
- ✓ Aeration control
- ✓ Sludge withdraw
- ✓ Maintaining mother liquor suspended solids (MLSS) in the reactor
- ✓ Optimal internal and external recycle rates

This ASM is developed purely based on the municipal WWTP but not the industrial fabricated WWTP model. ASM's are robust and sustained with different influent loading and characteristics to simulate successfully in WWTP.

1.1.2 Simulators for modelling and analysis of WWTP

Dynamic simulations of WWTP,s could be used to investigate the effect of various environmental studies, the system sensitivity of different parameters, and the applicability of various operational design and control configurations. Numerous research groups across the world use the freely available simulation models for diverse applications and they are included as pre-configured simulator packages in some commercial WWTP or developing the specific models in a programming software tool, for example, Matlab/Simulink. Commercial simulation configurations typically include enhanced libraries (C, N, P, and metals) of pre-determined operations that can be used to represent the entire WWTP and allow for easy creation and integrations of process platforms and model parameters. AQUASIM, SIMBA, SciLab, STOAT, BioWin, WEST, EFOR, GPS-X, and JASS are some of the most widely used commercial simulators. Given the following facts, the combination of Matlab/Simulink is an ideal solution to WWTP's:

- ❖ Significant computing potential
- ❖ Pre-determined toolbox and mathematical functioning
- ❖ Easily defined extensions and integrations
- ❖ Elucidate the dynamic study of WWTP into a set of mathematical equations.

1.1.3 Need for Process Control in WWTP

Suitable control configurations are needed to maintain the quality of discharge, monitor the WWTP, and minimize expenditures. Further

- Economy solutions are becoming highly crucial. As the loads on existing plants increase, the increased loads of the same volumes can be managed by control and optimization.
- Inflexible standards on processed wastewater.
- Penalties and taxes are linked to the quality of discharged water.
- Knowledge of environmental concerns by the general public is growing and becoming more and more focused on sustainability and energy use concerns.
- Integrated actuators and sensors have become expensive and maintenance of the sensors has become challenging in the wastewater environment.

In practice, the most frequently used control configurations are meant for dissolved oxygen control, nitrate control, ammonia-based aeration control, control of orthophosphates, total suspended solids, etc. The operation of WWTP's with lower operating costs and improved effluent quality has become essential in recent years. WWTP's are intricate, processes with nonlinear behavior. The complex nature of the microbes and huge disturbances in compositions and influent flow rates are accountable for the operation of WWTP's. Implementation of control strategies for the efficient operation of WWTP has become essential. Several control methodologies for WWTPs have been developed and tested from the perspective of control and process.

Fig. 1.2 depicts the usage of enabling technologies in wastewater treatment with their outputs of tapping the energy and sustainable financing. Over the last few decades, there has been an increase in research interests in the field of process control in wastewater treatment. BSM's and their advancements have served as important platforms for developing, testing, and comparing control technologies. The majority of WWTP control strategies that have been developed are based on BSM's and their enhancements (Gernaey et al. (2014)). Moreover, process selection and design tools can assist decision-makers in selecting appropriate treatment advancements for a given objective (Lema et al. (2017)). Fig. 1.3 depicts the benefits of employing controllers in WWTP.

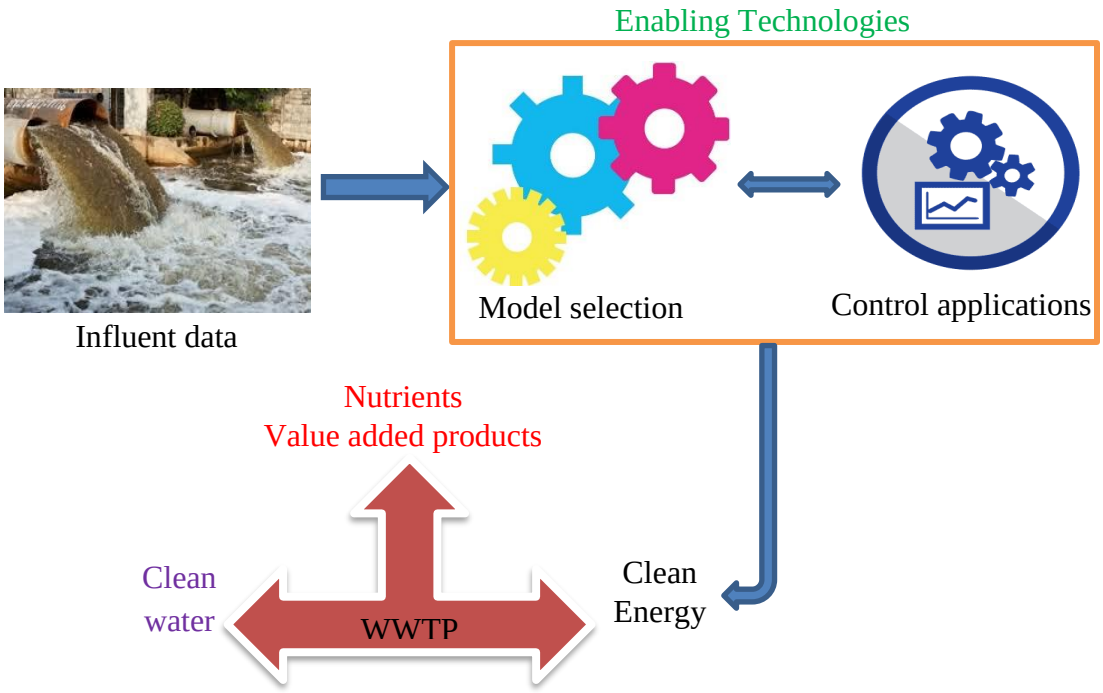

Figure 1.2 Enabling technologies in WWTP with their outputs

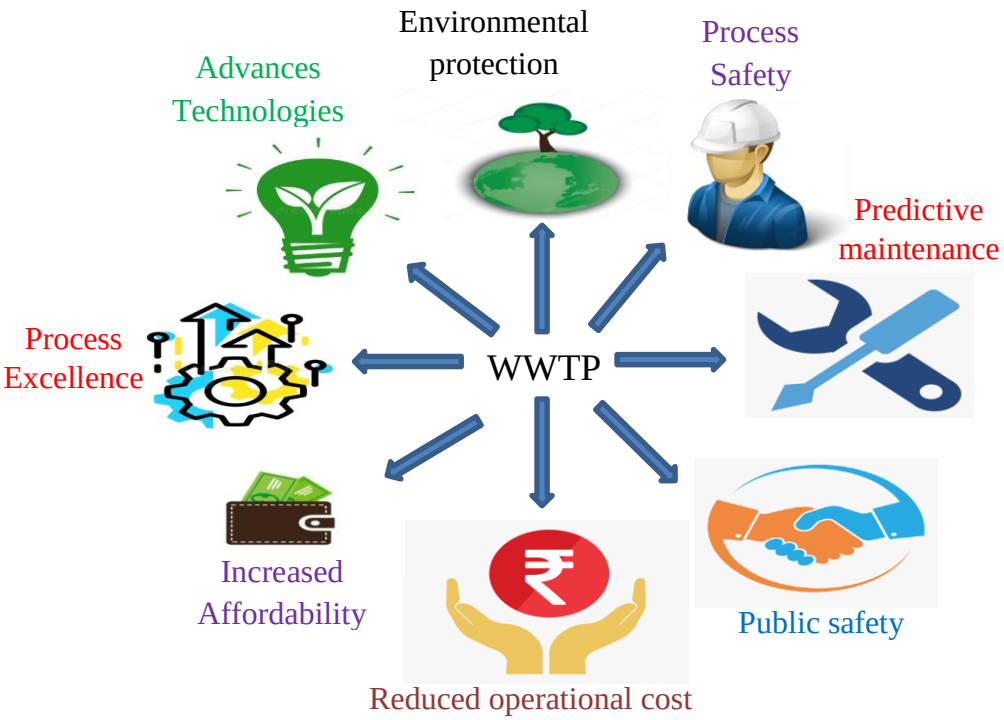

Figure 1.3 Benefits of employing controllers in WWTP

It is crucial to consider what incentives can encourage a system or individual to promote good performance for a control system to be successful. Rieger and Olsson (2012) provided important understandings about the employment of control systems. Process supervision can be tightened with automatic controllers, allowing operations to be closer to any constraints like effluent evaluation and cost. Moreover, the cost-benefit investigation is a useful tool for incorporating all parts of the control system. Process control plays an important role in wastewater treatment plants because they are operated at optimum conditions which lead to enhancing the plant's lifetime and decreases unit product cost (Agarwal et al. (2016)).

1.1.4 Control structures and algorithms

Controlling the operation of WWTPs has been done in a variety of ways as described in this section. Different types of control structures might be considered depending on the processes used in achieving the predefined goals. The control structure design is concerned with how the control system is set up, specifically which variables to control, which variables to regulate, and how these two sets of variables are combined to form control loops. In this research, some of the well-known control structures are applied for WWTP. Feed-back control (FB), Feed-forward control (FF), Cascade control, Supervisory control are designed and evaluated. Fig. 1.4 depicts the generalized framework of feedforward, feedback, and cascade control.

A controller's job is to maintain the process value at the set point. The PID controller is the most extensively used control algorithm for achieving this in-process control (Aström and Hägglund 1995). The PID controller deals with three sections P, PD, or PI. The proportional section reacts to current control errors, the integral section adds up earlier control errors, and the derivative section estimates the future control errors by utilizing the derivative of the control error.

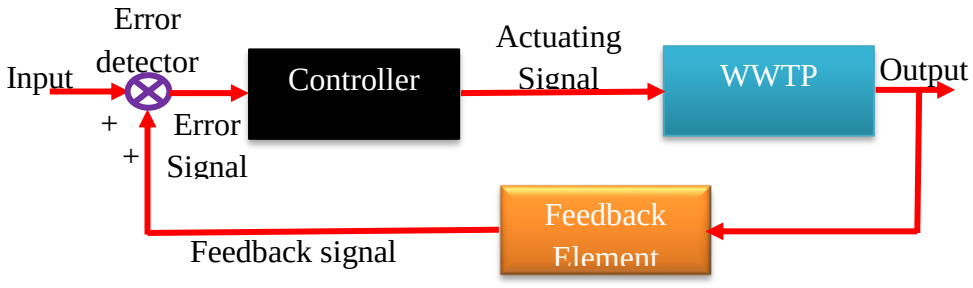

(A) Feed-forward

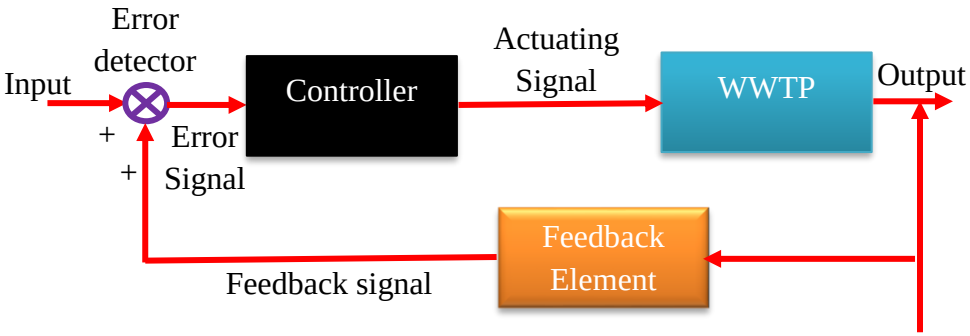

(B) Feed-back

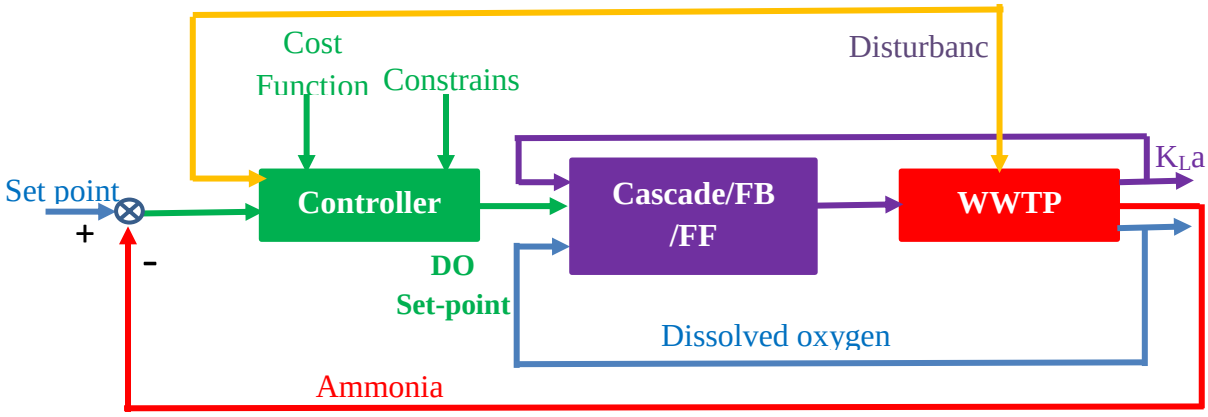

(C) Cascade control

Figure 1.4 Generalized control framework

The integral section is responsible for the integral action. Where the elimination of steady-state offset is achieved through integral action. The main drawback of PID is its linear nature, which may or may not apply to complex systems. The fractional-order PI D controller is a generalization of the integer-order PID controller, with the integration (λ) and differentiation orders (μ). The main attraction of fractional order controllers is due to the additional tuning parameters involved, and, which can be used to increase the overall robustness of the closed-loop system. Fig. 1.5 (C) depicts a simple fractional order PI controller design. Advanced control algorithms like MPC, Fuzzy, and ANN are widely used controllers in WWTP. Model predictive control (MPC) is a multivariable control technique that predicts future control actions in the input using process models. Process models, objective functions, and control rules are the essential aspects of MPC (Kouvaritakis and Cannon (2016)). Fig. 1.5 (A) depicts a simple MPC controller in WWTP. MPC has also been proved to be effective in various wastewater treatment applications using a linear process model (Steffens and Lant (1999); Charef et al. (2000); Sotomayor et al. (2002)). In all the processing

stages of wastewater treatment, FLC's have been used. It was also found that in various operating conditions, the FLC's have very good performance. Fig. 1.5(B) depicts a simple Fuzzy logic controller in WWTP.

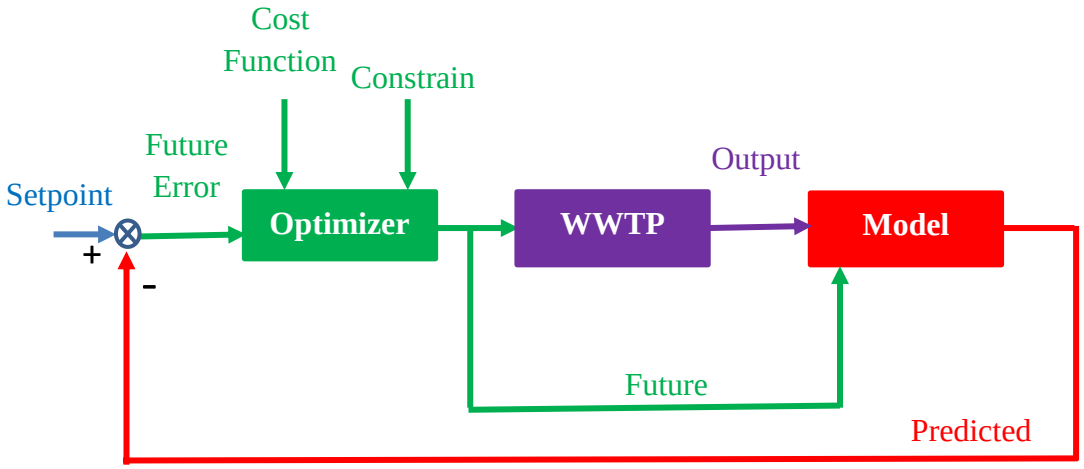

(A) A simple MPC scheme in WWTP

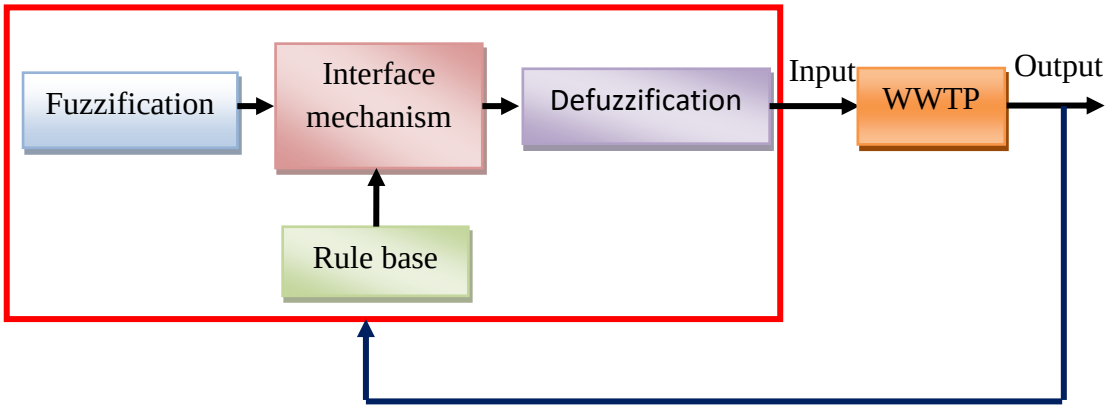

(B) A classical Fuzzy controller in WWTP

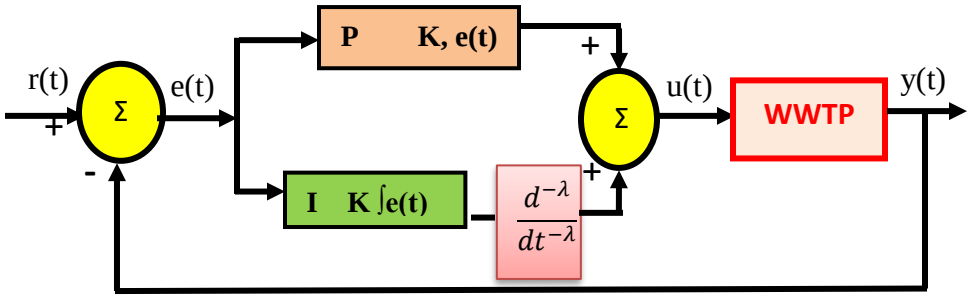

(C) A simple fractional-order PI in WWTP

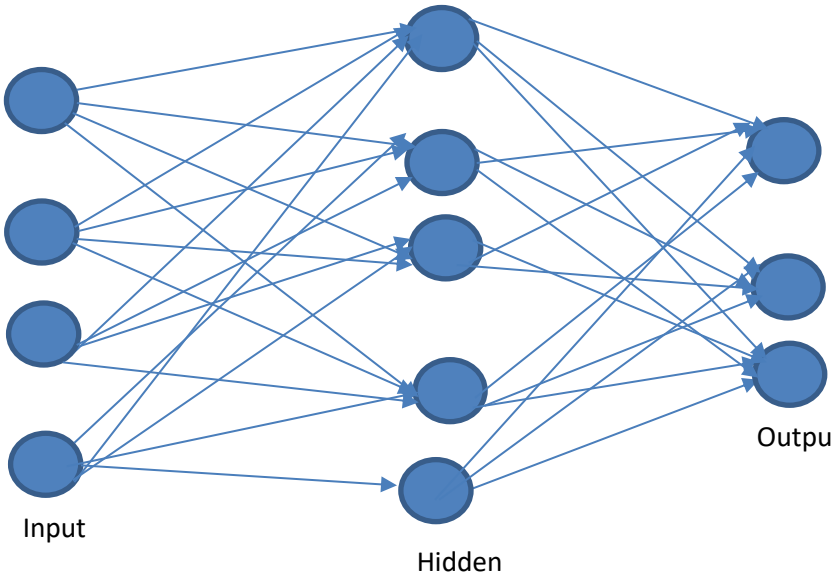

(D) A simple of ANN layers

Figure 1.5 Advanced control application in WWTP (A) MPC, (B) Fuzzy, (C) Fractional-order and (D) ANN

The direct control methods can have several failures depending on the process sensitivity, but the implementation of FLC's in wastewater treatment plays a key role in recent trends. For classic FLC, the control model is the way of the human knowledge base. FLC consists of three sections. In the primary section, MF's are fuzzified with input values to get Fuzzification. By using predetermined rules, fuzzy inputs and outputs are connected and then the outputs are determined by using the inference mechanism in the second section. The third section is to initiate strict output values in a computed way and is called defuzzification. Fuzzy logic control is used in WWTPs to control aeration for energy efficiency and to reduce nitrous oxide (N_2O) emissions according to Kalker et al. (1999); Fiter et al. (2005); Boiocchi et al. (2017). Artificial neural networking (ANN) depends on the artificial neurons with highly interconnected data processing units as a functioning. ANNs are generally trained using examples in order to address a specific problem. ANNs are capable of estimating WWTP performance based on the literature of Hamed et al. (2004); Ráduly et al. (2007); Güçlü et al. (2010); Huang et al. (2011); Liu et al. (2013). Fig. 1.5 (A), (B), (C), and (D) are depict the advanced control frameworks of (A) MPC, (B) Fuzzy, (C) Fractional-order, and (D) ANN in WWTP.

Sensors

Hardware sensor measurements can be difficult to manage or expensive to purchase, and so a trend has emerged towards adopting software sensors (soft sensors (SF)) in which models are combined with basic measurements to determine a variable that is highly difficult to estimate directly. The SF can be utilized as a "shadowing" sensor to offer information on sensor defects that have been estimated (Lumley (2002)). It is similar to an ordinary sensor aimed to calibrate at regular periods to maintain its prediction potentiality. Controlling simultaneous removal of nutrients (C, N, and P) will necessitate the development of sensor models to measure concentrations in the influent, effluent, or within the bioreactors. The set of sensor models consists of signal saturation, drift, measuring periods, noise, continuous measurement, and time response (Rieger et al. (2003); Rosen et al. (2008))

1.2 Modelling of the wastewater treatment process

Biological wastewater treatment process modeling is usually a multi-layered challenge. On a basic note, the main objective of the mathematical models in WWTP is to showcase the dynamic nature of the operation. Meanwhile, WWTPS's are generally notable for their intricate model building and a huge number of kinetic, stoichiometric, and state parameters to correlate. Due to the need for a satisfactory model for the proper explanation of simultaneous phenomena, the International Association for Water Quality (IWAQ, formally known as IAWPRC) developed a task group intending to develop a mathematical model of the wastewater treatment plant that can realistically predict the efficiency of single sludge systems which excites the process operations of carbon oxidation, hydrolysis, nitrification, denitrification, and proliferation of poly accumulating organisms (PAO's) based on Henze et al. (2000); Gujer et al. (2000); Gernaey et al. (2004); Riger et al. (2001). BSM1-P and BSM2-P as working scenarios are defined in this section. Both platforms of a simulation environment describe the plant layout, a simulation model, and test procedures, as well as performance evaluation criteria.

1.2.1 Benchmark simulation models.1-P (BSM1-P)

The WWTP framework is depicted in Fig. 1.6 which consists of seven bioreactors united in series, with an additional sedimentation tank. In the plant, the first two anaerobic reactors have a volume of 2000 m^3, the second two anoxic reactors have a volume of 2000 m^3, fully mixed. Additionally, the rest of the three aerobic reactors have a volume of 3999m^3 fully mixed and aerated. The

sedimentation tank volume is 6000m^3. Two recycle loops viz. (i) flow from the third aeration tank (Q_{intr}) to the anoxic reactor is 34500 m^3/d, and (ii) from the underflow (Q_r) of the sedimentation tank to influent flow is 18446 m^3/d. The WWTP is modeled for an average dry season flow (Q_{in}) rate of 18446 m^3/d. The sludge flow rate (Q_w) is fixed at 385 m^3/d and output effluent (Q_e). For assessment purposes, only the last 7 days are used for analysis even though 14 days are available. The simulation is run for zero to fourteen days. In the first seven days, the system reaches a dynamic 'pseudo' steady-state and remains in that state. For a fair comparison of different control algorithms, in the remaining seven days, any control algorithm can be implemented and the corresponding performance can be evaluated. To evaluate the control algorithms, the dynamic simulation can be run as many times as desired.

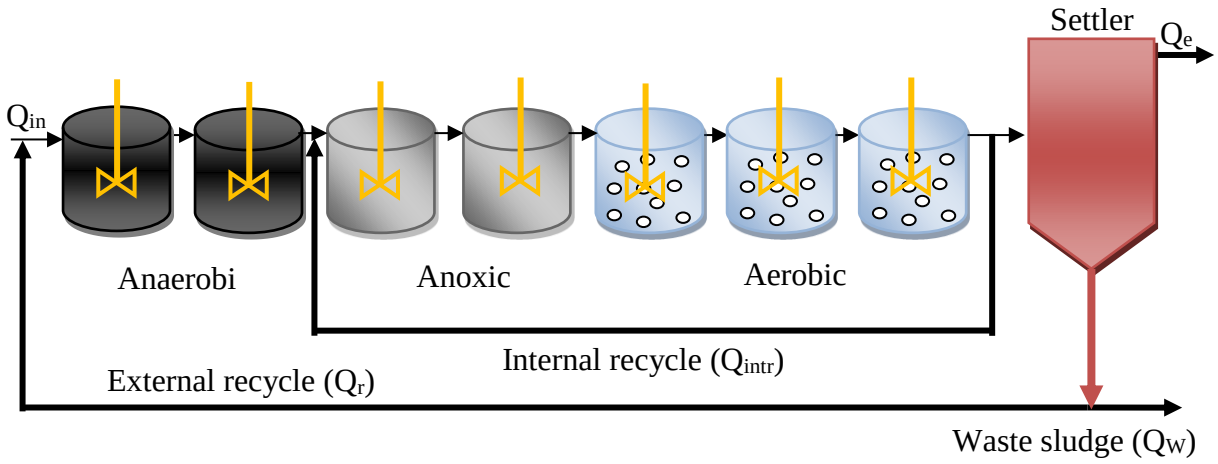

Figure 1.6 BSM1-P plant layout

1.2.2 Activated sludge model (ASM) description and model parameters

The activated sludge models are eminent mathematical models that are accountable for the biological and chemical reactions that take place in activated sludge systems (ASS). Literature-based on the ASM is tabulated in Table 1.1. Table 1.1 shows the substrates removal, process equations, state variables, and total parameters of six ASM are reported. In those ASM, ASM3bioP is selected for the process operation. Activated sludge model No. 3 (ASM3) is one more mathematical model developed to check the performance of biological WWTP. It inherently consists of the rate of oxygen consumption, nitrification and denitrification, and sludge production that could help in treating sewage wastewater. ASM3 addresses some other limitations of ASM1, such as nitrifier's decay rate difference under both aerobic and anoxic conditions, and includes the cell internal storage compounds (Gujer et al. (2000)). Similarly, an extension of the ASM3 model

was primarily developed (i.e., ASM3bioP) to predict biological phosphorus removal by including modified processes from the ASM2d model but without considering the fermentation of readily biodegradable substrates by Rieger et al. (2001); Solon (2015). ASM3bioP model has the biological P removal process which is elaborated in Fig. 1.7. PAO's are modeled in the cell internal system; all organic matter products are combined into one model structure (X_{PHA}) and the growth of PAO is responsible for the X_{PHA} as a substrate. Moreover, Oxygen and nitrate also influence the PAO's growth. ASM3 based on Gujer et al. (2000) was introduced to discuss the limitations of ASM1 for an instant the contrast in between lysis rates of nitrification in the anoxic and oxic environment. Further, it deals with cell internal storage issues. Another major variation between ASM3 and ASM1 is the COD rate.

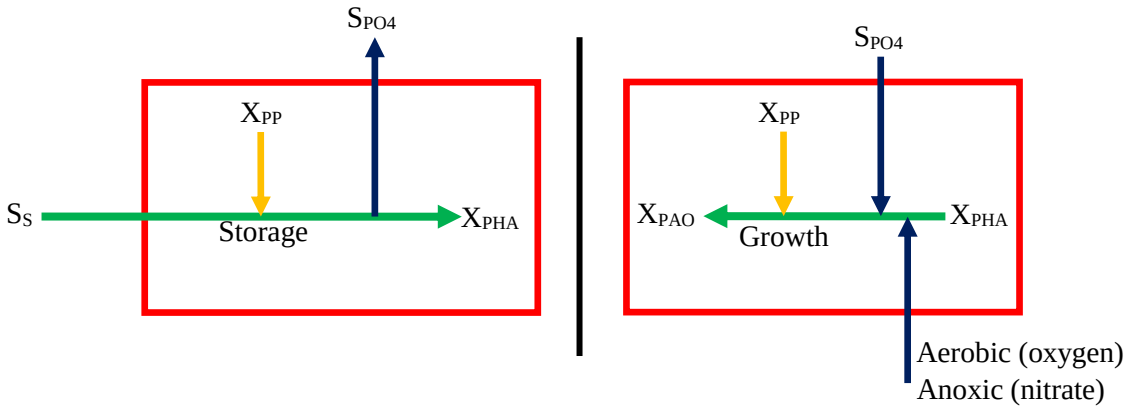

Figure 1.7 Description of P removal as included in the ASM3bioP model

Table 1.1 Selection of ASM for the operation

Models	Refs.	Substrates	Process	State variables	Total parameters
ASM1	Henze et al. (2000)	CN	8	13	26
ASM2d	Henze et al. (2000)	CNP	21	19	74
ASM3	Gujer et al. (2000)	CN	12	13	46
ASM3bioP	Rieger et al. (2001)	CNP	23	17	83
ASM2d+TUD	Meijer (2004)	CNP	22	18	98
UCTPHO	Hu et al. (2007)	CNP	35	16	66

The biological model of the reactors is simulated by Activated Sludge Model 3 bio–Phosphorous (ASM3-bioP). Twenty-three biological processes were considered to describe the biological phenomena happening in each reactor. The vertical transfer between layers in the settler is simulated by the double exponential settling velocity model. ASM3 has 13 state variables and with the addition of four new state variables related to bioP, the total numbers of state variables become 17. Further, ASM3 processes are enhanced with the ASM2d process which has bioP reactions without the precipitation reactions. ASM3 model contains hydrolysis, heterotrophic, and autotrophic with the addition of the above, P has less growth rate. Temperature dependencies of kinetic parameters, oxygen saturation concentration, and K_La (oxygen mass transfer coefficient) are also included in ASM3bioP at 15°C temperature. Table 1.2 shows the state variables with symbols and units by Solon (2015). A total of twenty-three biological processes were considered in ASM3-bioP are listed in the Appendix Table A1 and A2 Stoichiometric parameters matrix for the particulate components of ASM3 (Henze et al., 2000) and the EAWAG Bio-P module (Rieger et al. (2001)). Appendix Table A3 represents the kinetic rate expressions for ASM3 (Henze et al. (2000)) and Table A4 Kinetic rate expressions for the EAWAG Bio-P module (Rieger et al. (2001)).

Twenty-three processes are incorporated in ASM3-bioP are described below:

1) Hydrolysis
2) Heterotrophic organisms X_H
3) Aerobic Storage of X_{STO}
4) Anoxic Storage of X_{STO}
5) Aerobic growth
6) Anoxic growth
7) Aerobic endogenous Respiration
8) Anoxic endogenous Respiration
9) Aerobic respiration of X_{STO}
10) Anoxic resp. of X_{STO}
11) Aerobic endogenous Respiration
12) Anoxic endogenous Respiration
13) Storage of X_{PHA}
14) Aerobic storage of X_{PP}

15) Anoxic storage X_{PP}

16) Aerobic growth

17) Anoxic Growth

18) Aerobic endogenous Respiration

19) Anoxic endogenous Respiration

20) Aerobic lysis of X_{PP}

21) Anoxic lysis of X_P

22) Aerobic respiration of X_{PH}

23) Anoxic resp. of X_{PHA}

Table 1.2 State variables of ASM3bioP with average influent data

Compound	Symbol	Units	Average influent
Dissolved oxygen	S_O	$g(COD)m^{-3}$	0
Readily biodegradable organic substrate	S_S	$g(COD)m^{-3}$	90.34
Inert soluble organic	S_I	$g(COD)m^{-3}$	30
Ammonia+Nitrogen	S_{NH}	$g(N)m^{-3}$	39.40
Nitrate and nitrite	S_{NO}	$g\ (N)m^{-3}$	0
Dinitrogen	S_N	$g(N)m^{-3}$	0
Primarily orthophosphates	S_{PO4}	$g(P)m^{-3}$	8.86
Alkalinity	S_{HCO}	$mol(HCO3)m^{-3}$	7
Inert Particulate	X_I	$g(COD)m^{-3}$	51.20
Slowly biodegradable substrates	X_S	$g(COD)m^{-3}$	202.34
Heterotrophic Organisms	X_H	$g(COD)m^{-3}$	28.17
Cell internal storage	X_{STO}	$g(COD)m^{-3}$	0
Phosphate accumulating organisms	X_{PAO}	$g(COD)m^{-3}$	0
Polyphosphate	X_{PP}	$g(P)m^{-3}$	0
Primarily polyhydroxy alkanoates	X_{PHA}	$g(P)m^{-3}$	0
Nitrifying Organisms	X_A	$g(COD)m^{-3}$	0
Suspended solids	X_{TSS}	$g(SS)m^{-3}$	215.51

The mass balance equations are given in below:

$$r_1 = \frac{dZ_1}{dt} = \frac{1}{V_1}\left(Q_O Z_O + Q_r Z_r + r_1 V_1 - Q_1 Z_1\right) \tag{1.1}$$

Where $Q_1 = Q_O + Q_r$

$$r_2 = \frac{dZ_2}{dt} = \frac{1}{V_2}\left(Q_1 Z_1 + r_2 V_2 - Q_2 Z_2\right) \tag{1.2}$$

$$r_3 = \frac{dZ_3}{dt} = \frac{1}{V_3}\left(Q_2 Z_2 + Q_a Z_a + r_3 V_3 - Q_3 Z_3\right) \tag{1.3}$$

Where $Q_3 = Q_a + Q_2$

From K = 4 to 7

$$r_K = \frac{dZ_K}{dt} = \frac{1}{V_K}\left(Q_{K-1} Z_{K-1} + r_K V_K - Q_K Z_K\right) \tag{1.4}$$

Here Z is the concentration of the process, Where Q_a is concentration in the internal recycle rate, Q_r is concentration in external recycle and V is the volume of the reactors. Qr and Q_0 is the flow rate of influent, and all these two flow rates add to give influent flow to reactor1, r1. Whereas, Qa is added to the Qo in the third reactor. Similar equations can be written for all remaining six reactors as well using equations (1.1-1.4). Moreover, for aerated reactors, the dissolved oxygen dynamics will be represented in equation (1.5). In this equation, an extra term related to the amount of concentration of oxygen being supplied to aerobic reactors is added. S_O* notify the oxygen saturation coefficient, which is selected as 8 gO/m^3. Here K_La is the oxygen mass transfer coefficient for the k^{th} reactor. The Special case for O_2 in the aerobic tanks are considered:

$$\frac{dS_{O,K}}{dt} = \frac{1}{V}\left(Q_{K-1} S_{O,K-1} + r_K V_K + \left(K_L a\right)_K V_K \left(S_O^* - S_{O,K}\right) - Q_K S_{O,K}\right) \tag{1.5}$$

The amount of oxygen transferred to the aeration tanks should be equal to the amount of oxygen required by the microorganisms in the activated sludge process to oxidize the organic material and to maintain residual DO operating levels. When oxygen limits the growth of microorganisms, filamentous microorganisms may predominate, and the settleability and quality of activated sludge may be poor. On the other hand, an excessively high DO, meaning also a high flow rate, leads to high energy consumption and may also deteriorate the sludge quality. In practice, the DO concentration in the aeration tank should be maintained at about 1.5 to 4 gO_2/m^3 in the aerobic

aeration tanks, and 2 gO_2/m^3 is a commonly used value. Furthermore, if the nitrate consumption in the last predenitrification zone is not exceeding a certain level, excessive air consumption is not required in the aeration zones.

The most reasonable operating points for the nitrate concentration in the anoxic reactor need to be maintained in the interval 1−3 g N/m^3 when an internal recirculation is present and 1 g N/m^3 is the preferable value usually. Denitrification takes place in the anoxic reactors. It is carried out by ordinary heterotrophs and PAO biomass that convert the nitrate brought by the internal recirculation to anoxic reactor 3 (or 4) from aerobic reactor 7 into molecular nitrogen. In aerobic reactors, nitrification of ammonium to nitrate is performed by autotrophic organisms. On the other hand, the denitrification process (nitrate concentration in the anoxic reactor) is usually controlled by manipulating the internal recirculation flow rate from the last aerobic reactor. Table 1.3 represents the stoichiometric parameter values.

Table 1.3 stoichiometric parameter values

Parameters	Value
Heterotrophic max specific growth rate	3
Heterotrophic decay rate	0.3
Half saturation coefficient for heterotrophs	10
Oxygen half-saturation for heterotrophs	0.2
Nitrate half-saturation coefficient for denitrifying heterotrophs	0.5
Autotrophic max. specific growth rate	1
Autotrophic decay rate	0.2
Oxygen half-saturation coefficient for autotrophs	0.5
Ammonia half-saturation coefficient for autotrophs	1
Correction factor for anoxic growth of heterotrophs	0.8
Ammonification rate	0.01
Maximum specific hydrolysis rate	9
Half saturation coefficient for hydrolysis of slowly biodegradable substrate	1
Correction factor for anoxic hydrolysis	0.33
Rate constant X_{PHA} storage	6

The rate constant for X_{PP}	1.5
Rate constant lysis of X_{PP}	0.2
Rate constant for respiration of X_{PAO}	0.2
Maximum growth rate X_{PAO}	1

1.2.3 Secondary sedimentation tank

The secondary sedimentation tank is modeled as a non-reactive unit with ten layers (i.e. nil biological interactions). The feed layer is the sixth layer (counting from the top to the bottom). The area (A) of the settler is 1,500 m^2. Each layer (Z_m) has a height of 0.4 m, for a total height of 4 m. As a result, the settler volume is 6,000 m^3. equation 1.29 represents the solid flux because of gravity using a double exponential velocity by Takas et al. (1991). Fig .1.8 depicts the model of the secondary clarifier.

$$J_s = v_s(X_{sc})\, X_{sc} \tag{1.6}$$

$$v_s(X_{sc}) = max\,[\,0, min\{\, v_0', v_0(e^{-r_h(X_{sc} - X_{min})} - e^{-r_h(X_{sc} - X_{min})} \tag{1.7}$$

$$X_{min} = f_{ns}\, X_f \tag{1.8}$$

Where, X_{SC} is total sludge concentration, v_0 is maximum Vesilind settling velocity, v_0' is maximum settling velocity, r_p is flocculent zone settling parameter, r_h is hindered zone settling parameter, f_{ns} is a non-settleable fraction.

The upward (v_{up}) and downward (v_{dn}) velocities are calculated as shown in equations

$$v_{dn} = \frac{Q_u}{A} = \frac{Q_r + Q_w}{A} \tag{1.9}$$

$$v_{up} = \frac{Q_e}{A} \tag{1.10}$$

As per the notations above, the feed enters the settler at the 6th layer from the bottom and the sludge mass balance equation for the feed layer (m=6) are given in below:

$$\frac{dX_{sc,m}}{dt} = \frac{\frac{Q_f X_f}{A} + J_{sc,m+1} - (v_{up} + v_{dn})X_{sc,m} - min(J_{s,m}, J_{s,m-1})}{z_m} \tag{1.11}$$

Sludge mass balances for layers' m = 2 to 5:

$$\frac{dX_{sc,m}}{dt} = \frac{v_{dn}(X_{sc,m+1} - X_{sc,m}) + min(J_{s,m}, J_{s,m+1}) - min(J_{s,m}, J_{s,m-1})}{z_m} \tag{1.12}$$

For layer m = 1:

$$\frac{dX_{sc,1}}{dt} = \frac{v_{dn}\left(X_{sc,2} - X_{sc,1}\right) + min\left(J_{s,2}, J_{s,1}\right)}{z_1} \tag{1.13}$$

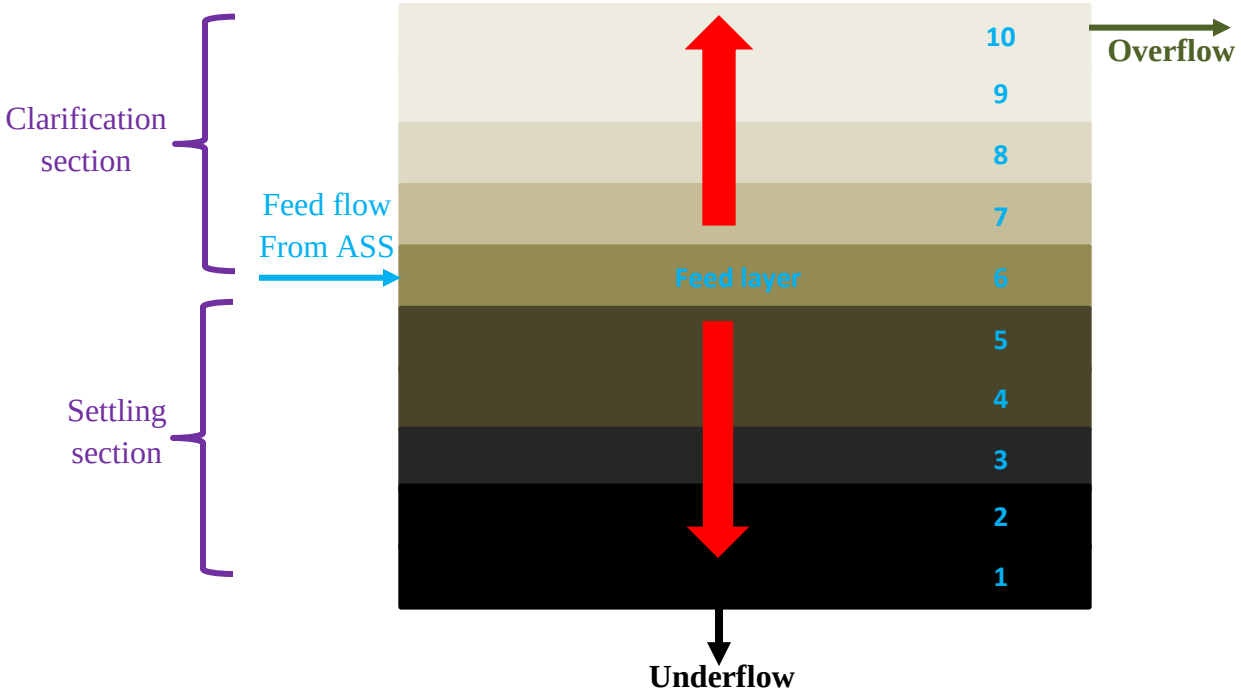

Figure 1.8 Model for secondary clarifier

For layers' m = 7 to 9:

$$\frac{dX_{sc,m}}{dt} = \frac{v_{up}\left(X_{sc,m-1} - X_{sc,m}\right) + J_{sc,m+1} - J_{sc,m}}{z_m} \tag{1.14}$$

For m = 10 (top layer):

$$\frac{dX_{sc,10}}{dt} = \frac{v_{up}\left(X_{sc,9} - X_{sc,10}\right) - J_{sc,10}}{z_{10}} \tag{1.15}$$

where, $J_{sc,j} = \begin{Bmatrix} \min\left(v_{s,10}X_{sc,10}, v_{s,9}X_{sc,9}\right) if\ X_{sc,9} > X_t \\ or \\ v_{s,10}X_{sc,10}\ if\ X_{sc,9} \leq X_t \end{Bmatrix}$

Where the threshold concentration X_t is 3000 g.m^{-3}.

The concentrations of soluble components are calculated considering each layer as a completely mixed volume.

For layer m = 6:

$$\frac{dZ_{sc,m}}{dt} = \frac{\frac{Q_f Z_f}{A} - (v_{up} + v_{dn}) Z_{sc,m}}{z_m} \quad (1.16)$$

For layer's m = 1 to 5:

$$\frac{dZ_{sc,m}}{dt} = \frac{v_{dn}(Z_{sc,m+1} - Z_{sc,m})}{z_m} \quad (1.17)$$

For layers' m = 7 to 10:

$$\frac{dZ_{sc,m}}{dt} = \frac{v_{up}(Z_{sc,m-1} - Z_{sc,m})}{z_m} \quad (1.18)$$

Where z_m is the height of m^{th} layer of the sedimentation tank.

Influent Data: In the ASM3bioP model, the compositions and characteristics of the influent wastewater vary from that of ASM2d influent data. Readily biodegradable organic substrate (S_S) is one of the ASM3bioP variables, whereas fermentable readily biodegradable organic substrate (S_F) and S_A (the fermentation products) are the combinations of S_S in ASM2d. In the steady-state simulation, it is found out that the removal of P was very intricate without increasing the composition of S_S. Furthermore, the S_S load raised 30% with the impact of the fraction of nitrogen, ammonia, and biodegradable nitrogen. In addition to the above, orthophosphate is also improved to maintain the orthophosphate to ammonia ratio in the influent data based on Gernaey et al. (2004).

The influent data of orthophosphates (S_{PO4}), ammonia nitrogen (S_{NH}), total suspended solids (X_{TSS}), readily biodegradable organic substrate (S_S), and flow rate (Q_o) are shown in Fig. 1.9 for the dry season. In the influent data, ammonia load changes within a few hours while suspended solid concentrations lower at 13 and 14 days which shows the weekend effect and lower activity. Similarly, for the dynamic storm influent condition, two short storm events are identified. First, on the 9th day, where Q_o and X_{TSS} composition is increased, and then on the 11^{th} day. The particulate and soluble pollutants are lower during this second storm occurrence.

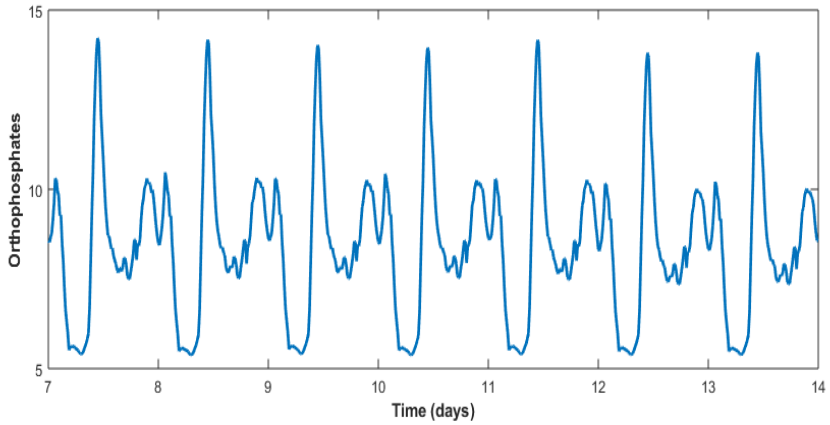

(A) Readily biodegradable organic substrate

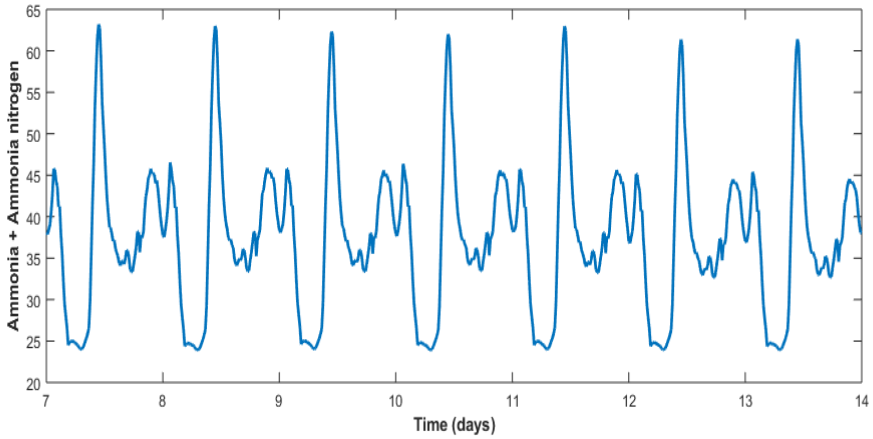

(B) Ammonia Nitrogen

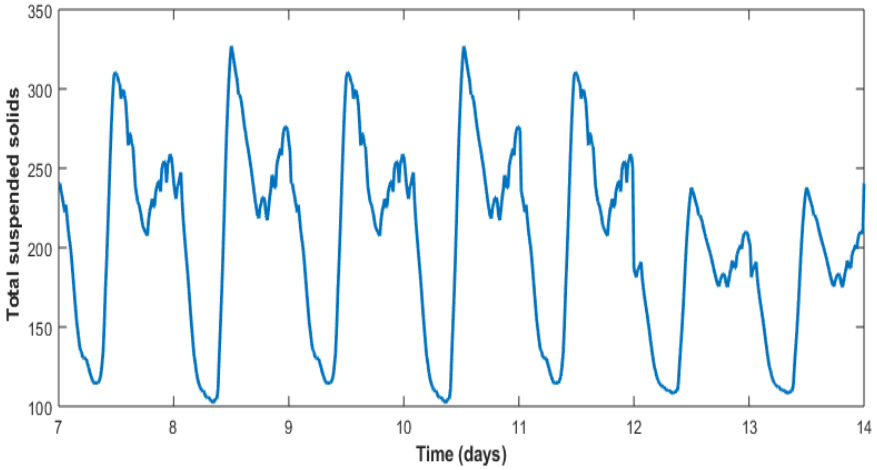

(C) Primarily orthophosphates

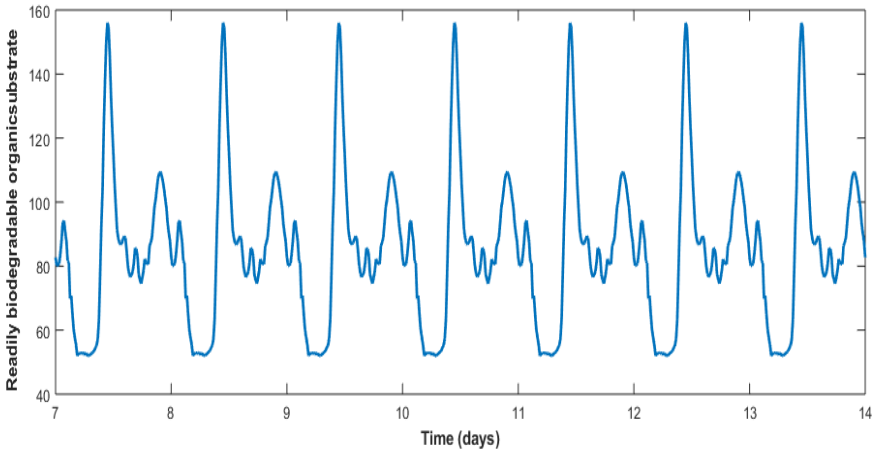

(D) Suspended solids

Figure 1.9 Influent scenario: S_S, S_{NH}, S_{PO4}, and X_{TSS} profiles

1.2.4 Plant performance evaluation criterion

The Effluent Quality index (EQI) defines the amount of effluent to surface waters averaged over the assessment time interval related to the weighting factors of discharge loads of composition which will impact more on receiving water body. Dynamic simulations are carried out by considering initially dry, rain, and storm season data files (14 days), and the performance is evaluated. Performance assessments were carried out to predict the economic basis with EQI for both the combined P and N removal in the benchmark simulation framework of WWTP (BSM1-P). The performance assessment which was initially implemented for BSM1 for N removal is now extended for P removal by Copp (2002); Gernaey et al. (2014). Equations. (1.19) and (1.20) describe the effluent quality index (EQI).

$$EQ = \frac{1}{1000\left(t_f - t_0\right)} \int_{t_0}^{t_f} KU_{(t)}\, Q_{e(t)} dt \tag{1.19}$$

$$KU_{(t)} = KU_{TSS(t)} + KU_{COD(t)} + KU_{BOD(t)} + KU_{TKN(t)} + KU_{NO_3(t)} + KU_{P_{tot}(t)} \tag{1.20}$$

The t_o and t_f in the equation. (1.42) represents the starting and ending intervals of time for computing the EQI while the KU_t notify the average load of polluted concentrations in the influent and effluent data: Generally, it consists of TSS, BOD_5, COD, TKN, NO_3 (nitrate), S_{NH} (ammonia) and TP in equation (1.20). Thus the corresponding expression for KU_t is given in equation 1.21).

$$\mathrm{KU_t} = \mu_t\, \mathrm{G_t} \tag{1.21}$$

Where μ_t (g^{-1}) are weighting factors ascribe every component of the pollution. Table 1.4 shows the weighting factors. Moreover, the composition of different elements (G_t) is estimated by using the following equations from (1.22)-(1.28).

$$G_{SS} = X_{TSS} \quad (1.22)$$

$$G_{COD} = S_S + S_I + X_I + X_S + X_H + X_{PAO} + X_{PHA} + X_A \quad (1.23)$$

$$G_{BOD} = 0.25\left(S_S + \left(1 - f_{S_i}\right)X_S + \left(1 - f_{XI_H}\right)X_H + \left(1 - f_{XI_P}\right)(X_{PAO} + X_{PHA}) + \left(1 - f_{XI_A}\right)X_A\right) \quad (1.24)$$

$$G_{TKN} = S_{NH} + i_{P,S_S}S_S + i_{N,S_I}S_I + i_{N,X_I}X_I + i_{N,X_S}X_S + i_{N,BM}(X_H + X_{PAO} + X_A) \quad (1.25)$$

$$G_{N_{tot}} = G_{TKN} + G_{NO_3} \quad (1.26)$$

$$G_{NO_3} = S_{NO_3} \quad (1.27)$$

$$G_{P_{tot}} = S_{PO_4} + i_{P,S_I}S_I + i_{P,X_I}X_I + i_{P,X_S}X_S + i_{P,BM}(X_H + X_{PAO} + X_A) + X_{PP} \quad (1.28)$$

Table 1.4 Weighting factors for μ_t values

Factors	μ_{TSS}	μ_{COD}	μ_{TKN}	μ_{NO}	μ_{BOD5}	$\mu_{P_{tot}}$
Values	2	1	30	10	2	100

The corresponding conversion factors in equations (1.24), (1.25) and (1.28) are considered as suggested by Henze et al. (2000), Gujer et al. (2000), Rieger et al. (2001), Solon (2015).

The assessment of the OCI Operational cost index (OCI) is necessary to calculate the cost for different control algorithms. The OCI is represented in equation. (1.29).

$$OCI = 3CA + ME + 5SP + AE + PE + MA \quad (1.29)$$

All the energies like aeration (kWh/d), pumping (kWh/d), mixing (kwh/d) energy respectively are incorporated in the equations. (1.30), (1.31) and (1.32). Here aeration power is needed to aerate bioreactors, pumping is used to alter the flow rate from one end to another end and for internal, external flow patterns. SP is defined as the rate of deposition concerning sludge given in equation (1.32).

The aeration energy (AE) is described as (Nopens et al., 2010; Hongyang et al., 2018):

$$AE = \frac{S_O^{sat}}{1800\ T}\int_{t_o}^{t_f}\sum_{i=1}^{7} V_i\, K_L a_i(t)\, dt \quad (1.30)$$

Where K_La_i notify the coefficient of mass transfer for oxygen

S_o^{sat} notify the oxygen saturation

The pumping energy (PE) is represented as:

$$\mathrm{PE} = \frac{1}{\mathrm{T}}\int_{t_o}^{t_f}\left(0.008\ \mathrm{Q_{exr}}(t) + 0.004\ \mathrm{Q_{intr}}(t) + 0.05\ \mathrm{Q_w}(t)\right)\mathrm{dt} \tag{1.31}$$

Where Q_{intr} is the internal recycle (m^3/d), Q_{exr} is the external recycle (m^3/d), Q_w is the wastage flow (m^3/d).

SP is the sludge production that is calculated based on the solids accumulated in the reactors and in the settler and also considering the solids purged. The sludge production (SP) includes the TSS from wastage and the solids accumulated. In general, the unit for TSS is g SS/m^3. Eq. (1.32) provides the sludge production (SP) cost as a function of TSS. TSSa and TSSs terms are already multiplied with the corresponding volumes and hence the units for TSSa and TSSs are kg SS. TSSa is the amount of solids in the bioreactors, and TSSs is the amount of solids in the sedimentation tank. TSSw is the amount of solids in the wastage and its unit is kg/m3. As the units for TSSw are represented in kg/m3, in eq. (1.32), it is multiplied with Qw which is the wastage flow having unit as m3/day.

$$\mathrm{SP} = \frac{1}{\mathrm{T}}\left(\mathrm{TSS_a}(t_f) - \mathrm{TSS_a}(t_o) + \mathrm{TSS_s}(t_f) - \mathrm{TSS_s}(t_o) + \int_{t_o}^{t_f}\mathrm{TSS_w} * \mathrm{Q_w}\ \mathrm{dt}\right) \tag{1.32}$$

The mixing is provided to avoid the biomass settling in the non-aerated reactors (anoxic and anaerobic reactors) and the mixing energy (ME) is represented as:

$$\mathrm{ME} = \frac{1}{\mathrm{T}}\int_{t_o}^{t_f}\mathrm{ME}(t)\,\mathrm{dt} \tag{1.33}$$

Where

$$\mathrm{ME}(t) = 24\sum_{i=1}^{7}\begin{cases}0.005 * \mathrm{V_i} & \text{if } \mathrm{K_L a_i} \le 20\mathrm{d^{-1}}\\ 0 & \text{if } \mathrm{K_L a_i} \ge 20\mathrm{d^{-1}}\end{cases}$$

Carbon addition (kg COD/d) is described as:

$$CA = \frac{CON_{CA}}{t_o * 1000}\int_{t_{start}}^{t_{end}} Q_{CA}\,dt \tag{1.34}$$

Here, Q_{CA} is the sum of carbon flow rate added and CON_{CA} is the concentration of added carbon

Metal addition (kg COD/d) is described as:

$$MA = \frac{CON_{MA}}{t_o * 1000}\int_{t_{start}}^{t_{end}} Q_{MA}\,dt \tag{1.35}$$

Here, Q_{MA} is the sum of carbon flow rate added and CON_{MA} is the concentration of added metal. Carbon addition (CA): External carbon source (methanol or acetic acid) is used as an alternative method for activated sludge system for removal of nutrients; the availability of readily degradable carbon substrate may limit the denitrification rate. A control approach is initiated and a metabolizable COD is directly added in the process where denitrification occurs temporarily. This method helps to increase the rate of denitrification on-demand, thereby minimizing the accumulation of nitrate and nitrite during times of peak loading. Carbon source is also added in the anaerobic tank to favor biological phosphorus removal and it will increase operational costs on high dosages are reported in Olsson et al. (2005); Guerrero et al. (2014).

Metal addition (MA): Metal is added (ferric chloride) to wastewater in the form of insoluble metal phosphate and an insoluble metal hydroxide. For metal addition, the formed precipitates with metals govern the alkalinity and concentration of orthophosphates in wastewater. Because of the conflict between phosphate and hydroxide, reaching a very low concentration of P effluent requires an increase in the amount of metal addition. As the concentration of dissolved phosphorus (effluent) decreases, more hydroxides of the metal will form. To achieve low phosphorus effluent limits, an increased dosage of metal addition is needed. Ultimately, phosphorus will reach chemical equilibrium without any further reduction. Generally, a metal dosage is added to the aerobic reactor and it will increase operational cost on high dosages are reported in Gernaey et al. (2002); Guerrero et al. (2014 In addition, based on the legal requirements, the effluent quality needs to be maintained.

1.3 Plant-wide modeling of wastewater treatment

BSM2-P is a BSM1-P extension that was created to incorporate plant-wide operations in a WWTP based on the literature of Flores-Alsina et al. (2016); Flores-Alsina et al. (2020). The sludge treatment operation is also included. The BSM2 protocol is made up of a full model of a general WWTP, a control structure, a benchmarking process, and a set of evaluation criteria. Model-based influent load generation as elucidated in (Solon et al. 2017, Flores-Alsina et al, 2016; Gernaey et al. 2011)) is used to generate dynamic influent load data to execute the performance of plant-wide scenarios of the wastewater treatment plants. The daily average dynamic mass flow rates are provided in Table 1. More information about the handling of influent generation is illustrated in Solon (2017); Snip et al. (2016). Dynamic simulations are performed for 609 days with steady-state simulation for 300 days. S: COD is the ratio of added sulfate ((Solon et al. (2017)). The last

one-year data is used for the performance assessment of the plant. State variables of ASM2d, units with notations, and average influent data are reported in Appendix Table D1.

1.3.1 Model scenario

The plant-wide model of BSM2-P is the resemblance of BSM2 plant but the modification is done in the activated sludge unit (ASU). In ASU extra two anaerobic reactors are added followed by anoxic and aerobic reactors (A^2/O) to enhance phosphorus removal and to improve PAO's with a competitive dominance over other nitrogenous bacteria. The plant-wide model of BSM2-P consists of ASU, primary (PSU) and secondary (SSU) sedimentation unit, thickener (THK), anaerobic digestion (ADU) unit, storage (SU), and dewatering (DU) unit with internal and external recycles. Fig. 1.10 depicts the plant-wide model of BSM2-P and Table 1.5 represents each process unit of WWTP of BSM2-P with their working function and physical configurations. The reaction rate expressions for all the state variables in the ASM2d model are described by Gernaey et al. (2014) and these expressions are considered in the present work.

Table 1.5 Elucidation of plant-wide model processes units and physical configurations

Process unit	Working function	References	Configurations
PSU	Non-reactive	(Otterpohl 1995)	900m^3
SSU	Double-exponential velocity function reactive	(Guerrero et al. (2013); Flores-Alsina et al. (2012)	6000m^3
ASU	ASM2d	(Flores-Alsina et al. 2016)	4500m^3
ADU	ADM1	(Batstone et al. 2002)	3400m^3
THK	Reactive	(Gernaey et al. 2014)	Underflow 30.9 m^3/d
DU	Reactive	(Gernaey et al. 2014)	9.6 m^3/d sludge and 168.9 m^3/d reject water
SU	non-reactive	(Gernaey et al. 2014)	160m^3

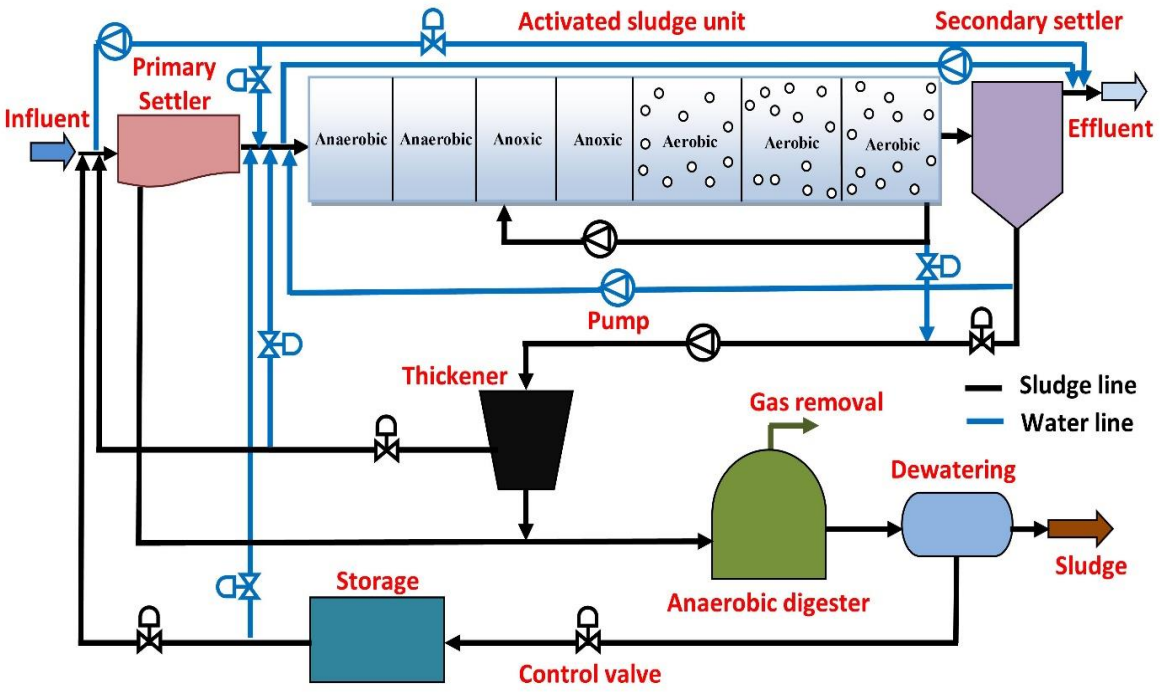

Figure 1.10 Plant-wide model layout for BSM2-P

1.3.2 Plant-wide evaluation criteria

The subscript 'ef' indicates the effluent discharge. θ_i signify the weighting factors of different pollutants to convert into basic pollution units are tabulated in Table 3. i_{COD_i} denotes the COD compounds, i_{N_i} denotes the nitrogen compounds, i_{P_i} denotes the phosphorus compounds, T signifies the total assessment time interval (364 days) and Q_{ef} denotes the discharge flow rate (m^3/d). The corresponding conversion factors for f_i are reported in (Solon (2017); Gernaey et al. 2014)). All the concentrations are addressed in g/m^3 units.

$$EQI = \frac{1}{T \cdot 1000} \int_{t_{start}}^{t_{end}} \Big(\theta_{TSS} TSS_{ef}(t) + \theta_{COD} COD_{ef}(t) + \theta_{NKJ} NKJ_{ef}(t) + \theta_{NO} S_{NO_{ef}}(t) + \theta_{BOD_5} BOD_{5_{ef}}(t) + \theta_{P_{org}} P_{org_{ef}}(t) + \theta_{P_{inorg}} P_{inorg_{ef}}(t) \Big) Q_{ef}(t)\, dt \quad (1.36)$$

$$COD_{ef} = S_{F_{ef}} + S_{A_{ef}} + S_{I_{ef}} + X_{I_{ef}} + X_{S_{ef}} + X_{B,H_{ef}} + X_{PAO_{ef}} + X_{PHA_{ef}} + X_{B,A_{ef}} + i_{COD_{S_{Fe(II)}}} S_{Fe(II)_{ef}} + i_{COD_{S_{IS}}} S_{IS_{ef}} + i_{COD_{X_{SO}}} X_{S^o_{ef}} + X_{SRB_{ef}} \quad (1.37)$$

$$NKJ_{ef} = S_{NH_{ef}} + i_{N_{S_F}} S_{F_{ef}} + i_{N_{S_I}} S_{I_{ef}} + i_{N_{X_I}} X_{I_{ef}} + i_{N_{X_S}} X_{S_{ef}} + i_{N_{BM}} \left(X_{B,H_{ef}} + X_{PAO_{ef}} + X_{B,A_{ef}} + X_{SRB_{ef}} \right) \quad (1.38)$$

$$P_{org_{ef}} = X_{PP_{ef}} + i_{P_{S_F}} S_{F_{ef}} + i_{P_{S_I}} S_{I_{ef}} + i_{P_{X_I}} X_{I_{ef}} + i_{P_{X_S}} X_{S_{ef}} + i_{P_{BM}} \left(X_{B,H_{ef}} + X_{PAO_{ef}} + X_{B,A_{ef}} + X_{SRB_{ef}} \right) \quad (1.39)$$

$$BOD_{5_{ef}} = 0.25 \begin{pmatrix} S_{F_{ef}} + S_{A_{ef}} + \left(1 - f_{S_I}\right) X_{S_{ef}} + \left(1 - f_{X_{IH}}\right) X_{B,H_{ef}} \\ + \left(1 - f_{X_{IP}}\right) \left(X_{PAO_{ef}} + X_{PHA_{ef}} \right) + \left(1 - f_{X_{IA}}\right) \left(X_{B,A_{ef}} + X_{SRB_{ef}} \right) \end{pmatrix} \quad (1.40)$$

$$P_{inorg_{ef}} = S_{PO_{4_{ef}}} \quad (1.41)$$

$$S_{NO_{ef}} = S_{NO_3} \quad (1.42)$$

$$TSS_{ef} = X_{TSS} \quad (1.43)$$

Operational cost is a weighted summation of costs associated with the production of sludge (SP) (kg ss/d), methane (PM) (kg.CH_4/d), pumping (PE), aeration (AE), mixing (ME) and heating (HE) energies (KWh/d), internal and external recycles are provided (m^3/d). All individual components are addressed in (Solon (2017); Gernaey et al. (2014)). Thus the OCI is estimated as below:

$$OCI = AE + PE + z_{PS} \cdot SP + ME - z_{PM} \cdot PM + \max(0, HE - 7PM) \quad (1.44)$$

z_i denotes the weighting factors of z_{PS} is 3 and z_{PM} is 6.

Aeration, pumping, mixing energies are addressed in the equations (1.45), (1.46), and (1.47). Here aeration power is needed to aerate bioreactors, pumping is used to alter the flow rate from one end to another end and for internal, external flow patterns.

The aeration energy (AE) is described as (kWh/d):

$$\mathrm{AE} = \frac{S_O^{sat}}{1800 \cdot T} \int_{t_o}^{t_f} \sum_{i=1}^{7} V_i \cdot K_L a_i(t)\, dt \quad (1.45)$$

Where K_La_i signifies the oxygen mass transfer coefficient, V_i notifies the volume of the reactors and oxygen saturation coefficient. T is the length of evaluation time (364 days)

The pumping energy (PE) is defined as (kWh/d):

$$\mathrm{PE} = \frac{1}{T} \int_{t_o}^{t_f} 0.004 \cdot Q_{int} + 0.008 \cdot Q_r + 0.050 \cdot Q_w + 0.075 \cdot Q_{PU} + 0.060\, Q_{TU} + 0.004 \cdot Q_{DO}\, dt \quad (1.46)$$

Where Q_{intr} is the internal recycle (m^3/d), Q_{exr} is the external recycle (m^3/d), Q_w is the waste flow (m^3/d), Q_{PU} is the primary clarifier underflow, Q_{TU} is the thickener underflow and Q_{DO} is the dewatering overflow.

The sludge production (SP) is expressed as (kg/d):

$$\mathrm{SP} = \frac{1}{\mathrm{T}\cdot 1000} \cdot \left(\mathrm{X_{TSS}(t_f)} - \mathrm{X_{TSS}(t_o)} + \int_{t_o}^{t_f} \mathrm{TSS_X}(t)\, \mathrm{Q_X(t)}\, \mathrm{dt}\right) \quad (1.47)$$

$$X_{TSS}(t) = X_{TSS,ASU}(t) + X_{TSS,SSU}(t) + X_{TSS,PSU}(t) + X_{TSS,ADU}(t) + X_{TSS,SU}(t)$$

With $X_{TSS,X}(t) = TSS_X(t) \cdot V_X$

Where Q_X (t) is the sludge flow and TSS_X is the total amount of solids in the sludge flow stream (after dewatering in BSM2-P). X_{TSS} is elucidated as the sum of TSS mass present in an individual process unit. The subscripts refer to the concern process units.

The mixing energy (ME) is defined as (kWh/d):

The mixing is highly necessary to avoid the biomass settling in the non-aerated and aerated reactors like all ASU tanks and anaerobic digester and the mixing energy (ME) is defined as (kWh/d):

$$\mathrm{ME} = ME_{ASU} + ME_{ADU} \quad (1.48)$$

Where

$$ME_{ASU} = \frac{24}{T} \int_{t_o}^{t_f} \sum_{i-1}^{i=7} \begin{bmatrix} if\ K_L a_i < 20d^{-1} & 0.005 \cdot V_i \\ if\ K_L a_i \geq 20d^{-1} & 0 \end{bmatrix} \cdot dt$$

$$ME_{ADU} = 24 \cdot 0.005 \cdot V_{ADU}$$

Where, V_i is the i^{th} tank volume (m^3) and 0.005 kW/m^3 is the mixing power consumption factor in ASU. V_{ADU} is the volume of liquid in ADU and the mixing power consumption factor 0.005 kW/m^3.

Methane production (kg CH_4/d) is defined as: The average methane production per day value is defined by using the equation. (1.49).

$$\mathrm{PM} = \frac{P_{atm}\cdot 16}{T\cdot R\cdot T_{OT}} \int_{t_o}^{t_f} \frac{1}{P_{tg}(t)} \cdot P_{g,CH_4}(t) \cdot Q_g(t) \cdot dt \quad (1.49)$$

Where, P_{gCH4} (bar) partial pressure of methane gas produced in the headspace, R denotes the universal gas law constant i.e $8.3145.10^{-2}$ bar m^3 $kmol^{-1}$ k^{-1}, T_{OT} represents the operating temperature of the digester (308.15 K), P_{tg} is the total gas pressure in the headspace, P_{atm} is atmospheric pressure (1.013 bar) and Q_g is the gas flow rate of produced gas.

Net heating energy is described as:

$$HE^{net} = \max(0, HE - 7 \cdot PM) \quad (1.50)$$

Where HE is the amount of energy required to get the anaerobic digester up to operating temperature, as shown in the equation below (1.51):

$$\mathrm{HE} = \frac{24}{86400\cdot T} \int_{t_o}^{t_f} P_{H2O} \cdot C_{H2O} \cdot \left(T_{OT} - T_{adu,i}(t)\right) \cdot Q_{ad}\,(t).\, dt \quad (1.51)$$

$$T_{ADU,i} = \frac{T_{PSU} \cdot Q_{PSU}(t) + T_{THK}(t) \cdot Q_{THK}(t)}{Q_{ADU}(t)} \qquad \text{Here, } Q_{ADU}(t) = Q_{PSU}(t) + Q_{THK}(t)$$

Where, P_{H2O} is the density of water (1000 kg/m^3), C_{H2O} is the specific heat capacity of water (4.186 KJ kg^{-1} ^{o}C^{-1}). $T_{ad,i}$ is the temperature of ADU influent, T_{OP} is the optimal temperature of ADU. Q_{ad} is the flow rate to the ADU (m^3/d).

Table 1.6 Weighting factors for EQI.

Weighting factors of EQI (θ_i)							
Weighting factors	θ_{TSS}	θ_{COD}	θ_{NKJ}	θ_{NO}	θ_{BOD_5}	$\theta_{P_{org}}$	$\theta_{P_{inorg}}$
Value	2	1	30	10	2	100	100

Following stringent regulations is a top priority for wastewater treatment plants. The legal constraints to be followed are the same as BSM1, i.e., TP is less than 2 gP/m^3; TN is less than 18 gN/m^3; BOD_5 is less than 10 g/m^3; COD is less than100 gCOD/m^3; TSS is less than 30 g/m^3, and S_{NH} is less than 4 gN/m^3.

Chapter 2

Literature Review

Chapter 2

Literature Review

Concerns about the impact of modern human life on the natural cycle have sparked several research areas that aim to address a portion of the issue in some way. Many efforts are being made these days to focus on cleaner and greener energy sources as well as production, transportation, and, of course, wastewater treatment. The use of various control techniques is aimed at improving the plant's efficiency. Numerous works in the literature propose various methods for regulating WWTPs. The majority of the work use BSM1 as a working scheme. Here, BSM1 is dealing with mainly organic matter and nitrogen. The present work use BSM1-P as a working scenario. Where it deals with organic matter, nitrogen, and phosphorous. In some case studies, the primary emphasis is on preventing effluent limit violations by direct controlling effluent variables. Other studies look at the trade-off between operating costs and effluent efficiency, but they don't address effluent violations. This is typically accomplished through a simple control strategy (control of dissolved oxygen in aerated reactors and nitrate-nitrogen concentration in the anoxic tanks or hierarchical control structures (Ammonia-based aeration control) that regulate dissolved oxygen set-points based on certain plant issues, solid retention time control (SRT control), metal and carbon dosages based on the requirements. BSM2-P has been used as another research platform in a plant-wide scenario. Some of them are interested in the design of control approaches in the WWTP. Especially, the proposed control strategies are aimed at dissolved oxygen rates in aeration, ammonia-based aeration control, regulating the wastage flow for the control of total suspended solids, and the addition of carbon and metal dosages. The BSM1-P and BSM2-P model, developed by the International Water Association (IWA) task group primarily for simulating a sewage treatment plant, has a wide range of literature. The scientific and research community now accepts this as a basic model for wastewater treatment plants.

The standardization of the model is necessary from a control and operational perspective because various control procedures have been suggested in the literature, but their evaluation and correlation, either realistic or simulation basis, is difficult. This is due to the wide range of time constants inherent in the activated sludge process, as well as the variability of the influent load, the intricate nature of biological and biochemical phenomena.

Temperature is a foremost element that shows the impact on biomass activity which is important to maintain efficient biological activity. Additionally, physiochemical characteristics like dissolved oxygen, settling velocity change, mixed liquor concerning change in temperature, which ultimately help in modeling and prediction of activated sludge system. Typically, in the global context, the average room temperatures vary for local atmospheric and environmental conditions. The temperature rise is mostly because of the varying sudden change in seasonal weather around the world. This work focuses intending to signify the temperature effects on phosphorous, nitrogen, and organic matter removal in BSM1-P and BSM2-P platforms. In this chapter, the literature is reviewed on BSM1-P and BSM2-P model schemes and the effect of temperature on BWWTP. In the last decade, diverse research is done based on their optimal control and design, with their objective functions of A^2/O that have been summarized in Table 2.1, with the majority of them seeking to determine the most profitable pollutants abatement approaches. Table 2.2 summarizes the studies that explain the making of existing A^2/O run more efficiently. Thus, it is important to understand that the original optimality of the simulated solution is highly dependent on the optimization problem conceptualization. The A^2/O (anaerobic, anoxic, and oxic) process is a well-established platform to remove N and P simultaneously in municipal WWTP today i.e introduced by Oehmen et al (2010); Zhou et al. (2015); Zhang et al. (2016). Regarding P, the approach of EBPR implementation is sustainable to meet the stringent regulations in the discharge flow but few researchers have proposed a successful design in WWTP for enhancing P-removal.

2.1 Literature based on BSM1-P control strategies

Real-Time Expert System is implemented in a wastewater treatment pilot plant to remove nutrients and organic matter biologically. It showed the great performance to control the pilot plant of WWTP is introduced by Baeza et al. (1999). A distributed control system (Knowledge-Based Expert System (KBES) constructed with G2©) is proposed in A^2/O configuration in the pilot plant is introduced by Baeza et al. 2002. Performance of the two-level control approach for the pre-denitrification system with the aim of the principal controller to balance the S_{NO} concentration in desired effluent concentrations is designed by Cho et al. (2002). Activated sludge model 2d (ASM2d) model in BSM1-P with two control loops (dissolved oxygen and nitrate) with PI controllers is tested with dry, rain, and storm data and is compared with open-loop and reported that a trade-off between operational cost and effluent quality exists is introduced by Gernaey et al. (2004). Biological phosphorus removal (BPR) was an intricate activity when contrast with N and

COD removal. It involves many processes with interactions among different biological reactions. Therefore, mathematical modeling and simulations will help to quantitatively assess this interactivity. Feed-forward (FF) control based on influent and nonlinear MPC with the addition of a penalty function on BSM1 and showed a low index of effluent efficiency and acceptable energy usage for aeration and pumping is designed by Shen et al. (2008). Shen et al. (2009); Cristea et al. (2008) are developed feedforward control for nitrogen removal in a pilot-scale A^2O (anaerobic-anoxic-oxic) process for municipal wastewater treatment and obtained improved nitrogen removal. Structured control of DO is important because it has more influence on aeration energy.

A two-level control strategy is proposed then the systematic track of the DO path in the BSM1 framework is shown by Brdys et al. (2009). Control options using the TSS controller with a high ratio of food to microbes in the reactor in the BSM2 framework reduced the risk and effect of bulking sludge are designed by Flores-Alsina et al. (2009). Feed-forward controllers have been applied in WWTP's taking into account the effluent quality and performance improvement especially for improving biological N and carbon (C) removal based on the Baeza et al. 2002; Nopens et al. (2010). Ostace et al., (2011) applied model predictive control (MPC) by considering a reactive secondary settler model and achieved reduced operational cost index (OCI) with improved effluent quality index (EQI). Although EBPR is considered a prominent approach, the inter-activity between N and P is still facing a removal failure in complete-scale treatment plants because of nitrate interactions in phosphorus uptake. These failures are influenced by the COD/P ratio and the organic matter in the influent, which are the primary parameters to understand the process Guerrero et al. 2011. It is implemented based on the ASM2d model. Xu and Vilanova (2013) developed different control strategies based on BSM1-P and observed that ammonia nitrogen and chemical oxygen demand (COD) of the effluent are under the limit, whereas other effluent parameters violated the constraints.

In BSM1-P, a novel control application with cascade and override control in combination with metal and carbon dosages are tested in the carbon-limited wastewater. It was found that the control application shows a better effluent with optimal cost by Guerrero et al. (2014). A fuzzy control framework is built to reduce the concentration of phosphorus in effluent water and found that fuzzy control shows better results in removing P compared with the PI control loop (Xu and Vilanova, 2015 a, b). Valverde-Pérez et al. (2016) applied control strategies for enhanced biological

phosphorus removal with two control frameworks on a sequence batch reactor and continuous flow reactor. An activated sludge process with P removal (Enhanced biological phosphorus removal) is introduced to enhance EQI. Under some circumstances, N and P removal is not possible because of deficit COD in wastewater content. So, either an external carbon source is added or chemical addition for P precipitation is generally preferred as a technical solution for efficient removal of P from COD limited wastewater. These dosages are expensive and lead to an increase in plant operating costs reported in Garikiparthy et al. (2016). Sdeghassadi et al. (2018) developed nonlinear MPC based on BSM1 and showed improved tracking of set-points.

BPR can be achieved by introducing PAO's in the sludge to inlet flow which has VFA (volatile fatty acid) in a reactor that has nil dissolved oxygen and nitrate achieved (Bunce et al. (2018)). In recent studies, signifies the application of the cascade approach in the DO design by Santín et al. (2015); Crisan et al. (2018). As far as energy savings in a real-time wastewater plant is concerned, hierarchical control strategies are proposed to obtain the required amount of DO to oxidize ammonia to nitrate. Fault detection on the benchmark models are evaluated by Baklouti et al. (2018). Hongyang et al. (2018) developed MPC based on the BSM1-P model to maintain an adequate amount of nitrate concentration as well as dissolved oxygen. It was observed that the control performance improved by 95% in all three weather (dry, rain, storm) conditions with MPC controller, with a focus to reduce ammonia fluctuations, a strategy with MPC/FF controllers was implemented at the base level to control S_{NO} and DO, and with the fuzzy controller at a higher level to manipulate the DO. Similarly, MPC at the supervisory level is also proposed to amplify the plant performance for reducing the cost and to improve the effluent quality by the design of Santín et al. (2016).

Artificial neural network (ANN) is designed to predict the set point of DO implemented by Santin et al. (2019). In the Activated sludge process, ammonia-based aeration control (ABAC) with a solid retention time (SRT) control approach is developed to balance the SRT, DO, and ammonia to maintain both treatment efficiency and energy economies in the plant according to Schraa et al. (2019). All these works are carried out by using BSM1 as the working platform. TN concentration attained regulation limits by using three control loops based on inorganic P, ammonia, and suspended solids concentration (Luca et al. (2019)). To predict the DO, artificial neural networks are used to satisfy delays from sensors and filters to get the desired set-point (Santin et al. (2019)).

The heuristic fuzzy controller is tested and found that all the pollutants meet stringent regulations with high-quality DO (Piotrowski et al. (2020)). Hierarchical control strategies on BSM1 are developed and found that there is an improvement in effluent quality and at low cost (Tejaswini et al. (2020)). The result is effluent ammonia nitrogen and total nitrogen are reduced with the little energy economy. A sensor-mediated (coupled with residual ammonia controls and DO set-point) approach is implemented on a granular sludge reactor to remove nutrients in wastewater and showed that maintaining stable aerobic granular sludge will help to improve the performance is designed according to Bekele et al. (2020).

On the other hand, the proliferation of poly accumulating organisms (PAO's) is responsible for the P removal through anaerobic and aerobic phases in the activated sludge system (AS) by Rampho et al. (2005); Ersu et al. (2010). The A^2O (anaerobic, anoxic, and oxic) process is a well-established platform to remove N and P simultaneously in municipal WWTP today i.e introduced by Oehmen et al. (2010); Zhou et al. (2015); Zhang et al. (2016); Massara et al. (2018). Regarding P, the approach of EBPR implementation is sustainable to meet the stringent regulations in the discharge flow but few researchers have proposed a successful design in WWTP for enhancing P-removal., Thus, with a reasonable amount of P and N removal, it is challenging to practice safe discharge and re-use of water by Machado et al. (2009); Ostace et al. (2013). Several investigations are proposed with slight adjustments of the process by replacing the positions of the anoxic and anaerobic move to give an improved phosphorus rate of 5-8% is reported by Zhang et al. (2000); Liu et al. (2008); Li et al. (2017). Different bio P models like MUCT, UCT, BDP-5 stage, A^2/O, and JHB are tested to find the best P removal process by Guerrero et al. (2013). Anoxic, anaerobic followed by aerobic with no internal recycle, this type of process is referred to as a reversed A^2O (R-A^2O) process with cost and effluent indexes. Mostly, this process is adopted by China and Japan in their WWTPs are reported in Bo 2006; Kang et al. (2011).

In some cases, the R-A^2O process doesn't show better results in the removal of nutrients when compared to A^2/O for both P and N. Mathematical models are used for WWTP to investigate the intricate concentrations of processes (chemical, biochemical and biological) in the effluent is presented by Fang et al. (2011); Hu et al. (2016). ASM2d and ASM3bioP ASS are used to simulate the R-A^2/O (Fang et al. (2016); Zhou et al. (2011)). Some investigations have shown better outcomes for R-A^2/O compared with A^2/O and other studies show contradictory results are

reported by Liu et al. (2008); Zhou et al. (2011). In the work of Chen et al., 2007, it is observed that microorganisms are responsible for the cycle function of aerobic and anaerobic processes that cause the efficient removal of N and P in the R-A^2/O. In the R-A^2O process, denitrification needs to satisfy the carbon source and another section of R-A^2O enters into the anaerobic section directly to maintain the anaerobic environment. In this manner, the PAO's can be improved to enhance P uptake and the P removal process is strengthened based on the results of Chen et al. (2007). This kind of process phenomenon is not well known yet. Thus a different pattern of studies are performed to test the EQI and OCI and to choose a better-optimized model. BNR processes are studied with the addition of carbon sources, which includes the accumulation of carbon sources within microbes are reported (Hu et al. (2016)). Carbon addition causes low nitrate concentration with high operational cost by Wang et al. (2017). In recent years, China is widely using R-A^2/O as the biological process in WWTP based on the literature of Xie et al. (2018). Water quality and microbial communities are analyzed with the addition of carbon sources by Chen et al. (2020).

2.2 Literature based on BSM2-P control strategies

The plant-wide model takes the attention among researchers for a long time run and the whole plant is controlled by the usage of water and sludge lines in WWTP by considering all process interactions based on the literature of Jeppsson et al. (2007); Nopens et al. (2009); Gernaey et al. (2014). WWTP's are considered as an integrated process, where all the individual unit processes are updated based on the process interactions. consequently, in recent years' wastewater engineering has boosted the advancements of enhanced modeling tools to address these issues. Studies on possibilities of control applications like sludge control approaches, biogas production in primary settler, the handling of the anaerobic digester, and phosphorus modeling with interactions of sulfur and iron cycles are incorporated in plant-wide models based on the literature of Barker and Dold (1996); Henze et al. (2000); Volcke et al. (2006); Grau et al. (2007); Ekama (2009); Ruano et al. (2011); Jeppsson et al. (2013); Flores-Alsina et al. (2014); Flores-Alsina et al., (2014).

The Benchmark simulation model (BSM2-P) Flores-Alsina et al. (2012) is used this is the integrated version of BSM1-P which includes both water and sludge treatment process units. As for as, a well-known plant-wide model is BSM2. Based on this plant-wide model, different control applications are studied like PI, ANN, and sludge-based strategies, hierarchal control approaches

are reported in Santin et al. (2015); Barbu et al. (2018); Tejaswini et al. 2020). To explore the total plant-wide model, researchers are switched their interest towards BSM1-P to BSM2-P. PI-based $S_{O,7,}$ and cascade PI in the control of ammonia and total suspended solids strategies are used. It was found that OCI and EQI are maintained trade-offs and compared with open-loop better results are found Solon et al. (2017). Sludge management strategies like bio-solids beneficiation facility (BBF) are studied. This resultant will improve solubility, sludge dewaterability and handle high sludge loads with change in the microbial population is noticed by Flores-Alsina et al. (2021).

2.3 Effect of temperature on the biological activity and treatment

In accordance with the geographical area, the mean yearly temperature of wastewater varies. For example, in Latin America, the temperature usually ranges from 3 to 27^{o}C. Whereas in Africa, Asia, and Middle East countries, the temperature goes from 28 to 45^{o}C. The temperature of wastewater is a very crucial parameter as it plays a significant role in the happening reaction rates and metabolic rates of microbes in the wastewater[1]. Stringent effluent limits must be followed while treating wastewater from the municipal and industrial sectors irrespective of the ambient and operating temperature. WWTP is facing many complications based on the active biomass for nitrogen removal (N) in treating industrial and municipal influents. The nitrification rate limits the extent of nitrogen. The nitrification rate is known to be the rate constraint step for N removal. Additionally, phosphorous removal based on uptake of acetate in the anaerobic section is crucial in influencing the amount of PAO's and thus the amount of P removed. In the literature, the effect of temperature on the kinetic processes in a typical WWTP is not extensively studied, and hence in this paper, this is addressed. The lower temperature has less impact on hydrolysis and fermentation. Short-term temperature advancements influence stoichiometry and kinetic variables. While long-term temperature advancements impact biomass activity.

Generally, the optimal temperatures for biological operations are in the range of 25 to 35^{o}C. The nitrification process ends when the temperature touches 50^{o}C and at 15^{o}C methane yielding bacteria becomes inert. Moreover, at 5^{o}C, autotrophic nitrifying microbes nearly cease functionally based on the investigation by Metcalf and Eddy (2003). The effluent quality has proved an optimistic assurance with a temperature range from 10 to 30^{o}C are reported by Collins et al. (1973). On investigating the temperature effect on bio-P removal, it was found that the rate of aerobic phosphorus uptake becomes extreme in the range of 15 and 20^{o}C are noticed by Baetens et al. (1999). Despite the solid retention time (SRT) and settling sludge compositions, with the rise in

temperature from 25^{o}C, the nitrogen removal happens simultaneously along with denitrification and nitrification reactions based on Görgün et al. (2002).

The flocculants in activated sludge after the settling process are investigated when the temperature varies from 3^{o}C to 15^{o}C by Ghanizadeh et al. (2001). Additionally, it is noticed that on temperature rise, the suspended solids from the effluent increase, and COD removal decreases. An investigation based on the temperature effects by considering the temperature from 9 to 30^{o}C in a tannery wastewater treatment in an SBR to assess the nitrogen removal. Moreover, it is observed that above 20^{o}C the effluent quality meets the effluent regulations presented by Murat et al. (2004). A remarkable increment is observed in the removal of COD and SS by raising the temperature from 15^{o}C to 35^{o}C in an up-flow micro aerobic sludge system. When temperature changes from 20^{o}C to 8^{o}C, the resultant removal rates of COD and SS are reduced based on De Kreuk et al. (2005); Meng et al. (2019). The up-flow anaerobic sludge blanket system is studied by changing the temperature from 6^{o}C to 32^{o}C to know the bio-kinetic rates for the treatment of sewage wastewater by Singh and Viraraghavan (2002). Temperature is a foremost element that shows the impact on biomass activity which is important to maintain efficient biological activity. Additionally, physicochemical characteristics like dissolved oxygen, settling velocity change, mixed liquor concerning change in temperature, which ultimately helps in modeling and prediction of activated sludge system is presented in Lippi et al. (2009). The rate of biological violations either becomes double or becomes half for every 10 to 15^{o}C of temperature rise.

According to Van't Hoff's rule, the biological activity rate doubles with every 10^{o}C rise in the temperature. The results of temperature impact on BNR in various studies are conflicting with each other. Many studies stated that phosphorous removal efficiencies exceed at higher temperatures (20-37^{o}C) (Brdjanovic et al. (1997)). Poly accumulating organisms (PAO) govern microorganisms at low temperatures (10^{o}C) despite the influence on carbon matter. Moreover, the temperature effect did not confer metabolic advantages to glycogen accumulating organisms above PAOs despite considering aerobic metabolism based on the literature of López-Vázquez et al. (2008). In a recent investigation, temperature effects are studied based on the activated sludge model (ASM1) on the BSM1 platform the kinetic parameters. It was noticed that, for temperatures less than 20^{o}C and greater than 30°C, the effluent constraints deviated from the stringent limits reported by Tejaswini et al. (2019).

Table 2.1 Summary of key process models and control parameters

key process models and control parameters → References	Process layout	Biological & settler model	Open/close loop	Decision variable	Algorithm/Method of computing	Objective function	Constrains	Study/ dynamic profile
(Xie et al. 2011)	A^2/O	Calibrated ASM2d, Not mentioned	Open loop	All are time-independent and continuous	Genetic	Min. Contaminants effluent	---	dynamic
(Fang et al. 2011)	A^2/O	ASM3bioP, Not mentioned	Open loop	All are time-independent and continuous	Genetic	Min. Contaminants effluent	---	dynamic
(El-Shorbaghy et al. 2011)	A^2/O	ASM3bioP, Point-settler with variable	Open loop	All are time-independent and continuous	GAMS simulator	Min. investment, operation, and maintains cost	Volume of reactor & effluent	steady
(Guerrero et al. 2012)	A^2/O	Modified ASM2d, Takacs	Closed loop	Time-varying	Random generator	Min. investment, operation, maintain cost, related to solid separation issues	---	dynamic
(Liu et al. 2012)	Primary clarifier + A^2/O	ASM2d, Takacs	Closed loop	All are time-independent and continuous	Multi-object Genetic-NSGAII	Min. Contaminants Effluent, process cost	---	steady

(Ostace et al. 2013)	A^2/O	Modified ASM2d Takacs	Closed loop	All are time-independent and continuous	Pattern search	Min. process cost	---	dynamic
(Nguyen et al. 2013)	A^2/O	ASM2d Takacs model (Takacs et al. 1991)	Closed loop	Time-varying	Pattern search	Min. process cost	---	dynamic

Table 2.2 Control strategies and performance indices of BSM1-P

Control strategies and performance indices → / References	ASM	Control goal	Control Algorithm	Control variables	Manipulating variables	Effluent quality (EQI)	Operational cost (OCI)	Remarks
(Gernaey et al. 2002)	A^2/O (ASM2d)	Effluent quality	PI, metal, and carbon dosages	Dissolved oxygen (DO)	Oxygen Mass transfer coefficient (K_La)	Improved EQI	OCI is increased	Better in P removal
(Gernaey et al. 2004)	A^2/O (ASM2d)	Effluent quality, Cost reduction	PI	DO and nitrate	K_La and internal recycle(Q_{intr})	Improved EQI	OCI increases	selection of oxygen set-point

(Ingildsen et al. 2005)	A^2/O (ASM2d)	Effluent quality, Cost reduction	PI	Different DO, nitrate, ammonia, TSS and phosphate	K_La , higher-level DO set point, Q_w and Q_{intr}	Improved EQI	OCI increases	Improved P removal
(Machado et al. 2009)	A^2/O (ASM2d)	Effluent quality, Cost reduction	RGA based PI control	Ammonia, nitrate, TSS and phosphate	higher level DO set point, Q_w ,Q_{intr} and purge flow rate	Improved EQI	Reduced OCI	EQI controlled based on cost setpoint
(Shen et al. 2010)	A^2/O (ASM2d)	Effluent quality, Cost reduction	PID	Dissolved oxygen (DO)	Oxygen Mass transfer coefficient (K_La)	Improved EQI	OCI reduction achieved	Better in P removal
(Guerrero et al. 2011)	A^2/O (ASM2d)	Effluent quality, Cost reduction	PI Cascade feed-forward	DO, ammonia Nitrate and TSS	K_La , higher level DO set point, Q_w and Q_{intr}	Improved EQI	OCI increases	Optimized through set-point
(Rieger et al. 2012)	A^2/O (ASM3bioP)	Effluent quality, Cost reduction	On-Off and PID	DO and ammonia (S_{NH})	K_La and DO set-point is determined by higher level	Improved EQI	OCI minimized	Reduced energy consumption

(Liu et al. 2012)	A^2/O (ASM2d)	Effluent quality, Cost reduction	Cascade MPC and PI	DO, ammonia and nitrate	K_La , higher-level DO set point and Q_{intr}	Improved EQI	OCI increases	Improved removal rates of N and P
(Xu et al. 2013)	A^2/O (ASM2d)	Effluent quality, Cost reduction	PI	Different DO, TSS and nitrate	K_La, Q_w and Q_{intr}	Improved EQI	OCI increases	Trade-off between OC and EQI
(Ostace et al. 2013)	A^2/O (ASM2d)	Effluent quality, Cost reduction	Pattern search	COD-P control, Ammonia, nitrate,	higher-level DO set point, Q_w, K_La and Q_{intr}	Improved EQI	Reduced OCI	Optimized reference operation provided
(Guerrero et al. 2014)	A^2/O (ASM2d)	Effluent quality, Cost reduction	PI and override control	Nitrate, phosphate	Q_{intr} and set point of nitrate	Improved EQI	OCI increases	P removal is enhanced
(Xu et al. 2015)	A^2/O (ASM2d	Effluent quality, Cost reduction	Fuzzy and PI	DO and nitrate	K_La and Q_{intr}	Improved EQI	OCI increases	Fuzzy control show improved EQI then PI

(Xu et al. 2015)	A^2/O (ASM2d	Effluent quality, Cost reduction	Fuzzy	DO and nitrate	K_La and Q_{intr}	Improved EQI	OCI increases	Fuzzy control show better P removal
(Hongyang et al. 2018)	A^2/O (ASM2d)	Effluent quality, Cost reduction	PI and MPC	DO and nitrate	K_La and Q_{intr}	Improved EQI	OCI increases	MPC show good tacking performance

Operation at normal temperatures minimizes land requirements, improves conversion processes, improves removal efficiencies, and makes the use of certain treatment processes possible. In WWTP methods, the temperature is regarded as the most demanding factor, especially for biological WWTP. Thus, the temperature of wastewater is identified as a significant parameter that influences biological treatment, marine life, and the water's suitability for useful purposes based on the literature of Shahzad et al. (2015); Brehar et al. (2019). Increasing the temperature of wastewater results in changes in the species of fish that live in the water body, the solubility of oxygen in water (a decline in the saturation concentrations), the oxygen adsorption mechanism, the rate of activity in bacteria, and the rate of gases transported to and from water by Von Sperling et al. (2005).

Temperature fluctuations in WWTP's have received relatively less attention towards a whole plant-wide model and control viewpoint. The complexity of biochemical reactions necessitated less exposure to temperature regulation in WWTP processes. In general, WWTPs are operated under ambient temperatures of the environment. Variations in climatic conditions will largely influence effluent quality (EQI), operational cost, and overall productivity. In current times temperature effect is studied by using an up-flow micro aerobic sludge system. The outcome results show that at 17°C, the removal efficiency of nitrogen is improved results are reported in Meng et al. (2019). Alsawi (2020) noticed that kinetic parameters largely influence the productivity of WWTP's and temperature changes influence the process performance. Nitrogen and carbon removal efficacy is improved at the lower temperatures of 10-15^{o}C for diary effluent in the fixed-bed reactor system presented in the paper of Hamdani et al. (2020).

Based on the literature survey the following important research gaps are identified:

- There is no literature on the design of basic and advanced control strategies like PI, MPC, Fuzzy, and ammonia-based aeration control (ABAC) in the BSM1-P (ASM3bioP process) platform.
- The application of PI in plant-wide BSM2-P (ASM2d Process) has been reported but the implementation of advanced control strategies like MPC and Fuzzy is not studied.
- The effect of temperature is not studied based on the seasonal variations in the global context on the simulation platform.

2.4 Motivation

Today, adopting new optimized techniques is a top incentive for maintaining legislative regulations of the pre-existing WWTP. Therefore, the optimized treatment techniques can include either redesigning the process structure or it can be enhanced with advanced process control strategies. All these lead to the regulation of the pollutant concentration of nitrogen (N), carbon (C), and phosphorus (P) in the effluent with a low operating cost. Although many implementations and developments have been published in the literature, a large number of WWTPs are still operated without upgradation due to a lack of proper understanding of modeling, control, and optimization tools to monitor the issues in meeting stringent WWTP effluent quality. One of the driving factors behind the increased use of advanced control strategies in wastewater treatment is plant complexity and the high number of unit operations. Control and monitoring of the entire WWTP are extremely difficult because various unit operations are dependent on chemical, biochemical, mechanical, and biological phenomena. Furthermore, a WWTP is characterized by regular changes in environmental conditions such as feed flow rate, temperature, influent nutrient concentrations, and toxic material concentration peaks, all of which may cause serious problems in biological wastewater treatment. These variations can have a major impact on process efficiency, leading to process failures in some cases.

To meet stringent regulations: Using advanced control strategies to achieve the effluent consistency specified in regulations is advantageous. Additionally, the effluent concentration can be kept more constant, and operation faults disturbing the treatment can be reduced. The management of the whole plant becomes more complex as the number of unit operations increases, becoming, for example, plant-wide treatment processes. By using modern control applications, the effluent quality can be effectively regulated, allowing even stringent environmental regulations to be met.

Cost minimization: According to Olsson et al. (2005) good plant management and proper usage of controllers have been shown to increase the ability of a nutrient removal WWTP by 10-30%. As the efficiency of the processes improves, the area needed for new WWTP's decreases, resulting in lower construction costs. Furthermore, substantial cost savings in nutrient removal plants could be realized by reducing the amount of energy required for aeration and the use of different chemicals.

Temperature effect on WWTP: Temperature plays an important role in many WWTPs. In WWTP methods, the temperature is regarded as the most demanding factor, especially for biological WWTP. Thus, the temperature of wastewater is identified as a significant parameter that influences biological treatment, marine life, and the water's suitability for useful purposes. Stringent effluent limits must be followed while treating wastewater from the municipal and industrial sectors irrespective of the ambient and operating temperature. WWTP is facing many complications based on the active biomass for nitrogen removal (N) in treating industrial and municipal influents. The nitrification rate limits the extent of nitrogen. The nitrification rate is known to be the rate constraint step for N removal. Additionally, phosphorous removal based on uptake of acetate in the anaerobic section is crucial in influencing the amount of PAO's and thus the amount of P removed. In the literature, the effect of temperature on the kinetic processes in a typical WWTP is not extensively studied, and hence in this thesis, this is addressed. The lower temperature has less impact on hydrolysis and fermentation. Short-term temperature advancements influence stoichiometry and kinetic variables. While long-term temperature advancements impact biomass activity. The wastewater treatment process has evolved into a production process in which effluent quality control is critical. Because poor treatment process operation can result in significant production losses and environmental issues, enhancing optimum operation and advanced control techniques has the potential to successfully operate the wastewater treatment facility.

2.5 Objectives

1. To develop lower-level control strategies for WWTP
2. To develop supervisory level control strategies for WWTP
3. To develop integrated supervisory and override control strategies for WWTP
4. To develop control strategies based on plant-wide WWTP models
5. To evaluate different biological WWTP configurations
6. To study the effect of temperature on WWTP,s.

2.6 Organization of the thesis

The organization of the thesis is as follows:

Chapter 2 presents a literature overview on various aspects of BWTP of control schemes and the effect of temperature and motivation and objectives

Chapter 3 elucidates the design and implementation of lower-level Control Strategies for BSM1-P.

Chapter 4 describes the design and implementation of higher-level Control Strategies for BSM1-P.

Chapter 5 elucidates the design and implementation of integrated supervisory and override Control Strategies for BSM1-P.

Chapter 6 describes the design and implementation of Control Strategies for BSM2-P

Chapter 7 Evaluation of three different A^2/O processes and the applications

Chapter 8 provides the effect of temperature in BWTP and plant-wide level

Chapter 9 provides a summary and conclusions.

Chapter 3

Design of Lower-level Control Strategies on BSM1-P

Chapter 3

Design of lower-level control strategies on BSM1-P

3.1 Lower-level control approach on BSM1-P

This chapter introduces lower-level control for the BSM1-P plant, which is based on the default strategy. It considers two loops: controlling dissolved oxygen concentration in tank 7 ($S_{O,7}$) by manipulating the oxygen mass transfer coefficient (K_La_7), and controlling nitrate concentration in reactor 4 ($S_{NO,4}$) by manipulating the internal recycle flow rate (Q_a). This is accomplished in the current work by employing various controllers such as proportional-integral (PI), Model predictive controller (MPC), and Fuzzy logic controller (FLC). Table 3.1 represents the control approaches for chapter 3.

Table 3.1 Control approaches for this chapter

Label	L1 (Default PI)	L2 (MPC)	L3 (Fuzzy)
Characteristics	S_{NO} and DO controller	S_{NO} and DO controller	S_{NO} and DO controller
Measured Variable	S_{NO} in tank4 and S_O in tank7	S_{NO} in tank4 and S_O in tank7	S_{NO} in tank4 and S_O in tank7
Set-point/Value	1 gN/m^3 and 2 gO_2/m^3	1 gN/m3 and 2 g O_2/m3	1 gN/m^3 and 2 g O_2/m3
Manipulated Variable	Internal recycle (Q_{intr}) and mass transfer coefficient (K_La_7)	Q_{intr} and K_La_7	Q_{intr} and K_La_7
Control Classification	PI	MPC	Fuzzy

3.1.1 Design and implementation of proportional integral controller

The PI controllers can be framed using a wide variety of techniques accessible in the literature. In the present report, Skogestad internal model control (SIMC) method is used to design the PI controllers by Grimholt and Skogestad (2018). The way of approach is depicted in the flow diagram in Fig.3.1.

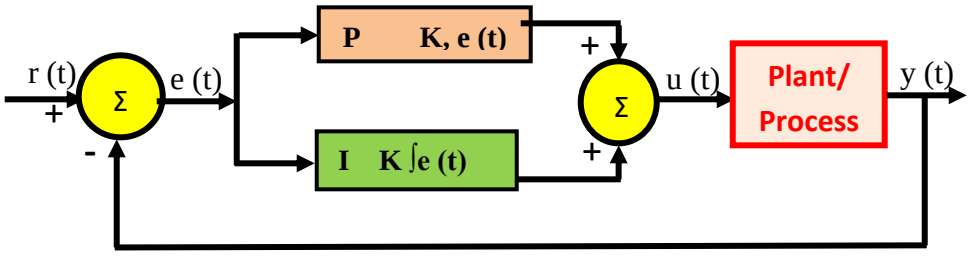

Figure 3.1 PI feedback control loop

The first-order plus time order delay (FOPTD) model as prescribed in equation (3.1) is identified for the design of the PI controllers for each loop.

$$G(s) = \frac{K_P e^{-d}}{TS+1} \tag{3.1}$$

Where, K_P denotes the process gain, d denotes the delay and T signifies the time constant of the system. For more clarification, the identification method and designed controllers are elucidated distinctly in Fig.3.2. Procedure for identification of different models used in this work identification of FOPTD/State space (SS) model for lower level is elaborated briefly in Appendix A. The lower-level identification Matlab file is reported in the Appendix from Figure A1.

PI controllers are designed for the two control loops independently based on the corresponding linear model. These models for both the loops are developed based on the system identification technique from the open-loop data. The operating point (steady-state values) for the DO loop is 2 g/m3 of DO when K_La is 252 day^{-1}. Similarly, the operating point for S_{NO} loops is 1 g/m^3 of nitrate when the internal recycle flow is 34,500 m^3/day. The reason to consider this operating point is as follows. In practical operation, the DO levels in the aeration reactor need to be maintained around 2 gO/m^3. Furthermore, if the nitrate consumption in the last pre-denitrification zone is not exceeding a certain value, excessive air consumption is not required. Similarly, the nitrate concentration in the anoxic reactor needs to be maintained in the interval 1–3 gN/m^3 when an internal recirculation is present and 1 g N/m^3 is preferable. For identification, a random input signal of 10% variance, having a mean value of 252 day^{-1}, is given in the K_La and observed its effect on DO. Similarly, for S_{NO}, a random signal with a mean value of 34,500 m^3/day and a variance of 10% is given in Q_{intr}. The corresponding input and output data for both loops is given in Fig. 3.3 for the control loop structure (CLS-2) which is shown in Fig. 3.4.

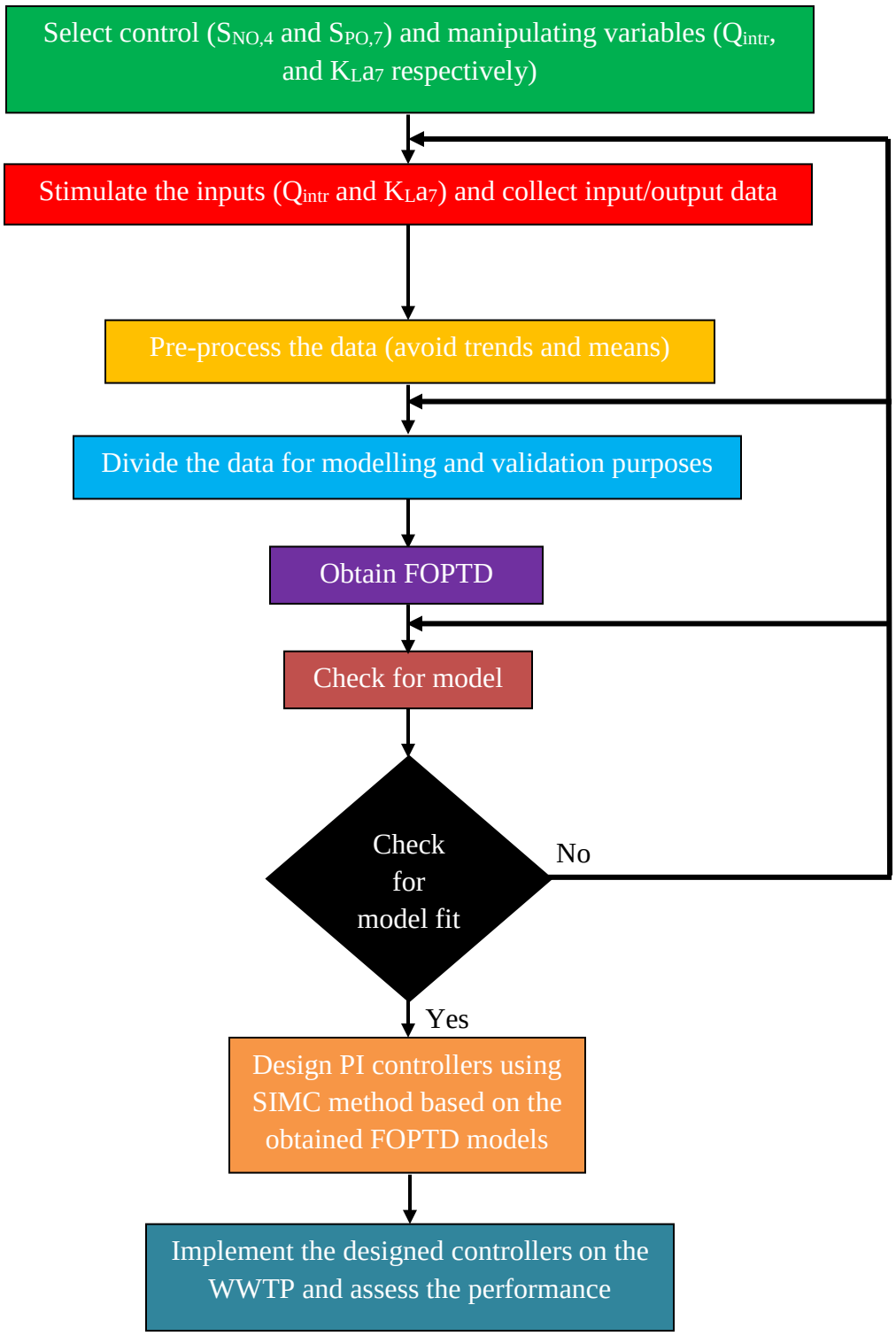

Figure 3.2 System identification method and controller design

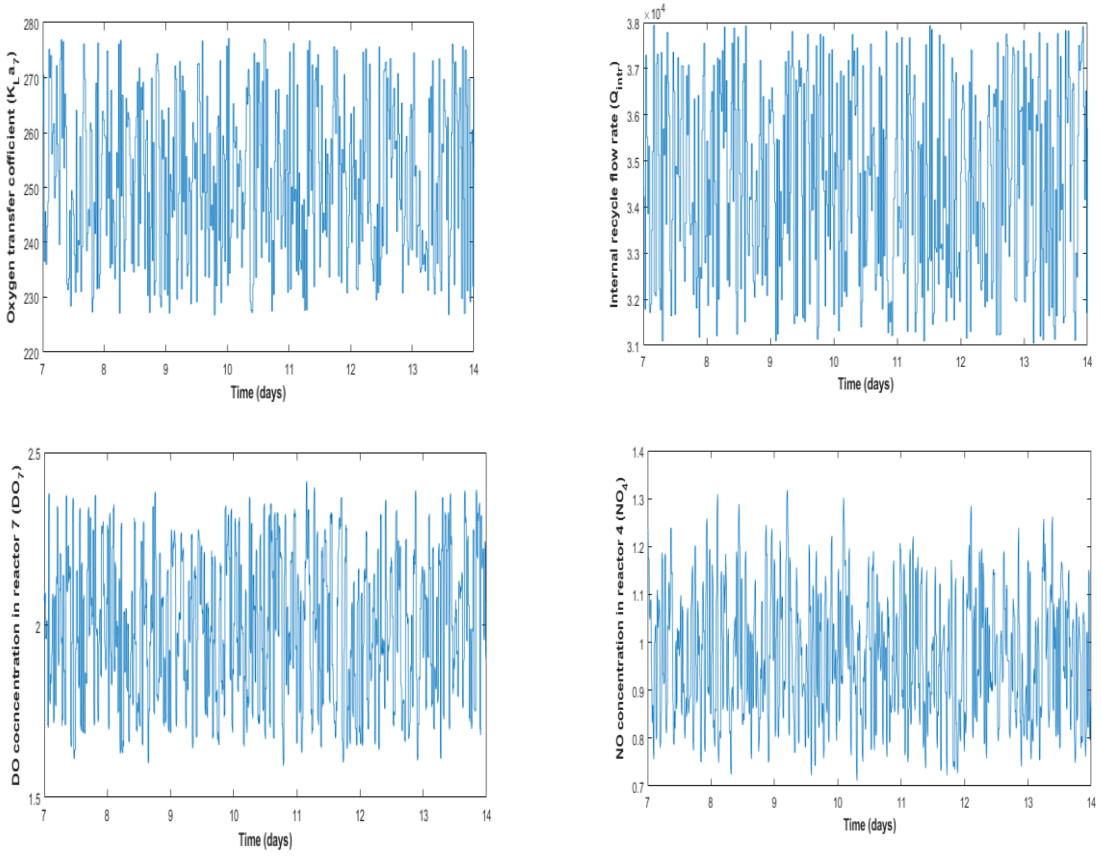

(A) (B)

Figure 3.3 Input and output data for (a) DO and (b) S_{NO}

From this data, the prediction error minimization (PEM) method is used to identify the models. Based on the models, using the SIMC method by Grimholt and Skogestad (2018), PI controllers are designed for each loop. For CS-2, (control of S_{NO} in reactor 4 and DO in reactor 7), the respective obtained FOPTD model parameters are: K_P = 0.0000699, T_i = 0.012214 and T_d = 0.0016771, K_P = 0.013907, T_i = 0.001414 and T_d = 0.0063646. Based these models, PI controllers are designed using SIMC method and are obtained as K_c = 52889.40, T_i = 0.012214 (S_{NO} loop) and K_c = 7.987, T_i = 0.00141 (DO loop). A similar design is followed for the design of PI controllers for all control strategies. Similarly, seven other control strategies (CS) are developed by choosing different combinations (CS1 – CS8) of reactors 5, 6, and 7 for DO with reactors 3 and 4 for S_{NO} and are given in Table 3.2. Appendix Figure A2 represents the BSM1-P Matlab/Simulink diagram with default controllers.

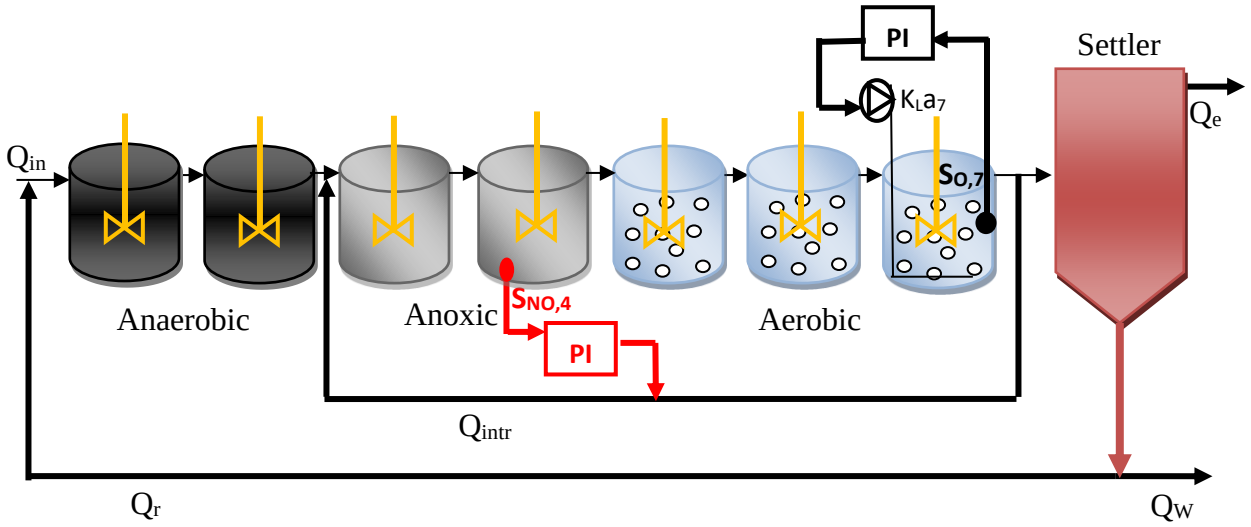

Figure 3.4 CS2-Configuration (Default control strategy)

Table 3.2 Different control approaches for varying DO and S_{NO}

Type	Control of DO in	Control of S_{NO} in
CS1	Reactor 7	Reactor 3
CS2	Reactor 7	Reactor 4
CS3	Reactors 5, 6 & 7	-
CS4	Reactor 6 & 7	-
CS5	Reactor 6 & 7	Reactor 3
CS6	Reactor 6 & 7	Reactor 4
CS7	-	Reactor 4
CS8	Reactors 5, 6 & 7	Reactor 3

The corresponding simulation results for the PI controller for dry weather influent are given in Table 3.3. For comparison, the plant layout without any control scheme (open-loop) is also considered and the corresponding results are also given in Table 3.3. The effluent quality is determined in terms of BOD, COD, P, NH_4, TN, and TSS. The variations of these parameters cause a variation in the effluent quality index. The general standard limits on these parameters are given in Table 3.3. Further, the percentage violation of P, TN, and NH over a total range of operating time is also tabulated. Besides the effluent quality index, the results of OCI are also tabulated which is evaluated based on AE, PE, ME, and SP used in the process. Of all the

parameters reported COD, BOD and TSS were below the standard limit whereas other parameters are not. Of all the combinations (CS1 – CS8), the pollutant considerations for CS1 and CS2 are better than CS3-CS8. In the former case, the OCI of CS2 is far better than CS1. The OCI and EQI are also plotted and are shown in Fig.3.5. Generally, the plant performance is evaluated based on the lower value of EQI and OCI. Fig.3.5. elucidate that the OCI value is better for CS2 and EQI value is better for CS1. Since the driving parameter for the present approach is EQI and hence CS2 is considered better than other combinations. Simulated studies are also conducted for both open-loop and PI controllers under the storm and rain influent climate seasons and observed that PI controller provides improved tracking performance when compared to open loop. It is observed that OCI and EQI are better under closed-loop conditions when compared with open loops.

Table 3.3 Comparision of different control apporaches from CS1 to CS8

Pollutants	Limit	Open loop	CS1	CS2	CS3	CS4	CS5	CS6	CS7	CS8
S_{NH}	4	6.0	5.5	6.04	4.7	5.4	4.9	5.5	4.5	4.0
TSS	35	13.6	13.7	13.6	13.5	13.6	13.7	13.6	14.6	13.6
TN	18	16.5	17.9	16.1	15.8	16.1	17.9	15.9	15.7	17.9
TP	2	3.5	3.4	3.5	3.8	3.6	3.5	3.6	3.9	3.8
COD	125	44.7	44.8	44.7	44.74	44.7	44.8	44.7	46.5	44.8
BOD	10	1.7	1.8	1.7	1.7	1.7	1.8	1.7	1.8	1.7
IQI		72152	72152	72152	72152	72152	72152	72152	72152	72152
EQI		13411	13169	13239	13415	13267	13250	13255	13518	13384
SP		2973	3017	2973	2938	2963	3004	296	2983	2977
Performance plant assessment										
AE		4336.6	4269.3	4255.7	4603.8	4378	4427.9	4371.5	4384	4703.2
PE		304.8	238.6	352.5	304.8	304.8	231.5	316.8	320.2	227.3
ME		480	480	480	480	480	480	480	330	480
OCI		18753	18830	18681	18854	18748	18920	18741	18898	19060
Percentage of effluent violations (%)										
TP		65.7	90.7	67.7	71.8	68.8	65.6	69	91.9	70.3
TN		38.0	43.6	26.3	27.6	33.3	56.8	27.9	15.6	56.6
S_{NH}		66.2	46.5	66.3	60.1	63.8	60.4	64.5	55.8	50.4

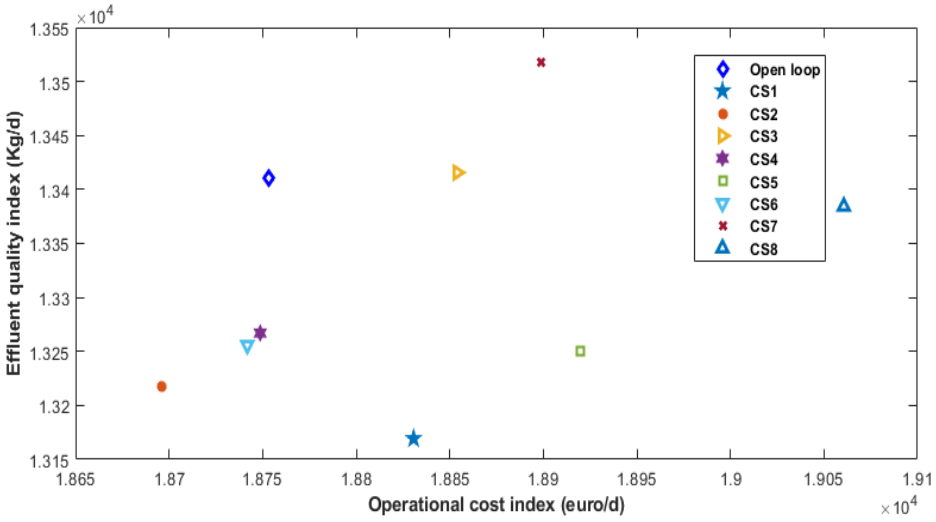

Figure 3.5 Comparisons of different control approaches based on EQI and OCI

3.1.2 Design and implementation of the model predictive controller (MPC)

To control the processes that contain multiple variables and to achieve the desired objectives with constraints, MPC can be used to do so which is an advanced control strategy. According to Maciejowski et al. (2002) by using a plant-wide model, a control problem is defined as the desired objective function in MPC. The tuning parameters here in this process are prediction (p) and control (m) horizons, where (p > m). The basic process framework for the MPC is given in Fig.3.6. For the implementation of MPC, an objective function is used that is represented in the equation. (3.2):

$$j = \sum_{i=1}^{p} \underbrace{\left|\left|\Gamma_h\left(h(G+l/G) - r(G+l)\right)\right|\right|^2}_{} + \sum_{I=1}^{m} \underbrace{\left|\left|\Gamma_{\Delta j}\left(\Delta j(G+l-1)\right)\right|\right|^2}_{} \qquad (3.2)$$

The first term indicates the objective of minimization of error between predicted outputs and setpoint and the second term indicates the objective to find optimal values Δ_j such that error is minimized. Where $h(G+l/G)$ is the variable of the controller at future instant $G+l$, predicted by the model at present instant G and $\Gamma_{\Delta j}$ and Γ_h refers to input and output rate weights respectively. The plant's non-linear model is linearized around an operating point and using the prediction error

method (PEM), a linear state-space model is obtained. Thus the prediction model is used in the MPC. From equation (3.3) is given as a state-space model for MPC:

$$\left\{\begin{matrix} h(k+1) = Sh(k) + Og(k) \\ b(k) = Ph(k) + Kg(k) \end{matrix}\right\} \quad (4.3)$$

Where h (k) denotes the state vector and S, O, P, K denotes the matrices of the state space.

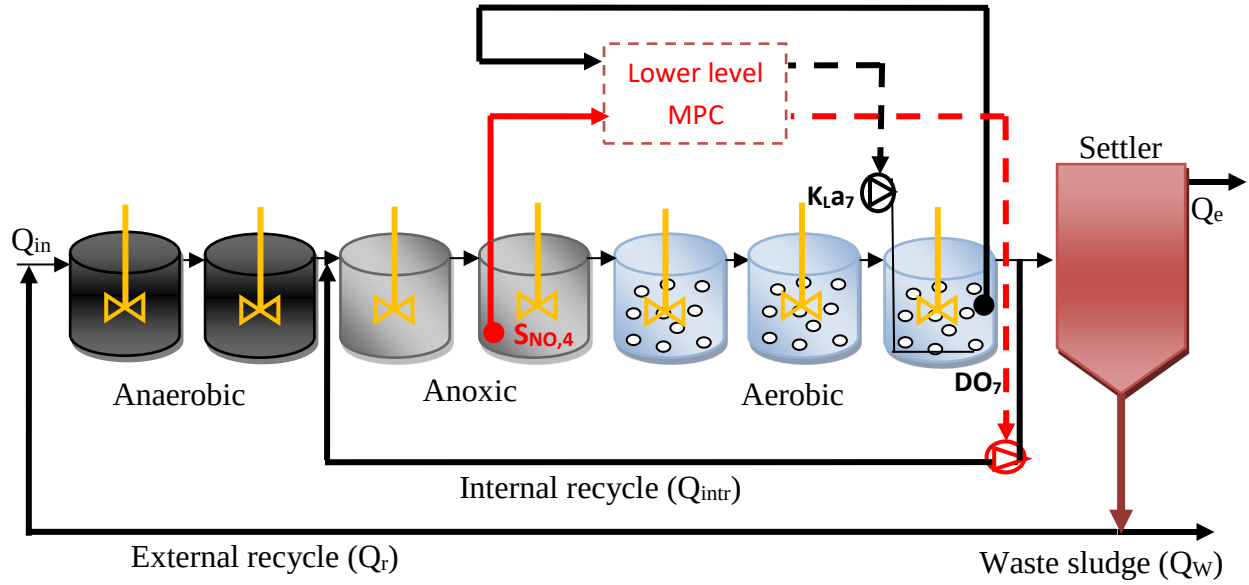

Figure 3.6 MPC implementation for the WWTP

The data of the output variables (S_{O7}, S_{NO4}) are obtained by making changes to manipulated variables (K_La_7, Q_{intr}) with a maximum variation of 10% around its operating point (252 d^{-1} for K_La_7 and 34500 m^3/d for the internal recycle flow rate). This data set is used to derive the 3rd order state-space model by the PEM method. BSM1-P with lower-level MPC Matlab/Simulink file is reported in Appendix Fig. A3.

The obtained linear state-space model is

$$A=\begin{bmatrix} 0.3926 & -0.05 & 2.38e-5 \\ 0.1014 & 0.3318 & 0.2935 \\ 0.011339 & 0.5385 & 0.536 \end{bmatrix} \quad B=\begin{bmatrix} 1.005e-05 & -0.0002057 & -7.092e-05 \\ 1.775e-06 & -0.003394 & -3.07e-17 \\ -3.381e-06 & 0.002697 & 5.606e-17 \end{bmatrix}$$

$$C=\begin{bmatrix} 3.319 & -0.552 & -0.2939 \\ 0.4232 & -2.5 & 1.602 \end{bmatrix} \quad D=\begin{bmatrix} 0 & 0 & 0 & 0 \\ 0 & 0 & 0 & 0 \end{bmatrix}$$

The selected values to tune the MPC tunning parameters are Nc = 2 and Np = 10, Δt (Sampling time) = 0.0001 days. The weights selected for DO_7 control are Γ_G= 1, $\Gamma_{\Delta j}$ = 0.01, and for S_{NO4}

control are Γ_G = 1, $\Gamma_{\Delta j}$ = 0.0001. The developed MPC is implemented and simulation studies are carried out for dry influent. The corresponding closed-loop performances are shown in Fig.3.7. For comparison, closed-loop results obtained with PI controllers (CS2 configuration) are also shown in Fig.3.7. The corresponding manipulated variables responses are also given. Results depict that MPC provides better tracking performance. Both PI and MPC provide improved performance when compared to open-loop operation.

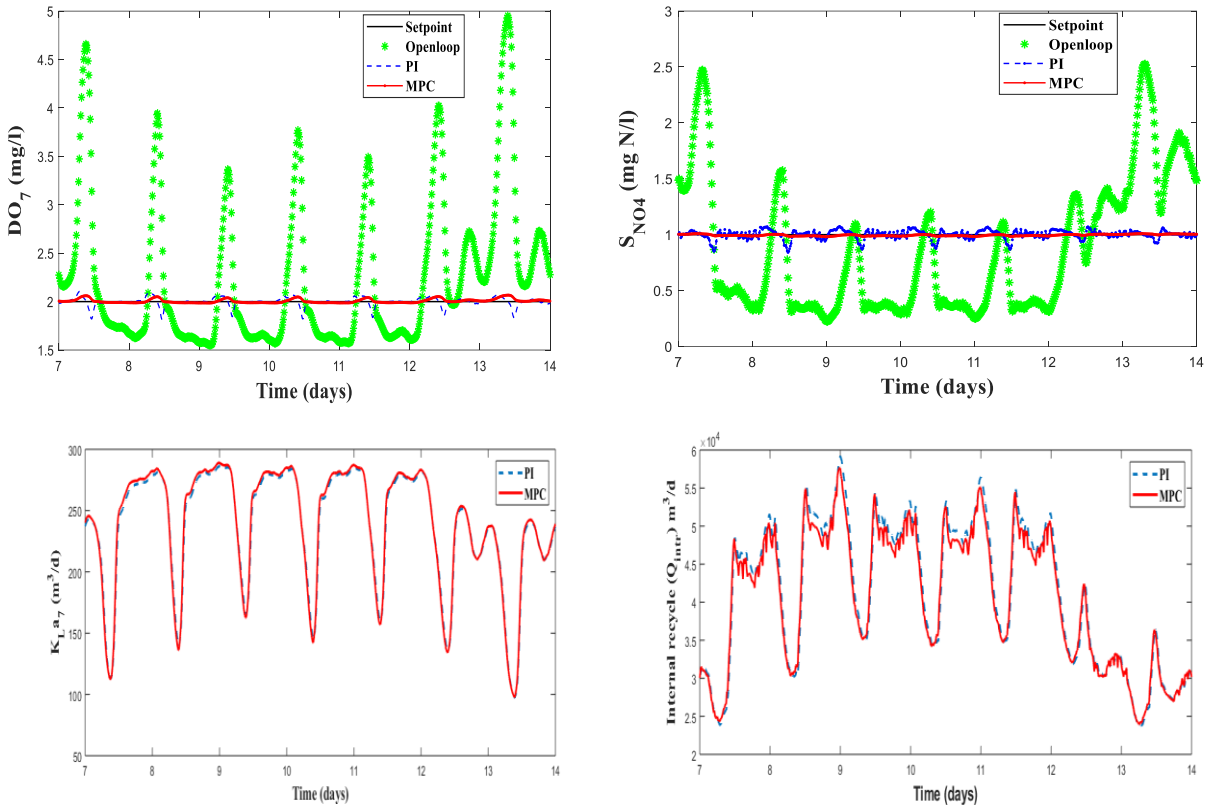

(A) (B)

Figure 3.7 Tracking of DO_7 and S_{NO4} with PI and MPC controllers for dry influent

3.1.3 Design and implementation of the fuzzy logic controller (FLC)

In all the processing stages of wastewater treatment, FLC's have been used. It was also found that in various operating conditions, the FLC's have very good performance. The direct control methods can have several failures depending on the process sensitivity, but the implementation of FLC's in wastewater treatment plays a key role in recent trends. The operation of the wastewater treatment systems can be influenced by several unpredictable factors, due to the intricate nature of wastewater treatment systems, classical techniques showed considerable difficulties when

attempting to control them automatically. Therefore, a soft computing method like FLC is practiced to be a good concept for controlling these time-varying, non-linear and ill-defined systems. It is observed from the literature that fuzzy control or law (FLC) is used to solve the most advanced control and processing units in WWTP. This is accomplished by using fuzzy rules that are identical in the design of human inference. In FLC based on IF-THEN statement rules for control signals. In FLC, using fuzzy rules is required which are identical in the design of human inference. Mamdani technique is chosen for the FI function and the centroid technique is chosen for the defuzzification method. A short description of FI and centroid is elucidated below. AS reported for the fuzzy laws: (I) if x, y is A1 and A2 then L1 is z, (II) if x, y is A2 and A2 then L2 is z and the indication of k1 is x, m1 is y, while k1 and m1 are rigid inputs. Fig.4.10 depicts the evaluation of the grey region. In the approach of fuzzy law, the group was exemplifying between a FE and an FS. A class of membership is proposed if equal to 1 signifies the elemental x related to FS and it is equal to 0 implies that x doesn't relate to the FS. In Fig.3.8, it was observed that the k1 slightly own to A1 and A2, and the category membership is defined and independently. The MS of m1 to FS, B1, and B2 were notified and accordingly. This is the way of crisp inputs to fuzzy inputs conversion which is termed fuzzification. Further, the resultant outcomes of MF are reached by rule (I). It is estimated by the equation. (3.4).

$$\theta_i(c) = min\{\theta(m1|A1),\theta(m1|A1)\} \tag{3.4}$$

This MF elucidates the importance of selecting the FS (L1). The resultant outcomes for MF were achieved by rule (II) for the present situation (k1 is x is and m1 is y) is regarded to rules(I) and (II) accordingly. Therefore, the resultant decision was combined with the MF's, as depicted in Fig.3.8. By evaluating the gray region with centroid, the fuzzy and the defuzzify output are necessary. The defuzzified output (C1) represented in Fig.3.8 is computed by equation. (3.5):

$$C1 = \frac{\sum_i u_i \int \theta(i)}{\sum_i \int \theta(i)} \tag{3.5}$$

Here u_i represents the center of the MF, the outcome of rule(I), and shoes the region under the membership operation. Where refers to the centroid technique to estimate C1. The second loop and third loop are similar to CS(I). For classic FLC, the control model is the way of the human knowledge base. FLC consists of three sections. In the primary section, MF's are fuzzified with input values to get Fuzzification. After, by using predetermined rules, fuzzy inputs and outputs are

connected then the outputs are determined by using the inference mechanism. The third section is to initiate strict output values in a computed way and is called defuzzification.

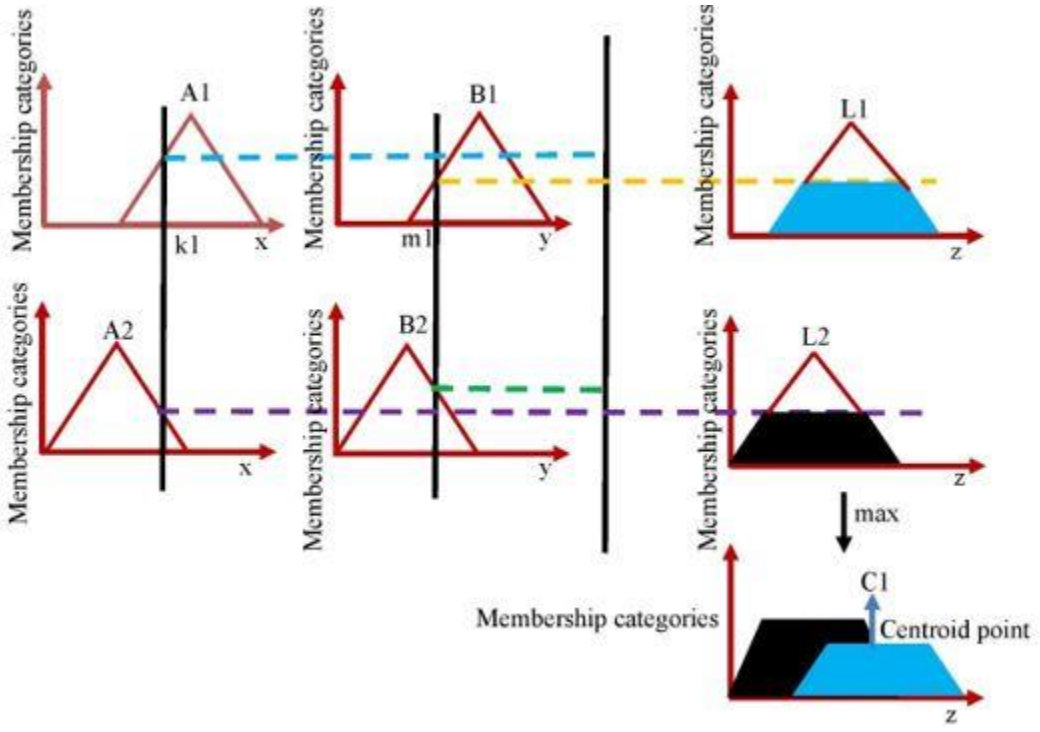

Figure 3.8 Mamdani fuzzy inference

The membership functions of DO for output and input functions are depicted in Fig.3.9. The membership functions of input and output data of DO are depicted in Fig. 3.9 (A), (B), and (C). FLC with applications of BSM1-P with three mechanisms blocks is depicted in Fig.3.10. Here in the FLC, the input variables are considered as the feedback error 'E' and high-order error 'ED'. Consequently, the output variables are considered as manipulating variables in the control configuration. Hence, for FLC for the design of the DO loop the input variable is selected as the mass transfer coefficient (K_La), and for the design of the S_{NO} loop; the input variable is selected as the internal recycle (Q_{intr}). On coupling, both these outputs and input, the membership function (MF) has to be selected. In this study, Mamdani fuzzy interface method is chosen and MF's are selected as a triangular shape functioning. Based on the simulation data, the usage of a rules-based system is obtained before developing the FLC framework. In the last aeration tank, the 'E' input variable scale is maintained from -30 to 30 g/m^3 and the 'ED' input variable scale is maintained from -25 to 25 g/m^3. The output variable scale of K_La in the last reactor is 200 to 280 d^{-1}. Further, in the second anoxic tank, the input variable scale of 'E' is maintained from -30 to 30 g/m^3 and 'ED' of the input variable scale is maintained from -25 to 25 g/m^3.

Table 3.4 Selection of DO rules for FLC

	NL	NI	NS	Z	PS	PI	PL
NL	PL	PL	PL	PL	PI	Z	Z
NI	PL	PL	PL	PL	PI	Z	Z
NS	PI	PI	PI	PI	Z	NS	NS
Z	PI	PI	PS	Z	NS	NI	NI
PS	PS	PS	Z	NI	NI	NI	NI
PI	Z	Z	NI	NL	NL	NL	NL
PL	Z	Z	NI	NL	NL	NL	NL

Table 3.5 Selection of nitrate (S_{NO}) rules

	NL	NS	Z	PS	PL
NL	PL	PL	PL	PS	Z
NS	PS	PS	PS	Z	NS
Z	PS	PS	Z	NS	NS
PS	PS	Z	NS	NS	NS
PL	NS	NL	NL	NL	NL

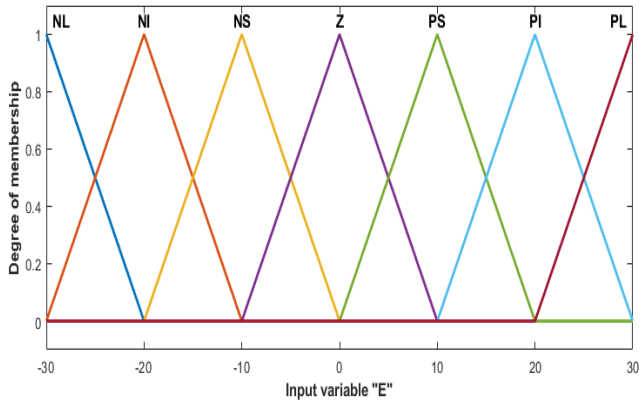

(A) MF of error of tank 7 for DO

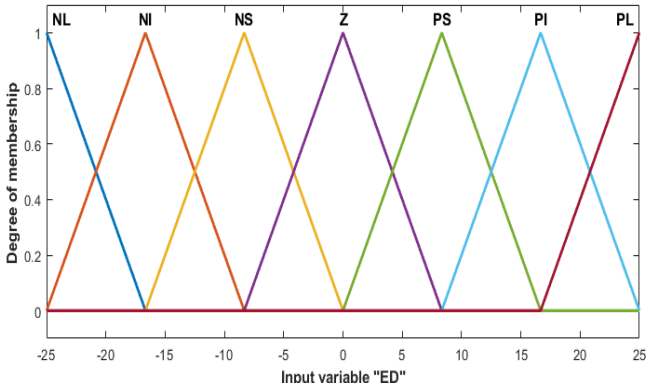

(B) MF of differentiation of error of tank 7 for DO

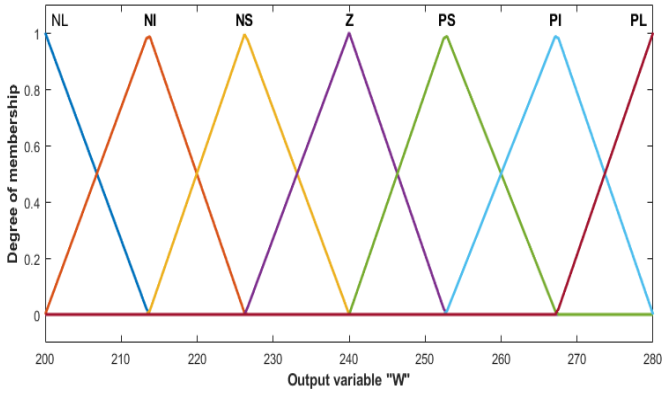

(C) MF of K_La7 in tnak7

Figure 3.9 MF's of input and output data of DO in tank7 by using K_La_7

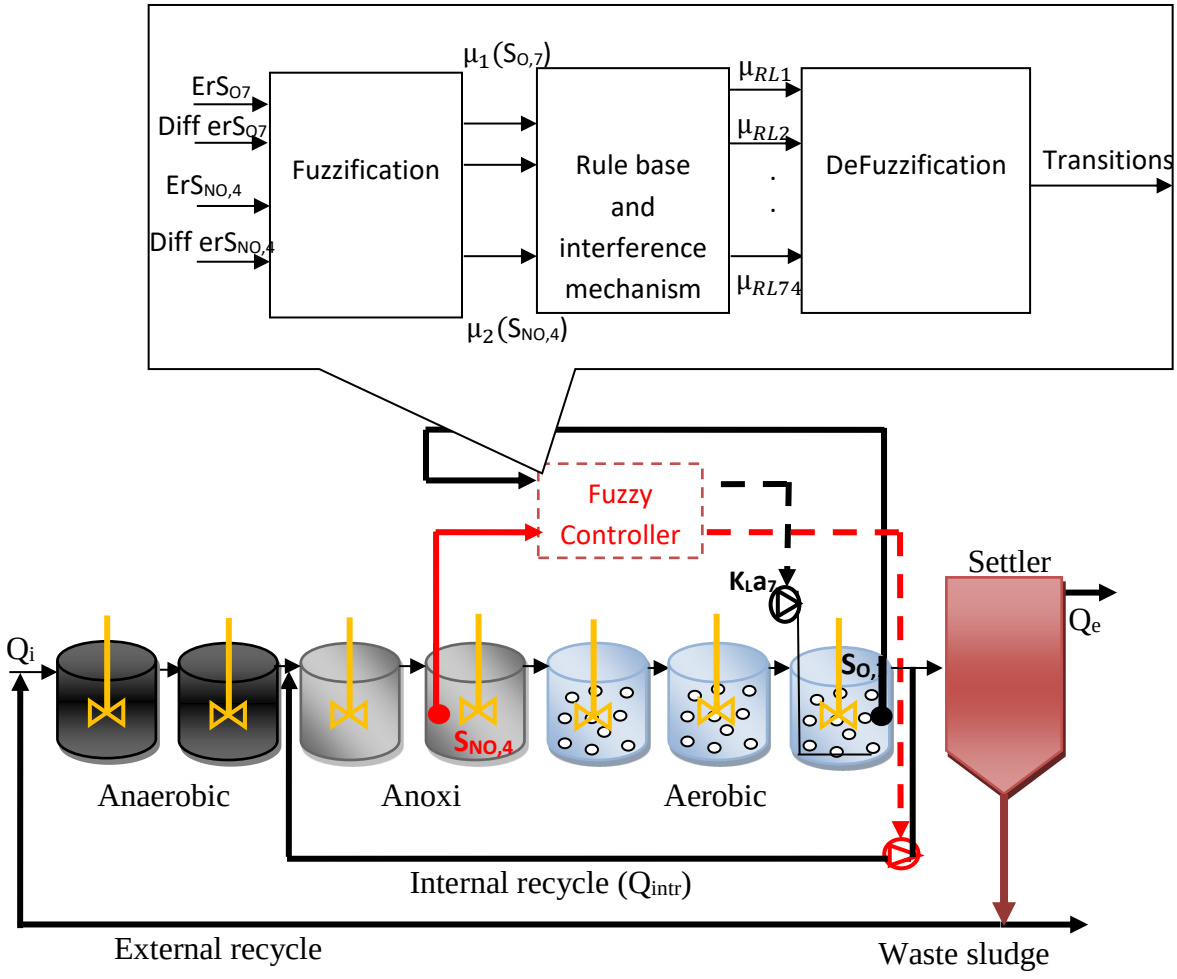

Figure 3.10 Fuzzy logic control of BSM1-P platform

The scale of the output variable of Q_{intr} is 20100 to 45000 d^{-1}. A total of seven MF are chosen for each individual and NL, NI, NS, Z, PS, PI, and PL where N, Z, P, L, I, and S are negative, zero, positive, big, medium, and small. Similarly, MF's of NO is also selected. The coupling of DO and S_{NO} fuzzy logic consists of 74 rules are implemented by the usage of IF-THEN statement conditions. The Fuzzy rules of both DO and S_{NO} are elucidated in Tables 3.4 and 3.5. BSM1-P with lower-level fuzzy logic controller (FLC) Matlab/Simulink file is reported in Appendix Fig. A4.

3.2 Simulation results and comparison

The comparative results using PI, MPC, and Fuzzy control strategies are discussed in this section. However, the major interest in this paper is focused to understand the effluent concentrations TP, TN, and S_{NH}. The comparative results of these three effluent concentrations are plotted and are shown in Fig.3.11 to 3.13. Major intrigue is not shown to compare the results of COD, BOD_5, and TSS using different control strategies as the results obtained are quite similar and are within the limits as given in Table 3.6. The applied control strategies improved plant performance. Fig.3.11 to 3.13 show that amongst all the control strategies implemented, the results obtained using MPC are much favorable for both ammonia and nitrogen removal. MPC gives efficient removal of N and ammonia when compared to PI and FLC. Note that all comparisons are carried out based on the average concentrations of individual effluent components. Accordingly, effluent quality and global plant performance which includes energy estimations and overall cost are determined. FLC, when compared to open-loop, provides better performance. Whereas in MPC, both OCI and EQI are decreased compared to open-loop which means better control is achieved. The implementation of fuzzy logic controllers is more advantageous for the P removal. MPC provided good improvement in OCI but the improvement is not significant for EQI when compared with fuzzy control and PI control.

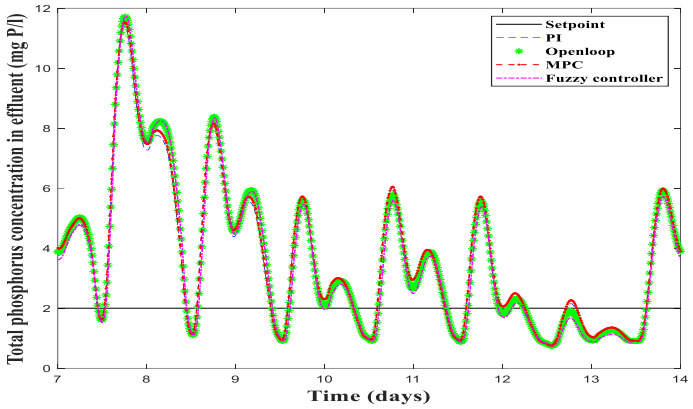

Figure 3.11 TP concentration with open-loop, PI, MPC, and fuzzy controllers

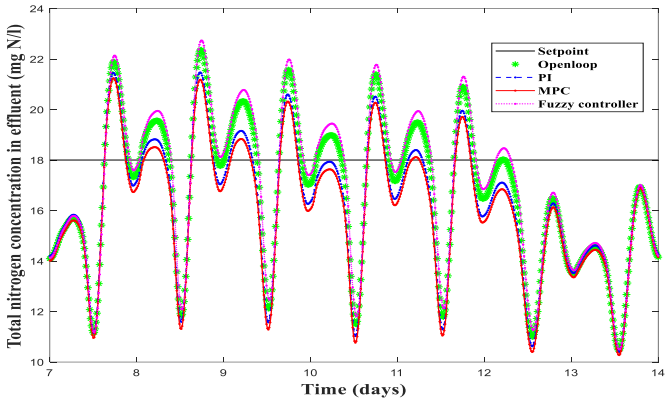

Figure 3.12 TN concentration with open loop, PI, MPC, and fuzzy controllers

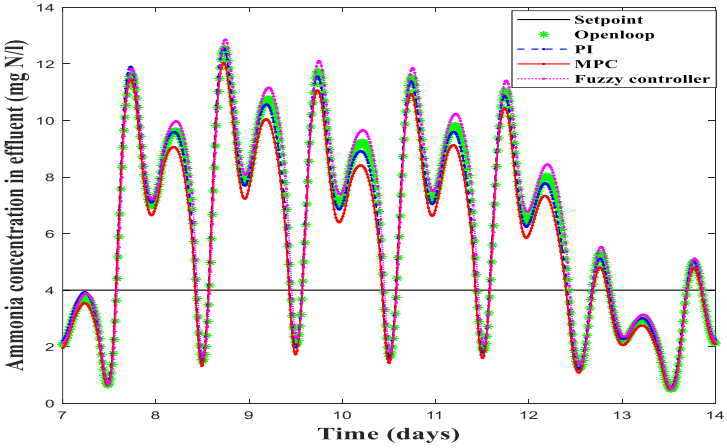

Figure 3.13 S_{NH} concentration with open loop, PI, MPC, and fuzzy controllers

Table 3.6 Average effluent concentrations of PI, MPC, and fuzzy

Average effluent concentrations				
Components	Open-loop	PI	Fuzzy	MPC
S_{NH}	6.0845	6.0535	6.3318	5.6954
TSS	13.681	13.6701	13.73	13.685
TN	16.5053	16.0053	16.7901	15.764
TP	3.588	3.5498	3.4921	3.6465
COD	44.7533	44.7371	44.7845	44.7893
BOD	1.782	1.7852	1.7975	1.789
IQI	72152.229	72152.229	72152.229	72152.229
EQI	13411.043	13239.202	13381.956	13243.485
Performance plant assessment				
SP	2973.4521	2969.9099	2989.8759	2956.6811
AE	4336.6933	4254.6108	4264.4945	4262.6957
PE	304.818	331.4486	295.1637	329.3818
ME	480	480	480	480
OCI	18753.284	18681.109	18739.131	18619.642

3.3 Summary

Different control frameworks from CLS1 to CLS8 in the BSM1-P plant layout under the ASM3bioP framework are implemented. In comparison, it is observed that the effluent pollutant considerations for CLS1 and CLS2 are better than CLS3–CLS8. In the former case, the operational cost index of CLS2 is far better than CLS1. Further, the obtained EQI and OCI values using the PI controllers are also applied to rain and storm data are compared with that of open-loop data. Additionally, in this study, PI, fuzzy, and MPC controls are implemented and the performances are compared to monitor DO and S_{NO} tracking. The simulation outcomes signify that three of them can attain good performance and of three control strategies. MPC provided better OCI and EQII results. For the removal of phosphorus, the application of a fuzzy controller showed better results than PI and MPC but with high OCI. PI, MPC, and fuzzy controllers are compared with the open-

loop. The Percentage of improvement on EQI for PI - 1.8%, MPC - 1.3%, and Fuzzy - 0.3% and the Percentage of reduced OCI are PI - 0.3, MPC - 0.7%, and Fuzzy - 0.07.

Chapter 4

Design of Supervisory-level control strategies on BSM1-P

Chapter 4

Design of supervisory-level control strategies on BSM1-P

4.1 Combination of both lower level and higher-level control strategies on BSM1-P

The importance of hierarchical level control is discussed in this section. The controllers in the lower level control section were tasked with maintaining the dissolved oxygen set-point. The higher-level controller's job is to manipulate the DO controller's set-points based on the ammonia concentration in the tank. Various processes in ASM3bioP result in the biological treatment of S_{NH} and S_{NO}. Here, the default control (PI) strategy is considered a lower-level control. This consists of two PI controllers as given in Fig.3.4, in which DO_7 is controlled by manipulating K_La_7 in the seventh reactor. The desired set-point value for DO_7 is 2 mg/l. The other control loop is responsible for maintaining S_{NO4} at 1 mgN/l by regulating Q_{inr}. The main contribution of the present work is the development of a two-level hierarchical strategy with a supervisory layer as shown in Fig. 4.1. The task in the higher-level control is to determine DO_7 values (setpoints for the lower level) by controlling S_{NH7} in the seventh reactor. These DO_7 values are sent as set points to the lower DO_7 loop. Thus, the higher-level control loop helps to find the setpoints to the lower loop. As far as the lower-level controller is considered, S_{NO4} and DO_7 are controlled by manipulating Q_{intr} and K_La_7. If S_{NH7} is more, higher DO is essential for better nitrification. Nitrification oxidizes ammonium to nitrate and denitrification reduces nitrate to nitrogen gas. In the aeration tank, if DO is too high, ammonia will decrease but nitrate will increase. On the other hand, if the DO is too low, ammonia will increase and the nitrate available for denitrification will decrease. Moreover, the level of aeration will impact energy usage.

Thus, the DO setpoint must be properly selected. At a lower level, default two PI and MPC controllers are used and at a higher level, MPC and fuzzy controllers are designed. The default DO set-point of 2 can be modified according to the needs of the WWTP. It can be lower if the ammonium load is lower and higher if the ammonium load is higher. Moreover, it should be always maintained at the lowest value that is useful to maintain the concentration below the discharge limits, to have the lowest operational costs. Table 4.1 represents the control approach for chapter 4. The identification of the state-space model for higher-level is reported in Appendix B.

Table 4.1 Designed control approaches

Label	L1 (Default PI)	L2 (Lower level MPC)	L3 (Default PI+ Higher level MPC)	L4 (Lower level MPC+ Higher level MPC)	L5 (Default PI+ Higher level MPC)	L6 (Lower level MPC+ Higher level MPC)
Characteristics	S_{NO} and DO controller	S_{NO} and DO controller	$S_{NO,}$ DO, and S_{NH} controller	$S_{NO,}$ DO, and S_{NH} controller	$S_{NO,}$ DO, and S_{NH} controller	$S_{NO,}$ DO, and S_{NH} controller
Measured Variable	S_{NO} in tank4 and S_O in tank7	S_{NO} in tank4 and S_O in tank7	S_{NO} in tank4 DO and S_{NH} in tank7	S_{NO} in tank4 DO and S_{NH} in tank7	S_{NO} in tank4 DO and S_{NH} in tank7	S_{NO} in tank4 DO and S_{NH} in tank7
Set-point/Value	1 gN/m^3 and 2 g O_2/m^3	1 gN/m^3 and 2 g O_2/m^3	1 gN/m^3, DO set-point is determined by higher level	1 gN/m^3, DO set-point is determined by higher level	1 gN/m^3, DO set-point is determined by higher level	1 gN/m^3, DO set-point is determined by higher level
Manipulated Variable	Internal recycle (Q_{intr}) and mass transfer coefficient (K_La_7)	Q_{intr} and K_La_7	Q_{intr} , K_La_7 and Set-point for DO controller	Q_{intr} , K_La_7 and Set-point for DO controller	Q_{intr} , K_La_7 and Set-point for DO controller	Q_{intr} , K_La_7 and Set-point for DO controller
Control Classification	PI	MPC	PI and MPC	MPC and MPC	PI and Fuzzy	MPC and Fuzzy

4.1.1 Lower level PI and higher-level MPC control scheme

Open-loop data is generated for both DO and S_{NO} loops and accordingly control relevant models are developed. The corresponding control layout is shown in Fig.4.4. The mass transfer coefficient (K_La_7) is a manipulating variable for the DO control. For a value of 252 d^{-1} the DO concentration in the seventh reactor is observed as 2 gO_2/m^3. A random input signal is given in K_La by considering a variation of ±10% in the nominal value of 252 d^{-1} and the corresponding output data (DO) is collected in the seventh reactor. The internal recycle (Q_{intr}) is a manipulating variable for S_{NO} control. For a value of 34500 m^3/d, the S_{NO} concentration in the fourth reactor is observed as 1 gN/m^3. A similar kind of approach is also carried out to monitor the value of S_{NO} by providing a random signal to Q_{intr} with a variation of 10%. Matlab/Simulink file for Higher Level Identification is depicted in Appendix Fig. B1. Now the output data of S_{NO} and DO is used to develop FOPTD models using the prediction error minimization method. From these models, by using the Skogested internal model control method (SIMC) by Grimholt and Skogestad (2018), each loop is designed with PI controllers. PI-MPC Control Configuration in BSM1-P in Fig.4.1. In order to develop the linear model for a higher level, S_{NH7} has been identified by varying DO_7, with a variation of ±10% whose steady-state value is 3 gN/m^3 in the seventh reactor. The corresponding ammonia data is collected whose steady-state value is 3.45 gN/m^3 in the last reactor. Therefore, the data set is used to drive the third-order state-space model using the PEM technique. For MPC, in higher-level m=2 and p=10, Δt is 0.0001 days are selected. The following weights have been used for DO_7 by manipulating ammonia in reactor seven. Γ_G= 1, $\Gamma_{\Delta j}$= 0.01. A third-order state-space model is achieved by manipulating DO to monitor ammonia with the prediction error method:

$$A=\begin{bmatrix} 0.8594 & -0.2136 & 0.1737 \\ -0.1037 & 0.7195 & -0.0285 \\ -0.05527 & -0.2764 & 0.36416 \end{bmatrix} \quad B=\begin{bmatrix} -0.03123 \\ -0.1148 \\ -0.2162 \end{bmatrix}$$

$$C=[2.249 \quad -0.1324 \quad 0.1145] \quad D=[0]$$

Simulation studies are carried out with the corresponding controllers. Fig.4.2 (a) depicts the variable DO set-point assigned by a higher-level and its tracking by the lower-level controller for the data. Fig.4.2(b) depicts the set-point tracking with default PI (DO_7 and S_{NO4}) controllers. If ammonia is high, then it needs high DO for better nitrification. If ammonia is low, it requires less DO which results in less S_{NO}. The DO consumption in the seventh tank impacts the S_{NO} level in the fourth tank as depicted in Fig.4.2 (b). In comparison, the performance of MPC-based control

is not superior to that of the default PI controller for set-point tracking of S_{NO}. Similar results are obtained for all the remaining cases as well while tracking the set-point of S_{NO}. PI-MPC configuration on BSM1-P of Matlab/Simulink file is depicted in Appendix Fig.B2.

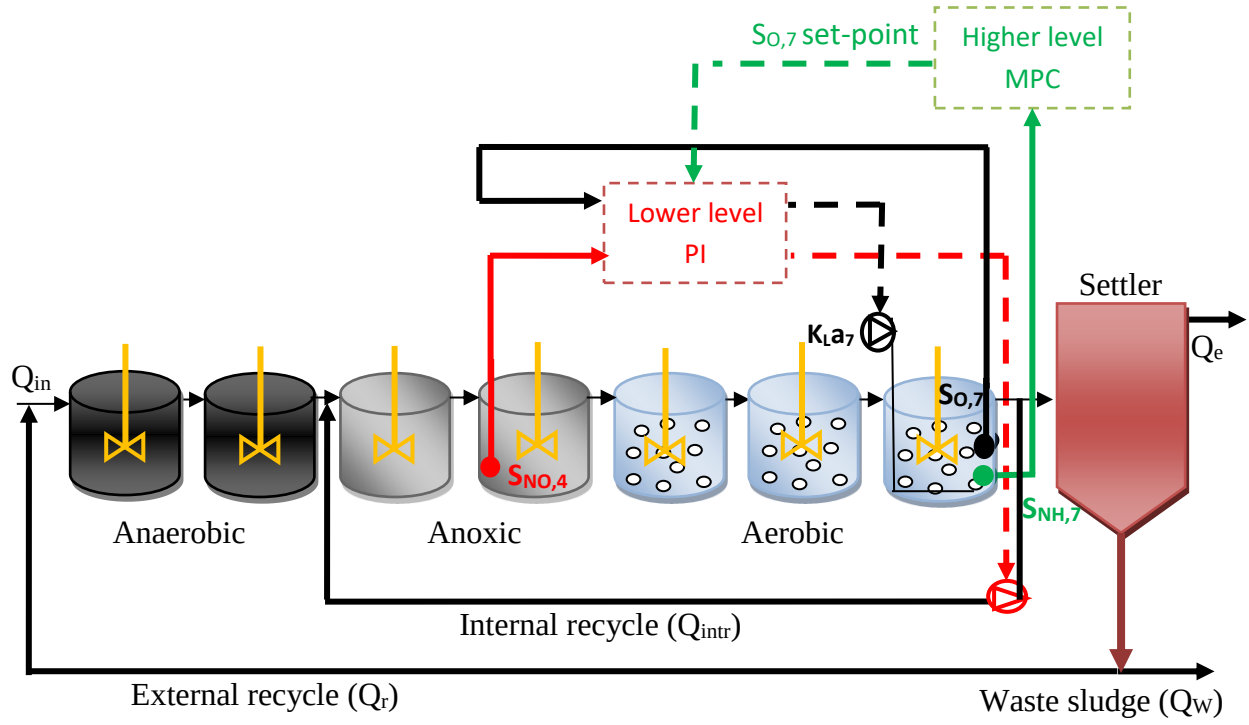

Figure 4.1 PI-MPC control configuration in BSM1-P

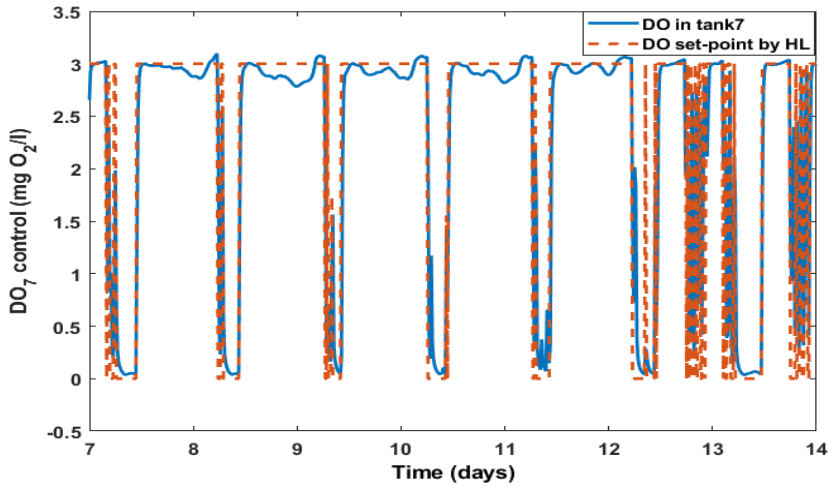

(A)

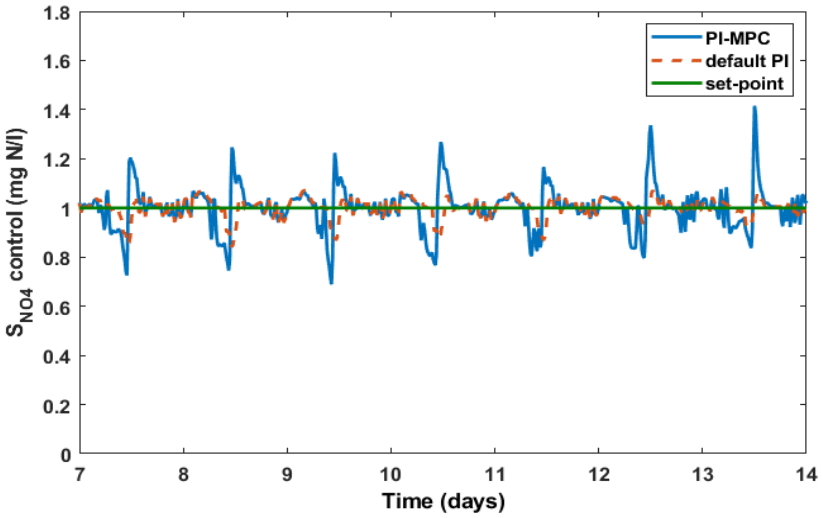

(B)

Figure 4.2 (A) DO tracking in the seventh reactor (B) Nitrate tracking in the fourth reactor

4.1.2 Lower level MPC and higher level MPC control scheme

Here, MPC was developed for a lower level as well as for a higher-level loop. For the lower level, system identification is carried out for obtaining the data of DO_7 and S_{NO4} by manipulating K_La_7 and Q_{intr} by considering a variation of 10% in the operating point which $252d^{-1}$ for K_La_7 and 34500m^3/d for the internal recycle flow rate with maintaining the steady-state of DO_7 is 2 gO_2/m^3 in the last reactor and S_{NO4} is 1 gN/m^3 in the fourth reactor. The corresponding control layout is shown in Fig.4.3. MPC-MPC Control Configuration in BSM1-P in Fig.4.3. In the higher level, S_{NH7} was observed by varying DO_7. The corresponding ammonia data is recorded. The tuning parameters for MPC for the lower-level model are m=2 and p=10 and Δt is 0.0001 days. For DO_7 control, Γ_G=1 and $\Gamma_{\Delta j}$= 0.01 are considered and for S_{NO} control, Γ_G = 1 and $\Gamma_{\Delta j}$= 0.0001 are used. The tuning parameters for MPC for the higher-level model are m=2 and p=10. Δt is 0.0001 days. In the higher level, for DO_7 loop Γ_G=1 and $\Gamma_{\Delta j}$=0.01 are selected. The identified state-space model is given below for both the lower-level and higher-level loops.

MPC lower-level state-space model :

$$A=\begin{bmatrix} 0.3926 & -0.05 & 2.38e-5 \\ 0.1014 & 0.3318 & 0.2935 \\ 0.011339 & 0.5385 & 0.536 \end{bmatrix} \quad B=\begin{bmatrix} 1.005e-05 & -0.0002057 & -7.092e-05 \\ 1.775e-06 & -0.003394 & -3.07e-17 \\ -3.381e-06 & 0.002697 & 5.606e-17 \end{bmatrix}$$

$$C=\begin{bmatrix} 3.319 & -0.552 & -0.2939 \\ 0.4232 & -2.5 & 1.602 \end{bmatrix} \quad D=\begin{bmatrix} 0 & 0 & 0 & 0 \\ 0 & 0 & 0 & 0 \end{bmatrix}$$

MPC higher-level state-space model :

$$A=\begin{bmatrix} 0.9119 & 0.1414 & 0.01841 \\ 0.1625 & 0.7227 & 0.0923 \\ 0.05881 & -0.1619 & 0.9543 \end{bmatrix} \quad B=\begin{bmatrix} -0.05254 \\ 0.08427 \\ 0.05361 \end{bmatrix}$$

$$C=[1.728 \quad -0.01105 \quad 0.0073] \qquad D=[0]$$

Fig.4.4 (a) depicts the computation of DO set-point by a higher-level controller and its tracking by the lower-level controller for dry seasonal conditions. It is also noticed that average values for all the effluent variables are almost under the limit except for ammonia and phosphorus as shown in Table 3. Fig.4.4 (b) depicts the set-point tracking of S_{NO} in the fourth reactor and DO with default PI controllers. MPC-MPC configuration on BSM1-P of Matlab/Simulink file is depicted in Appendix Fig.B3.

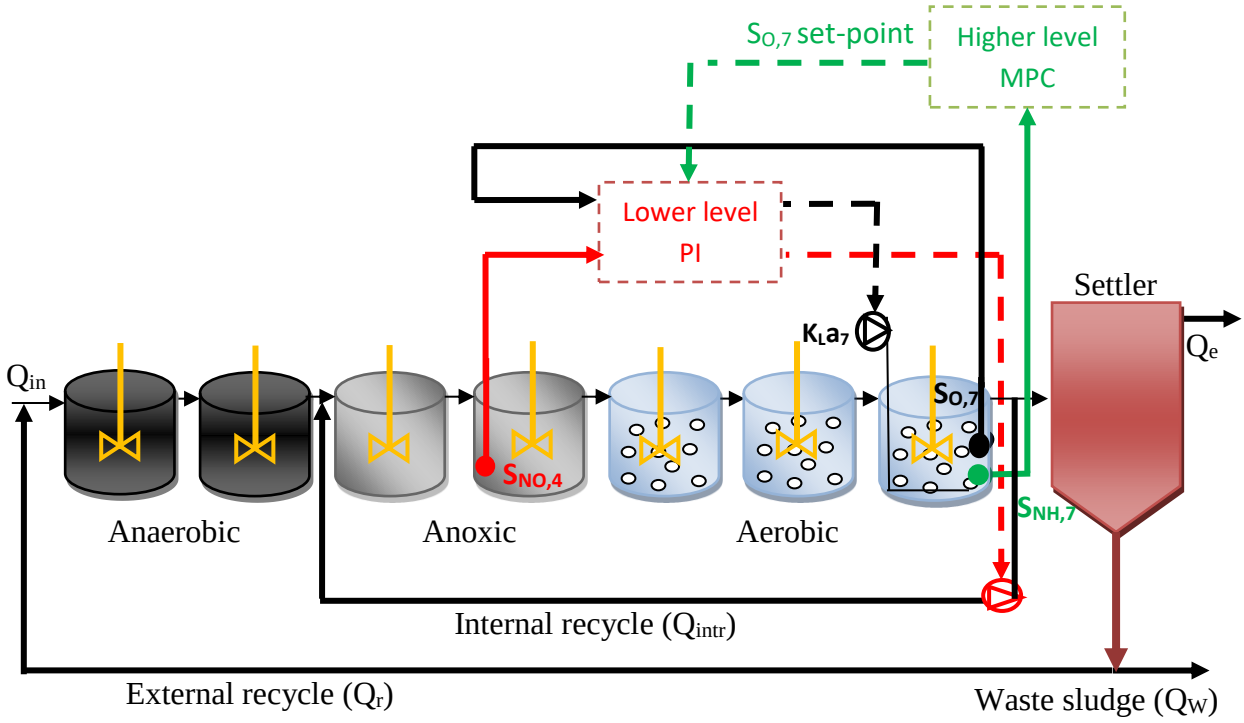

Figure 4.3 MPC-MPC control configuration in BSM1-P

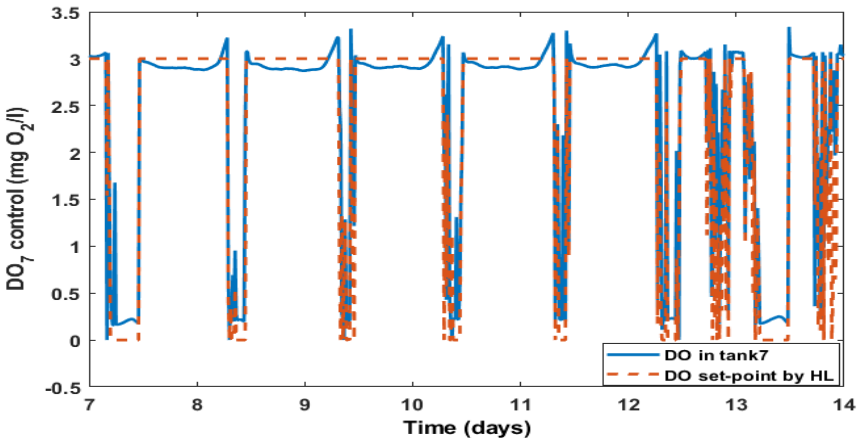

(A)

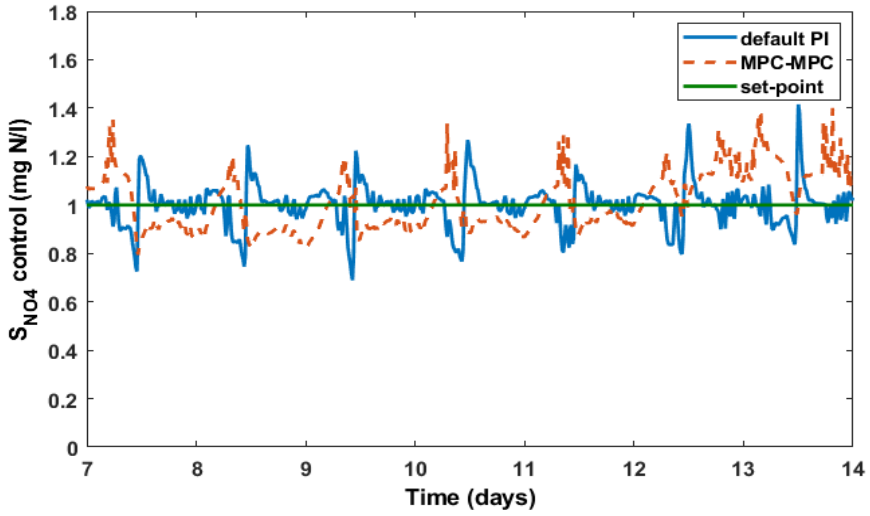

(B)

Figure 4.4 (A) DO tracking in the seventh reactor (B) Nitrate tracking in the fourth reactor

4.1.3 Lower level PI and higher level fuzzy control scheme

Lower Level (default PI) is similar to control scheme 1. In the fuzzy logic controller at a hierarchical level, the DO set-point is manipulated in the seventh reactor to reduce the effluent violations in ammonia in reactor 7. The deciding rules for higher level fuzzy controller logic is reported in the Appendix B. The selected range studied for the membership functions (MF) of DO and ammonia in reactor 7 is 0-5 mgO_2/l, and 0-20 mgN/l respectively. Gaussian-shaped-bell curve is selected as an MF for two variables and they are partitioned in three linguistic rules individually, "low, "medium" and "high". For controlling the DO loop, the three rules are described below:

- ❖ IF Ammonia level is “low” then DO set-point is “low”
- ❖ IF Ammonia level is “medium” then DO set-point is “medium”
- ❖ IF Ammonia level is “high” then DO set-point is “high”

On a combination of these rules, a lower and higher-level control framework is made. The MF for output and input for the PI-Fuzzy depicts in Figs.4.5 (A) and 4.5 (B). In this case, for the lower level, a default PI approach is used and FLC configurations are designed at a higher level. For proper oxidation of ammonia to nitrate (nitrification) in the seventh reactor, sufficient care needs to be taken to maintain the dissolved oxygen concentration in such a way that it should not be decreased before achieving proper nitrification. BSM1-P with PI-Fuzzy Configuration of Matlab/Simulink file is depicted in Appendix Fig.B4.

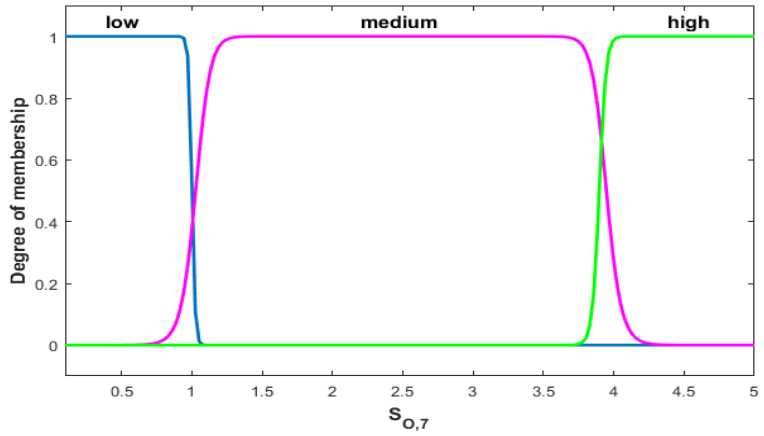

(A)

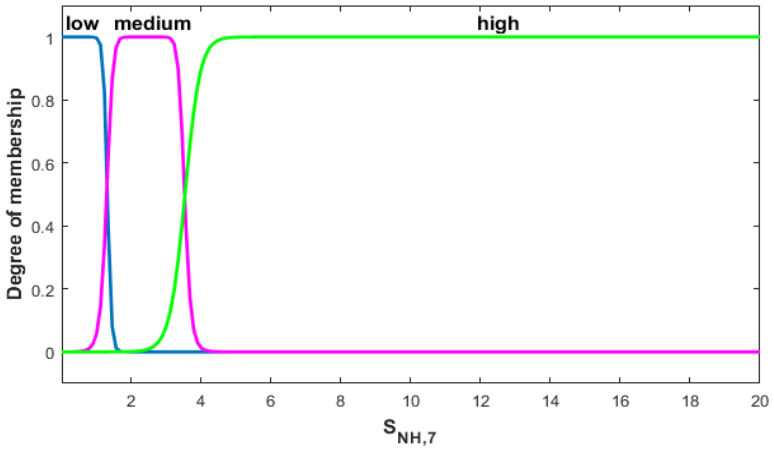

(B)

Figure 4.5 (A) MF of output for DO concentration (PI-Fuzzy) (B) MF of input for ammonia concentration (PI-Fuzzy).

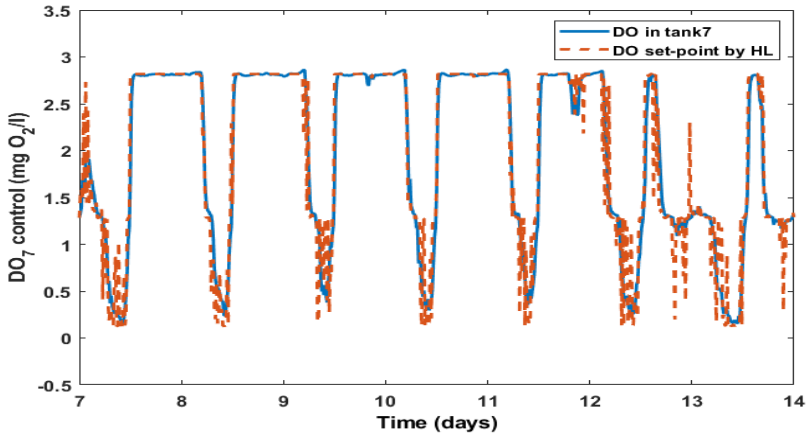

(A)

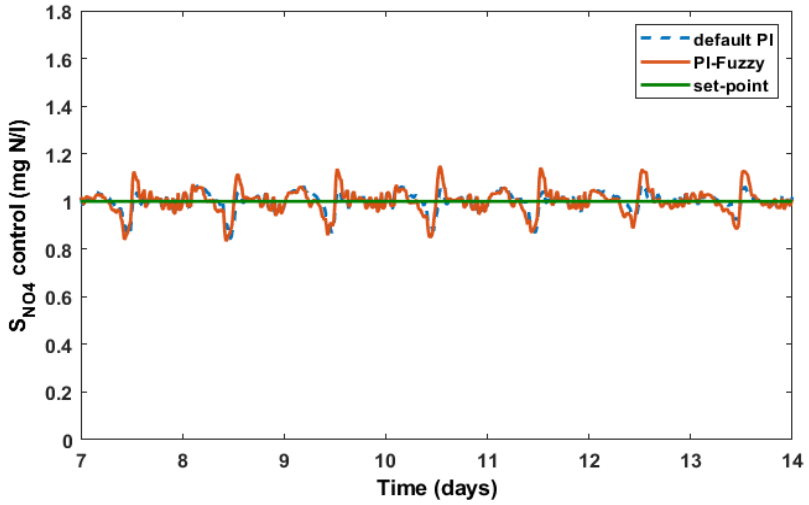

(B)

Figure 4.6 (A) DO tracking in the seventh reactor (B) Nitrate tracking in the fourth reactor

Based on this requirement, membership functions of the two process variables are developed in fuzzy logic control. The oxygen concentrations in the range of 1–4 mgO_2/l are considered normal and thus acquire a complete degree of belongingness to the fuzzy set as the medium. Above 4 mgO_2/l concentration, high values are considered in the fuzzy set which is a straight line at 1 as shown in Fig.4.5(A). The values of ammonia concentration in the range of 0-1 mgN/l are considered as low and in the range of 2-4 mgN/l are considered as the medium. Accordingly, the fuzzy sets are defined and shown in Fig.4.5 (A and B). This kind of approach clearly signifies the degree of belongingness of a variable to the fuzzy set. The principal goal of executing this strategy is to alter the DO set-point in tank7 based on ammonia concentration. While the HL control (fuzzy)

is tested for the DO loop only. The set-point of the S_{NO} loop remains constant by HL. But both DO and S_{NO} loops are associated because of interaction effects between them. Fig.4.6(A), DO tracking in the seventh reactor (B) Nitrate tracking in the fourth reactor are depicted. MPC-MPC Control.

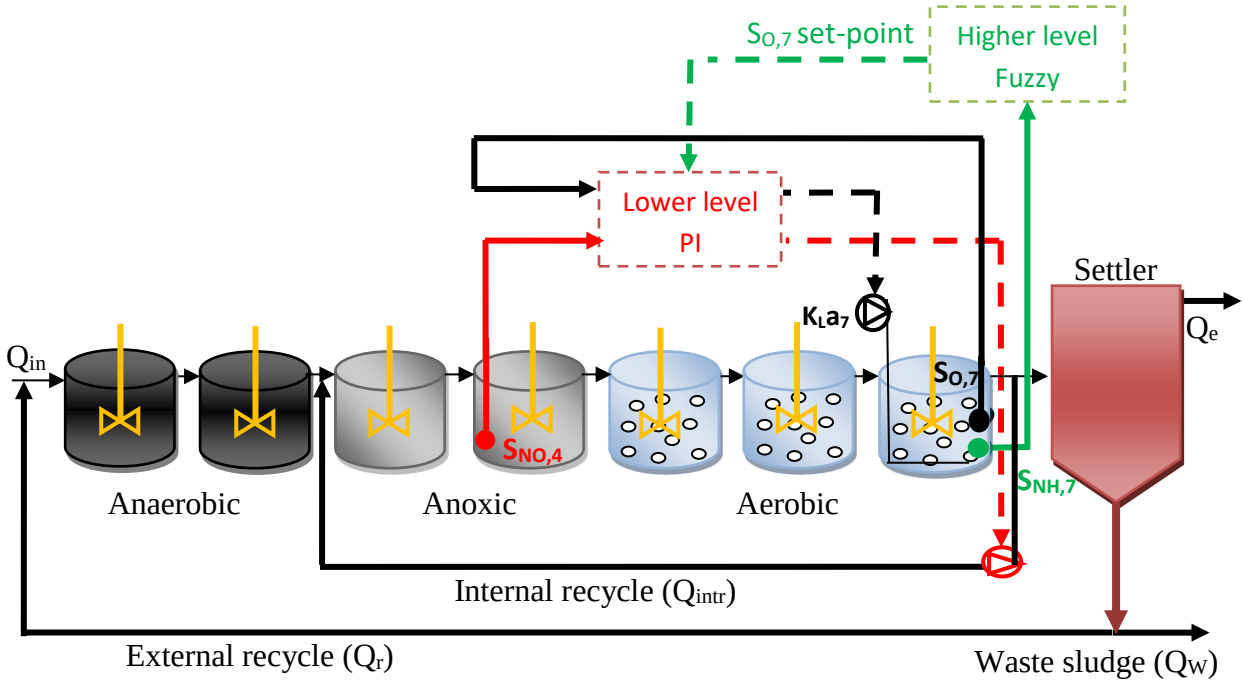

Figure 4.7 PI-Fuzzy control configuration in BSM1-P

4.1.4 Lower Level MPC and Higher Level Fuzzy Control Scheme

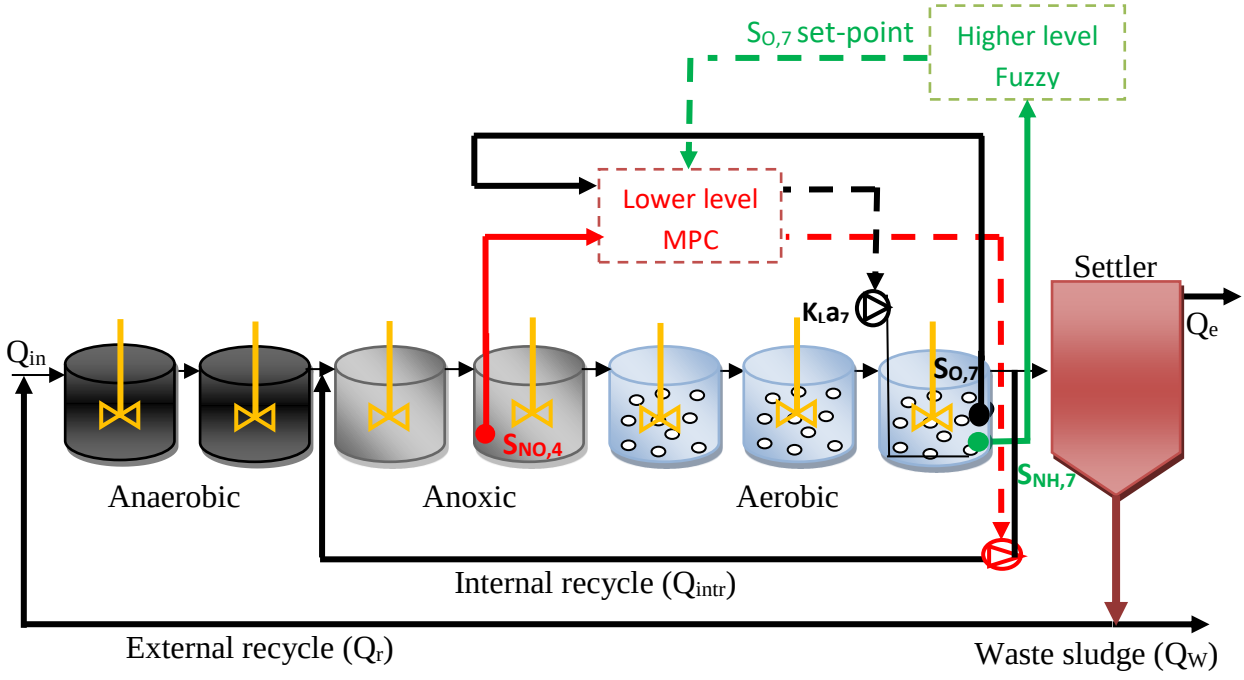

Figure 4.7 MPC-Fuzzy control configuration in BSM1-P

Lower level MPC is similar to control scheme 2 and hierarchical Fuzzy is similar to control scheme 3. MPC-Fuzzy Control Configuration in BSM1-P is depicted in Fig.4.8. Fig.4.9 (A) depicts the DO_7 set-point tracking response and Fig.4.9 (B) depicts the nitrate tracking for this configuration in comparison with default PI for dry weather. The results depict there is an improvement in tracking response even in the presence of disturbances. BSM1-P with MPC-Fuzzy Configuration of Matlab/Simulink file is depicted in Appendix Fig.B5.

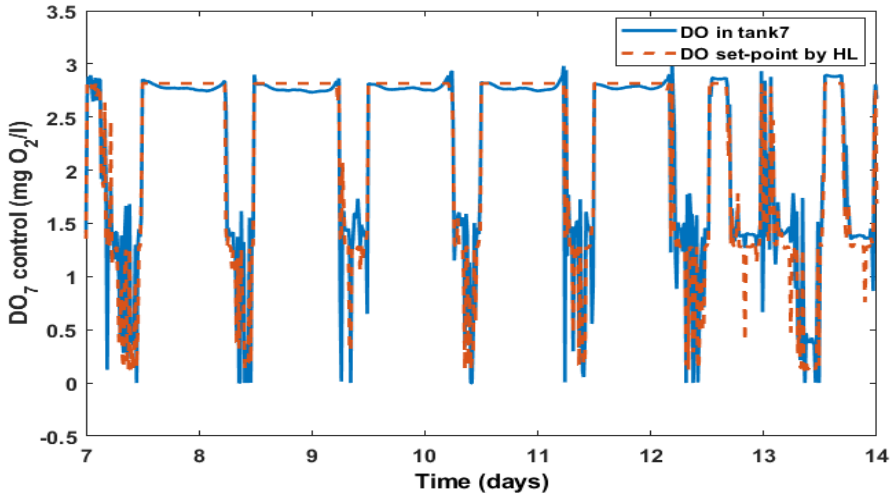

(A)

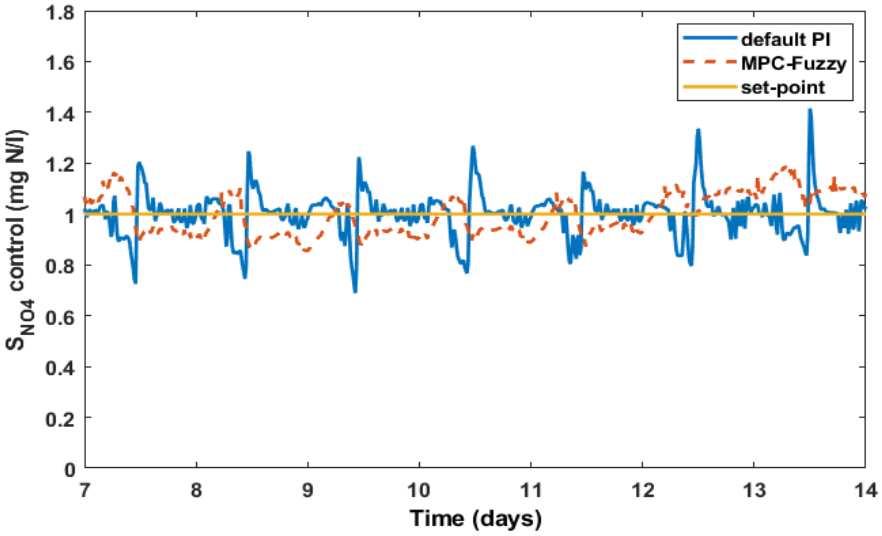

(B)

Figure 4.8 (A) DO tracking in the seventh reactor (B) Nitrate tracking in the fourth reactor

4.2 Simulation Results and Comparision

The corresponding average concentrations of the effluent with all hierarchical control approaches and performance indices for dry influent are given in Table 4.2. It was observed that the value of EQI is improved by 5.7% on comparing the default strategy in the case of dry weather conditions. It can be observed that there is a trade-off between OCI and EQI for all the control strategies chosen. Whereas in the case of the dry season, a considerable change in the value of EQI is observed in comparison to the default strategy. A significant change is observed in the value of OCI in all the control strategies, a trade-off is maintained between EQI, OCI, and improvement as well. In the dry season, it is observed that the percentage of violation values of PI-MPC and MPC-MPC when compared with default PI are greater in the case of TP and is lesser in the case of TN and ammonia. MPC-MPC shows better effluent quality and slightly high operating costs. Similarly, it was observed that the percentage of violations for PI-Fuzzy and MPC-Fuzzy are higher in the case of S_{NH4} and TP when compared with default PI and is less in the case of TN, as shown in Fig.4.10. From Table 4.2, it was observed that the average effluent concentrations attain stringent regulations except for ammonia and phosphorus. MPC-MPC shows better-optimized ammonia removal, PI-MPC shows optimized phosphorus removal. It can be noticed that the OCI increases and EQI decrease for all the control strategies chosen from Fig.4.11. Sludge production is slightly high in PI-MPC and low in MPC-MPC. The effluent concentrations are compared for all control strategies and are depicted in Fig.4.12 (A), (B), and (C). Similarly, in the rainy season and stormy season, the percentage of violation values of all hierarchical control strategies is less than the default PI values in the case of S_{NH}, TN, and TP.

Controller implementation for dry weather condition

On comparing with default PI, PI-MPC showed an improved EQI of 3.8% with a 1.3% increase in OCI, and with MPC-MPC EQI improved by 5.7% with an increase of 1.4% in OCI. On the other hand, PI-Fuzzy and MPC-Fuzzy showed an improvement of 1.9%, 5.2% in EQI with an increased OCI of 0.4% and 1.3% respectively. For Dry season data, the MPC-MPC controller showed the optimal results when compared with PI-Fuzzy, PI-MPC, and MPC-Fuzzy strategies.

Controller implementation for rainy weather conditions

On comparing with default PI, PI-MPC showed an improved EQI of 8% with 1.3% of increased OCI, and with MPC-MPC EQI improved by 6.1% with an increase of 4.3% in OCI. On the other hand, PI-Fuzzy and MPC-Fuzzy showed an improvement of 4.4%, 4.8% in EQI with an increased

OCI of 0.4% and 1%. For rainy season data, the PI-MPC controller showed the optimal results when compared with all other control approaches used in the present study. Appendix Table B1 is tabulated for the comparison of PI-MPC, MPC-MPC, PI-Fuzzy, and MPC-Fuzzy schemes for the rain season.

Controller implementation for storm weather condition

On comparing with default PI, PI-MPC showed an improved EQI of 9.6%, increased OCI of 1.6%. MPC-MPC resulted in an improvement of 4.3% in EQI and 1.3% in OCI. On the other hand, the other two control strategies, PI-Fuzzy and MPC-Fuzzy showed an improvement of 5.9%, 9.8% in EQI, and 1.5%, 1.7% in OCI. For storm season data, the PI-Fuzzy controller showed optimal results when compared to other control approaches. Appendix Table B2 is tabulated for the comparison of PI-MPC, MPC-MPC, PI-Fuzzy, and MPC-Fuzzy schemes for storm season.

Table 4.2 Compared results of PI, PI-MPC, MPC-MPC, PI-Fuzzy, and MPC-Fuzzy

Average effluent concentration		Default PI	PI-MPC	MPC-MPC	PI-Fuzzy	MPC-Fuzzy
Components	Limit			`		
S_{NH}	4	6.05	5.31	5.04	5.48	5.38
TSS	30	13.67	13.72	13.78	13.72	13.77
TN	18	16.005	15.35	15.45	15.53	15.50
TP	2	3.54	3.38	3.58	3.54	3.60
COD	100	44.73	44.79	44.88	44.81	44.87
BOD_5	10	1.78	1.79	1.80	1.799	1.80
Performance plant assessment						
IQI		72152	72152	72152	72152	72152
EQI		13239	12741	12484	12978	12548
SP		2969	2983	2953	2972	2956
AE		4254	4431	4544	4355	4528
PE		331	338	333	330	332
ME		480	495	495	482	489
OCI		18681	18945	18949	18769	18934

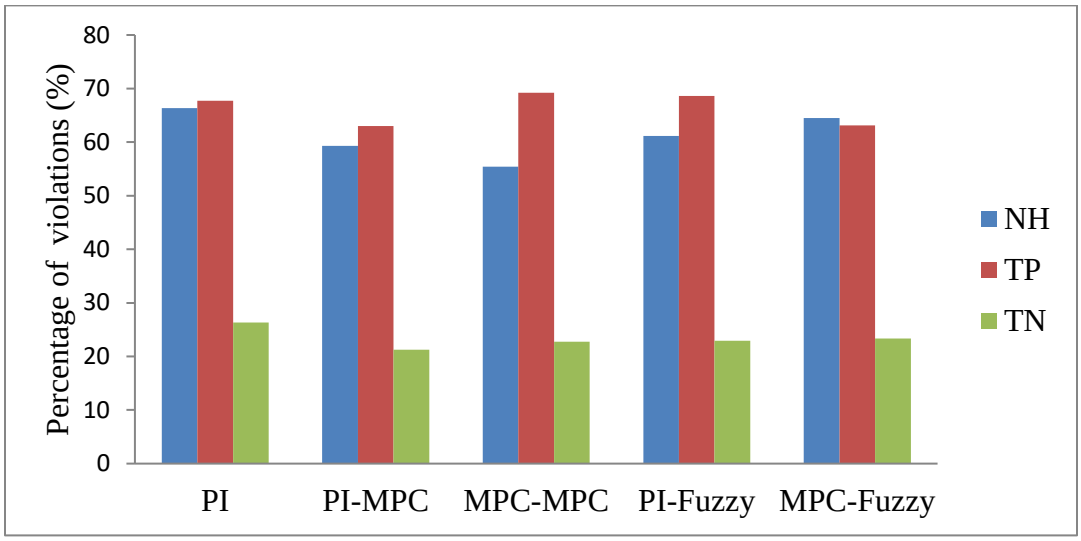

Figure 4.9 Comparison of Percentage of violations for all control strategies

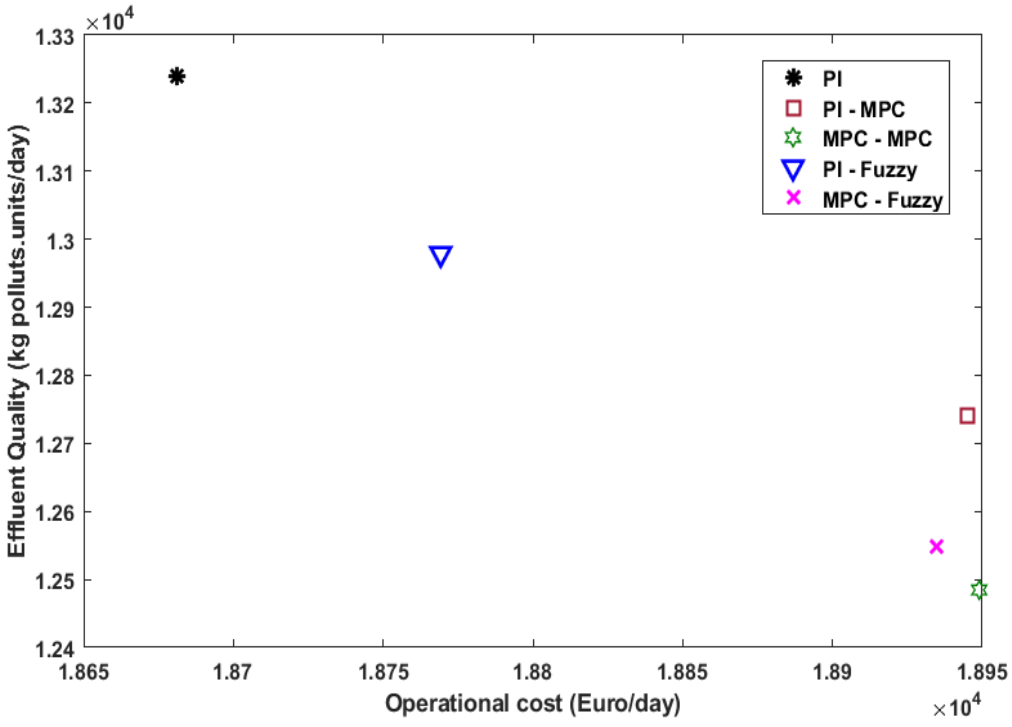

Figure 4.10 Comparison of EQI and OCI for all control strategies

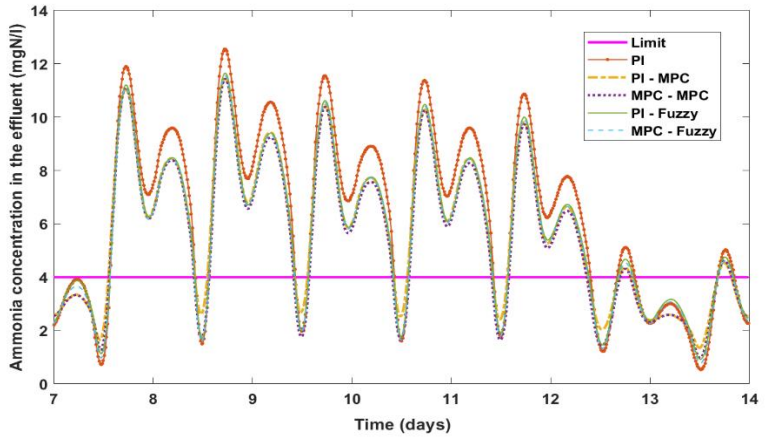

(A)

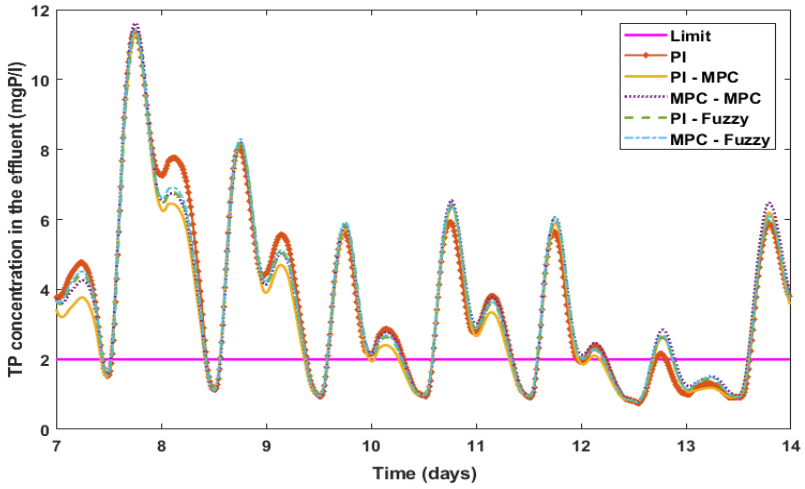

(B)

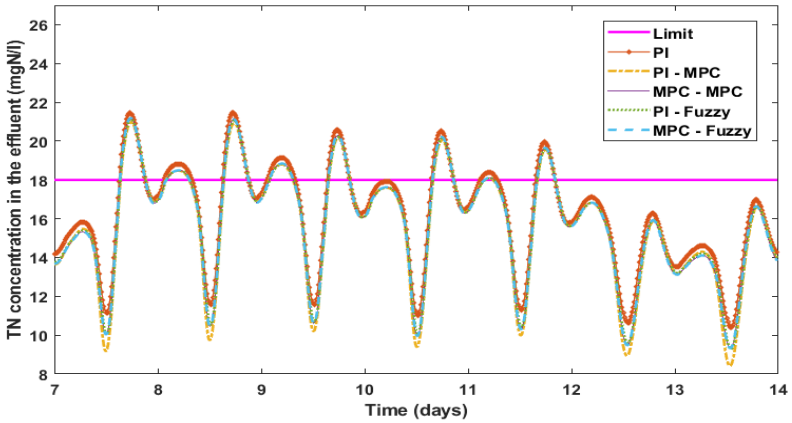

(C)

Figure 4.11 PI, PI-MPC, MPC-MPC, PI-Fuzzy, and MPC-Fuzzy controllers for (A) Ammonia (B) TP (C) TN concentration in the effluent

4.3 Summary

In chapter 3 used a BSM1-P simulation platform with ASM3bioP as a bioprocess and implemented PI, MPC, and Fuzzy based controllers. They found that operational cost is decreased with improved effluent quality. These control designs show improved effluent quality of 2%, 1.4% and 0.4% with decreased operational cost of 0.3%, 0.7% and 0.07% respectively. All these control approaches are focused only on DO and S_{NO}. In the present work, an additional ammonia controller is added to the DO loop. By using four different control combinations PI-MPC, MPC-MPC, PI-Fuzzy, and MPC-Fuzzy, the performance is compared with default PI. In this study, dry, rain, and storm season conditions are used. MPC-MPC, PI-MPC, and PI-MPC showed improved EQI of 5.7%, 8%, and 9.6% with an increase of 1.4%, 1.3%, and 1.6% in OCI.

Ammonia removal is improved by 18% with the MPC-MPC control framework and provided better effluent quality. Aeration energy is high in all hierarchical control applications with respect to mixing energy when compared to PI. MPC in the higher level provides better tracking performance and is favorable for both TN and total ammonia removal. MPC shows efficient removal of ammonia and TN when compared to FLC and PI. Also, the tracking for S_{NO} and DO_7 with PI controllers is slightly better. However, the percentage of violations for ammonia and total phosphorus is less when compared to default PI controllers. This study helps to select appropriate control strategies and provides guidelines for the operators in wastewater utilities and serves as a decision support tool.

Chapter 5

Design of integrated supervisory and override control strategies on BSM1-P

Chapter 5

Design of integrated supervisory and override control strategies on BSM1

5.1 Supervisory layer with three DO loops with override control strategies on BSM1-P (SOPCA control scheme)

There will be a limitation for the removal of biological phosphorus when the carbon source is more complex than volatile fatty acids (VFA) and when the nitrate enters the anaerobic phase. The nitrate detrimental effect was not to inhibit the phosphorous release process but to prevent the fermentation process for VFA production (Guerrero et al., 2011). Hence, the objective is to control P (P in tank7) below its effluent limit. For achieving this, a supervisory control layer is used which requires the measurement of P in the 7th reactor. As the total P limit is 2 gPm^{-3}, a set point of $S_{PO,7}$ is selected, and based on the P measurement, the supervisory layer computes the nitrate set point to the intermediate override control layer as shown in Fig.5.1. The setpoint considered for S_{PO} is 1.68 gPm^{-3}. The reason for selecting this value is based on the legal upper limit for effluent phosphorous which is 2 gPm^{-3}. By maintaining the set point of effluent phosphorous below this value, it is expected that the effluent phosphorous will follow the upper limit without any violations. However, S_{PO} is influenced by the amount of nitrate levels in the anoxic reactors. Hence, the nitrate set point is computed at the supervisory layer by keeping a pre-determined set point for S_{PO}. If the computed nitrate setpoint is greater than 16 g N m^{-3}, the nitrate set point to the lower level loop needs to be 1 gNm^{-3}. On the other side, if the computed nitrate values are less than 16 gNm^{-3}, the corresponding setpoint to the next control layer would be 0.1-1 gNm^{-3}. In the anoxic section, when P increases, the setpoint of nitrate in the anoxic section would be decreased by optimizing the Q_{intr}. The control approach is rooted in a cascade implementation with a pair of PI feedback controllers and integrated with override control to inhibit the overflow of S_{NO} (Nitrate) in the discharge. For a clear understanding, the proposed control loops are:

- Supervisory loop: In tank7, orthophosphates ($S_{PO,7}$) is regulated by manipulating the set point of S_{NO}. The P set point selected in tank 7 is based on $S_{NO,7.}$
- Intermediate (Override) loop: In tank7, if the nitrate concentration is above 16 gN/m^3, change the set point to 1 gN/m^3. If the nitrate concentration is less than 16 gN/m^3, maintain the set point between 0.1 - 1 gN/m^3.
- Lower level loop: In tank4, control the $S_{NO,4}$ by manipulating the $Q_{intr.}$

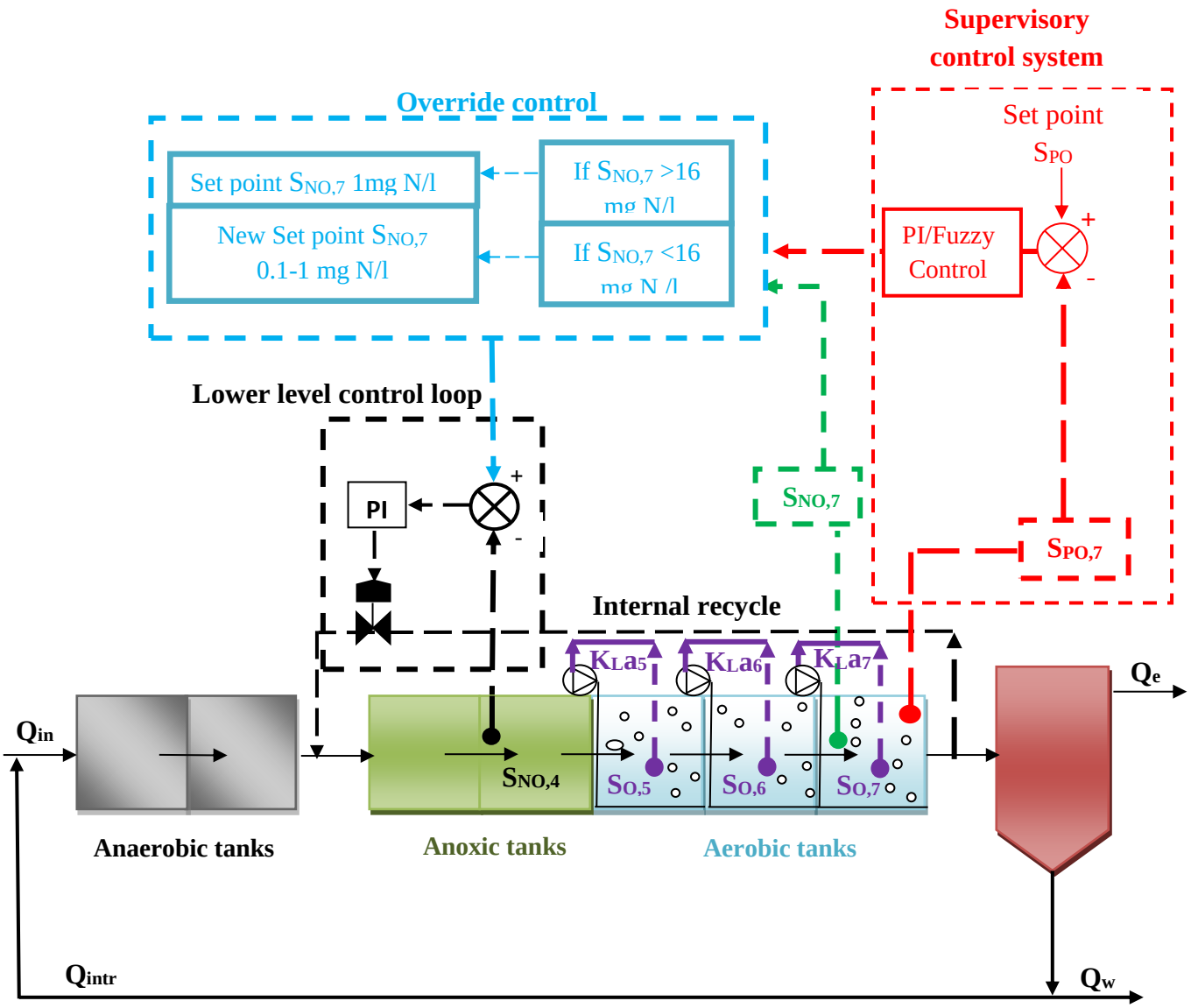

Figure 5.1 SOPCA control approach for P removal

The override control setpoint of $S_{NO,7}$ as 16 g N m^{-3} in tank7 is selected based on the concentration of $S_{PO,7}$ limit value. If nitrate concentration increases, the orthophosphates also increase. Here, in this case, 16 gNm^{-3} is an optimal setpoint for both nitrate and orthophosphate. The SOPCA approach is useful to remove P by adjusting the nitrate inlet into the anoxic tank. Due to this, the anaerobic fraction in the plant will increase. If the anoxic tank volume decrease results in an increase of TN in the effluent, this leads to denitrification of nitrate. The upper limit for TN is 18 gNm^{-3}. Thus, an override control loop is selected: here the cascade loop is disabled while the nitrate composition in the discharge is above 16 gNm^{-3}. This value was considered for being a warning range less than 18 gNm^{-3}, the legal discharge limit for TN. In this framework, the secondary loop is operative with a nitrate set point of 1 gNm^{-3}. Additionally, the last three (tank 5, 6, and 7) aerobic

reactors are tested for different S_O (2, 3, 1, 1.5, and 2.5) setpoints by manipulating the corresponding oxygen mass transfer coefficients (K_La_5, K_La_6, and K_La_7). In the next sections, the supervisory layer is explained in detail.

5.1.1 Supervisory layer: Use of fuzzy logic control scheme

Many chemical and biological processes are controlled using fuzzy logic control (FLC). This is achieved by employing fuzzy rules that are identical to those used in human inference design. FLC is used on the WWTP in this study. FLC is based on IF-THEN statement rules for the computation of the control signals.

In tank7, P is regulated by manipulating the set point of $S_{NO,4}$ which is passed as set-point to tank4. Usually, the input variables considered are the feedback error (E) and the differentiation of feedback error as (ED). These two variables are selected as inputs for the FLC. Accordingly, output variables are considered as manipulating variables (W) which is $S_{NO,7}$. To combine the output and input variables, the membership function (MF) should be selected. A triangular function is selected as shown in Fig.5.2 (A-C). FLC consists of three sections as shown in Fig.5.3. In the primary section, MF's are fuzzified with input values to get fuzzification as given in Table 5.1. By using the predetermined rules, fuzzy inputs and outputs are connected as shown in Table 5.1 and then the outputs are determined by using the inference mechanism. For the third section, defuzzification takes place to compute the output values. A total of 9 rules are followed and are given below. Mamdani technique is chosen for the fuzzy interface function and the centroid technique is chosen for the defuzzification. BSM1-P with SOPCA (PI-Fuzzy) Configurations file of Matlab/Simulink is depicted in the Appendix of Fig.C1.

Ru1: If (error is P) and (differror is R) then (nitrate is B)
Ru2: If (error is P) and (differror is C) then (nitrate is B)
Ru3: If (error is P) and (differror is S) then (nitrate is E)
Ru4: If (error is O) and (differror is R) then (nitrate is A)
Ru5: If (error is O) and (differror is C) then (nitrate is A)
Ru6: If (error is O) and (differror is S) then (nitrate is A)
Ru7: If (error is Q) and (differror is R) then (nitrate is B)
Ru8: If (error is Q) and (differror is C) then (nitrate is B)
Ru9: If (error is Q) and (differror is S) then (nitrate is B)

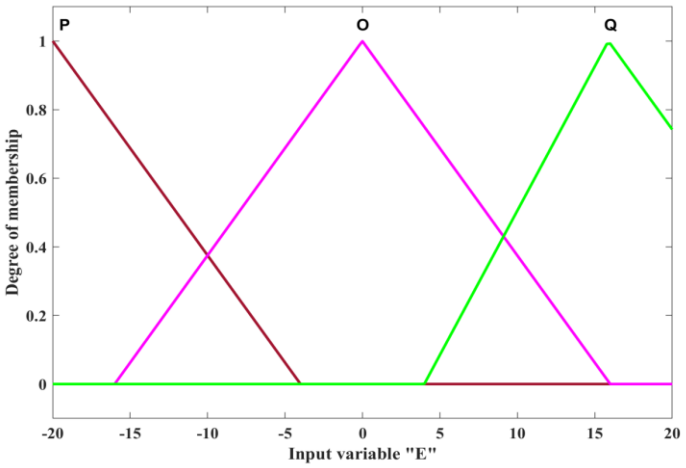

(A) Membership of E of tank 7 for $S_{PO,7}$

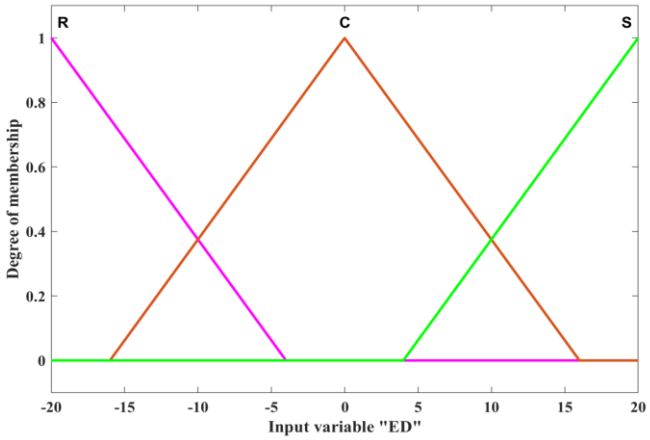

(B) Membership of ED of tank 7 for $S_{PO,7}$

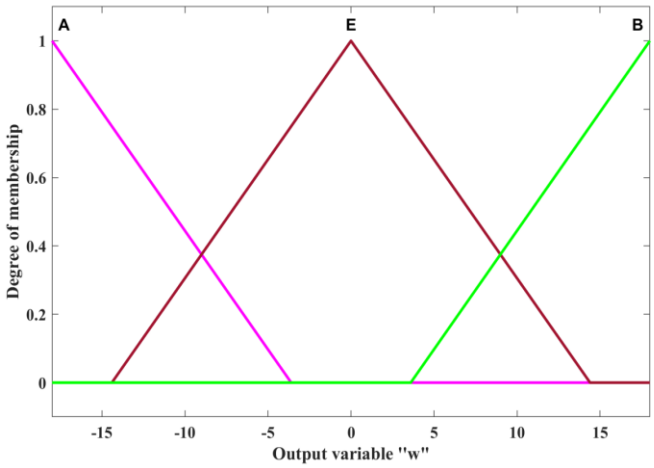

(C) Membership of W of tank 7 for $S_{NO,7}$

Figure 5.2 Membership functions for fuzzy rules

Table 5.1 Linguistic functions and MF's for control inputs and outputs

Linguistic Variable					
Linguistic value	Range	MF	Characteristic ranges		
1	Lower	Triangular shaped	-36	-20	-4
2	Medium	Triangular shaped	-16	-0.009778	16
3	Higher	Triangular shaped	3.99	15.88	31.87
Linguistic Variable (differential error)					
Linguistic value	Range	MF	Characteristic ranges		
1	Lower	Triangular shaped	-36	-20	-4
2	Medium	Triangular shaped	-16	-0.009778	16
3	Higher	Triangular shaped	3.99	20	36.01
Linguistic Variable					
1	Lower	Triangular shaped	-32.4	-18	-3.6
2	Medium	Triangular shaped	-14.4	3.5e-15	14.4
3	Higher	Triangular shaped	3.6	18	32.4

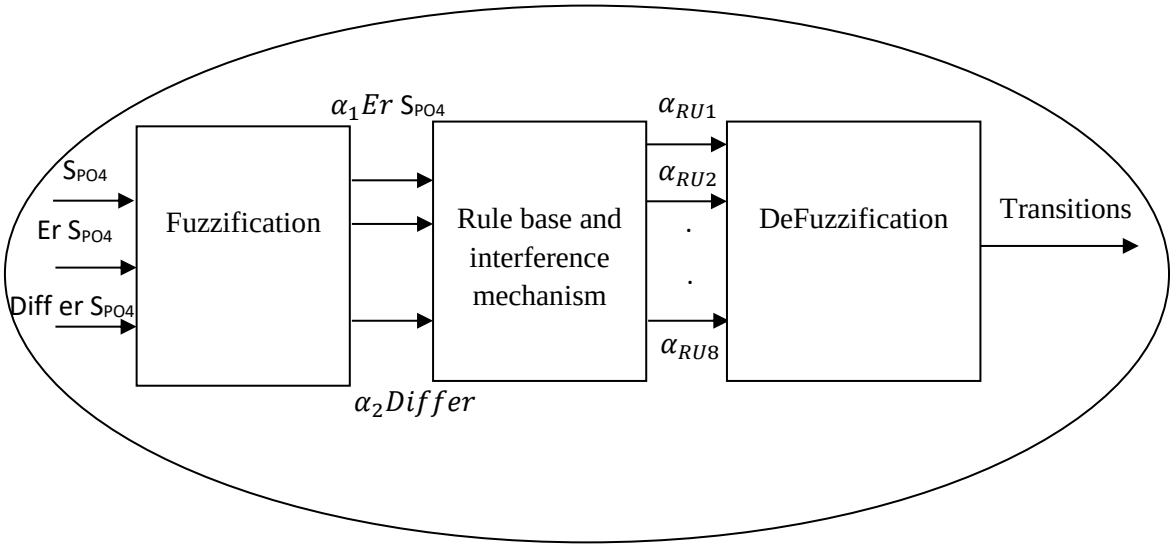

Figure 5.3 Flow diagram of fuzzy controller

Table 5.2 DO Control set points for SOPCA (PI-Fuzzy) [I] to SOPCA (PI-Fuzzy) [VIII]

Control approaches SOPCA (PI-Fuzzy) with additional DO controllers in aerobic reactors	S_O set points for the last three aerobic reactors		
	S_{O5}	S_{O6}	S_{O7}
SOPCA(I)	1	1	2
SOPCA (II)	1	1.5	2
SOPCA (III)	1.5	1.5	2
SOPCA (IV)	1	3	2
SOPCA (V)	2	2	2
SOPCA (VI)	2	3	2
SOPCA (VII)	3	1.5	2.5
SOPCA (VIII)	3	3	2

Other than the SOPCA control approach, additional dissolved oxygen (S_O) loops are added. Table 5.2 shows the various S_O setpoints by manipulating K_La in the last three reactors. In SOPCA (PI-Fuzzy), eight different S_O setpoint combinations of control strategies are implemented in the last three reactors. In this scheme, three PI control strategies are designed independently with model-based data. PEM is used to develop models for both loops with the open-loop data. For this, ±10% variance change in the inputs of oxygen mass transfer coefficients (K_La_7, K_La_6, K_La_5) are given randomly whose steady-state values are 91, 127, and 155 m^3/d. The corresponding output data of S_O is collected whose steady-state value is 2 gO_2/m^3 in all three reactors. Similarly, with fixed input change of ±10% variance is given in Q_{int} whose steady-state value is 21900 m^3/d. The corresponding output data of $S_{NO,4}$ is collected whose steady-state value is 0.1848 gN/m^3 in all fourth reactors with an additional override control loop. Fig.5.4 depicts the scheme of SOPCA (V). In the supervisory layer, fuzzy is chosen with the above fuzzy scheme of MF's. The corresponding obtained input and output data are depicted in the Appendix data are depicted in Fig.C3. PEM is utilized to determine the model. By using the obtained models, a SIMC method is used to design controllers for both the loops. The parameters of the PI controller are: a) For S_{O7}: K_p (Proportional control gain)=12.042 and T_i (Integral time) =0.010586,S_{O6}: K_p=17.549 and T_i=0.0055903,S_{O5}: K_p=6.92 and T_i=0.0014262 b) For $S_{NO,4}$: K_p=28533.61 and T_i=0.031488.

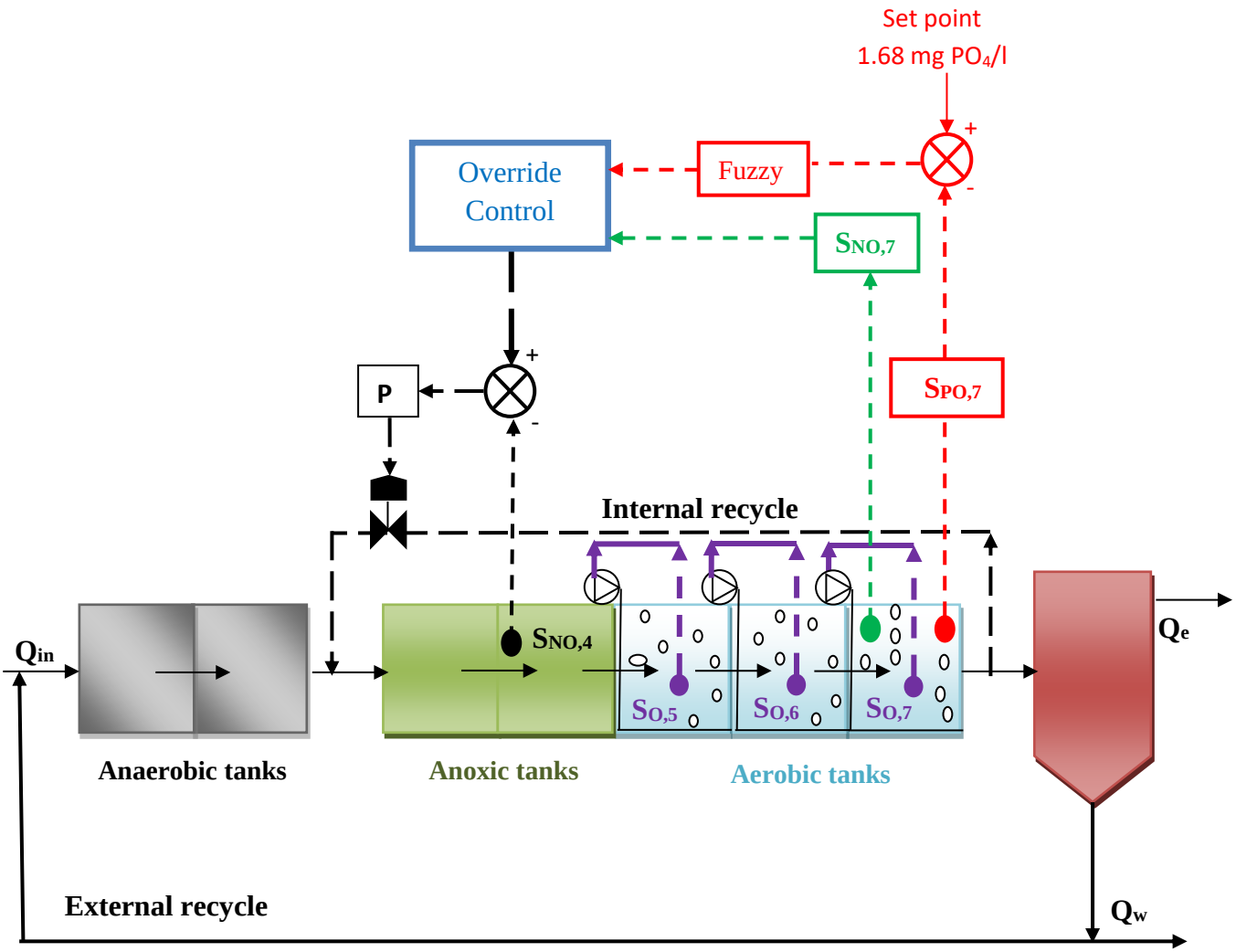

Figure 5.4 Scheme of SOPCA (V) control approach for P removal

5.1.2 Simulation results and comparison

The simulation outputs of SOPCA (PI-Fuzzy) with additional S_O control approaches have been computed. The corresponding average effluent values are given in Table 5.3. In comparison, of the eight control strategies (I to VIII), it was found that TN and ammonia are under the limits. Plant performance with energy assessments like aeration, pumping, sludge production, and mixing energies are determined. It is noticed that the average composition of P is largely influenced by S_O which is directly proportional to the formation of orthophosphates. P removal is contradictory with N and ammonia removal while all controls are applied with respect to nitrate. The results with three S_O control loops showed better results than single S_O control and SOPCA (PI-Fuzzy) without the S_O control approach. From the perspective of effluent discharge of percentage of violations, TP plays a key role in EQI improvement. The optimized TP removal is best observed in SOPCA (I), whereas, TN and ammonia removal are good with SOPCA (VIII) as depicted in Fig.5.5. From

the analysis of different SOPCA control schemes with additional S_O loops, optimal results in terms of EQI and OCI are observed for SOPCA (I) as shown in Fig.5.6. Comparison between the average effluent concentrations of removal rate efficiencies of SOPCA (I-VIII) and effluent limits is carried out and the results are reported in Table 5.3. It can be observed that the pollutant removal rates for S_{NH}, TSS, TN, COD, and BOD_5 for SOPCA(VIII) scheme showed improvement of 62.5%, 65.1%, 2.4%, 59.2%, and 87.4%. On the other hand, an improved removal rate for TP is obtained when SOPCA (I) scheme is used in which an improvement of 28.5% is obtained.

Comparison with default PI controllers of SOPCA (I) to SOPCA (VIII): The default control strategy uses PI controllers for both loops in which DO and nitrate are controlled by manipulating oxygen mass transfer coefficient and internal recycle rate in seventh and fourth reactors respectively in chapter 3 (Shiek et al., 2021). Among the eight control strategies (I to VIII) in which fuzzy logic controller is used in the supervisory layer, SOPCA (I) shows the lower operational cost with improved effluent quality. On comparing with the default PI, SOPCA (I) showed an improved EQI of 37.4% with an increase of 7.6% in OCI. Also, on comparing with the default PI, all the pollutant concentrations of removal rates are improved except nitrogen. For example, on comparing with default PI, the improved removal efficiency obtained is 57.2%, 22.6%, 59.6%, 8.7%, and 27.5% for S_{NH}, TSS, TP, COD, and BOD_5 respectively. On comparing with operational performance assessment with default PI with eight control strategies SOPCA (I) to (VIII), an increment is observed for AE, ME, and SP. In the case of pumping energy, it is high in the default PI compared to other controllers.

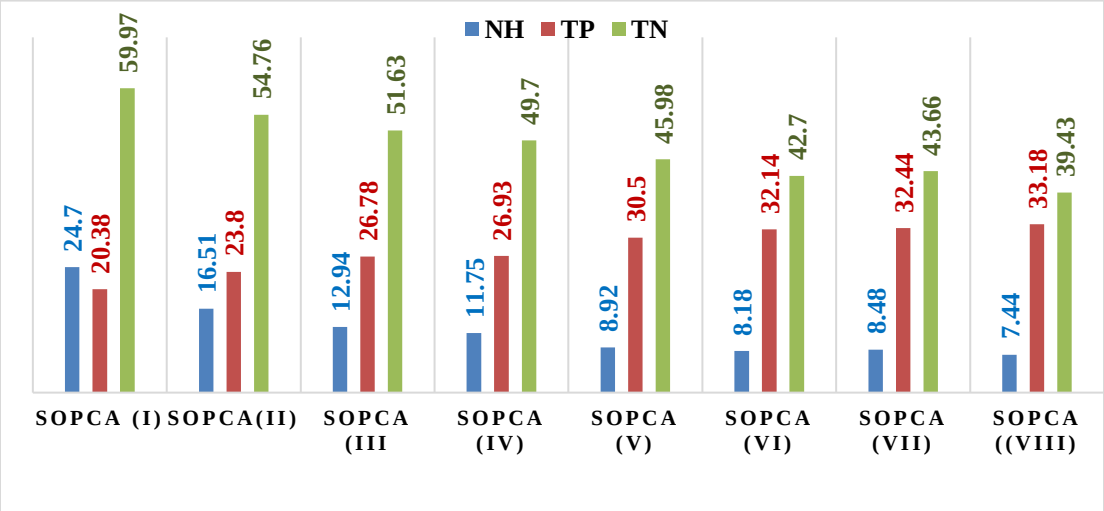

Figure 5.5 Percentage of violations of S_{NH}, TP, and TN for SOPCA (I) and SOPCA (VIII)

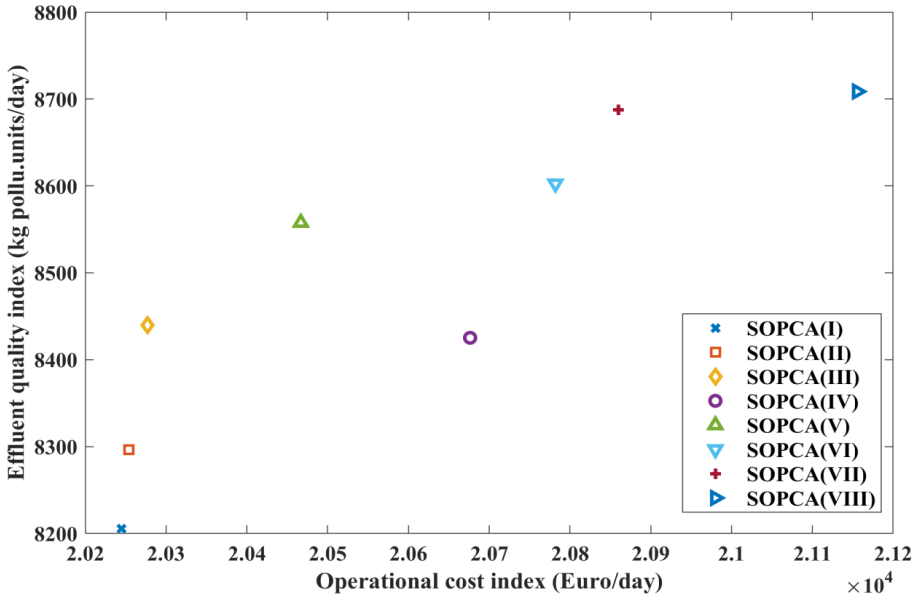

Figure 5.6 Comparative analysis of OCI and EQI for SOPCA (I) and SOPCA (VIII)

Table 5.3 Average concentration values of effluent discharge with different combinations of S_O for aerobic reactors in SOPCA (PI-Fuzzy) scheme

Average concentrations of effluent		SOPCA control strategies (I-VIII)							
Components	Limit	SOPCA (I)	SOPCA (II)	SOPCA (III)	SOPCA (VI)	SOPCA (V)	SOPCA (VI)	SOPCA (VII)	SOPCA (VIII)
S_{NH}	4	2.58	2.21	1.95	1.88	1.68	1.58	1.61	1.50
TSS	30	10.57	10.54	10.51	10.51	10.48	10.48	10.47	10.45
TN	18	18.79	18.40	18.11	18.01	17.74	17.62	17.65	17.56
TP	2	1.43	1.6	1.76	1.77	1.90	1.98	2.00	2.05
COD	100	40.83	40.84	40.84	40.84	40.84	40.85	40.85	40.84
BOD_5	10	1.2939	1.287	1.28	1.27	1.27	1.27	1.26	1.26
	Performance plant assessment								
AE		4408.7	4533.1	4666.4	5077.1	4967.5	5332.7	5418.6	5762.9
SP		3079	3054.2	3030.5	3028.3	3006.8	2995.1	2994.7	2983.9
ME		1164	1164	1164	1164	1164	1164	1164	1164
PE		210.2	216.2	221.9	222.1	228.6	233	233.4	233.5

5.2 Supervisory layer: Use of PI control scheme

In this scheme, from section 5.1.1 the control approach is similar to PI controller application for lower control loop and the last three S_O control strategies are designed independently based on the identified models with the additional override control loop. The control tracking the performance of S_O for three aerobic reactors and also for SOPCA (PI-PI) with eight S_O setpoint combinations of the last three aerobic reactors (IX to XVI) of control strategies are implemented and are given in Table 5.4. The systematic approach for model identification and implementation of control is elaborated in the flow diagram from Fig.5.7. In this section the supervisory layer, the PI controller is chosen. Fig.5.8 depicts the control scheme of SOPCA (XIII) varying S_O is 2 gO_2/m^3 is maintained as the set points in the last three aerobic reactors. For $S_{NO,7}$ loops, a random input signal with 10% is given in nitrates (setpoint of 0.1848) and the corresponding input and output data is noted. The corresponding output data of $S_{PO,7}$ is collected whose steady-state value is 1.68 gP/m^3 in the last reactor. The corresponding obtained input and output data are depicted in the Appendix data are depicted in Fig.C3. Again, PEM is utilized to determine the model. By using these models, based on the SIMC method, the parameters of the PI controller are obtained as a) For $S_{O,7}$: K_p= 12.042 and T_i=0.010586, S_{O6}: K_p=17.549 and T_i=0.0055903, S_{O5}: K_p=6.92 and T_i=0.0014262 b) For $S_{NO,4}$: K_p=28533.61 and T_i=0.031488. For $S_{PO,4}$ controller: K_p=-0.1055 and T_i=0.07213. BSM1-P with SOPCA (PI-Fuzzy) configurations file of Matlab/Simulink is depicted in the Appendix of Fig.C2. DO control tracking performance in the three aerobic reactors are depicted in Appendix Fig.C4.

Table 5.4 DO Control set points for SOPCA (PI-PI) [IX] to SOPCA (PI-PI) [XVI]

Control approaches SOPCA (PI-PI) with additional DO controllers in aerobic reactors	S_O set points for the last three aerobic reactors		
	S_{O5}	S_{O6}	S_{O7}
SOPCA (IX)	1	1	2
SOPCA (X)	1	1.5	2
SOPCA (XI)	1.5	1.5	2
SOPCA (XII)	1	3	2
SOPCA (XIII)	2	2	2

SOPCA (XIV)	2	3	2
SOPCA (XV)	3	1.5	2.5
SOPCA (XVI)	3	3	2

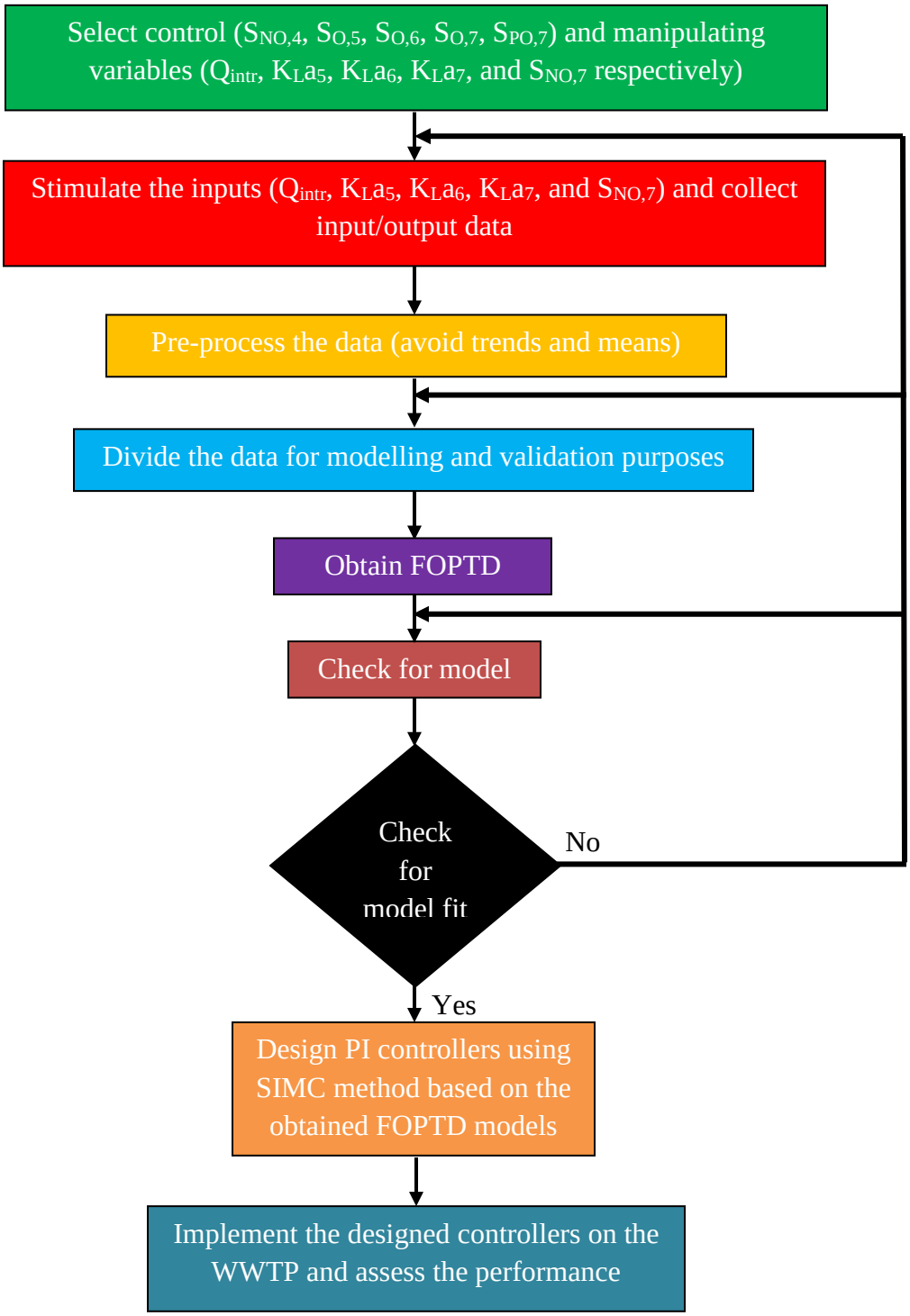

Figure 5.7 Systematic approach for model identification and implementation of control

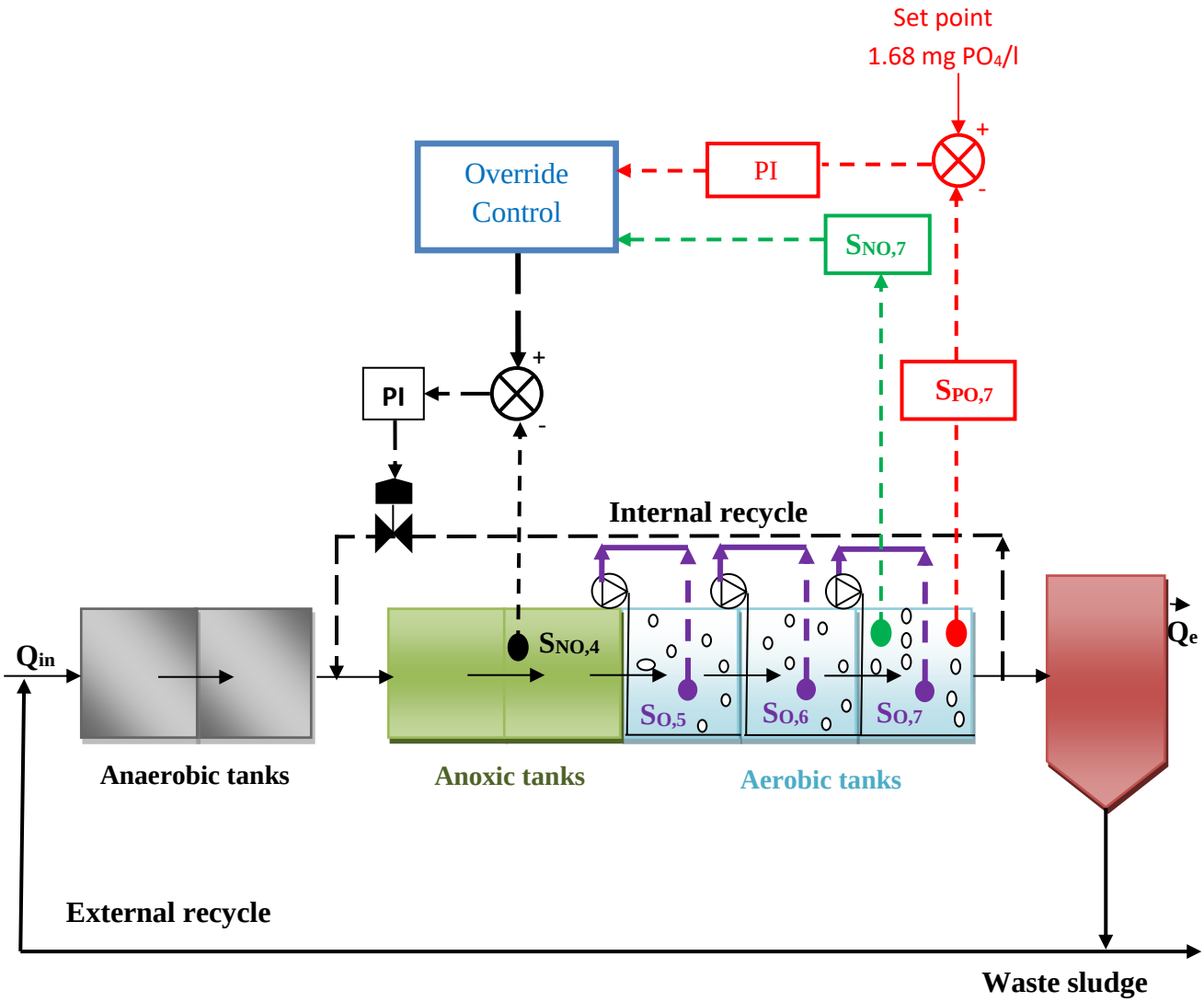

Figure 5.8 Scheme of SOPCA (XIII) control approach for P removal

5.2.1 Simulation results and comparison

The optimized results in terms of EQI and OCI are observed with SOPCA (IX) scheme as shown in Fig.5.10. The comparative analysis for the last seven days of SOPCA (I) and SOPCA (IX) results of TP and TN are depicted in Fig.5.11 (a, b) and it can be observed that SOPCA (IX) showed better results. Comparison between the average effluent concentrations of removal rate efficiencies of SOPCA (IX-XVI) control strategies and effluent limits is done and the results are reported in Table 5.5. Here, the removal rate for S_{NH} when SOPCA (XIV) is used improved by 60.5%. For TSS and BOD_5, SOPCA (XV) scheme provided an improvement of 65.1% and 87.4%. On the other hand, the TP, TN, and COD are improved when SOPCA (IX) scheme is used and the improvement is obtained as 20.5%, 11%, and 59.2% respectively. The percentage of violations of S_{NH}, TP, and TN for SOPCA (IX) and SOPCA (XVI) is depicted in Fig.6.9. In the operation

performance assessment data, an increase in S_O set point lead to an increase in the AE rate. From Tables 5.3 and 5.5, it is observed that the AE intake is high in SOPCA (VIII) and SOPCA (XVI) and low in SOPCA (I) and SOPCA (IX). As far as ME is concerned, it remained constant throughout all SOPCA control strategies. For SP, the highest values are recorded in SOPCA (I) and SOPCA (IX), the lowest in SOPCA (VIII) and SOPCA (XIV). Further, among the other eight control strategies (IX to XVI) in which PI controller is used in the supervisory layer, SOPCA (IX) shows the lower operational cost with improved effluent quality as shown in Table 5.5.

On comparing with the default PI: SOPCA (I) showed an improved EQI of 39% with an increase of 6.2% in OCI. Also, on comparing with the default PI, all the pollutant concentrations of removal rates are improved except COD. The improved removal efficiency is obtained as 54.4%, 22.5%, 0.61%, 55.1%, 8.7%, and 28% for $_{SNH}$, TSS, TN, TP, and BOD5 respectively. On comparing the costs with the default PI, all the eight control strategies showed increased AE and ME. In the case of pumping energy, it is high with the default PI. The sludge production rates are improved with SOPCA (XIV to XVI).

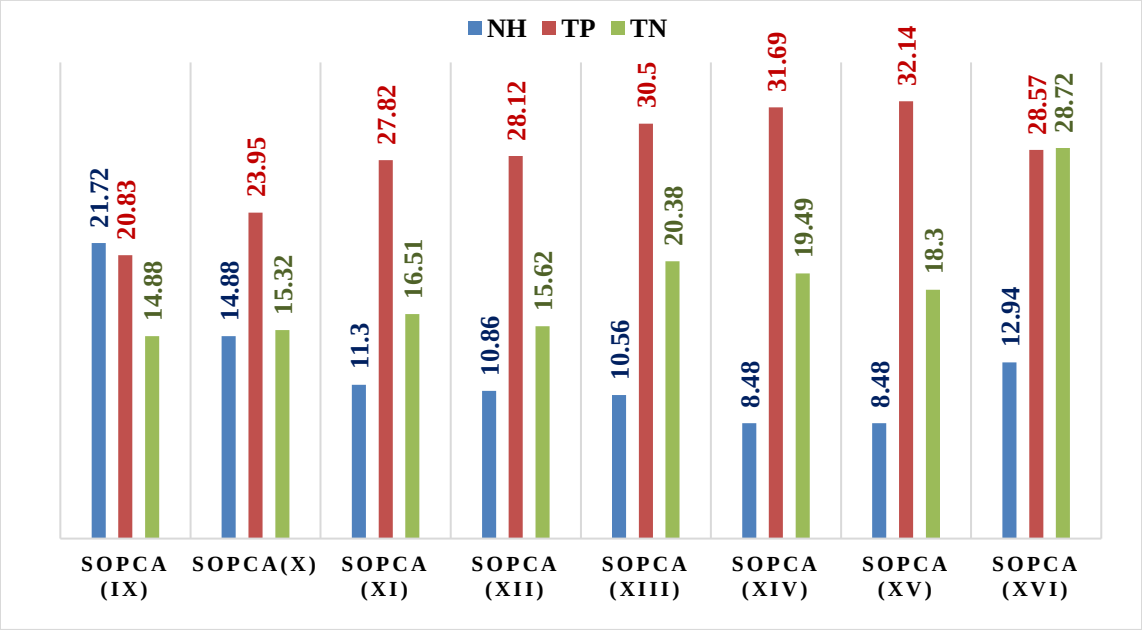

Figure 5.9 Percentage of violations of S_{NH}, TP, and TN for SOPCA (IX) and SOPCA (XVI)

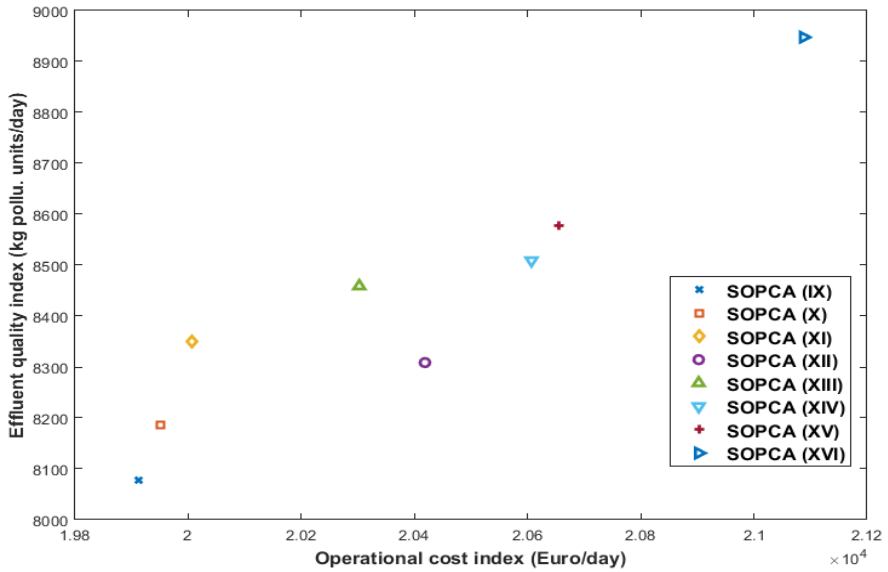

Figure 5.10 Comparative analysis of OCI and EQI for SOPCA (IX) and SOPCA (XVI)

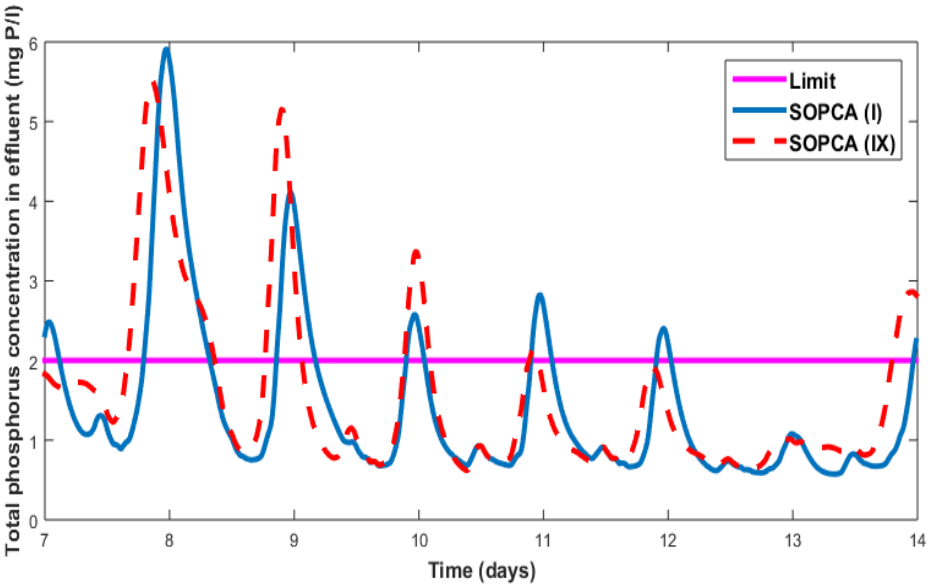

(A) Comparison of the effluent of TP concentrations

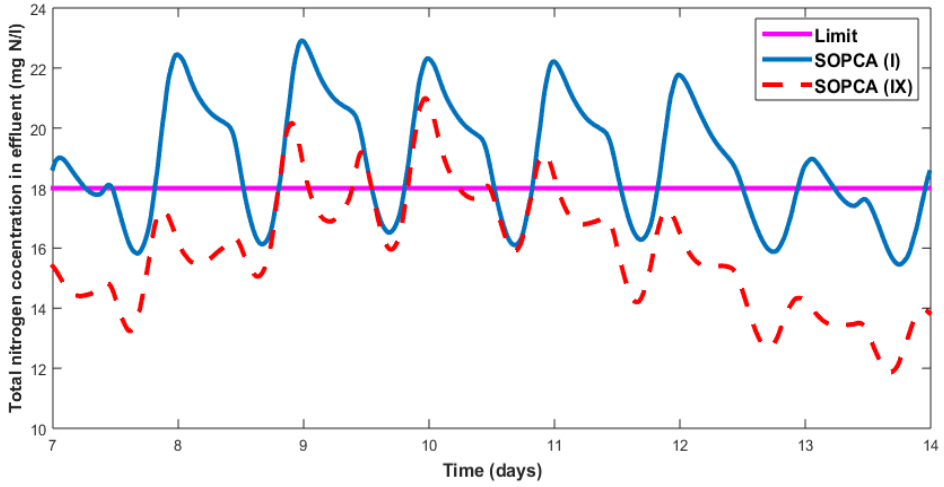

(B) Comparison of the effluent of TN concentrations

Figure 5.11 Comparison of effluent discharge of TP and TN on SOPCA (I) and SOPCA (IX) control schemes

Table 5.5 Average concentration values of effluent discharge with different combinations of S_O for aerobic reactors in SOPCA (PI-PI) scheme

Average concentrations of effluent		SOPCA control strategies (IX-XVI)							
Pollutants	Limit	SOPCA (IX)	SOPCA (X)	SOPCA (XI)	SOPCA (XII)	SOPCA (XIII)	SOPCA (XIV)	SOPCA (XV)	SOPCA (XVI)
S_{NH}	4	2.75	2.31	1.99	1.92	1.75	1.58	1.61	1.97
TSS	30	10.54	10.51	10.49	10.48	10.48	10.46	10.45	10.45
TN	18	16.04	16.07	16.24	16.25	16.79	16.64	16.51	17.26
TP	2	1.59	1.74	1.89	1.87	1.95	2.02	2.06	2.14
COD	100	40.84	40.84	40.85	40.84	40.85	40.85	40.85	40.86
BOD_5	10	1.289	1.28	1.27	1.27	1.27	1.26	1.26	1.26
	Performance plant assessment								
AE		4341.4	4475.1	4620.5	5033.1	4936.7	5308.5	5389.2	5713
SP		3015.8	2996.7	2978.5	2978.9	2975.4	2961.4	2955.4	2973
ME		1164	1164	1164	1164	1164	1164	1164	1164
PE		259.2	257.3	255.5	254.1	247.7	250.2	252	265.6

5.3 Summary

In the earlier works on the seven reactor A^2O (Anaerobic, anoxic and oxic) bioprocess system, different control approaches have been developed (Ostace et al., 2013). Chapter 3 used a bioprocess of ASM3bioP in the BSM1-P simulation framework and designed default PI, MPC, and Fuzzy controllers to control S_O and S_{NO}. The comparison is done at the limit value of 2 gP /m^3 for phosphorus. They observed that P in the effluent is increased by 42.8%, 44.4%, and 41.1% respectively for the three control schemes and they also observed that EQI is improved with slightly lower operational costs. Maheswari et al., (2020) used the same simulation platform and designed four case studies based on a nested control loop on three-stage biological treatment for ammonia changes. They observed that EQI is improved with higher operational costs. Their control approaches are compared for P and it is noticed that the P in the effluent is increased by 48.5%, 48.4%, 46%, and 47.3%. From chapter 4 using the same ASM3bioP bioprocess with BSM1-P, an ammonia-based aeration control (ABAC) is designed with four different combinations of controllers like PI-MPC, MPC-MPC, PI-Fuzzy, and MPC-Fuzzy. These control approaches are compared and observed that the P in the effluent was increased by 40.8, 44.1%, 43.5%, and 44.4% respectively for the corresponding control schemes. In their study, the ammonia removal rate is improved by 18% in the case of MPC-MPC but P removal is not affected much. In all these studies, the goal is not to design control strategies to improve P removal instead ammonia removal.

In this chapter, the main focus is on phosphorus removal, and hence Supervisory and Override P Control Approach (SOPCA) is designed with three additional S_O control loops in the aeration tanks. The comparison is done at the limit value of 2 g P m^{-3} for phosphorus. Here, the Supervisory Layer of Fuzzy and PI control schemes show improved results with P in the effluent by 28.5% and 20.5% only. Moreover, TN and ammonia are under the effluent regulatory limits.

Chapter 6

Development of control strategies based on plant-wide WWTP models

Chapter 6

Design of control strategies for plant-wide models with simultaneous removal of nitrogen and phosphorus

This chapter introduces PI controllers for the BSM2-P plant, which is based on the default strategy. It considers two loops: controlling dissolved oxygen concentration in tank 7 ($S_{O,7}$) by manipulating the oxygen mass transfer coefficient (K_La_7), and controlling nitrate concentration in tank 4 ($S_{NO,4}$) by manipulating the internal recycle flow rate (Qa). In another approach, a lower-level control framework is implemented to DO in the sixth reactor by regulating the K_La of fifth, sixth, and seventh reactors in the biological treatment process. Here PI is used at the lower level whereas Fuzzy and MPC are used at the supervisory level. The supervisory level is based on the ammonia-based aeration control (ABAC) to later the DO setpoint corresponds to the ammonia concentration. Table 6.1 reports the functioning of control strategies on BSM2-P. Appendix Table D.1 represents the state variables of ASM2d, units with notations, and average influent data are provided. Appendix Fig.D1 depicts the open-loop Matlab/Simulink file for BSM2-P

Table 6.1 Functioning of control strategies

Attributes	PI controller	Lower level	PI (Lower level) +MPC (Supervisory level)	PI (Lower level) +Fuzzy (Supervisory level)
Control variable	$S_{O,7}$ and $S_{NO,4}$	$S_{O,6}$	$S_{NH,6}$	$S_{NH,6}$
Set-point	2 gO_2/m^3 & 1 gN/m^3	2 gO_2/m^3	DO set-point is determined by higher level	DO set-point is determined by higher level
Regulating variables	K_La_7 and internal recycle	K_La in the last three reactors	Set-point for DO controller	Set-point for DO controller
Control design	PI	PI	PI and MPC	PI and Fuzzy

6.1 Control strategies for plant wide-models

6.1.1 PI control approach:

The default control approach is associates with two control loops of PI: In ASU the last aerobic tank (tank7) $S_{O,7}$ and the second reactor of anoxic (tank 4) $S_{NO,4}$ is controlled. The regulated variables are oxygen mass transfer coefficient (K_La) and internal recycle (Q_{intr}) respectively. The set-points are chosen according to the requirements of the WWTP. In the practical process, the level of $S_{O,7}$ in the oxic reactor required to be retained from the range of 1.5 to 4 $gO_2/m^{3,}$ and the practiced value is 2 gO_2/m^3 in WWTP. Moreover, the most advisable working points for the nitrate level in the anoxic tank are required to be carried from the range of 1-3 gN/m^3 and the practice value is 1 gN/m^3 is recommended usually. The models are developed using the attained open-loop data for each $S_{NO,4}$ and $S_{O,7}$ control loops. By using their regulating variables to select the required setpoint. For the values of 88000 and 73, the concentrations of S_{NO} and DO are reported as 2 gO_2/m^3, 1 gN/m^3 respectively. In the seventh and fourth reactor, a random input signal with a $\pm$10% variation in the obtained values. The attained resulting output data for S_{NO} and DO is collected. The S_{NO} and DO output data are now used to build FOPTD models using the method of prediction error minimization. Each loop is modeled with PI controllers from these models using the Skogested internal model control method (SIMC), and the FOPTD model is described (Grimholt & Skogested (2018) in the below: A first-order plus time order delay (FOPTD) model as given in the equation. (3.1) is identified for the design of PI controllers for each loop. For control of S_{NO} in bioreactor 4 ($S_{NO,4}$) and DO in bioreactor 7 ($S_{O,7}$), the respective obtained FOPTD model parameters are given in below:

K_P =0.000026144, T_i = 0.012515 and T_d = 0.000875.

K_P =0.04538, T_i =0.010085 and T_d =0.

Based on these models, PI controllers are designed using the SIMC method and are obtained for S_{NO} and DO loops are like K_c =35748.16, T_i= 0.01215, and DO loop is K_c =11.015, T_i = 0.010085. The corresponding simulation results are tabulated in Table 6.3. The resultant tracking performance of S_O and S_{NO} is depicted in Fig.6.1 (A) and (B). The PI control approach is depicted in Fig.6.2 (A). Identification file for BSM2-P of Matlab/Simulink file is depicted in Fig.D2.

6.1.2 Lower level control approach

In this approach, a close-loop control framework contains a PI controller. It is able to control S_O in the sixth tank at a set-point of 2 mgO_2/l by regulating the K_La_6. Further, the oxygen mass transfer coefficient in tank 5 and tank 7 by a factor of 1 and 0.5 respectively are manipulated (Solon et al. 2017). The lower level control approach is depicted in Fig.6.2 (B). BSM2-P with lower-level PI configuration Matlab/Simulink file is depicted in Appendix Fig.D3.

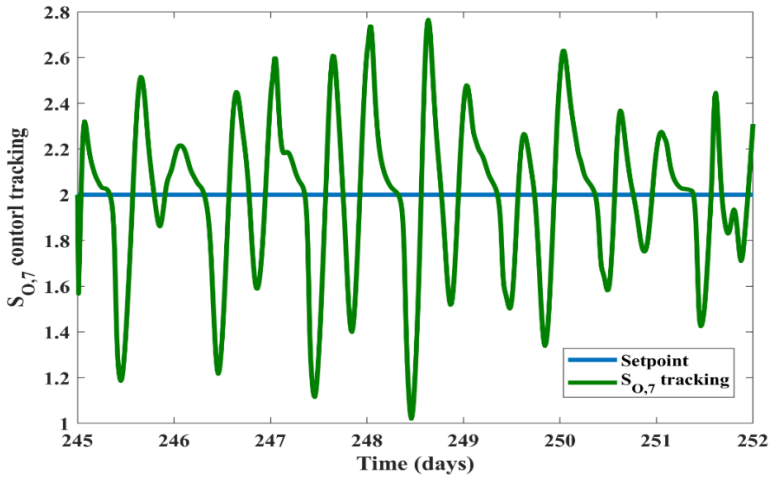

(A)

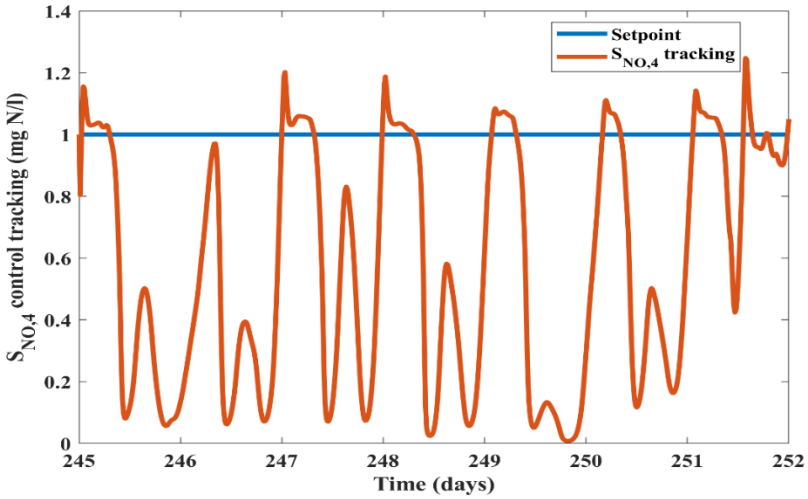

(B)

Figure 6.1 Control tracking (A) Dissolved oxygen and (B) Nitrate

6.1.3 Ammonia-based aeration control (ABAC) approach

This approach is based on cascade (MPC/Fuzzy) controllers for ammonia control ($S_{NH,6}$) by manipulating the $S_{O,6}$ set point in the aeration tank6. Here the $S_{O,6}$ in the aeration tank6 is controlled by regulating the airflow rates of reactors 5, 6, and 7 like the same as lower-level control.

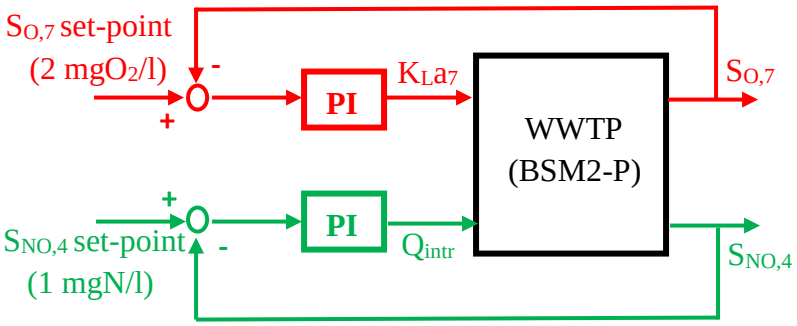

(A)

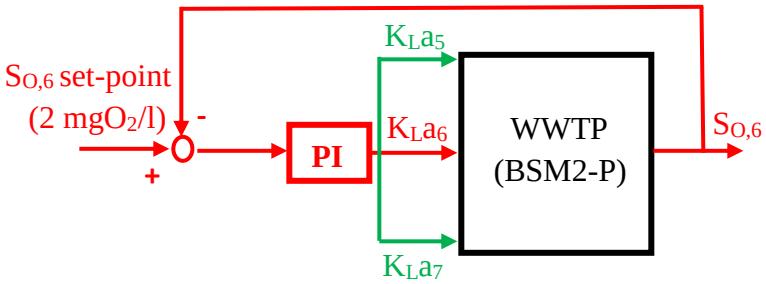

(B)

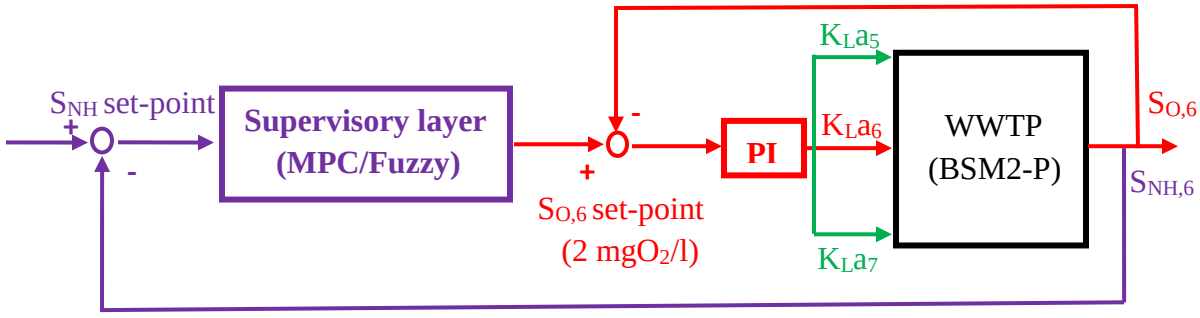

(C)

Figure 6.2 Control frameworks for BSM2-P (A) PI controllers (B) Lower level control (C) Supervisory level control framework with lower level

6.1.4 PI-MPC

The PI controller implemented for BSM2-P is used at the lower level in this control strategy, where MPC is implemented for the supervisory layer. $S_{NH,6}$ in tank 6 and S_O setpoint to be given to lower-level is the controlled and manipulated variables for supervisory layer. For system identification

of the design model for the supervisory layer, the S_O setpoint is varied by $\pm 10\%$ around the operating point, and the resulting S_{NH} concentration is collected. The prediction error method is used to drive the 3rd order state-space model for this data set (Ljung (1999)). The identified state-space model for the supervisory layer is expressed below. For supervisory layer MPC, the sampling time of control is 0.05 days (72 minutes), prediction and control horizons are 10, 2 respectively, and rate of change of regulated variable 0.1 are used.

MPC supervisory-level state-space model :

$$A=\begin{bmatrix} 0.7231 & 0.1351 & -0.03826 \\ -0.3957 & -0.2845 & 0.01298 \\ -0.0068 & -0.0477 & -0.1704 \end{bmatrix} \quad B=\begin{bmatrix} -0.09427 \\ -0.75 \\ -1.994 \end{bmatrix}$$

$$C=[1.306 \quad 0.074 \quad -0.01624] \quad D=[0]$$

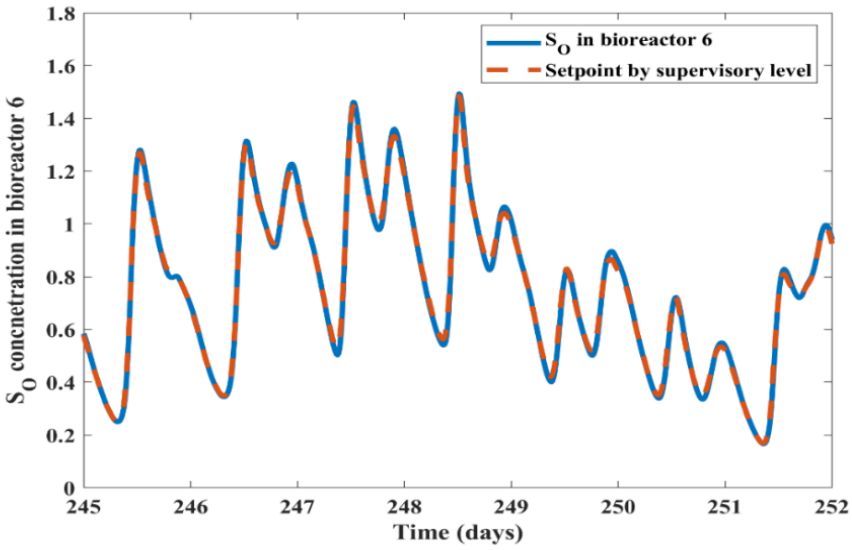

Figure 6.3 Dissolved oxygen tracking in the sixth bioreactor (PI-MPC)

Fig.6.3 depicts the computation of S_O by a supervisory level and its tracking by the lower-layer controller for 245 to 252 days for users to make a better comparison purpose. The performance evaluation was done in the period of 245 to 609 days. Fig.6.3 depicts that a good supervisory setpoint tracking is achieved by using the PI-MPC controller design framework in the sixth bioreactor. The resultant average concentrations of nutrient removal, energy usages, and greenhouse gas emissions, and performance of plant with cost assessment are reported in Table 6.3 and compared with the other three control frameworks. Identified models for controller designs are reported in the Appendix C.

6.1.5 PI-Fuzzy

Fuzzy Controller manipulates the S_O set-points at a supervisory layer to minimize ammonia peaks. The membership functions (MF) of $S_{O,6}$ and $S_{NH,6}$ are considered in the ranges of 0-4 mg O_2/l and 0.1-20 mg N/l, respectively. The MF's for both input and output variables are in a Gaussian bell-shaped curve, which is divided into three linguistic variables, "high," "low," and "medium," as shown in Figures 6.4(A) and (B). Total three rules are framed according to the S_O control loop (Tejaswini et al 2020). The corresponding linguistic variables for "high," "low," and "medium," are tabulated in Table 6.2. Figure 6.4(C) depicts that a good supervisory setpoint tracking is achieved by using the PI-Fuzzy controller design framework in the sixth bioreactor. The simulated results are reported in Table 6.3. Fig.D4. depicts the BSM2-P with lower-level PI-Fuzzy Configuration for Matlab/Simulink file.

If ammonia level is "low" then S_O (dissolved oxygen) level is "low"

If ammonia level is "high" then S_O level is "high"

If ammonia level is "medium" then S_O level is "medium"

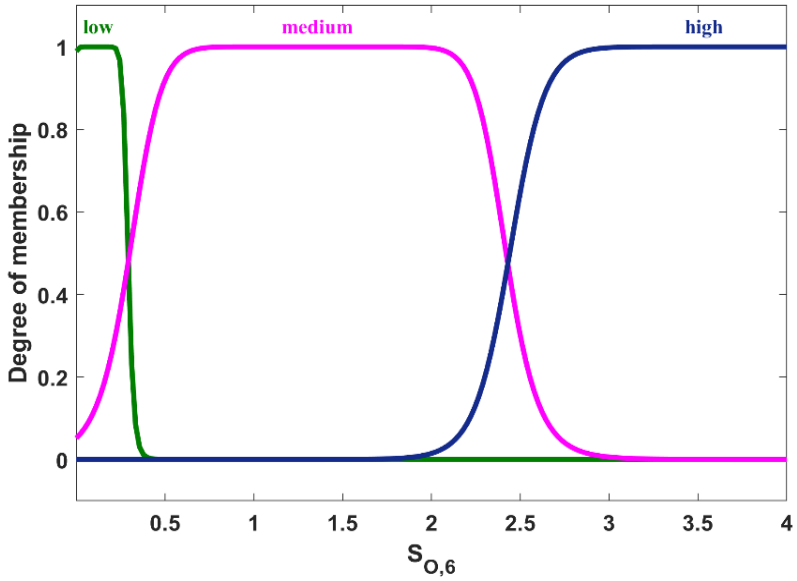

(A) Membership function of output

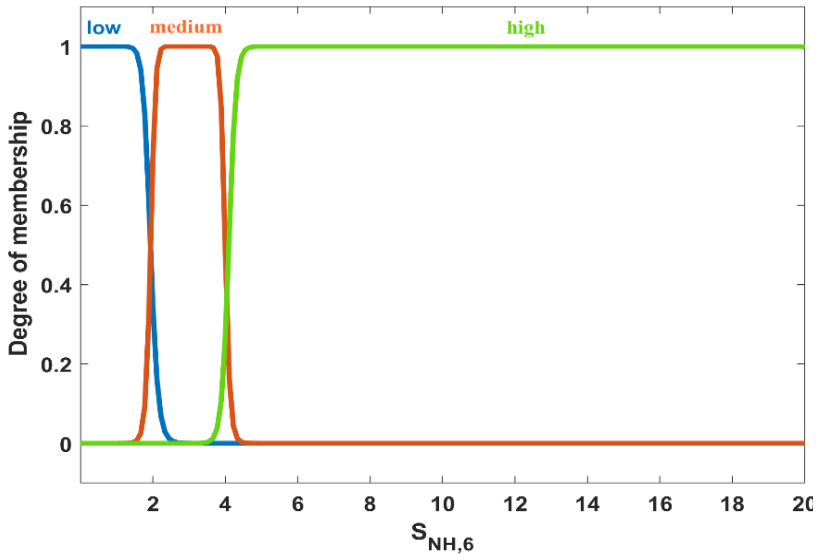

(B) Membership function of input

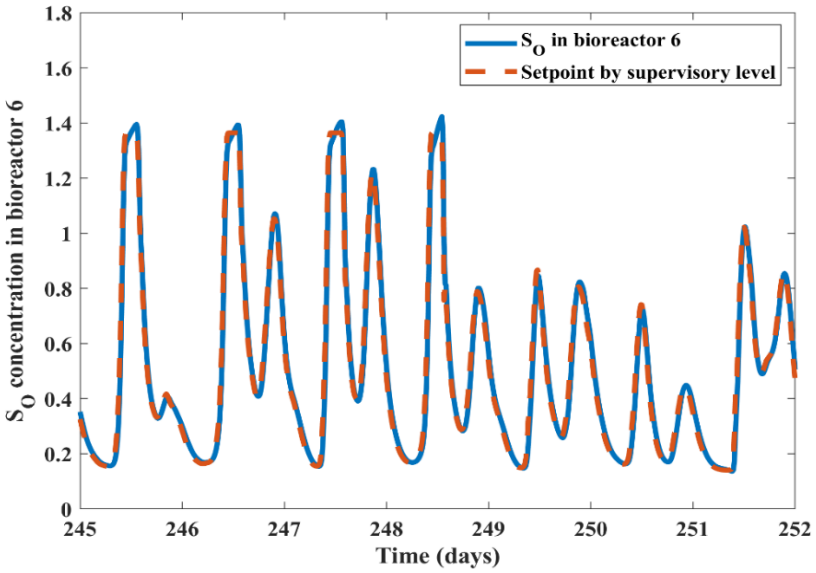

(C) corresponding tracking performance of dissolved oxygen

Figure 6.4 Membership functions rules (A) Output (B) Input and (C) corresponding tracking performance

Table 6.2 Linguistic functions and MF's for control inputs and outputs

Linguistic Variable (Output)					
Linguistic value	Range	MF	Characteristic ranges		
1	Lower	Gaussian bell-shaped shaped	0.175	5.4	0.11

2	Medium	Gaussian bell-shaped shaped	1.06	5.87	1.36
3	Higher	Gaussian bell-shaped shaped	3.56	18	6
Linguistic Variable (Input)					
Linguistic value	Range	MF	Characteristic ranges		
1	Lower	Gaussian bell-shaped shaped	1.89	9.18	0.034
2	Medium	Gaussian bell-shaped shaped	1.02	7.75	2.96
3	Higher	Gaussian bell-shaped shaped	8.26	42.2	12.36

6.2 Comparison of four control design frameworks on BSM2-P

The simulation outputs of four control designs (PI controllers, lower-level PI, supervisory-level PI/MPC, and Fuzzy) frameworks are computed. The corresponding average values of effluent concentrations are given in Table 6.3. Nitrification oxidizes ammonium to nitrate and denitrification reduces nitrate to nitrogen gas. Then a high DO improve nitrification, but an excess of nitrate perhaps is not fully denitrified in the anoxic reactors due to a lack of COD. Moreover, phosphorous removal is largely influenced by dissolved oxygen which is directly proportional to the formation of orthophosphates. From Table 6.3, on comparing with lower-level the ammonia, TP, TSS, and TN removal concentrations are improved. For ammonia, TP, TSS, and TN the removal efficiency is improved by 36%, 33.6 1.02%, and 11.3% in PI-MPC, PI-Fuzzy, PI-MPC, and PI-Fuzzy controllers respectively. Figure 6.5(D) depicts the bar harps of all the average values of energy usages like aeration, pumping, mixing, heating, consumed energies (kwh/d), and sludge production rate (kg ss/d). From the bar graph, it was observed that aeration and consumed energies are high in the case of PI-MPC and low in the case of the PI-Fuzzy controller.

The sludge production rate and heat energy are high in the PI-Fuzzy controller are reported. Compared to all controllers Fuzzy shows less aeration energy to get better nutrient removal with a slight increase in cost. On literature, it is showing that the Fuzzy control is favorable for the better removal of phosphorous. On comparing with lower-level PI, PI-Fuzzy showed an improved EQI of 21.1% with a 0.52% increase in OCI. On comparing with four control strategies there is a trade-off between OCI and EQI. Overall, in comparison with lower-level PI control ammonia is improved at PI-MPC, and TP is improved at PI-Fuzzy. In both cases, PI-MPC and PI-Fuzzy showed improved EQI with an increase of OCI. On comes to greenhouse gases like methane, hydrogen, and carbon dioxides of average production rates are reported in Table 6.3. From the

observations of the table, it is noticed that PI-fuzzy shows high methane, Hydrogen, carbon dioxide, and gas flow production rates of 28.7%, 4.87%, 6.8%, and 3.2% on comparing with lower-level PI. PI-fuzzy and PI-MPC show good outcomes for TP and ammonia in terms of percentage of violations. The percentage of violations is reported in Table 6.3. PI-Fuzzy showed good removal efficiency in the phosphorus. Moreover, PI-Fuzzy shows lower OCI with PI-MPC. The effluent concentrations of ammonia, TN, and TP are compared for all four control frameworks with their corresponding pollutant limit value are depicted in Fig.6.5(A)(B)(C), and (D). Nitrogen and phosphorous removed to the ratio of OCI is achieved high in the case of PI-Fuzzy.

Table 6.3 Comparison of average concentration values of effluent for four control strategies

Parameters	PI controllers	Lower level PI control	PI-MPC	PI-Fuzzy
S_{NH}	1.05	0.96	0.57	1.28
TSS	15.39	15.54	15.38	16.23
TN	9.07	9.81	9.86	8.7
TP	4.54	4.05	4.4	2.69
COD	42.17	42.04	42.17	41.95
BOD_5	2.43	2.42	2.45	2.50
IQI	97875.71	97875.71	97875.71	97875.71
EQI	14625.98	13715.37	14391	10824.9
Average production rates				
Methane	1029	1024	1035	1438
Hydrogen	0.00392	0.00393	0.0039	0.0041
Carbon dioxide	1504	1527	1517	1640
Gas flow	2630	2635	2646	2722
OCI	10959.1	10949	11810	11007
Average percentage of violations				
TP	86.71	72.5	70.4	38.4
S_{NH}	2.71	3.12	0.21	1.28
TSS	0.025	0.062	0.048	0.58
BOD_5	---	--	--	0.0085
$N_{removed}$/OCI	0.08131	0.0800	0.0740	0.0815

$P_{removed}$/OCI	0.01044	0.0113	0.0098	0.0139

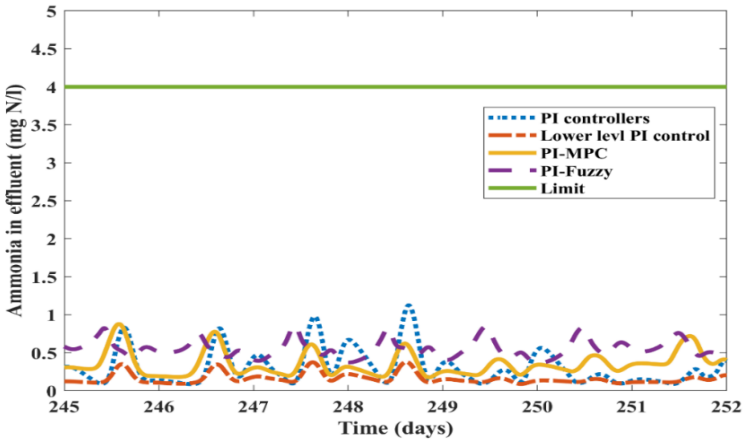

(A)

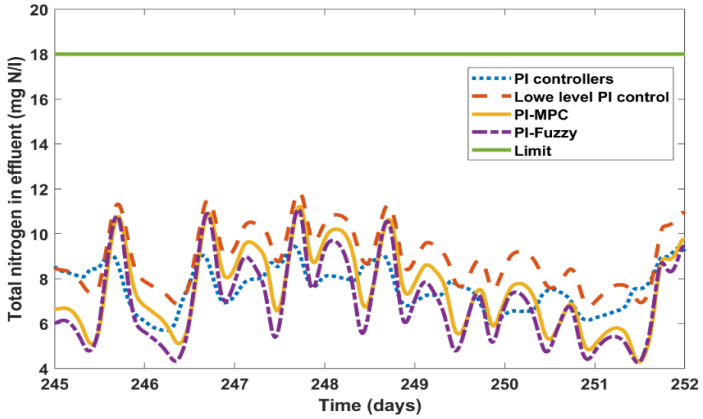

(B)

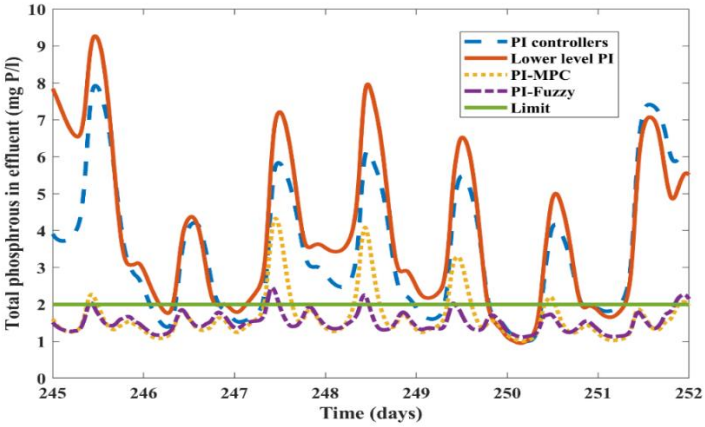

(C)

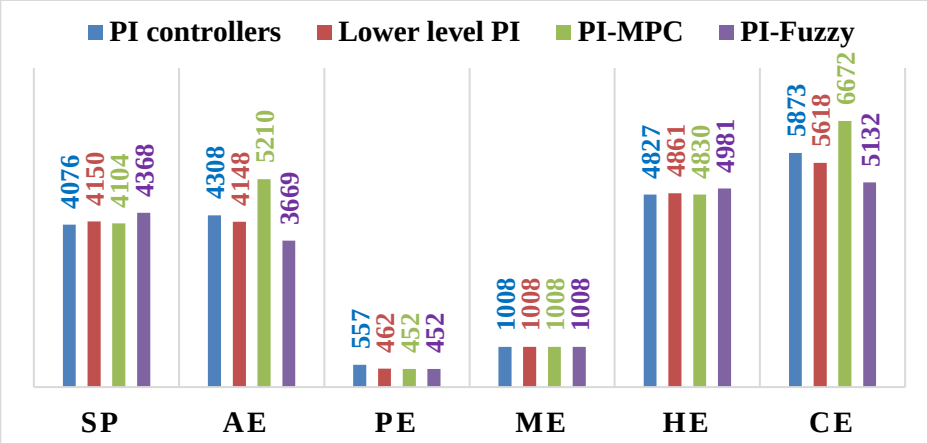

(D)

Figure 6.5 The effluent concentrations of (A) ammonia, (B) TN, (C) TP, and (D) bar graph for all the usages are compared for all four control frameworks with their corresponding pollutant limit values

PI controllers are designed to control DO by regulating the oxygen mass transfer coefficient with an additional aeration-based ammonia controller and control TSS by regulating the external recycle. The control strategy showed significant improvement in both effluent quality and operating costs. The control designs show improved EQI of 31% with decreased OCI of 6.9% with an open loop. As far as pollutant concentration is concerned, TN and TP are improved by 17% and 42.1% respectively Solon et al. (2017). In the present work, an ammonia-based aeration controller at the supervisory level is designed. By using two different control combinations, PI-MPC and PI-Fuzzy, the performance is compared with Solon et al. (2017). PI-Fuzzy showed improved EQI of 13.5% with an increase of 13.6% OCI. Phosphorus and TN removal is improved by 29.7% and 5.4% respectively with the PI-Fuzzy control framework and produced better EQI. PI-Fuzzy shows a high production rate of methane when compared to Solon et al. (2017).

6.3 Summary

A seven reactor configuration (anaerobic, anoxic, and aerobic) is used in a plant-wide level biological wastewater treatment process model (BSM2-P) to design advanced control strategies. A lower-level and supervisory-level (ABAC) design framework is made. Here PI is at a lower level whereas MPC and Fuzzy are used as a supervisory-level PI-Fuzzy showed improved effluent quality and better removal rates of phosphorus. Greenhouse gas emission production rates are high in the case of the PI-Fuzzy controller. In each control application case, there is a trade-off between EQI

and OCI. In comparison with PI (one loop), PI-Fuzzy showed an improved EQI of 21.1% with a 0.52% increase in OCI. Of all the compared outcomes, PI-Fuzzy shows better EQI and increased OCI. PI-Fuzzy showed high production rates of greenhouse gas emissions and low consumption of aeration energy. The percentage of violations of total phosphorus showed less in the case of PI-Fuzzy.

Chapter 7

Analysis of different reactors combinations and configurations for biological WWTP

Chapter 7

Analysis of different reactors combinations and configurations for biological WWTP

7.1 Evaluation of three different A^2/O processes

In this chapter, three different biological wastewater treatment processes consisting of anaerobic, anoxic, and aerobic reactors are evaluated. A^2O process (anaerobic, anoxic, and aerobic reactors with internal and external recycles), Reverse R-A^2O process (anoxic, anaerobic, and aerobic reactors with external recycle), and Inverted I-A^2O process (anoxic, anaerobic, and aerobic with internal and external recycles) are considered. Dissolved oxygen (DO) is maintained in the respective aerobic reactors using a PI controller. Furthermore, metal and carbon addition is done.

7.1.1 Biochemistry in the WWTP and biological activity

In the biological treatment section, different designs of A^2/O processes are suggested to improve both N and P removal. To achieve this, different combinations of anoxic, anaerobic, and aerobic reactors are used as a part of biological treatment with suitable reactor volumes. The ASM2d by Gernaey et al. (2004) was chosen as one of the mathematical models to illustrate the removal process of both N and P. ASM2d model with the biological P removal process is elaborated in Fig.7.1. PAO's (ploy accumulating organisms) are modeled in the cell internal system and further, all organic matter products are combined into one model structure (X_{PHA}). The growth of PAO is responsible for the X_{PHA} (polyhydroxy aldehydrates) as a substrate. Moreover, Oxygen and nitrate also influence the PAO's growth.

Anaerobic phase reactions: PAO's utilize poly-P and glycogen stored in their cells as energy sources that allow for the absorption of VFA (volatile fatty acid). VFA's are converted and retained to PHA on PAO cells. As the uptake of VFA, PAO's drop orthophosphates into the mixed liquor. PAO's do not develop in the anaerobic phase but their ability to consume food interims of VFA's provides them with a competitive advantage on bacteria.

Aerobic phase reactions: In the aerobic phase, PAO's use PHA for metabolism and cell growth as a source of carbon and energy. PAO's also restore their glycogen and ploy-P supplies in the aerobic phase. PAO's can take in excess phosphate from the mixed liquor and the EBPR process to replenish their stored polyphosphate.

First, the influent flow and return sludge enter into the anoxic section. Here denitrification is responsible for denitrifying bacteria where NO is shifted into N_2. After the anoxic section, the WW enters into the anaerobic section by a pre-denitrifying process where it largely impacts the anaerobic environment by the presence of nitrate. In the anaerobic section, the carbon matter in WW is shifted to PHA and other organic matters. The detailed mechanism of the biological P removal process included in the ASM2d model is depicted in Fig.7.1.

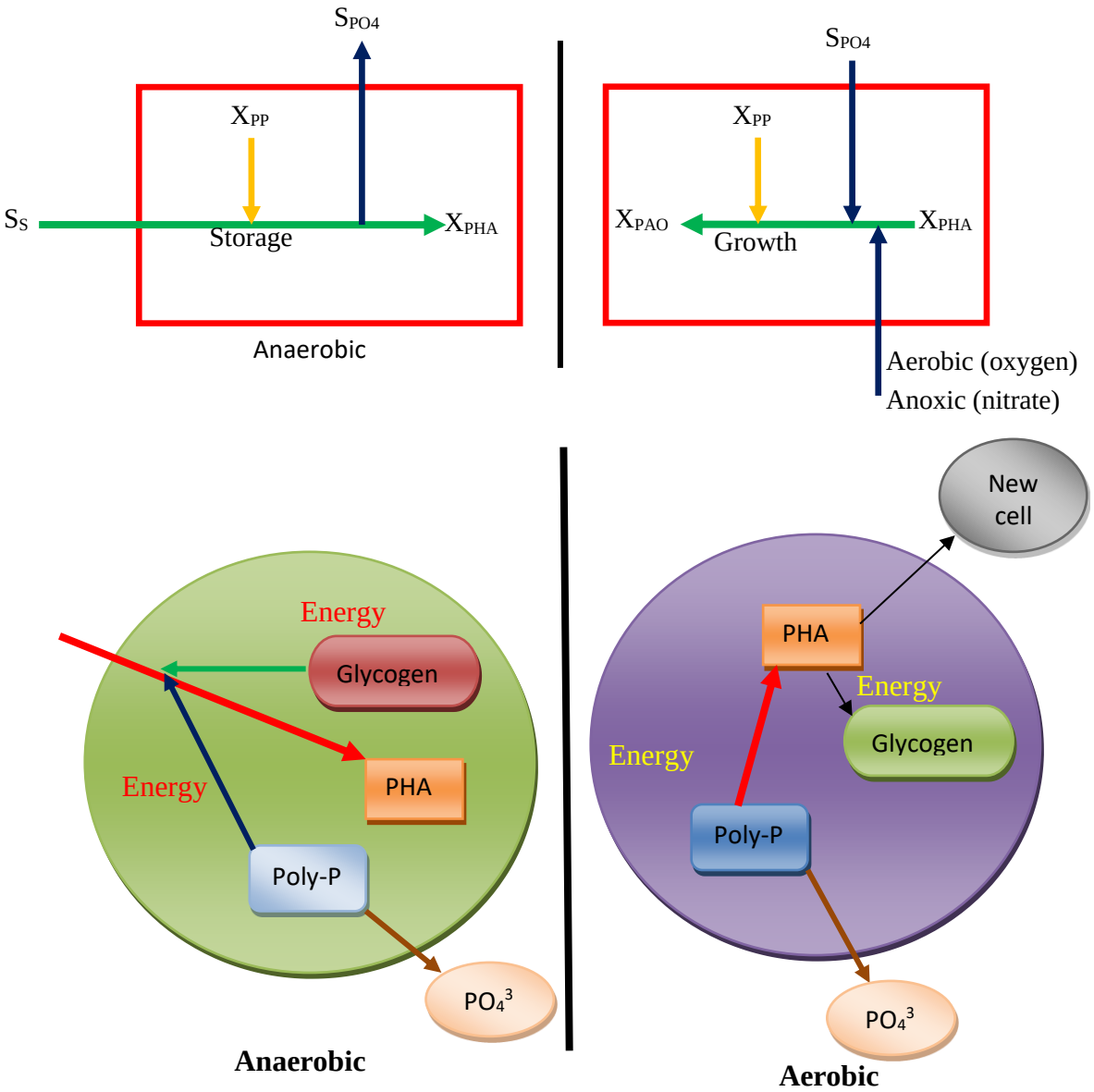

Figure 7.1 Detailed mechanism of biological P removal process included in the ASM2d model

Thus the accumulations of PHA and PAO are used to enhance the phosphorus uptake. If the PAOs directly enters into the aerobic section from the anaerobic section, the biochemical efficiency is high in the aerobic section. The enhancement of phosphorus uptake happens in the anaerobic section. This anaerobic and aerobic platform improves the N and P removal capacity based on Bo (2006).

7.1.2 Influent composition and process configurations

Model creation and simulation are performed using MATLAB/SIMULINK (Mathwork, Inc). The ASM1 model which has been used for the carbon and nitrogen removal simulation has 13 components and this model does not include the biological phosphorus process. In the ASM2d model, both N and P removal happens which consists of 19 components. The influent for the combined N and P removal simulation benchmark is based on available ASM2d influent composition is taken from Gernaey et al. (2002); Gernaey et al. (2004). The BSM1 platform consists of five bioreactors having a total volume of 5999 m^3 and the volume of the settler is 6000 m^3 which is broadly used in N removal platforms to stimulate control strategies by Copp (2002). For the extension of the model to include P removal, the ASS is replaced from ASM1 to ASM2d for P and N dynamic simulations are done based on Henze et al. (2000). To improve PAOs, anaerobic reactors are added to the BSM1-P layout according to Gernaey et al. (2004). Table 7.1 presents the process units, physical attributions, and model selection. The sedimentation tank model is represented by the non-reactive double exponential settling velocity model by Takács et al (1991). The three anoxic, aerobic, and anaerobic sections, are fully mixed but only aeration tanks are fully aerated. Kinetic parameters, oxygen mass transfer, and oxygen saturation factors are also embedded in ASM2d at 15^{o}C temperature is reported at Henze et al., (2000). Q_o and Q_e are the influent and effluent discharge labels in Fig.7.2. Different biological configurations (A) A^2/O, (B) R-A^2/O, and (C) I-A^2/O are depicted in Fig.7.2.

Table 7.1 Process units and models with physical parameters for different plant configuration

Process	Unit process	Biological process	Model	Volume (m^3)	Internal recycle (m^3/d)	External recycle (m^3/d)	Waste sludge (m^3/d)
A^2/O Fig.7.2(A)	Biological reactors	Anaerobic, anoxic,	ASM2d	6749	300%	100%	400

Gernaey et al. (2004)		and aerobic					
	Secondary Settler	Non-reactive	Takács model	6000	-------	------	-----
R-(A^2/O) Fig.7.2(B) Xie et al. (2018).	Biological reactors	Anaerobic, anoxic, and aerobic	ASM2d	6749	-------	200%	400
	Secondary Settler	Non-reactive	Takács model	6000	-------	------	-----
I-(A^2/O) Fig.7.3(C) Xu et al. (2014)	Biological reactors	Anaerobic, anoxic, and aerobic	ASM2d	6749	300%	100%	400
	Secondary Settler	Non-reactive	Takács model	6000	-------	------	-----

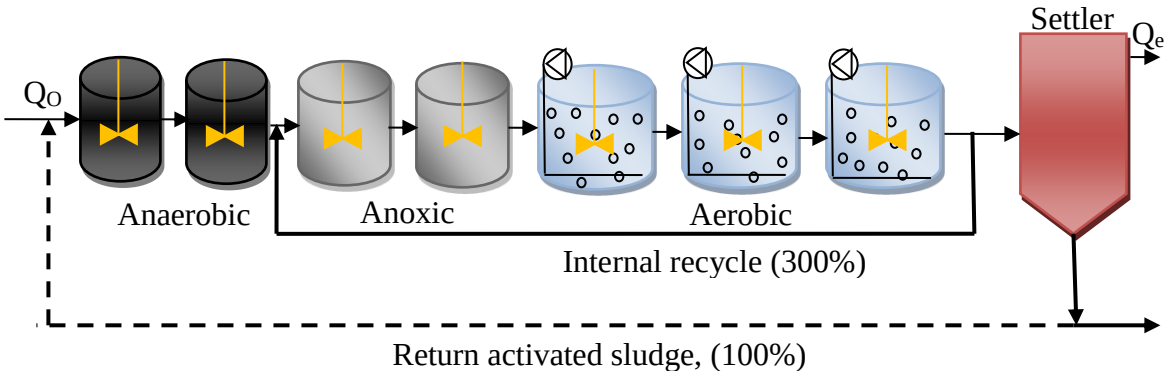

(A) A^2/O

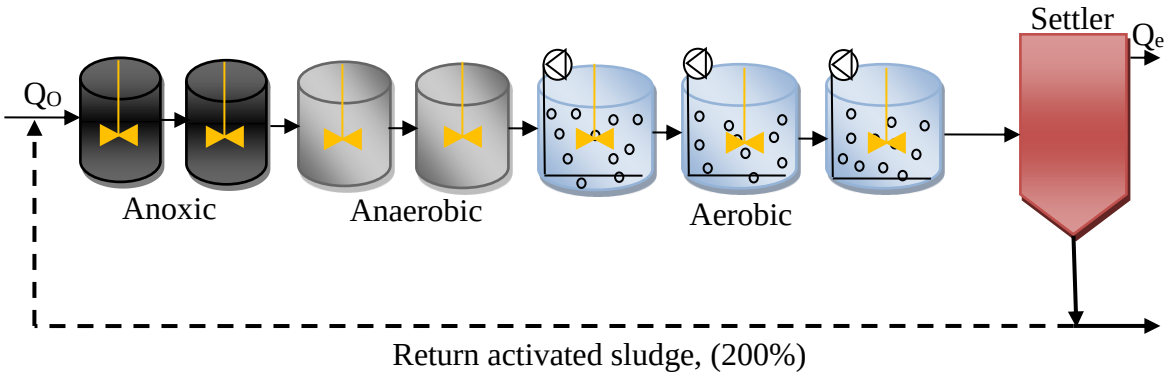

(B) R-A^2O

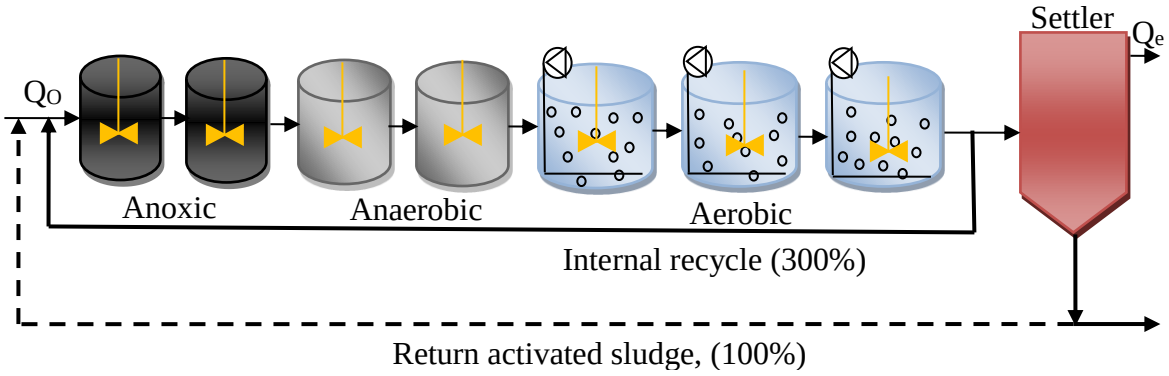

(C) I-A^2O

Figure 7.2 Different biological configurations (A) A^2/O, (B) R-A^2/O, and (C) I-A^2/O

7.1.3 Effluent quality evaluation

For the ASM2d model, the plant individual pollutant concentrations are changed but the operational cost is similar to ASM3bioP. EQI is determined as a weighted average sum of effluent concentrations. For dynamic simulation, fourteen days' data is available but the last seven days are considered as the plant performance assessment. ((Henze et al., 2000; Hongyang et al., 2018):

$$EQI = \frac{1}{1000(t_f - t_0)} \int_{t_0}^{t_f} KU_{(t)}\, Q_{e(t)} dt \qquad (7.1)$$

$$KU_{(t)} = KU_{TSS(t)} + KU_{COD(t)} + KU_{BOD(t)} + KU_{TKN(t)} + KU_{NO_3(t)} + KU_{P_{tot}(t)} \qquad (7.2)$$

The t_o and t_f in the equation. (7.1) represents the starting and ending intervals of time for computing the EQII while the KU_t notify the average load of polluted concentrations in the influent and effluent data. Generally, it consists of TSS (total suspended solids), BOD_5 (biological oxygen demand), COD (chemical oxygen demand), TKN (total kjendal nitrogen), S_{NO} (nitrate), S_{NH}

(ammonia), and TP in the equation. (7.2). Thus the corresponding expression for KU_t is given in the equation. (7.3).

$$KU_t = \beta_t G_t \quad (7.3)$$

Where β_t (g^{-1}) are weighting factors ascribe every component of the pollution. The weighting factor values are represented below. Moreover, the composition of different elements (G_t) is estimated by using the equations. (7.4) - (7.10).

The values of weighting factors are assigned each effluent component, the factors are considered as follows: $\beta_{SS} = 2, \beta_{COD} = 1, \beta_{TKN} = 20, \beta_{NO} = 10, \beta_{BOD_5} = 2, \beta_{TP} = 100$. Besides G_t, spontaneous concentrations of various nutrients are calculated corresponding to their 19 state variables:

$$G_{SS} = X_{TSS} \quad (7.4)$$

$$G_{COD} = S_F + S_A + S_I + X_I + X_S + X_H + X_{PAO} + X_{PHA} + X_A \quad (7.5)$$

$$G_{BOD} = 0.25\left(S_F + S_A + \left(1 - f_{S_i}\right)X_S + \left(1 - f_{XI_H}\right)X_H + \left(1 - f_{XI_P}\right)(X_{PAO} + X_{PHA}) + \left(1 - f_{XI_A}\right)X_A\right) \quad (7.6)$$

$$G_{TKN} = S_{NH} + i_{P,S_F}S_F + i_{P,S_A}S_A + i_{N,S_I}S_I + i_{N,X_I}X_I + i_{N,X_S}X_S + i_{N,BM}(X_H + X_{PAO} + X_A) \quad (7.7)$$

$$G_{N_{tot}} = G_{TKN} + G_{NO_3} \quad (7.8)$$

$$G_{NO_3} = S_{NO_3} \quad (7.9)$$

$$G_{P_{tot}} = S_{PO_4} + i_{P,S_F}S_F + i_{P,S_A}S_A + i_{P,X_I}X_I + i_{P,X_S}X_S + i_{P,BM}(X_H + X_{PAO} + X_A) + X_{PP} + \left(\frac{1}{4.87}\right) \quad (7.10)$$

7.2 Analysis of three processes R-A^2/O, A^2/O, and I- A^2/O

A comparative analysis on three combinations like A^2/O, R-A^2/O, and I-A^2/O with average pollutant concentrations, EQI, OCI, and percentage of violations are tabulated in Table 7.2. On comparing two processes R-A^2/O is having the optimized OCI with EQI. The average nutrient concentrations (TN, TP, S_{NH}) are shown in Table 7.2. Which notify the best removal efficiency is found in R-A^{2}O. The compared results of the last seven days are depicted in Fig.7.3 (A), (B), and (C). But in comparison, in R-A^{2}O, TSS is high, which leads to a slightly high EQI when compared to that of A^2/O. Note that the R-A^{2}O process is dealing with only external recycle whereas the other two processes are having internal and external recycles which causes high OCI.

On comparing EQI and OCI, the R-A^2O process shows a low OCI of 4.2% in comparison with A^2O. On comparing the percentage of violations between A^2/O and R-A^2/O, TP and ammonia removal is improved by 32.2% and 14.2% respectively. On seeing Table 7.2, R-A^2O shows a lower cost with better efficient quality in terms of nutrient removal of TP and ammonia. Based on this, R-A^2O is chosen as a research platform for further applications in WWTP.

Table 7.2 Average pollutant concentrations and operational costs of A^2/O, R-A^2/O, and I-A^2/O

Parameters	A^2/O	R- A^2/O	I- A^2/O
S_{NH}	6.354	4.73	6.22
TSS	14.90	17.13	14.06
TN	15.21	15.68	14.08
TP	3.75	2.98	8.400
COD	46.12	48.51	46.91
BOD_5	2.47	2.74	2.56
IQI	56776.9	56776.9	56776.9
EQI	5087.11	5220.01	7199.96
Performance plant assessment			
SP	3636.79	3518.43	3251.51
AE	2843.73	2843.73	2843.73
PE	388.92	315.13	388.92
ME	489.96	489.96	489.96
OCI	20561.87	19695.14	20710.78
Percentage of violations (%)			
TP	91.66	62.20	100
TN	7.29	10.26	0.744
S_{NH}	68.15	58.48	68.00

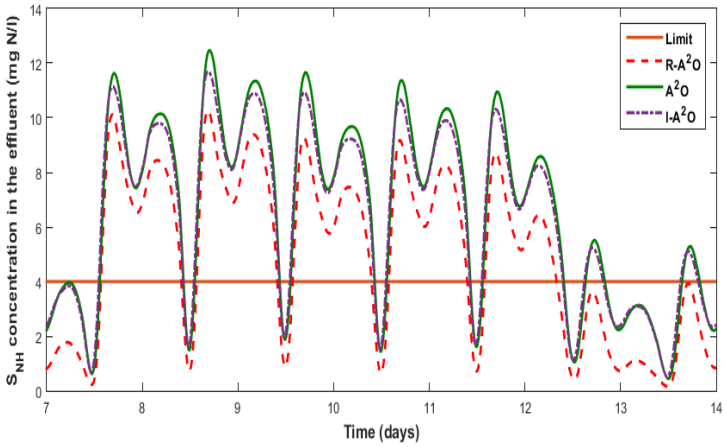

(A) Ammonia concentration

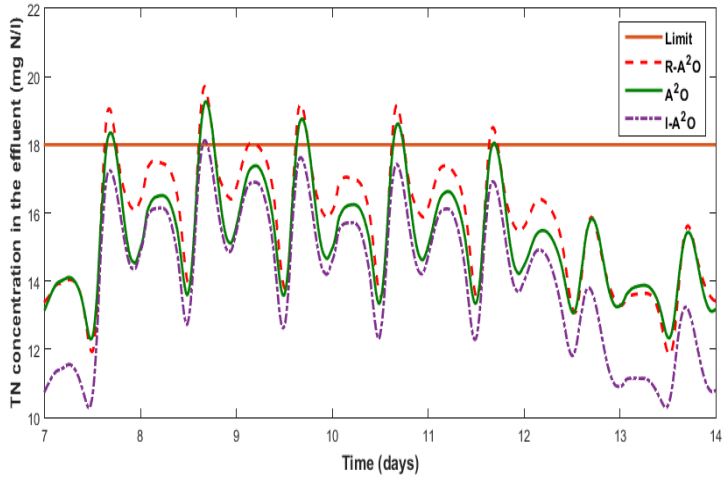

(B) Total nitrogen concentration

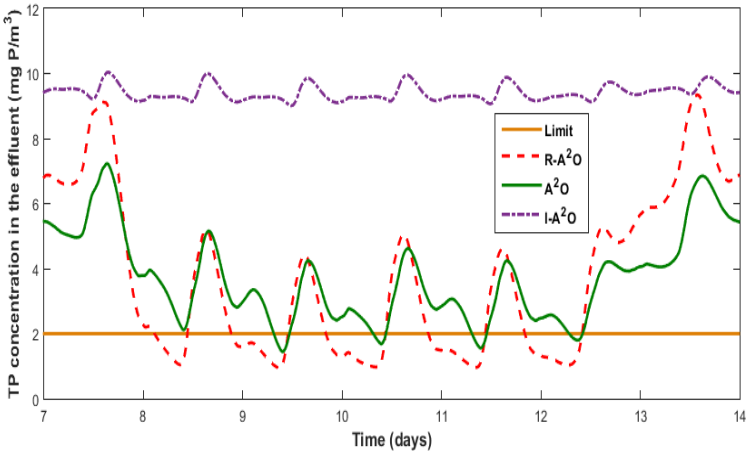

(C) Total phosphorous concentration

Figure 7.3 Ammonia, TN, and TP concentrations of A^2/O, R-A^2/O, and I-A^2/O

7.2.1 Carbon source addition (CA) in R-A^2/O

If CA is carried out in the first anaerobic reactor, then improved results in terms of enhanced efficiency for the removal of nutrients are obtained. Carbon addition in the R-A^2/O platform is depicted in Fig.7.4 (A). CA is usually carried out by adding carbon mass from 100 to 400 kgCOD/d is tabulated in the appendix Table E1. On the increase of carbon source, the OCI increases with the decrease of EQI as depicted in Fig.7.4 (B). Drastic changes in TSS and sludge production are observed with an increase in the carbon load. It is slightly impacting the rate of TN and ammonia. Different dosing methods for the addition of carbon sources through peristaltic pumps are studied in order to optimize the nutrient removal efficiencies with low carbon sources for urban domestic wastewater in the A^2/O system. From the bar graphs of Fig.7.4 (C), it can be noted that TP is lower on increasing the carbon loading whereas other pollutants are contradictory with (TN, ammonia, TSS, and COD) slight increase. Appendix Table E1 represents the average effluent data with increased carbon addition in R-A^2/O.

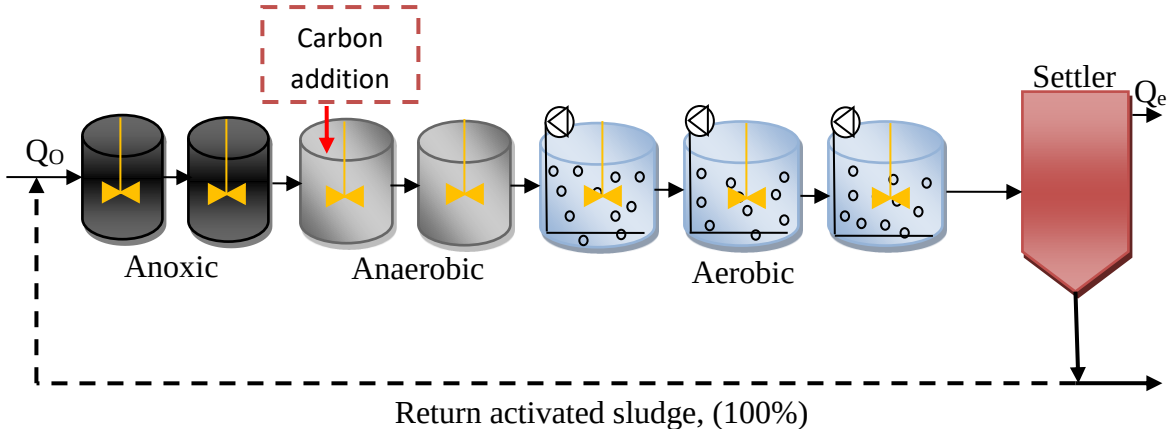

(A) Addition of carbon source in R-A^2/O

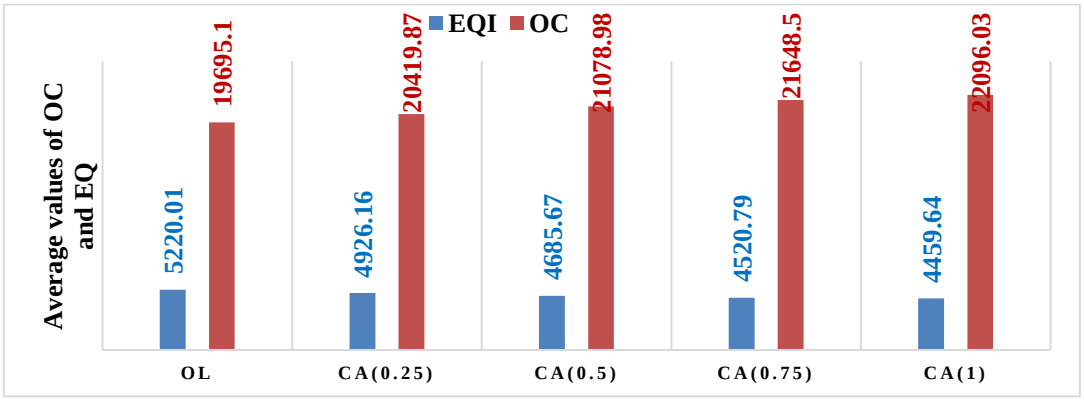

(B) EQI and OCI changes with increased dosages of carbon loading

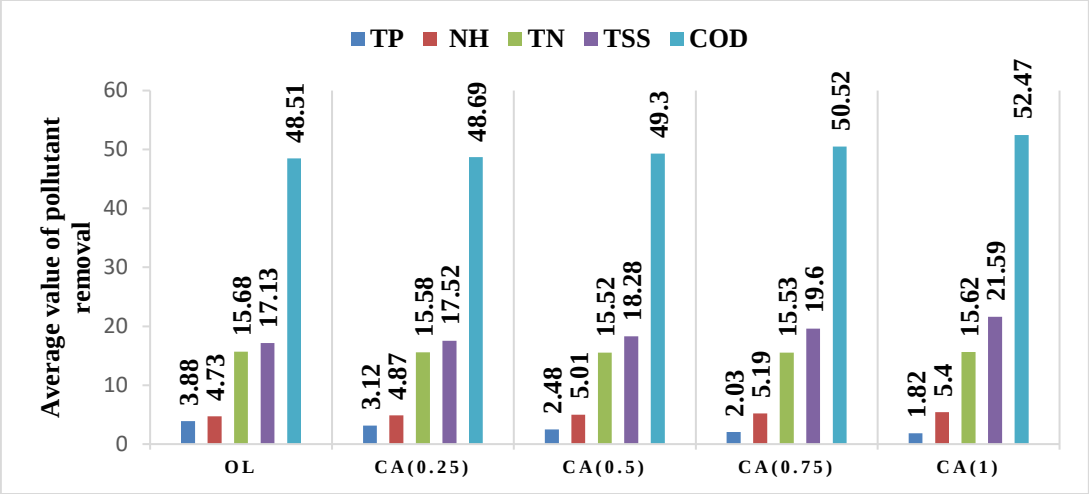

(C) Comparative analysis of pollutant removal with increased carbon dosages

Figure 7.4 (A) CA in R-A^{2}O process (B) Comparison of EQI and OCI (C) Comparison of pollutant removal

7.2.2 Metal load addition (MA) in R-A^2/O

MA in the last aerobic reactor showed the optimized result in terms of better efficiency for the removal of nutrients. Metal addition in the R-A^2/O platform is depicted in the appendix Fig. E2. Fig.7.5 (A) depicts the metal combination of both CA+MA in the R-A^2/O platform. Metal loading is carried out by adding metal mass from 250 to 1000 kgCOD/d is tabulated in the appendix Table E3. On the increase of metal sources, the OCI increases, and EQI decreases. Drastic changes in TSS and sludge production are observed with an increase in metal load. It is slightly impacting the rate of TN and ammonia. Loading of both carbon (400) and metal (1000) source in the R-A^{2}O shows the best removal efficiency of nutrients like ammonia, TN, and TP respectively.

From the bar graph in Fig.7.5 (B), it can be analyzed that TP is less when there is an increase in metal loading. But the combination of MA+CA maintaining the corresponding masses as 1000 and 400 kgCOD/d shows a slight increase in COD and TSS. On the other hand, other pollutants are decreased on comparing with MA dosages as shown in Fig.7.5 (B). A tradeoff between the EQI and OCI can be observed from these results. The effect on sludge production, OCI, and EQI is depicted in Fig.7.5 (C).

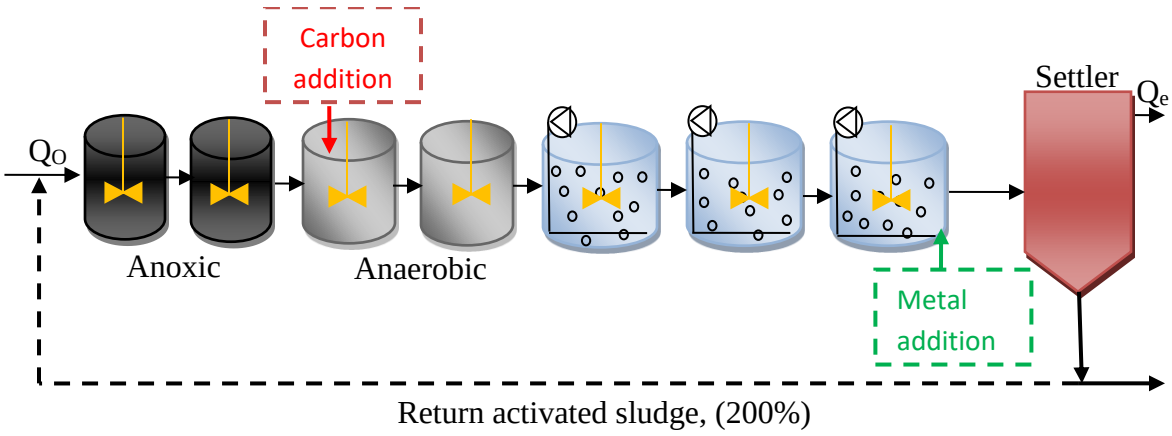

(A) Addition of carbon and metal source in R-A^2/O

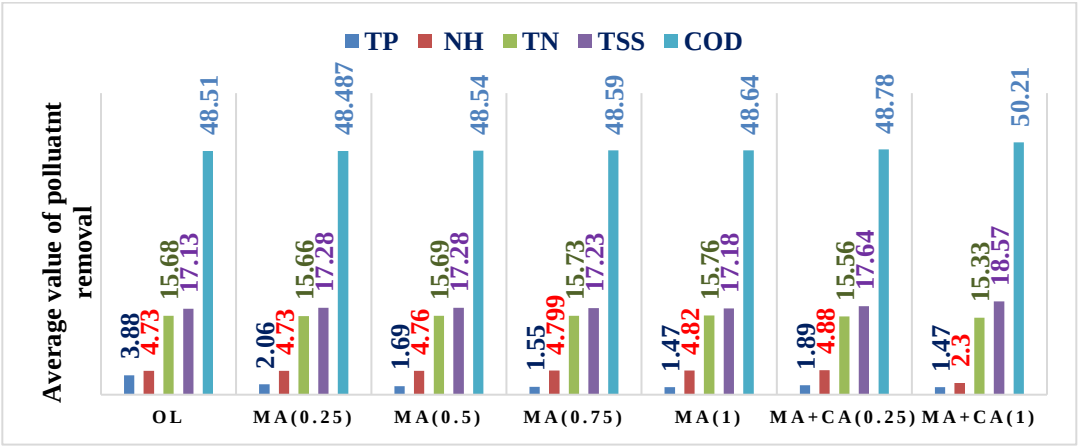

(B) Combined metal and carbon addition sources with corresponding pollutant removal

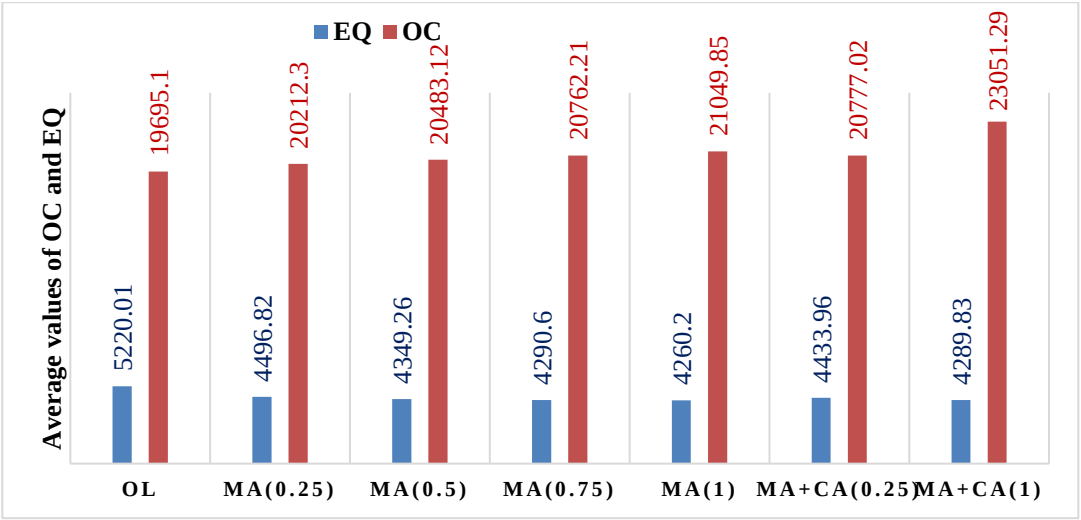

(C) Combined metal and carbon addition sources with corresponding OCI and EQI

Figure 7.5 (A) MA and CA in R-A^2O process (B) Comparison of EQI and OCI (C) Comparison of pollutant removal

7.2.3 Control of DO in the presence of metal and carbon additions

With the feedback controllers for maintenance of DO and S_{NO}, there is no significant effect on the effluent quality in the R–A^2O process. Whereas, it is not possible to control S_{NO} as no internal recycling is available to maintain the nitrification rate. The application of DO control schemes of the last three aerobic reactors with metal and carbon addition is depicted in Fig.7.6 (A). It is noticed that the average composition of P is largely influenced by DO which is directly proportional to the formation of orthophosphates which leads to the P. DO setpoint 2 gO_2/m^3 is regulated by manipulating the set point of K_La_5, K_La_6, and K_La_7 in the last three reactors. Identified models for controller design are reported in Appendix E. In this scheme, three PI control strategies are designed independently with model-based data. The system identification technique is used to develop linear models for both the loops with open-loop data. For this, 10% of random signals of variance with the value of K_La_5, K_La_6, and K_La_7 of 325, 222, and 120 m^3/d respectively are given in the DO. Additionally, metal and carbon source dosages are added to check how the EQI and OCI will impact the process and the corresponding layouts and tables are given in appendix E3.

In the DO application, ammonia & TN removal efficiency is very good but it is contradictory towards phosphorous removal is tabulated in the appendix E3. Fig.7.6 (C) depicts that ammonia is very low while maintaining the setpoint 2 gO_2/m^3 for DO in the last three reactors. If the DO setpoint is considered as 1,1 and 2 gO_2/m^3 (DO(1,1,2)), then improved results are obtained when compared to DO(2,2,2) Control. DO Control application with CA shows better removal of TN and ammonia. Moreover, MA is accountable for the better P removal as depicted in Fig.7.6(C). Fig.7.6(B) depicts the DO(2,2,2) control showing the higher aeration energy usage and increased EQI and OCI which is contradictory when compared to DO(1,1,2). In addition to both MA and CA and on maintaining the mass (1000 and 400 kgCOD/d) with DO(1,1,2) application, it shows high nutrient removal efficiency with high OCI. For the Appendix E from Figs. E1, E2, and E3 represent the three DO control applications, three DO control applications with metal and carbon addition. Appendix Table E3 represent the average effluent data with three DO control strategies with additional carbon and metal addition in R-A^2/O.

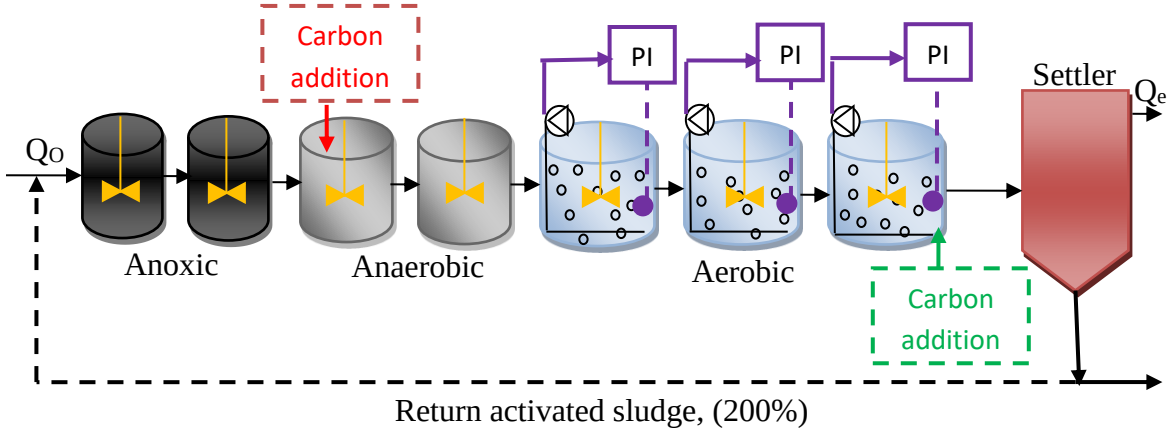

(A) Combined metal and carbon addition sources with three DO control loops

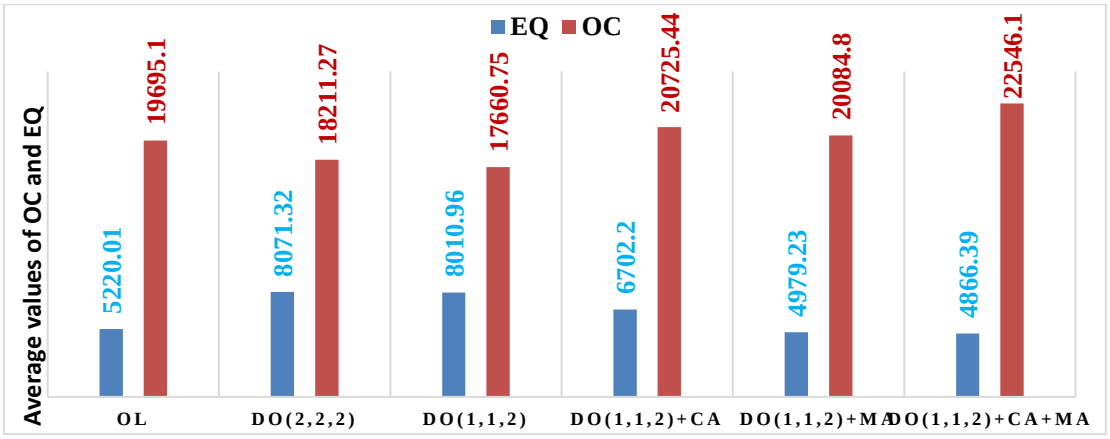

(B) Three DO control loops and addition of carbon and metal dosages of OCI and EQI

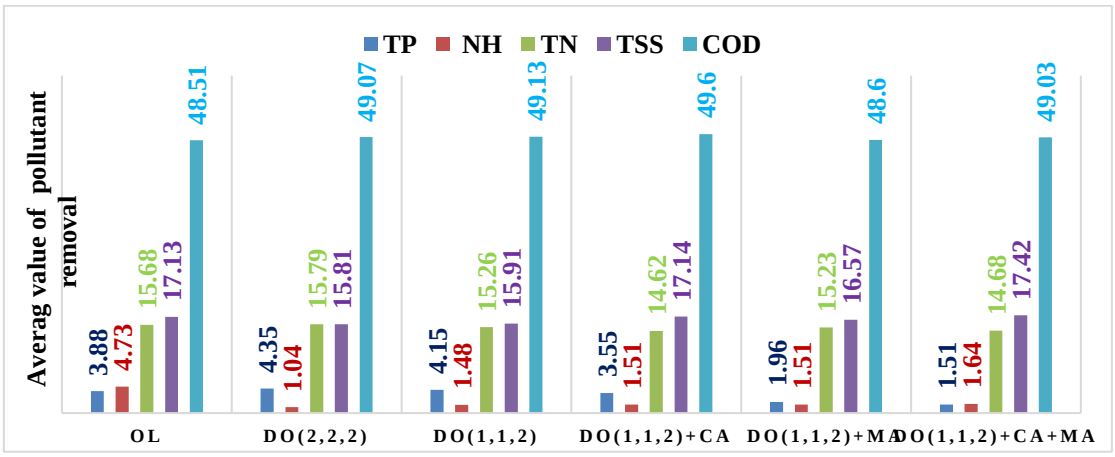

(C) Pollutant removal with three DO control loops and addition of carbon and metal dosages

Figure 7.6 (A) Three DO control loops and addition of carbon and metal dosages layout (B) Comparison of EQI and OCI (C) Comparison of pollutant removal

7.3 Overall comparative analysis on MA, CA, and DO control application

The overall comparisons of R-A^2/O, CA, MA, and control applications are given in Table 7.3. From Table 7.3, it can be observed that the application of three DO control loops with the addition of CA and MA shows better EQI and slight variations in OC. DO(1,1,2)+MA and CA application leads to less operational cost.

Table 7.3 Overall comparative analysis with carbon, metal additions, and DO control loops

Average concentration	Open loop (R-A^2/O)	CA 1(m^3/d)	MA 1(m^3/d)	MA and CA 1 (m^3/d)	$DO_{1,1,2}$ + MA and CA
S_{NH}	4.73	5.40	4.82	2.30	1.64
TSS	17.13	21.59	17.18	18.57	17.42
TN	15.68	15.62	15.76	15.33	14.68
TP	3.88	1.82	1.47	1.47	1.51
COD	48.51	52.47	48.64	50.21	49.03
BOD5	2.74	3.42	2.76	3.08	2.79
Carbon added	0	400	0	400	400
Metal added	0	0	1000	1000	1000
IQI	56766.9	56766.9	56766.9	56766.9	56766.9
EQI	5220.01	4459.64	4260.20	4289.83	4066.39
Performance plant assessment					
SP	3518.43	3839.19	3490.33	3609.14	3548.74
AE	2843.73	2843.73	2843.73	2843.73	2870.17
PE	315.13	315.13	315.13	315.13	323.45
ME	489.96	489.96	489.96	489.96	489.96
OCI	19695.1	22096.03	21049.85	23051.29	22546.10
Percentage of violations (%)					
TP	62.20	23.36	----	0.744	11.01
TN	10.26	11.60	11.75	7.73	11.60
S_{NH}	58.48	61.54	58.69	61.30	-----

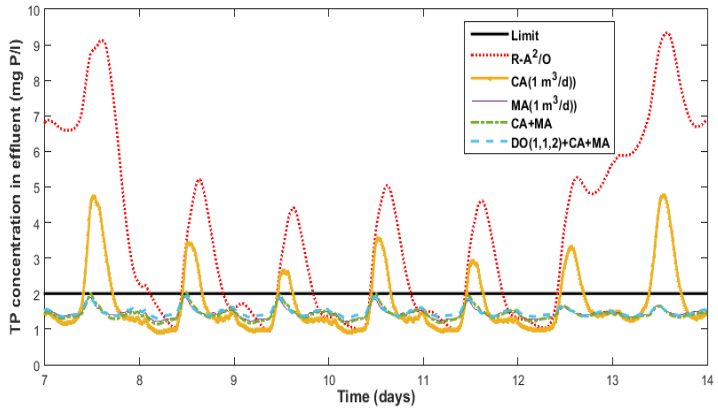

(A) TP concentration

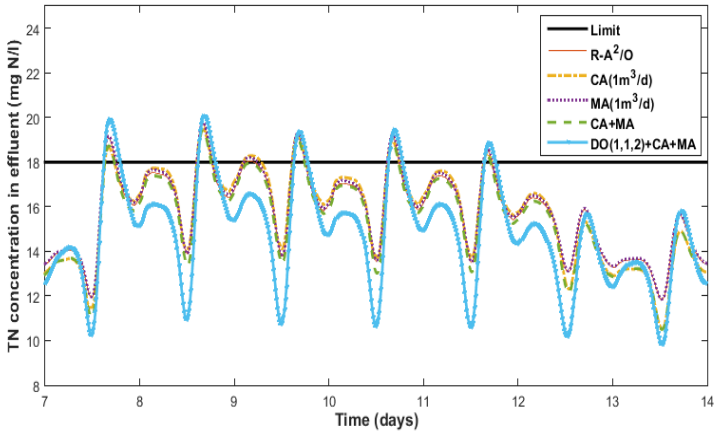

(B) TN concentration

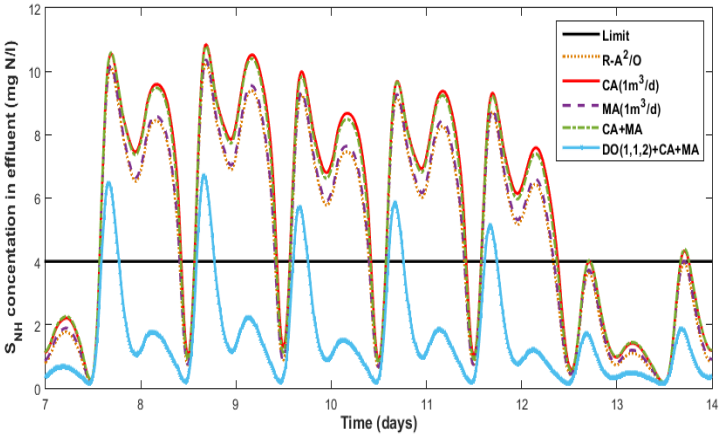

(C) Ammonia concentration

Figure 7.7 Overall comparative analyses on carbon, metal, and control loop applications with Ammonia, TN, and TP concentrations

Maintaining the DO setpoint range affects the economy in the aeration and pumping energy and the DO rate is also largely affecting the ammonia and it is almost negligible in the percentage of the violation. Different combinations of these applications with nutrient removal (TN, TP, and ammonia) are depicted in Fig.7.7 (A) (B) and (C). DO is responsible for high phosphorus violations but the addition of CA+MA causes the impact with efficient removal of TN and TP. On comparing the percentage of violations between R-A^2/O (open loop) and R-A^2/O with DO(1,1,2)+MA and CA, TP removal is improved by 82.3%. EQI is improved by 22.2% with an increased OCI of 12.6%.

7.3.1 Effect of temperature on the kinetic parameters

In this temperature analysis, three temperatures (10, 15, and 20^{o}C) are tested with respect to kinetic parameters. Hereby mainly targeting the autotrophic, heterotrophic, and ploy accumulating organisms, hydrolysis the growth and decay rates are changed based on their temperature. The kinetic parameters by varying temperature are mentioned in Henze et al. (2000); Gernaey et al. (2004). At 10^{o}C the results showed high violations and average pollutant concentration of ammonia, TN, and TSS where the microbes are functionally inactive for this particular temperature.

From Table 7.4, on comparing the two temperatures at 15 and 20^{o}C at the same data profiles, both EQI and OCI are good at 20^{o}C. As far as violations and average pollutant concentrations, nutrient removal efficiencies are better at 20^{o}C on comparing with 15^{o}C. The percentage of violations shows TP and TN removal efficiencies are contradictory in the range of 15 and 20^{o}C. On the other hand, ammonia is negligible at temperature 20^{o}C.

Table 7.4 Changing of temperature with respect to kinetic parameters

Parameters	10^{o}C	15^{o}C	20^{o}C
S_{NH}	12.22	4.73	2.55
TSS	20.16	17.13	16.02
TN	21.22	15.68	9.91
TP	3.16	3.88	2.39
COD	51.54	48.51	46.44
BOD_5	3.40	2.74	2.03

IQI	56776.9	56776.9	56776.9
EQI	6802.34	5220.01	4871.88
Performance plant assessment			
SP	3773.38	3518.43	3112.94
OCI	20696.09	19695.14	17769.59
Percentage of violations (%)			
TP	60.74	62.20	40.47
TN	96.27	10.26	25.59
S_{NH}	100	58.48	----
TSS	1.78	----	----

7.4 Summary

In this chapter, the comparative analysis on A^2O, R-A^2O, and I-A^2O are tested and it is found that R-A^2O shows the optimized results in OCI with slight high EQI. Hence, R-A^2O is taken as a benchmark and tested with different applications like carbon loading, metal loading, and control approaches to know how it will impact the EQI and OCI. It is noticed that the increase of metal and carbon dosages leads to lower EQI and higher OCI with better removal of nutrients. On comparing effluent quality (EQI) and operational cost (OCI), the R-A^2O process shows a low OC of 4.2% in comparison with A^2O with improved TP removal of 32.2%. The combination of both metal and carbon loading simultaneously in the process shows better efficient nutrient removal. The combination of DO control with metal and carbon additions resulted in optimized results in terms of EQI and nutrient (TN, TP, and ammonia) removal. EQI is improved by 22.2% with an increased OCI of 12.6% in comparison with the open-loop. Furthermore, the temperature is tested with three different ranges like 10, 15, and 20^oC with respect to changing kinetic parameters. These temperature analyses are tested with the same influent profile at 20^oC representing the best nutrient removal efficiency with lower operational cost.

Chapter 8

Effect of temperature on WWTPs

Chapter 8
Effect of temperature in biological wastewater treatment plants

The effect of temperature on the phosphorous, nitrogen, and organic matter removal in an activated sludge system (ASS) is assessed in this research. Benchmark Simulation Model No.1 (BSM1-P) with an ASS (ASM3bioP) is used and the temperature is chosen between 10°C to 35°C. The kinetic expressions for the maximum growth rate of heterotrophic biomass, autotrophic, and phosphate accumulating organisms and their decay rate are considered.

8.1 Model-based analysis of the effect of temperature on activated sludge process (BSM1-P)

The analysis of kinetic and stoichiometry parameters is considered to be a key role in optimizing the WWTP in terms of modeling, design, and enhancing the improvement of WWTP biologically. These parameters are highly dependent on the temperature and the sensitivity of biomass. In this study, the ASM3bioP model is executed in Matlab/Simulink environment by Solon (2015). The ASM3bioP model comprises 17 state variables that are related to the stoichiometric and kinetic variables to perform all twenty-three processes relating to anaerobic, anoxic, and aerobic decay of autotrophs and heterotrophs, growth of autotrophs and heterotrophs, hydrolysis, ammonification, and phosphorous uptake. The kinetic and stoichiometric parameters affected by temperature are evaluated at different temperatures and are given below equation (8.1) by Gernaey et al. (2014).

$$\theta_T = \theta_{T_{ref}} . \exp\left(\left(ln\left(\frac{\theta_{T_{ref}}}{z}\right)/5\right).\left(T - T_{ref}\right)\right) \quad (8.1)$$

Where θ_T the parameter value of temperature at T is, $\theta_{T_{ref}}$ is the measure of the parameter at a reference temperature T_{ref} and z is the temperature co-efficient. A reference temperature of 20ºC is considered by Rieger et al. (2002) and the variables are analyzed within the range of 10ºC-35ºC by changing the temperature values. The kinetic parameters selected to investigate the effect of temperature coefficients (TC) are given below:

Maximum heterotrophic growth rate (μ_{mH})

Maximum autotrophic growth rate (μ_{mA})

Heterotrophic decay rate(b_H)

Autotrophic decay rate (b_A)

Maximum growth rate of X_PAO (mu_{PAO})

Endogenous respiration rate of X_PAO (b_{PAO})

8.1.1 Effect of Temperature co-efficient on effluent quality

From the literature, it was observed that the kinetic parameters significantly affect the effluent quality. It is noted from equation (8.1) that the kinetic parameters strongly rely on the measure of temperature co-efficient 'z'. Thus, it is imperative to assess the impact of TC in detail. The range of 'z' chosen for kinetic parameters are:

μ_{mH}, 0.8 <z< 8

μ_{mA}, 0.6<z< 2

b_H, 0.05 <z< 1

b_A, 0.14 <z< 0.3

mu_{PAO}, 0.7 <z< 2

b_{PAO}, 0.08<z< 0.6

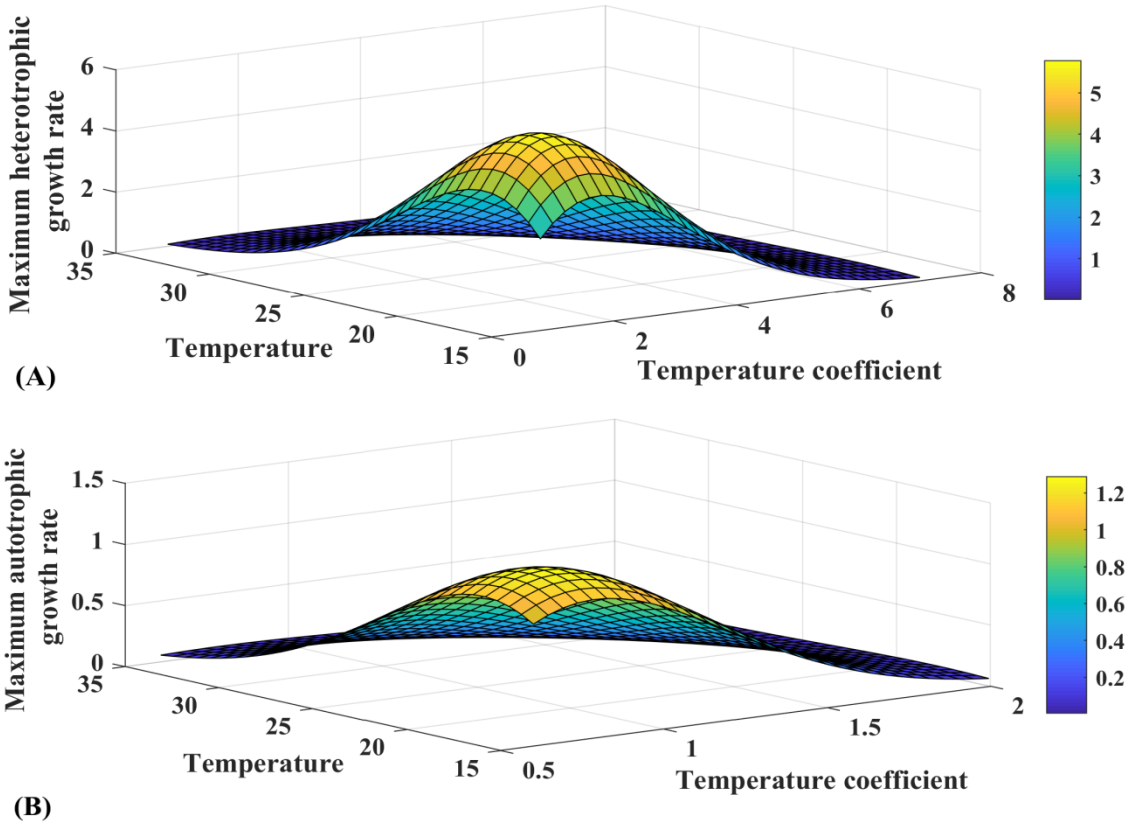

Figure 8.1 Effect of temperature and temperature co-efficient on (A) μ_{mH} and (B) μ_{mA}

By varying 'z' in these ranges and temperature between 15 – 35°C, simulations are carried out to understand the effect of this change on the kinetic parameters like μ_{mH},

$\mu_{mA}, b_H, b_A, mu_{PAO}, and\ b_{PAO}$. The corresponding graphs of μ_{mH} and μ_{mA} are shown in Fig.8.1 (A) and Fig.8.2 (B). It is observed that the kinetic parameters have shown the highest values between 15 –25°C and then observed decaying until 35°C and 10°C. The kinetic parameters are computed for the associating temperature co-efficient using equation (8.1) and the EQI is observed for individual values. Table 8.1 represents the effluent quality having both state and composite variables when the temperature coefficient is varied between 0.8–8 when the maximum heterotrophic growth rate is determined at 25°C.

8.1.2 Simulation results

The resultant variations in effluent quality and concentrations of $\mu_{mH}\ and\ \mu_{mA}$ at various temperatures are depicted in Figs. 8.1 (A) and 8.1 (B). Based on this other parameters are also found. For different temperatures, at 15°C, the EQI and TP are decreasing but at other higher temperature points (23 to 30°C) the EQI and TP are increasing by varying the TC from 0.8 – 8 and the corresponding graphs are depicted in Fig.8.2 (A) and (B).

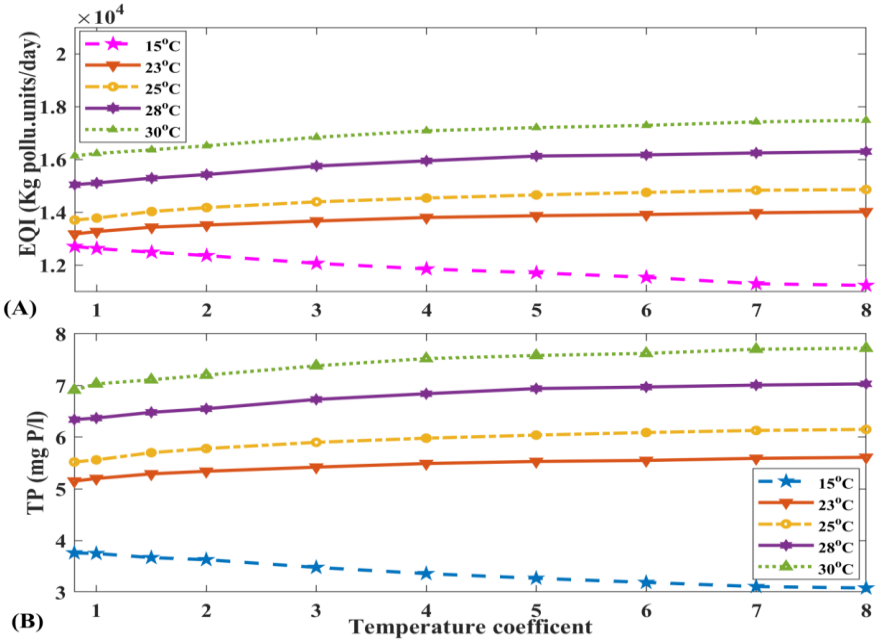

Figure 8.2 Effect of μ_{mA} at different temperatures on (A) EQI (B) and Total phosphorus

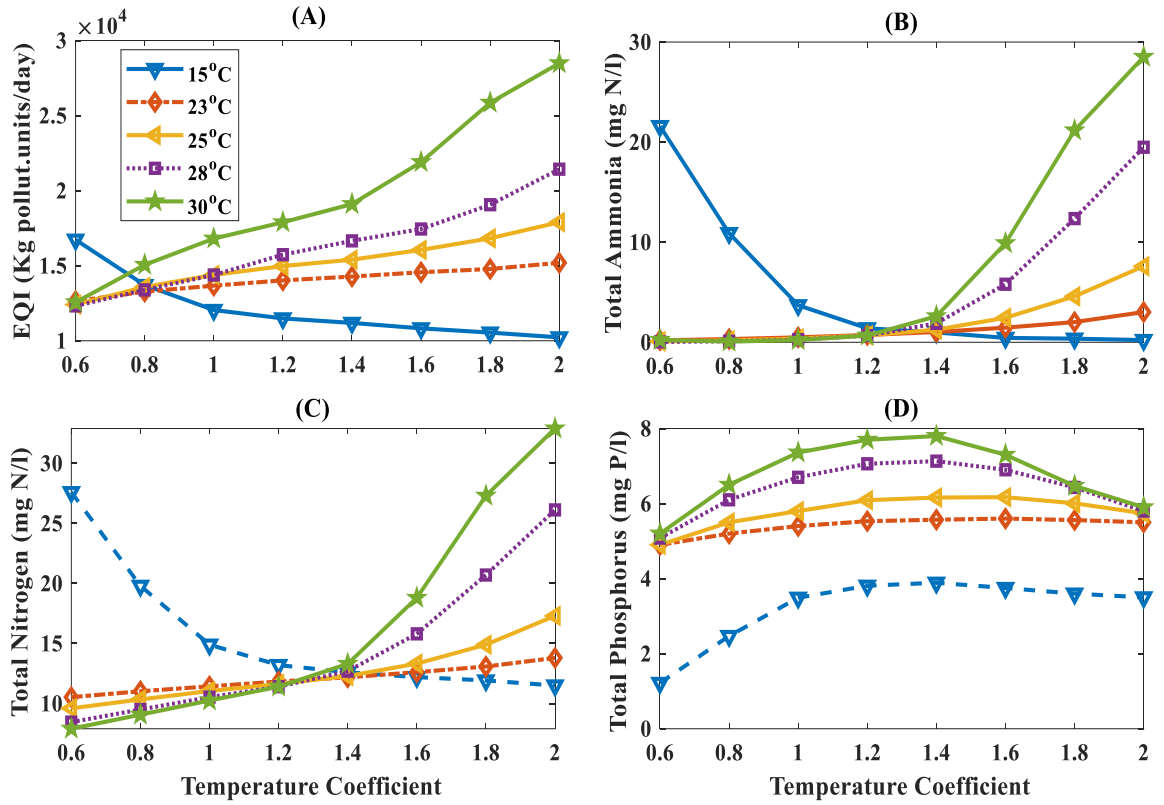

Figure 8.3 Effect of μ_{mH} at different temperatures on (A) EQI (B) Ammonia (C) Total nitrogen and (D) Total phosphorus

Effect of μ_{mA} at different temperatures by varying TC (0.6 to 2) and the corresponding nutrient removals are depicted in Fig.8.3(A), (B) (C) and (D). On seeing the graphs, at 15°C, the EQI, ammonia, and TN shows higher removal rate at the initial stages but as TC increases the corresponding removal rate is also improved. For other higher temperature measures (23 to 30°C) the removal rate is initially low but as there is a rise in TC the removal rate decreased. In TP, at 15°C the removal rate is much less than other temperature measures (23 to 30°C). EQI is directly proportional to the nutrient removal rate. So, if the rate of nutrient (C, N, and P) removal rate increases, then the EQI is also enhanced.

Further, corresponding decay rates (b_H and b_A) are also tabulated in Table 8.1. The effect of temperature coefficient for different compositions at various temperatures is depicted in Figs. 8.4 and 8.5. Effect of b_H at different temperatures by varying TC (0.05 to 1) and the corresponding nutrient removals are depicted in Fig.8.4(A), (B) (C) and (D). On seeing the graphs, at 15°C, the EQI, ammonia, and TN show a higher removal rate at the initial stages but as TC increases the

corresponding nutrient removal is improved. For other higher temperature measures (23 and 25^{o}C) the removal capacity is initially low but as there is a rise in TC the nutrient removal is enhanced. On the other hand, at 28 and 30^{o}C show lower nutrient removal rate is noticed on comparing with other temperatures.

Table 8.1 Effect of z on EQI when μ_{mH} is evaluated at 25°C

Tem co-eff →	0.8	1	1.5	2	3	4	5	6	7	8
Variables ↓	State variables									
S_O	1.99	1.99	1.98	1.9799	1.989	1.9894	1.977	1.9747	1.9592	1.94
S_S	0.13	0.13	0.135	0.1345	0.1339	0.1334	0.133	0.133	0.1328	0.131
S_I	30	30	30	30	30	30	30	30	30	30
S_{NH}	0.36	0.36	0.372	0.3765	0.36931	0.3711	0.3781	0.3728	0.3756	0.378
S_{NO}	9.71	9.7	9.68	9.6896	9.6859	9.7084	9.7383	9.737	9.75	9.78
S_{N2}	35.76	35.76	35.81	35.81	35.82	35.79	35.768	35.79	35.8004	35.82
S_{PO4}	5.006	5.05	5.2	5.285	5.41	5.49	5.5577	5.6133	5.6557	5.68
S_{alk}	3.57	3.57	3.57	3.5697	3.56	3.56	3.5619	3.56	3.55	3.37
X_I	6.48	6.45	6.42	6.5103	6.45	6.544	6.541	6.48	6.499	6.52
X_S	0.087	0.08	0.08643	0.0863	0.08616	0.08737	0.087	0.087123	0.08721	0.08727
X_H	3.12	3.141	3.2	3.228	3.25	3.3347	3.3529	3.344	3.35	3.36
X_{STO}	0.0033	0.00433	0.00708	0.01032	0.01816	0.02812	0.0391	0.050988	0.06426	0.06722
X_{PAO}	2.9	2.85	2.8	2.77	2.728	2.7043	2.67	2.6735	2.6696	2.692
X_{PP}	0.35	0.35	0.346	0.342	0.3369	0.33384	0.3292	0.3296	0.32878	0.3299
X_{PHA}	0.1	0.0999	0.0958	0.0934	0.09037	0.08428	0.0873	0.0863	0.08535	0.0851
X_A	0.39	0.394	0.39	0.3916	0.3934	0.3946	0.3946	0.396	0.39514	0.3945
X_{TSS}	12.2	12.24	12.23	12.26	12.27	12.136	12.136	12.158	12.1464	12.131
Composite variables										
TKN	1.32	1.31	1.32	1.326	1.31	1.32	1.33	1.323	1.33	1.33
TN	11.03	11.02	11	11.016	11.002	11.033	11.06	11.0614	11.08	11.085
TP	5.52	5.56	5.7	5.78	5.9067	5.98	6.0426	6.098	6.13	6.16
COD	43.23	43.16	43.14	43.21	43.14	43.29	43.26	43.2	43.2	43.2

BOD_5	1.36	1.35	1.35	1.35	1.34	1.36	1.35	1.3552	1.35	1.35
EQI	15969.0	15961.1	15826.5	15728.8	15753.7	15792.8	15800.9	15725.2	15747.6	15849.2

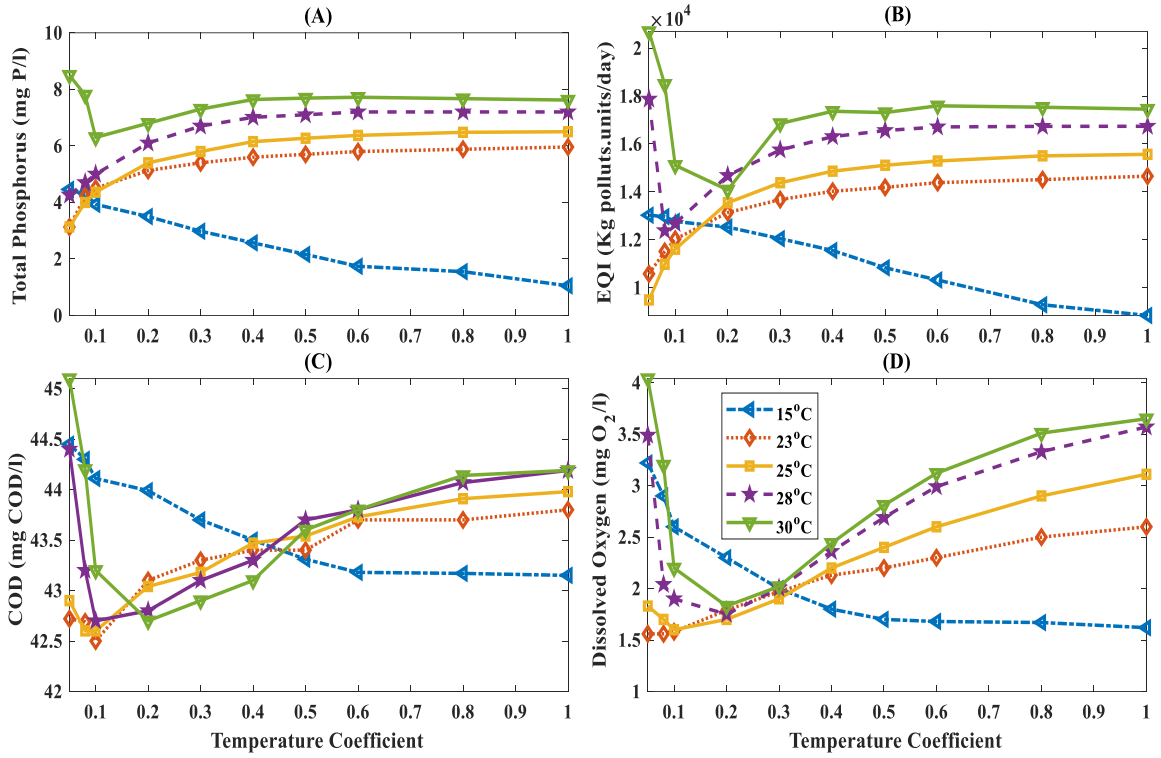

Figure 8.4 Effect of b_H at temperatures on (A) Total phosphorus, (B) EQI (C) COD, and (D) Dissolved oxygen

Effect of b_A at different temperatures by varying TC (0.14 to 0.3) and the corresponding nutrient removals are depicted in Fig.8.5 (A), (B) (C) and (D). On seeing the graphs of TP and ammonia, at 15°C TN and ammonia increasing linearly with respect to TC. But remaining temperature measures TN and ammonia is achieved better removal rate and independent on TC. By observing the graphs Fig.8.5 (A), and (C) reported that at 30°C, TN and ammonia achieved a better removal rate. Moreover, TP and EQI are enhanced in the case of lower temperatures and worsened at higher temperatures. Maximum decay and growth rate of X_PAO of resultant variations of effluent quality and concentrations at various temperatures are depicted in Figs.8.6 and 8.7 Effect of mu_{PAO} at different temperatures by varying TC (0.7 to 2) and the corresponding nutrient removals are depicted in Fig.8.6 (A), (B), and (C). From Fig.8.6 (A) and (B). It was noticed that at 15°C the EQI and TP are initially showing improved removal rate, as TC increases the removal rate decreases.

Furthermore, at higher temperatures, the removal rate shows a parabolic path with respect to TC. On the other hand, TN is enhanced in the case of higher temperatures and worsened at lower temperatures.

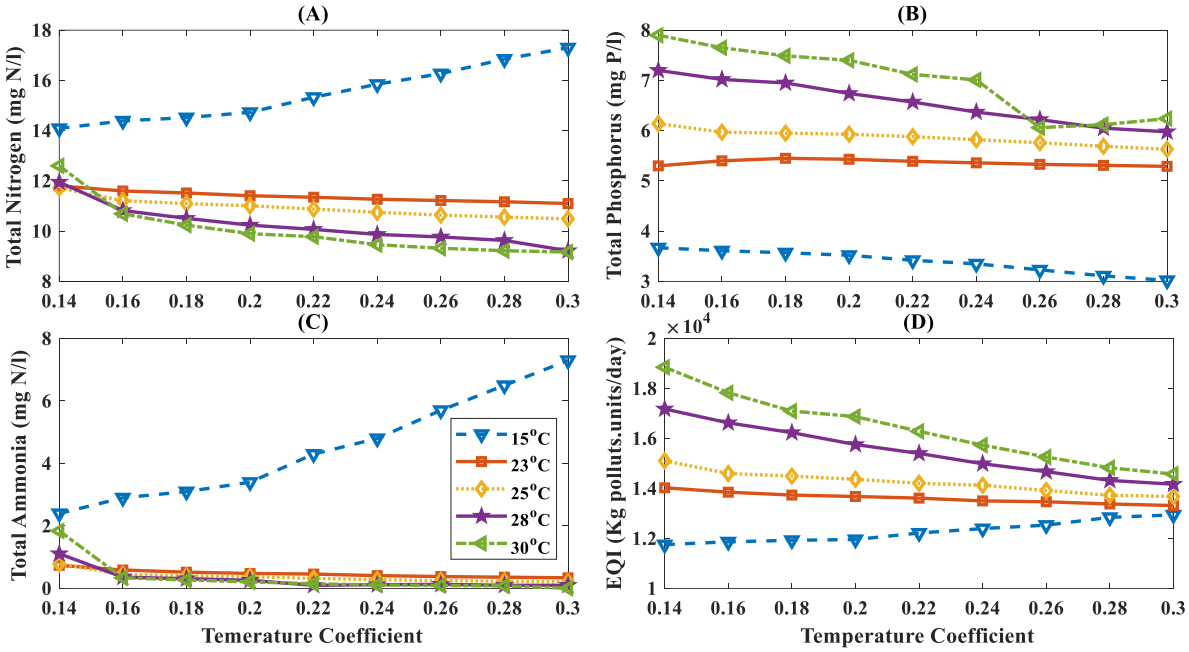

Figure 8.5 Effect of b_A at temperatures on (A) Total Nitrogen, (B) Total phosphorus (C) Ammonia, and (D) EQI

Effect of b_{PAO} at different temperatures by varying TC (0.08 to 6) and the corresponding nutrient removals are depicted in Fig. 8.7(A), (B), (C) and (D). It was noticed that at 15°C the EQI and TP are initially showing improved removal rate, as TC increases the removal rate decreases. At higher temperatures, it is observed that the EQI and TP are initially showing a lower removal rate. As TC increases the TP and effluent quality is improved. In the DO, the consumption is decreased as TC increases at lower temperature measures, and in higher cases, the consumption DO is increased on increasing TC. On the other hand, TN is enhanced in the case of higher temperatures and worsened at lower temperatures.

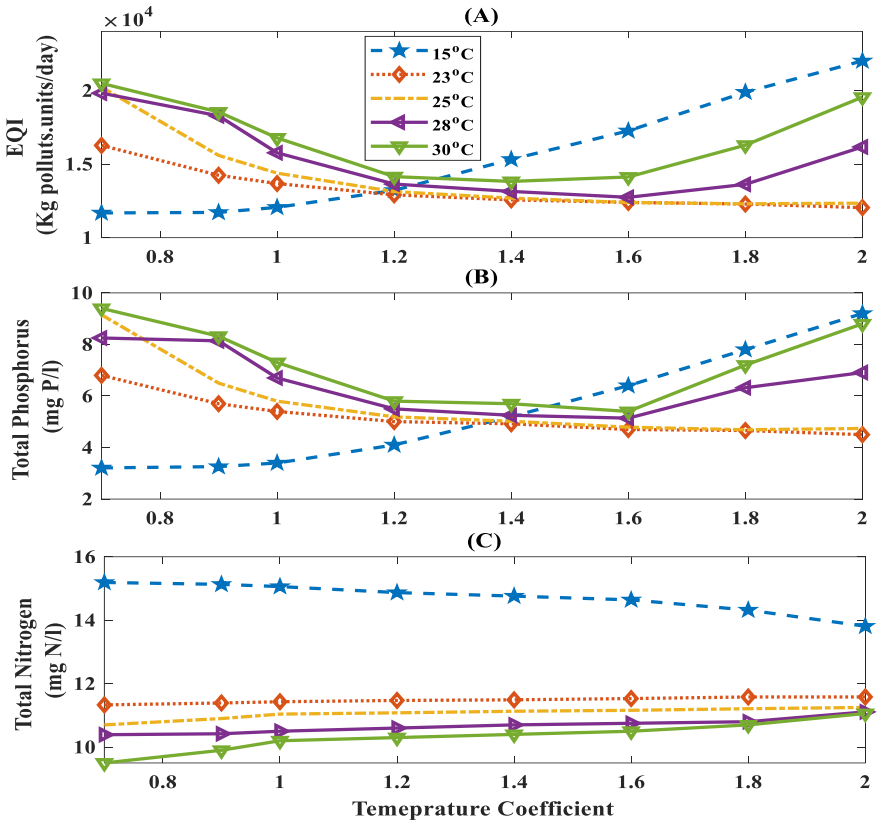

Figure 8.6 Effect of mu_{PAO} at different temperatures (A) EQI, (B) Total phosphorus, and (C) TN

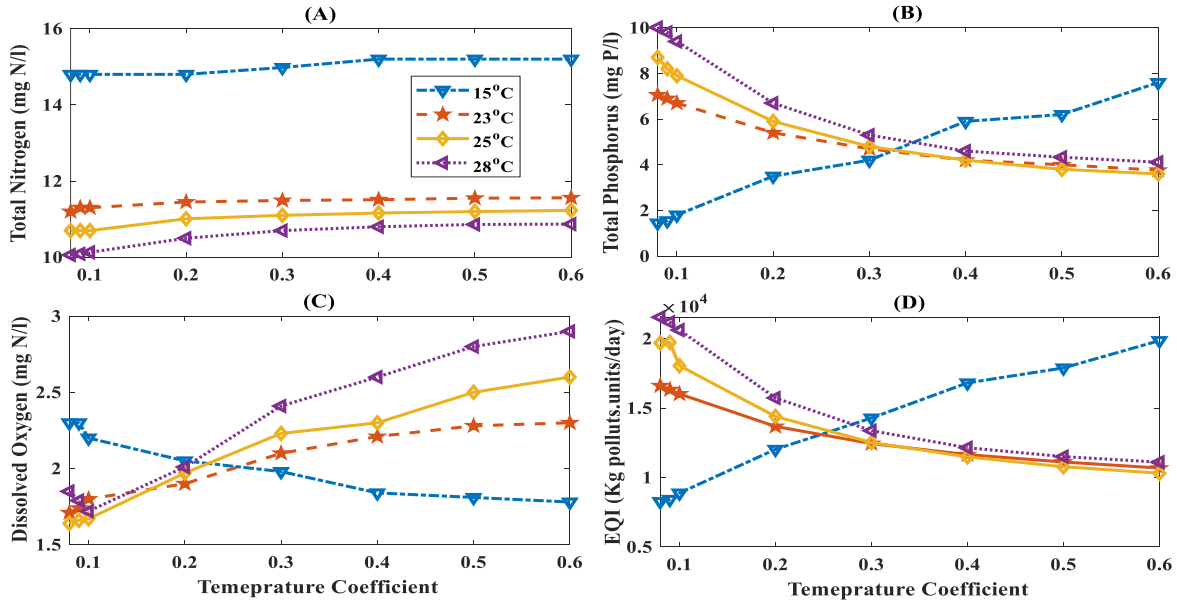

Figure 8.7 Effect of b_{PAO} at different temperatures (A) Total Nitrogen, (B) Total phosphorus and (C) Dissolved oxygen, and (D) EQI

8.1.3 Detail comparison of each individual pollutant concentrations

The impact of μ_{mH} on the quality of the effluent with varying temperature co-efficient is depicted in Fig.8.2. μ_{mH} is highly dependent on how the wastewater is treated and hence a huge range of results are noticed in the publications. Moreover, they are related to the structure of the reactor where the growth of biomass is happening. Additionally, it is noticed that the TP increases with the rise of temperature co-efficient and eventually leads to a rise in EQI.

The effect of μ_{mA} on the quality of effluent with different temperature coefficients is depicted in Fig.8.3. It impacts mainly S_{NH}, TN, TP, and EQI. Here the Kinetic parameter μ_{mA} play a key role to regulate the SRT at which the nitrifying bacterium is terminated. Generally, nitrification is carried out as a single-stage process, and it is relevant to the usage of μ_{mA} related to the removal of nitrogen-ammonia in the design. The effect of μ_{mA} in the effluent quality and concentrations of resultant variations of various temperatures are depicted in Appendix Table F2. The effect b_H on the quality of effluent with different temperature coefficients is depicted in Fig. 8.4. As the temperature increases, the corresponding state and composite variables also increases. The b_H effects almost all state and composite variables namely COD, TP, $S_{O,}$ and EQI. It is crucial to investigate b_H owing to its enormous impact on the estimated cell area for a particular SRT.

The effect of b_H in the effluent quality and concentrations of resultant variations of various temperatures are depicted in Appendix Table F1. Fig.8.5 depicts the effect of b_A in the quality of effluent with different temperature coefficients. The b_A rate effects mostly in TN, TP, $S_{NH,}$ and EQI. Biomass activity is terminated because of a critical effect on the ASP in a stable process. Aerobic and anoxic endogenous respiration causes biomass loss and requirements of energy not used for growth. The effect of b_A in the effluent quality and concentrations of resultant variations of various temperatures are depicted in Appendix Table F3.

The effect of mu_{PAO} in the effluent quality and concentrations of resultant variations of various temperatures are depicted in Appendix Table F4. The mu_{PAO} rate effects mostly TN, TP, and EQI. In the anaerobic section, PAO's incorporate fermentation products into storage products inside the cells with the discharge of P from stored Poly-P. In the aerobic section, energy is formed by the oxidation of storage products, and hence Poly-P storage inside the cell increases. The biomass activity rises owing to the growth of PHB composition as it falls with a rise in poly-p. All this leads to the decay of orthophosphate with a decrease in temperature and hence it influences on lower production of Poly-P.

The effect of b_{PAO}in the effluent quality and concentrations of resultant variations of various temperatures are depicted in the Appendix table figure F5. The b_{PAO} rate effect mostly in TN, TP, DO, and EQI. Aerobic and anoxic lysis of internal poly-phosphates takes care of the fact that cell internal poly-phosphates decay together with the biomass. Hence, the determination of decay rates inhabits a key role in the microbial process. Overall, the following observations are made.

8.1.4 Summary

- ✓ On considering 10^{o}C and 35^{o}C as the lower and upper-temperature ranges, at both the temperatures, it is observed that the simulation is stopped when stoichiometric parameters are reached beyond their limit.
- ✓ b_{PAO} is estimated with multiple temperature changes within the range of 10°C - 30°C, and finally, it is observed that the appropriate temperature ranges to get the simulation results is 15^{o}C – 28^{o}C.
- ✓ Generally, in phosphorous removal, it is noticed that at very low temperatures (5 to 10^{o}C), a higher sludge age is needed because of a decrease in the rate of the kinetic process.
- ✓ At (>10^{o}C), the anaerobic metabolism of GAO's, the anaerobic glycogen hydrolysis is completed and hence limiting the substrate uptake rate leading to the growth of the GAO's. With weather differences or geological areal differences, when the temperature (>25°C) is observed, the PAO's are at a lower level than GAO's production.

8.2 Effect of temperature using BSM1-P model with the fuzzy control application

The objective of this chapter is to report the effect of temperature (from 10^{o}C to 35^{o}C) on six kinetic parameters (growth and decay rates) by using the modified Arrhenius relation for the temperature dependency with the addition of a fuzzy controller (FLC) to monitor the effluent quality (EQI) and operational cost (OCI) in Wastewater treatment plants. A Benchmark simulation model (BSM1-P) is used to design the FLC, in order to check the plant performance and effluent quality that is affected by changing temperature. Two control loops like dissolved oxygen and nitrate are used by manipulating oxygen mass transfer coefficient and internal recycle in seventh and fourth reactors

8.2.1 Effect of temperature on activated sludge system

The analysis of kinetic and stoichiometry parameters is considered to be a key role in optimizing the WWTP in terms of modeling, design, and enhancing the improvement of WWTP biologically.

These parameters are highly dependent on the temperature and the age of biomass. A study state simulation is done on ASM3bioP as bioprocess and COD state fractions are used as an influent composition for analysis. ASM3bioP model has 17 state variables, which are related to heterotrophic and autotrophic decay and growth rates, hydrolysis, and bioP removal processes. Temperature dependencies have different biological kinetics and this is compensated for by interpolating the kinetic parameters to various temperatures. BSM1-P framework is used to analyze to base the change of temperatures concerning kinetic parameters. The kinetic and stoichiometric parameters affected by temperature are evaluated at different temperatures and the model used for the analysis is given in the below equation (8.2) (Copp JB, 2002; Gernaey et al., 2014). The kinetic parameters selected to investigate the effect of temperature coefficients are given below. The temperature changes concerning kinetic parameters are analyzed using equation (8.2). The six estimated kinetic parameters with the change of temperatures are presented in Table 8.2.

$$\alpha_T = \alpha_{T_{15}} . \exp\left(\left(\ln\left(\frac{\alpha_{T_{15}}}{\alpha_{T_{10}}}\right)/5\right).(T-15)\right) \quad (8.2)$$

Where α_T the considered parameter temperature (T) value and $\alpha_{T_{15}}$, $\alpha_{T_{10}}$is the defined benchmark parameter values at 10 and 15^{o}C (Henze et al. (2000); Gujer et al. (2000); Gernaey et al. (2004); Riger et al. (2001), Solon (2015)).

Maximum heterotrophic growth rate (μ_{mH})

Maximum autotrophic growth rate (μ_{mA})

Heterotrophic decay rate(b_H)

Autotrophic decay rate (b_A)

Maximum growth rate of X_PAO(mu_{PAO})

Endogenous respiration rate of X_PAO(b_{PAO})

Table 8.2 Kinetic parameters with respect to temperature changes

Temperature	Kinetic parameters in the change of temperature from the equation. 8.2					
Range (^{o}C)	μ_{mH}	b_H	μ_{mA}	b_A	mu_{PAO}	b_{PAO}
10	1.33457	0.133457	0.900144	0.450482	2.971301	1.803199
15	2.00093	0.200093	0.810584	0.298365	1.722885	0.600233
20	3	0.3	1	0.2	1	0.2

23	3.82520	0.382521	1.065027	0.157326	0.726149	0.103474
25	4.49790	0.449791	1.110711	0.134064	0.580422	0.066641
30	6.74372	0.674372	1.233678	0.088794	0.336553	0.022183
35	10.1108	1.011088	1.370259	0.059164	0.19593	0.007451

8.2.2 Design and implementation of fuzzy logic controller

In practical usage, the most frequently used control configurations using the specified control handles are:

DO control in aeration tank: In practice, DO is maintained in the range of 1.5-2 g/m^3set point by the operator. DO of 2 g/m^3 is required to provide maximum growth rate and if 1.5 g/m^3 is maintained the non-desirable reactions for the microbial growth terminate. K_La is accountable for the usage of DO concentration (Amand et al., 2013). If it is more than the 2 g/m^3 in aeration it will lead to more cost but there is no drastic change of effluent quality and is similar to the results of 2 g/m^3.

S_{NO} control in the anoxic tank: Q_{intr} is responsible for the S_{NO} concentration in closed-loop usage. In general, BSM1 uses a 1 gN/m^3 for the set point. For other sources like carbon dosages (Q_c) are also regulate S_{NO} concentration. Generally, in practice, open-loop control of S_{NO} is evaluated by choosing the suitable values of Q_{intr} and Q_c.

The control applications of WWTP are concentrated on the governing of AS process variables although the correlations of internal and external recycle rates, the effect of influent variations must be studied to obtain the optimized process operations from a global point of view. Here, in this paper, the controls that handle the ASP processes are the air diffusion rate in the aeration tank and the internal recycle rate as manipulated variables. The oxygen mass transfer coefficient (K_La) is accountable for the air flow rate; it depends on the dynamics of diffusion phenomena. For classic FLC, the control model is the way of the human knowledge base. FLC consists of three sections. In the primary section, MF's are fuzzified with input values to get Fuzzification. After, by using predetermined rules, fuzzy inputs and outputs are connected then the outputs are determined by using the inference mechanism. The third section is to initiate strict output values in a computed way and is called defuzzification. The membership functions of DO for output and input functions are depicted in Fig. 8.8.

FLC with applications of BSM1-P with three mechanisms blocks is depicted in Fig. 8.9. Here in the FLC, the input variables are considered as the feedback error 'E' and high-order error 'ED'. Consequently, the output variables are considered as manipulating variables in the control configuration. Hence, FLC for the design of the DO loop the input variable is selected as the mass transfer coefficient (K_La), and for the design of the S_{NO} loop; the input variable is selected as the internal recycle (Qintr). On coupling, both these outputs and input, the membership function (MF) has to be selected. In this study, Mamdani fuzzy interface method is chosen and MF's are selected as a triangular shape functioning. Based on the simulation data, the usage of a rules-based system is obtained before developing the FLC framework.

In the last aeration tank, the 'E' input variable scale is maintained from -30 to 30 g/m^3 and the 'ED' input variable scale is maintained from -25 to 25 g/m^3. The output variable scale of K_La in the last reactor is 200 to 280 d^{-1}. Further, in the second anoxic tank, the input variable scale of 'E' is maintained from -30 to 30 g/m^3 and 'ED' of the input variable scale is maintained from -25 to 25 g/m^3. The scale of the output variable of Q_{intr} is 20100 to 45000 1/d. A total of seven MF are chosen for each individual and NL, NI, NS, Z, PS, PI, and PL where N, Z, P, L, I, and S are negative, zero, positive, big, medium, and small. Similarly, MF's of S_{NO} is also selected. The coupling of DO and S_{NO} fuzzy logic consists of 74 rules are implemented by the usage of IF-THEN statement conditions. The Fuzzy rules of both DO and S_{NO} are elucidated in Tables 8.3 and 8.4. The membership functions of input and output data of DO are depicted in Fig. 8.8 (A), (B), and (C).

Table 8.3 Selection of DO rules for FLC

	NL	NI	NS	Z	PS	PI	PL
NL	PL	PL	PL	PL	PI	Z	Z
NI	PL	PL	PL	PL	PI	Z	Z
NS	PI	PI	PI	PI	Z	NS	NS
Z	PI	PI	PS	Z	NS	NI	NI
PS	PS	PS	Z	NI	NI	NI	NI
PI	Z	Z	NI	NL	NL	NL	NL
PL	Z	Z	NI	NL	NL	NL	NL

Table 8.4 Selection of nitrate (S_{NO}) rules

	NL	NS	Z	PS	PL
NL	PL	PL	PL	PS	Z
NS	PS	PS	PS	Z	NS
Z	PS	PS	Z	NS	NS
PS	PS	Z	NS	NS	NS
PL	NS	NL	NL	NL	NL

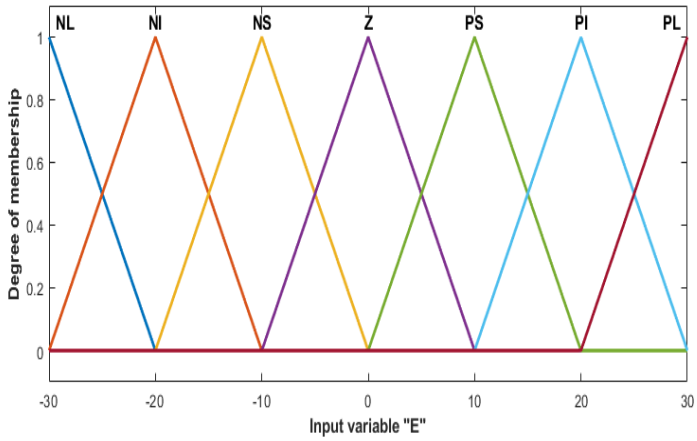

(A) MF of error of tank 7 for DO

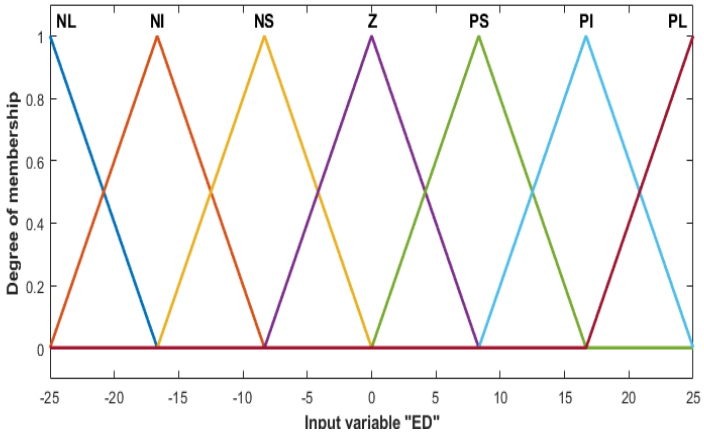

(B) MF of differentiation of error of tank 7 for DO

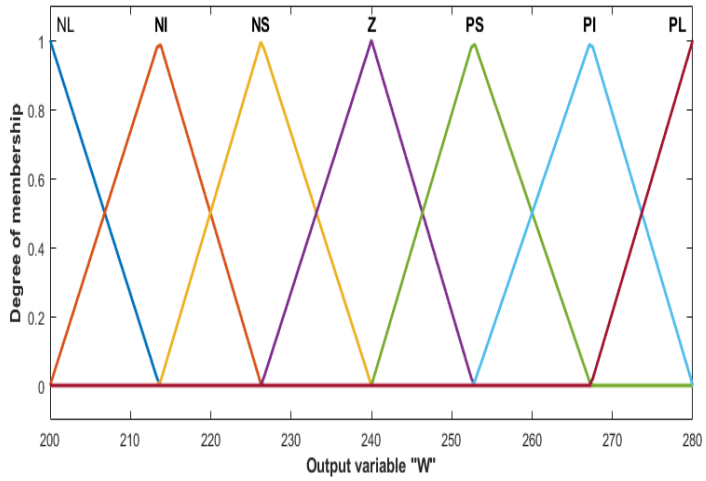

(C) MF of K_La_7 in tank7

Figure 8.8 MF's of input and output data of DO in tank7 by using K_La7

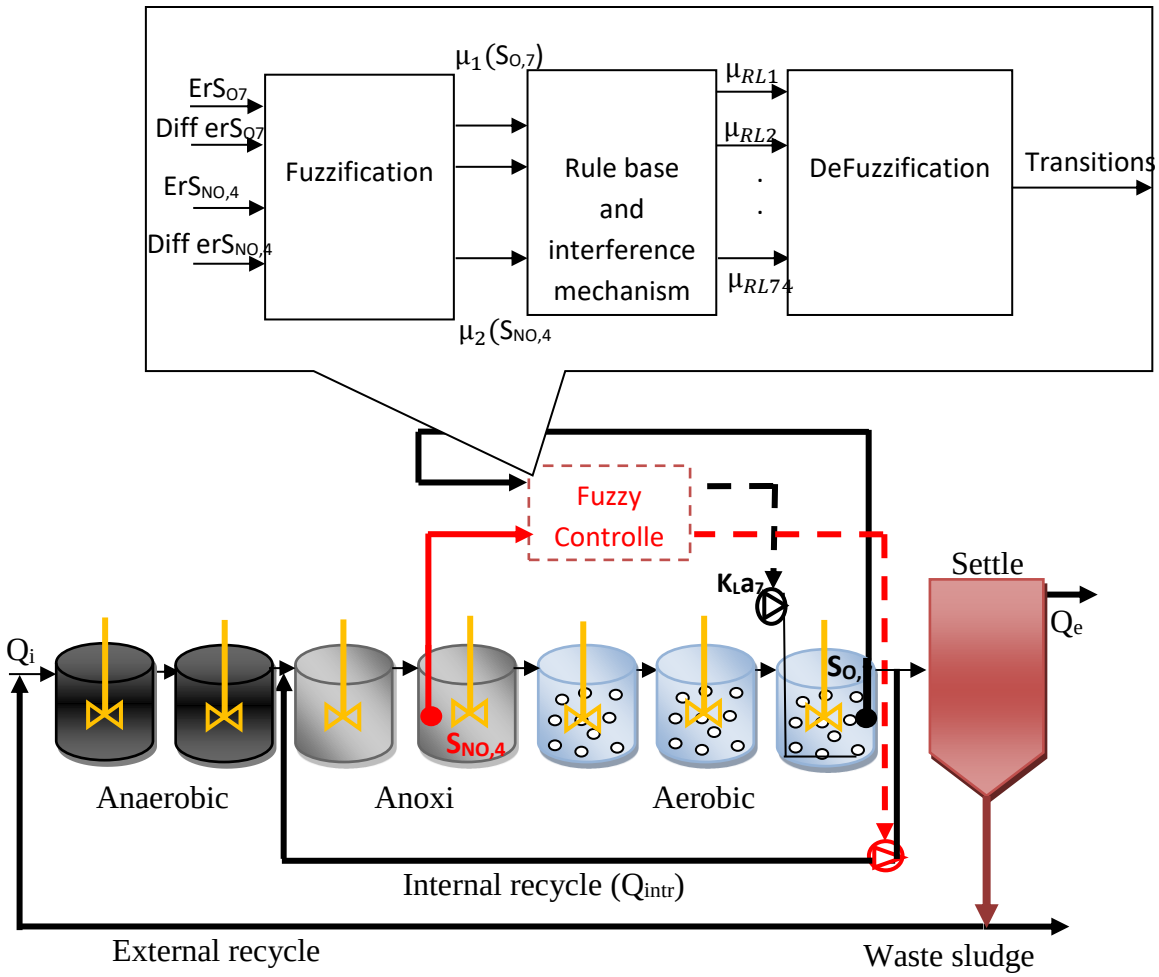

Figure 8.9 Fuzzy logic control of BSM1-P platform

8.2.3 Simulation results

Simulations are performed by varying the temperature from 15 to 35^{o}C and the results are analyzed. In this temperature range, at 10 and 35^{o}C, the effluent quality and nutrient removal efficiency are not good. This is due to the inert nature of microbial growth. Microbes that are responsible for the nitrification rate (nitrifiers) and Phosphorus uptake rate (PAO's) are nearly cease functioning. Improved removal of ammonia, phosphorus, and nitrogen efficiency is achieved at higher temperatures (20-30^{o}C). Based on the kinetic parameters, a higher P-release rate with higher temperatures is reported. Furthermore, at higher temperatures, the kinetic parameters of growth (Autotrophic, PAO, and heterotrophic) and the consumption of substrate rates are also increased. Overall, it has an impact on effluent discharge. The simulation outcomes of 15 to 30^{o}C are tabulated in Table 8.5. From Table 8.5, it can be observed that BOD_5 and TSS range is

increased on increasing temperature which is inversely proportional to TP, TN, ammonia, and COD. In the global index context, sludge production increases on increasing temperature which leads to high operational costs. OCI increases on increasing temperature with lower effluent quality with the application of FLC. A bar chart is plotted to describe the effluent quality and cost when the temperature changes from 15^{o}C to 30^{o}C and is depicted in Fig. 8.10. The effluent violations data for TN, ammonia, and TP from the last seven days are given in Fig.8.11 (A), (B), and (C). It can be observed that as the temperature increases, the effluent quality decreases with increased operational cost.

From Table 8.5, it was noticed that as temperature increases from 15^{o}C to 30^{o}C the consumption of aeration energy is slightly increased with respect to increased temperature. Additionally, here in this case of the control study, the sludge production is increased on increasing temperature. Overall the effect of both these sludge production and aeration energy will impact largely in the OCI. Moreover, a significant improvement in EQI with an increase in OCI is noticed. On comparing the EQI at 15^{o}C with other temperature ranges, evaluations in terms of improved percentage of EQI are reported. At the temperatures of 20, 23, 25, 30^{o}C, improved EQI's are reported as 16, 58, 68, and 72%. On the increasing temperature, there is a drastic improvement in EQI, but there is no improved response of EQI ongoing above 30^{o}C. Further, EQI worsens when compared to 15^{o}C. On comparing with OCI of 15^{o}C with temperature changes, evaluations in terms of percentage of OC are reported. At the temperatures of 20, 23, 25, 30^{o}C the OCI's of 5.1, 10.8, 13.5, and 16.8% are reported. As temperature rises the OCI also increases. Further, as EQI improved there is an increase in OCI, and find there is a tradeoff between OCI and EQI.

From Table 8.5, it was observed that on increasing temperature from 15 to 30^{o}C there is a slight change of COD and BOD_5. There is no drastic impact on these pollutants on changing temperature concerning kinetic parameters. On the other hand, other pollutants are drastically impacted. On seeing the TP, $S_{NH,}$ and TN at 15 and 30^{o}C, the percentage of improvements are noticed as 83.4, 87.5, and 40%. The temperature ranges from 20 to 25^{o}C are increased with deceased nutrient concentrations. Additionally, the percentage of nutrient (TP, $S_{NH,}$ and TN) violations show large variations at 15^{o}C but in the case of 30^{o}C there is no violation found to cross the discharge limit value. Whereas TP is observed above the limit value (100%) at 15^{o}C, but at 30^{o}C the TP violation is significant with a nil percentage of the violation. Not only TP but also ammonia and TN are also reported nil percentage of the violation. Thus, it will impact the significant improvement in EQI.

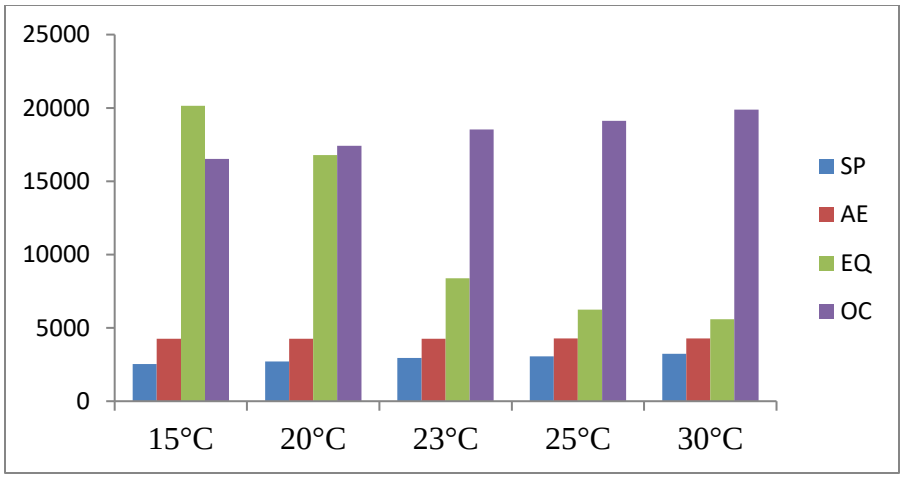

Figure 8.10 Bar graph on different temperatures with corresponding sludge production, aeration energy, operational cost, and effluent quality

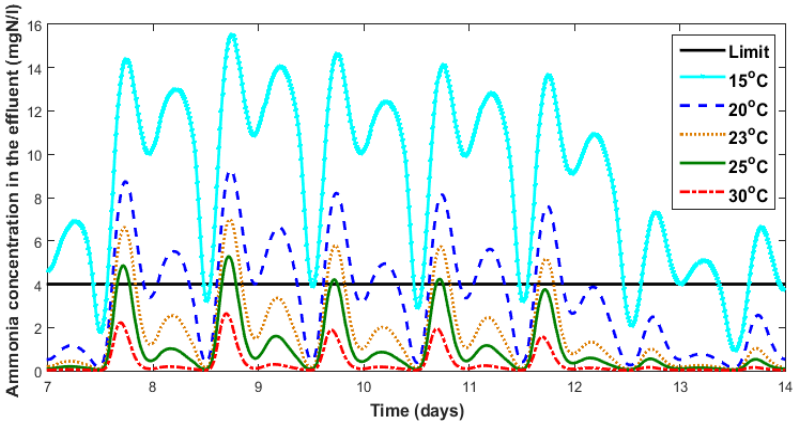

(A) Ammonia in the effluent

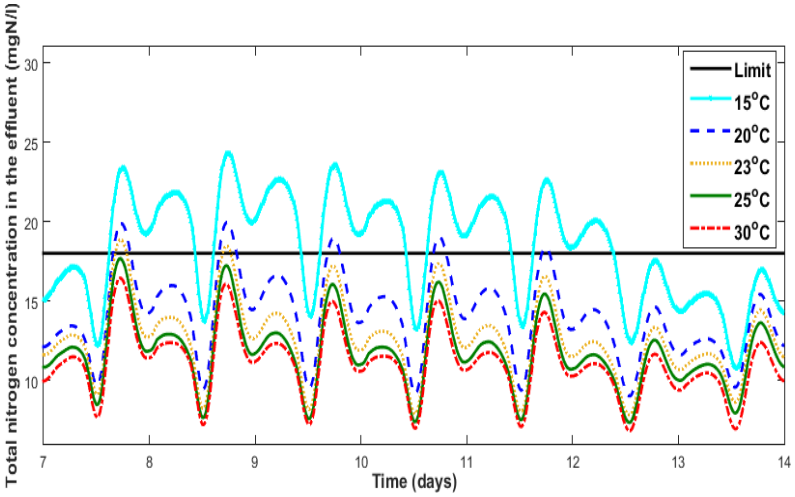

(B) TN in the effluent

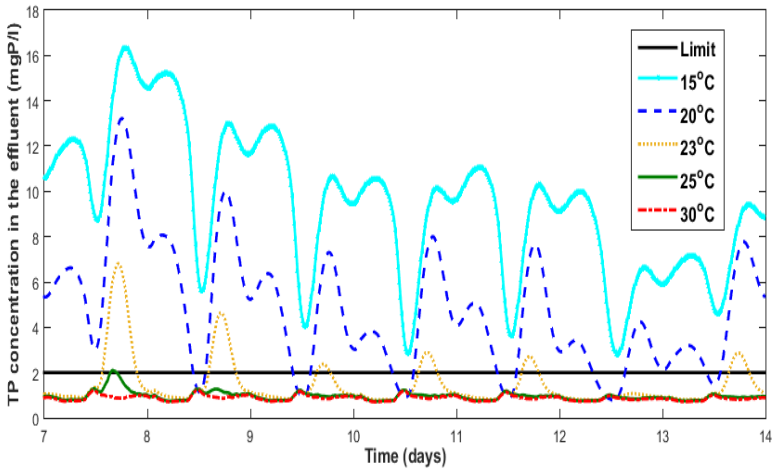

(C) TP in the effluent

Figure 8.11 Comparison of S_{NH}, TN, and TP for different temperatures with FLC

Table 8.5 Average effluent concentrations and operational cost index

Pollutants	Temperature changes with additional fuzzy controller				
Parameter	15°C	20°C	23°C	25°C	30°C
BOD_5	1.64	1.6	1.66	1.68	1.9
TP	7.45	5.21	2.12	1.54	1.232
S_{NH}	7.29	4.12	2.78	1.508	0.912
X_{TSS}	12.92	13.17	13.97	13.92	14.32
TN	18.14	14.44	12.41	11.55	10.88
COD	44.71	44.39	44.21	44.13	44.08
Operational cost assessment					
SP	2531.84	2715.49	2951.23	3067.05	3240.41
AE	4262.09	4265.45	4267.57	4275.74	4289.79
PE	295.44	295.99	296.09	295.03	295.66
ME	480	480	480	480	480
EQI	20142.52	16781.05	8377.55	6255.26	5600.21
OCI	16529.35	17423.7	18538.02	19129.11	19873.7
Percentage of violations (%)					
TP	100	82.44	18.30	1.286	---

TN	57.29	9.22	2.52	----	---
S_{NH}	77.04	39.43	12.64	5.506	----

8.2.4 Summary

Microbial behavior on the removal of phosphorous and nitrogen in an enhanced biological phosphorous removal process is studied at different temperatures. In this work, six kinetic parameters have been selected that deal with decay and growth rates of heterotrophic, autotrophic, and poly accumulating organisms by changing the temperature using the modified Arrhenius formula. While changing the kinetic parameters on the basis of temperature, additionally coupled S_{NO} and DO control loops are designed using fuzzy logic. For 10°C–35°C the microbes are inert as there is no response on the EQI and effluent violations. It can be observed that as the temperature increases, the EQI increases with increased OCI. On the other hand, the average pollutant concentrations like BOD5 and XTSS are slightly increased with increasing temperature, and mixing energy turned out to be a constant in all the cases because no changes happen in the mixing energy. At the temperatures of 20°C, 23°C, 25°C, and 30°C, the EQI is improved by 16%, 58%, 68%, and 72%, respectively. On the increasing temperature, there is a drastic improvement in EQI (low EQI value), but if the temperature is further improved (more than 30°C), then there is no improvement on the EQI. Further, EQI worsens when compared to the conditions at 15°C. Similarly, OCI is evaluated at different temperatures and is evaluated in terms of percentages. When the WWTP is operated at the temperatures of 20°C, 23°C, 25°C, 30°C, the corresponding OC improvement is obtained as 5.1%, 10.8%, 13.5%, and 16.8%, respectively. From 15°C to 30°C, there is a tradeoff between EQI and OC. On the comparison of temperature changes with additional FLC, it is observed that a better EQI is observed but with high OC at 30°C. Other pollutants like BOD_5, TSS, and COD are not affected severely by the temperature.

8.3 Effect of temperature in plant-level (BSM2-P) wastewater treatment process

In this chapter, the effect of temperature on phosphorous, nitrogen, organic matter removal, overall effluent quality, methane, and hydrogen production in an activated sludge system (ASS) is assessed in this research. For the plant-wide model of the ASS, the benchmark Simulation model (BSM2-P) with an ASS (ASM2d) is used and the temperature is selected between 10 to 35°C covering different seasons. A steady-state simulation is achieved to evaluate the effluent

compositions by changing kinetic parameters. A total of twelve kinetic expressions for the maximum growth rate of heterotrophic biomass, autotrophic, phosphate accumulating organisms and their decay rates, oxygen saturation, hydrolysis, fermentation, and oxygen saturation coefficient, oxygen mass transfer coefficients are also considered. Further, the anaerobic digestion model (ADM1) is also used with changing Physico-chemical parameters which are functions of temperature. The corresponding physicochemical parameters are analyzed in the range of 25 to 55°C. A total of seven Physico-chemical kinetic expressions for the acid-base equilibrium gases are considered which includes Henry's law coefficient for carbon dioxide, methane, hydrogen, and partial pressure of water.

8.3.1 Effect of temperature on oxygen mass transfer coefficient, and oxygen saturation coefficient changes

Temperature is known to affect the wastewater treatment process, primarily by affecting chemical and biological reaction rates. Temperature changes are thought to be the cause of biological activity. As a result, some model parameters are considered to be temperature-dependent to account for this. More subtle effects, such as microbes' culture changes may lead to a higher risk of bulking during certain seasonal conditions. This shows more attention towards the research community. The effects of temperature are measured using the Arrhenius relationship at Gernaey et al. (2014). The following equation can be used to change temperature-sensitive parameters in the default case. Based on the above equation (8.2, 8.3, and 8.4) the nine kinetic parameters (hydrolysis, decay, growth rates of autotrophic, heterotrophic, and ploy accumulation organisms), K_La and S_O^{satu} are computed based on the temperature changes by Gernaey et al. (2014). Temperature influences aeration efficiency and consequently energy utilization through K_La and S_O^{satu}. The oxygen solubility relies on temperature-dependent, increasing as the temperature drops. The S_O^{satu} is valid in the range of 273.15 K to 348.15 K.

$$S_O^{satu}(T) = \frac{8}{10.50237016} * 6791.5 * K(T_k) \quad (8.3)$$

$K(T_K) = 56.12e^{-66.7354+\frac{87.4755}{T^*}+24.4526*\ln(T^*)}$ and $T^* = T_k/100$. The term 8/10.50237016 is denoted as S_O^{satu} value at 15°C is exactly 8 g/m^3. Further, the temperature affects the K_La. The following is the widely accepted relationship between the K_La and temperature, as presented by ASCE (1993): Here $K_L$an in day^{-1} and T in degree centigrade.

$$K_L a(T) = 1.024^{(T-15)} * K_L a_{15} \quad (8.4)$$

The kinetic parameters chosen to examine the effect of temperatures are given below in Table 8.2. The twelve estimated kinetic parameters, $K_L a$ and S_O^{satu} with change in temperatures are presented in Table 8.2.

Table 8.6 Kinetic parameters, $K_L a$ and S_O^{satu} as temperature changes

Kinetic parameters	10°C	15°C	17°C	20°C	23°C	25°C	28°C
Hydrolysis rate	2	2.46	2.67	3	3.42	3.72	4.21
Maximum growth rate heterotrophic	3	4.23	4.85	6	7.32	8.40	10.33
Maximum rate of fermentation	1.5	2.11	2.41	3	3.64	4.17	5.12
Decay rate Heterotrophic	0.20	0.28	0.32	0.40	0.47	0.54	0.67
Storage rate constant for X_{PHA}	2	2.46	2.67	3	3.42	3.72	4.21
Storage rate constant for X_{PP}	1	1.23	1.33	1.5	1.71	1.86	2.10
Maximum growth rate of PAO	0.67	0.82	0.88	1	1.13	1.22	1.38
Lysis rate of X_{PAO}	0.10	0.14	0.16	0.20	0.24	0.27	0.33
Lysis rate of X_{PP}	0.10	0.14	0.16	0.20	0.24	0.27	0.33
Lysis rate of X_{PHA}	0.10	0.14	0.16	0.20	0.24	0.27	0.33
Maximum growth rate autotrophic	0.35	0.61	0.76	1.0	1.48	1.85	2.58
Decay rate autotrophic	0.05	0.09	0.11	0.15	0.23	0.29	0.41
$\mathbf{S_O^{satu}}$	8.9	8	7.6	7.2	6.8	6.6	6.34
$K_L a$ ($K_L a_5$ in the reactor 5) ($K_L a_6$ in the reactor 6) ($K_L a_7$ in the reactor 7)	$K_L a_5$-106 $K_L a_6$-106 $K_L a_7$-53	$K_L a_5$-60 $K_L a_6$-120 $K_L a_7$-120	$K_L a_5$-63 $K_L a_6$-126 $K_L a_7$-126	$K_L a_5$-67 $K_L a_6$-135 $K_L a_7$-135	$K_L a_5$-72 $K_L a_6$-145 $K_L a_7$-145	$K_L a_5$-76 $K_L a_6$-152 $K_L a_7$-152	$K_L a_5$-81 $K_L a_6$-163 $K_L a_7$-163

8.3.2 Simulation results

Simulations are performed by varying the temperature from 10 to 28^{o}C and the results are determined based on the seasonal conditions. In this paper, two performance platforms are used to test the temperature effect on the plant-wide benchmark model of BSM2-P. The results are based on the temperature effect on twelve kinetic parameters and $K_L a$ and S_O^{satu} which are obtained from equations (8.2, 8.3, and 8.4), and the values are reported in Table 8.7. It can be noticed that both platforms show similar removal rates but the attained average removal rates are different. At temperatures <5 and >30^{o}C, the effluent quality, and nutrient removal efficiency are not good. Temperature fluctuations during the year may have a significant impact on the composition of microbial communities. Each species has a minimum, optimum, and maximum temperature range that supports growth, similar to pH. This is due to the inert nature of microbial growth. Microbes that are responsible for the nitrification rate (nitrifiers) and Phosphorus uptake rate (PAO's) are nearly cease functioning.

On overall comparison, the pollutants like COD, S_{NH}, TN, and BOD_5 average removal rates are decreased on increasing temperature but at 28^{o}C onwards, these pollutants start decreasing the removal rate. Whereas for TSS, an improved removal rate is observed on increasing temperature. TP shows an increasing trend in decreasing the temperature. In the BSM2-P platform, the improved removal efficiency of S_{NH}, TN, TP, COD, and BOD_5 is attained at 17^{o}C, 20^{o}C, 10^{o}C, 20^{o}C, and 28^{o}C. The attained improved average removal rate efficiency is reported on comparing with 15^{o}C for S_{NH}, TN, TP, COD, and BOD_5 are 22.2%, 9.7%, 28%,1.7%, and 86.4%. The overall EQI and OCI are depicted in Fig. 8.12. As temperature increases, the EQI is also increasing. At 28^{o}C the OCI is improved by 8.29% but the EQI is increased by 33.9% on comparing with 15^{o}C. As the temperature increases from 10 to 15^{o}C in AS system, the average production rates of methane, hydrogen, CO_2, and average gas flow rates decrease. At 10 and 28^{o}C the average production rates are compared at 15^{o}C. The reported production efficiency rates for methane are improved by 16.82% at 10^{o}C and worsened by 19.85% at 28^{o}C. The reported production efficiency rates for hydrogen are improved by 33.3% and worsened by 30% at 28^{o}C. The reported production efficiency rates for CO_2 and gas flow rates are improved by 20%, and 16% at 10^{o}C and worsened by 45.6% and 28.6% at 28^{o}C.

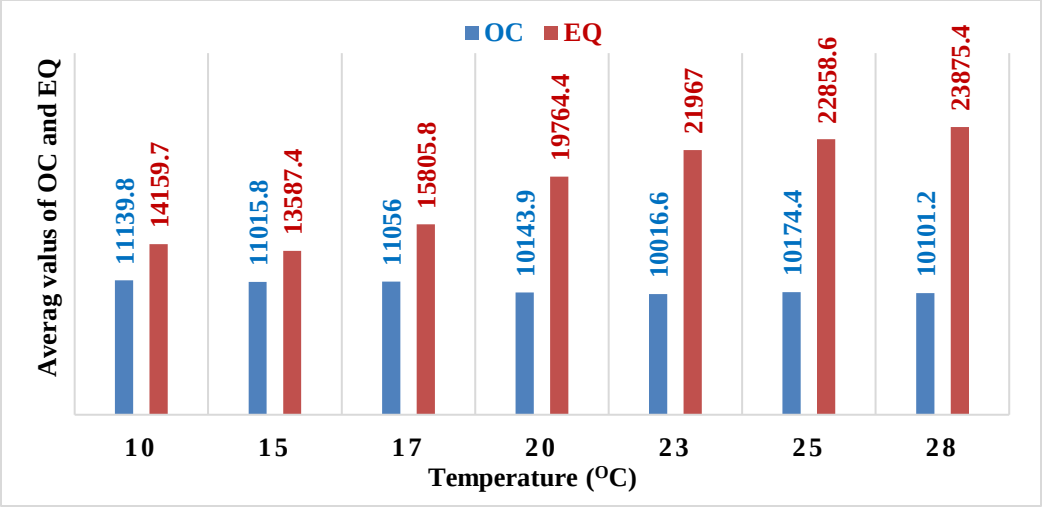

Figure 8.12 OCI and EQI of BSM2-P

Table 8.7 Average effluent concentrations for BSM2-P as temperature changes due to change in kinetic parameters

Performance assessment of BSM2-P platform							
Average effluent pollutants	10°C	15°C	17°C	20°C	23°C	25°C	28°C
S_{NH}	0.88	0.09	0.07	0.089	0.09	0.11	0.18
TSS	35.7	15.3	14.2	12.7	12.03	11.7	11.4
TN	10.3	6.2	5.7	5.6	6.3	6.6	6.8
TP	3.2	4.5	5.7	7.6	8.6	9.09	9.6
COD	60.1	41.3	40.8	40.6	40.7	40.8	41.16
BOD_5	5.3	1.7	1.44	0.9	0.60	0.43	0.23
Sludge production	4528.7	3867.9	3647.3	3320.1	3154.6	3087.92	3066.9
Aeration energy	3961.3	4000	3987.4	4052.4	4108.3	4182.9	4314.5
Pumping energy	452.3	452.3	452.3	452.3	452.4	452.4	452.4
Mixing energy	1388.3	1058.2	1405.3	954.47	1039.3	1213.1	1059.1
Heating energy	1667.3	1583.2	1531.4	1457.3	1419.6	1403.6	1388.7
Methane production	1000.1	856	806.1	745.4	715.3	700.4	686.6
Hydrogen production	0.004	0.003	0.0029	0.0025	0.0023	0.0022	0.0021
CO_2 production	1542	1232.4	1087.5	879.5	771.9	724.4	670.5
Average gas flow rate	2603.9	2176.5	2005.4	1778.5	1663	1609.5	1553.8

8.3.3 Effect of temperature based on anaerobic digestion model

Physico-chemical parameter values for the anaerobic digestion model (ADM1) by Batstone al. (2002) subjected to temperature change is studied based on the equation (8.5) given below by Gernaey et al. (2014):

$$\beta_T = g * \exp\left(((h/100)/R) * (1/T_b - 1/T_a)\right) \quad (8.5)$$

Here, β_T is the temperature (T_a) value at parameter, h and g are the temperature coefficients and R is the gas constant and T_b is the base temperature of the ADM1. A total of eight Physico-chemical parameters are used and studied the temperature effect and the resultant values are given in Table 8.8. The seven Physico-chemical parameters are $K_{H,co2}$, $K_{H,ch4}$ and $K_{H,h2}$ (Henry's law coefficient for carbon dioxide, methane, and hydrogen, k.mol.m^{-3}.bar^{-1}), Pgas, h_2o (partial pressure of water, bar), Ka,co_2 and $K_{a,IN}$ (acid-base equilibrium gases for acid, kmol.m^{-3}). ADM1 was created primarily to model sludge digestion in WWTPs where the normal process temperatures are 25°C or 55°C, which are thought to be suitable for thermo- and mesophilic digestion, respectively. Where optimal temperature for biogas production is at 55°C.

Table 8.8 Physico-chemical parameters as temperature changes

Parameters	Temperature ranges from 25-55^{o}C in the ADM1						
Temperature →	25^{o}C	30^{o}C	35^{o}C	40^{o}C	45^{o}C	50^{o}C	55^{o}C
Kw	$1.0*10^{-14}$	$1.54*10^{-14}$	$2.08*10^{-14}$	$2.94*10^{-14}$	$4.12*10^{-14}$	$5.72*10^{-14}$	$7.85*10^{-14}$
Ka,co_2	$4.46*10^{-7}$	$4.70*10^{-7}$	$4.94*10^{-7}$	$5.17*10^{-7}$	$5.42*10^{-7}$	$5.67*10^{-7}$	$5.92*10^{-7}$
$K_{a,IN}$	$5.62*10^{10}$	$7.94*10^{-10}$	$1.11*10^{-9}$	$1.53*10^{-9}$	$2.10*10^{-9}$	$2.84*10^{-9}$	$3.82*10^{-9}$
Pgas,h_2o	0.0313	0.0419	0.0557	0.0732	0.0955	0.1235	0.1585
$K_{H,co2}$	0.0350	0.0308	0.0271	0.0241	0.0214	0.0191	0.0171
$K_{H,ch4}$	0.0014	0.0013	0.00116	0.0011	$9.75*10^{-4}$	$8.97*10^{-4}$	8.28*10-4
$K_{H,h2}$	$7.80*10^{-4}$	$7.58*10^{-4}$	$7.38*10^{-4}$	$7.19*10^{-4}$	$7.01*10^{-4}$	$6.84*10^{-4}$	$6.68*10^{-4}$

8.3.4 Simulation results

In this study, it was noticed that AS temperature increases from 10 to 28^{o}C with changing phsyico-chemical parameters in ADM1 by using the temperature range (25 to 55^{o}C) from the equation. (8.5), and the corresponding average methane, CO_2 and, hydrogen production values are reported in Table 8.9. On comparing with 10 to 28^{o}C of AS temperature, 10^{o}C shows the better production rates of methane, hydrogen, and CO_2 from other temperatures. Whereas when ADM1 temperature

increases from 25 to 55°C, the average production rates are increasing. This is happening for all temperature changes for constant temperature of AS from 10 to 28°C. In this case, like temperature increases (10 to 28°C) the methane, hydrogen, and CO_2 production rates are decreasing. Moreover, rating trends are different from each other on constant AS temperature. The average production rates with improved efficiencies of methane, hydrogen, and CO_2 at 55°C on compared with an optimal temperature of 35°C of ADM1 are -0.89%, 57.6%, and 8.8% respectively with the constant AS temperature of 10°C and these are tabulated in Table 9.4. The average production rates with improved efficiencies of methane, hydrogen, and CO_2 at 55°C on compared with an optimal temperature of 35°C of ADM1 are -0.01%, 54.1%, and 7.8% respectively with the constant AS temperature of 28°C, and these are tabulated in Table 8.9.

Table 8.9 Average effluent concentrations for BSM2-P with the change of physio-chemical kinetic parameters

Parameter with average productions, kg d^{-1}	CT*, °C	Temperature, °C (ADM1)						
		25	30	35	40	45	50	55
Methane	10	1001.4	1001.9	1002.22	1002.10	1001.49	999.70	992.62
Hydrogen		0.0032	0.0038	0.0042	0.0047	0.0054	0.0068	0.0099
CO_2		1507.03	1551.48	1591.19	1626.51	1661.00	1697.44	1743.95
Methane	15	849.63	849.57	849.43	849.21	848.85	847.68	843.59
Hydrogen		0.0029	0.0032	0.0034	0.0038	0.0045	0.0057	0.008
CO_2		1178.49	1231.49	1248.21	1276.84	1305.56	1335.95	1376.04
Methane	17	797.24	797.29	797.24	796.89	796.38	795.29	791.18
Hydrogen		0.0026	0.0028	0.0031	0.0035	0.0041	0.0052	0.0082
CO_2		1030.42	1062.40	1090.43	1115.01	1139.03	1164.95	1200.91
Methane	20	733.60	733.66	733.66	733.38	732.93	731.77	726.99
Hydrogen		0.0022	0.0024	0.0027	0.0030	0.0035	0.0046	0.0074
CO_2		818.92	843.27	864.26	882.47	900.39	920.55	952.72
Methane	23	698.22	702.93	703.01	702.83	702.47	701.35	695.95
Hydrogen		0.0021	0.0022	0.0025	0.0028	0.0033	0.0043	0.0070

CO_2		722.4	734.94	753.04	768.79	784.51	802.86	833.99
Methane	25	687.92	688.13	688.28	688.16	687.87	686.82	681.32
Hydrogen		0.0020	0.0022	0.0024	0.0027	0.0032	0.0042	0.0068
CO_2		668.33	688.37	705.57	720.59	735.67	753.50	784.29
Methane	28	672.17	676.24	679.21	681.22	683.11	684.21	679.32
Hydrogen		0.0019	0.0020	0.0022	0.0024	0.0028	0.0035	0.0048
CO_2		644.2	648.37	665.57	688.59	695.67	705.50	721.29

*Constant temperature in ASM2d model

8.3.5 Summary

The improved removal efficiency of S_{NH}, TN, TP, COD, and BOD5 is obtained at 17, 20, 10, 20, and 28^{o}C temperatures respectively. The average percentage of removal is obtained as 22.2%, 9.7%, 28%, 1.7%, and 86.4% respectively for S_{NH}, TN, TP, COD, and BOD_5 which is higher when compared to the removal rate at 15^{o}C. At higher temperatures (55°C) the ADM1 showed improved production efficiency rates for carbon dioxide and hydrogen but at the lower level (25°C) it showed lower production efficiency rates. The average production rates of methane, hydrogen, and CO_2 at 55^{o}C are different by -0.01%, 54.1%, and 7.8% respectively when compared at the temperature of 28^{o}C.

Chapter 9

Summary and conclusions

Chapter 9

Summary and conclusions

9.1 Summary

In this thesis, an activated sludge system (ASM3bioP and ASM2d) is used in seven reactor configurations (anaerobic/anoxic/oxic) on BSM1-P and BSM2-P to design different control strategies. Lower-level control (controlling DO and S_{NO}) is designed by using advanced control strategies like PI, MPC, and Fuzzy. Supervisory-level control (ammonia-based aeration control) is added to Lower-level control by using the controllers like Fuzzy and MPC. By using four different control combinations PI-MPC, MPC-MPC, PI-Fuzzy, and MPC-Fuzzy are implemented. In another control, the framework is designed with a pair of PI feedback controllers (Supervisory layer, lower layer), override control with an additional three DO controllers. The performances of three biological treatment processes in a WWTP (A^2/O, R-A^2/O, and I-A^2/O) are studied to find the optimized configuration in terms of cost. Furthermore, a model-based analysis is studied to evaluate the effluent compositions with varying kinetic parameters accessed from varying temperature coefficients in the temperatures range from 10°C to 35°C for both secondary treatment and plant-wide level.

9.1.1 Design of lower-level control strategies on BSM1-P

A total of 8 control approaches are designed and implemented in the advanced simulation framework for assessment of the performance. The performance of the WWTP (effluent quality index and global plant performance) and the operational costs are also evaluated to compare the control approaches. Additionally, this chapter reports a comparison among proportional-integral (PI) control, fuzzy logic control, and model-based predictive control (MPC) to control dissolved oxygen (DO_7) and nitrate ($S_{NO,4}$) by manipulating oxygen mass transfer coefficient (K_La_7) and internal recycle (Q_{intr}) respectively.

9.1.2 Design of supervisory-level control strategies on BSM1-P

The supervisory control framework is used to alter the dissolved oxygen in the seventh reactor (DO_7) to control ammonia. Lower level PI, MPC, and Fuzzy are used to control the nitrate levels in the fourth reactor (S_{NO4}) by manipulating internal recycle (Q_{intr}) and DO_7 in the seventh tank by manipulating mass transfer coefficient (K_La_7). MPC and Fuzzy are designed in the supervisory layer to alter the DO_7 set-point based on the ammonia composition in the seventh reactor (S_{NH7}).

Model predictive control (MPC) and Fuzzy controllers are designed in a two-level hierarchical supervisory control framework.

9.1.3 Design of integrated supervisory and override control strategies on BSM1-P

The idea is to generate more organic matter with a reduction of nitrate concentration in the anoxic section so that more biological phosphorus removal happens. For this, the Supervisory and Override Control Approach (SOPCA) is designed based on the benchmark simulation model (BSM1-P) and is evaluated by considering dynamic influent. In the supervisory layer, proportional-integral (PI) and fuzzy controllers are designed. Additionally, three dissolved oxygen (DO) PI control loops in the last three aerobic reactors are designed. PI controller is designed for control of nitrate levels in the anoxic reactors and is integrated with override control and supervisory layer.

9.1.4 Development of control strategies based on plant-wide WWTP models

Control strategies based on proportional-integral (PI), model predictive control (MPC), and Fuzzy logic are developed and implemented on a plant-wide wastewater treatment plant. Four combinations of control frameworks are developed in order to reduce the operational cost and improve the effluent quality. As a working platform, a Benchmark simulation model (BSM2-P) is used. A default control framework with PI controllers is used to control nitrate and dissolved oxygen (DO) by manipulating the internal recycle and oxygen mass transfer coefficient (K_La). Hierarchical control topology is proposed in which a lower-level control framework with PI controllers is implemented to DO in the sixth reactor by regulating the K_La of the fifth, sixth, and seventh reactors, and Fuzzy and MPC are used at the supervisory level. This supervisory level considers the ammonia in the last aerobic reactor as a feedback signal to alter the DO set-points.

9.1.5 Analysis of different reactors combinations and configurations for biological WWTP

Three different schemes of wastewater treatment consisting of anaerobic, anoxic, and aerobic reactors are evaluated. A^2O process (anaerobic, anoxic, and aerobic reactors with internal and external recycles), Reverse R-A^2O process (anoxic, anaerobic, and aerobic reactors with external recycle), and Inverted I-A^2O process (anoxic, anaerobic, and aerobic with internal and external recycles) are considered. Dissolved oxygen (DO) is maintained in the respective aerobic reactors using a PI controller. Metal addition is carried out in the last aerobic reactor and carbon addition is carried out in the first anaerobic reactor in each process. Further, evaluation is carried out at

different temperatures (10, 15, and 20^{o}C) by changing the kinetic parameters in the model, and the effect of the operating temperature on EQI, OCI, and nutrient removal are also studied.

9.1.6 Effect of temperature on WWTPs

9.1.6.1 Model-based analysis of the effect of temperature on ASP (BSM1-P)

The effect of temperature on the phosphorous, nitrogen, and organic matter removal in an activated sludge system (ASS) is assessed in this research. Benchmark Simulation Model No.1 (BSM1-P) with an ASS (ASM3bioP) is used and the temperature is chosen between 10°C to 35°C. The kinetic expressions for the maximum growth rate of heterotrophic biomass, autotrophic, and phosphate accumulating organisms and their decay rate are considered. Total ammonia, nitrogen, and phosphorous in the effluent are analyzed.

9.1.6.2 Effect of temperature using BSM1-P model with fuzzy control application

The objective of this chapter is to report the effect of temperature (from 10^{o}C to 35^{o}C) on six kinetic parameters (growth and decay rates) by using the modified Arrhenius relation for the temperature dependency with the addition of a fuzzy controller (FLC) to monitor the effluent quality index (EQI) and operational cost index (OCI) in Wastewater treatment plants. A Benchmark simulation model (BSM1-P) is used to design the FLC, in order to check the plant performance and effluent quality that is affected by changing temperature. Two control loops like dissolved oxygen and nitrate are used by manipulating oxygen mass transfer coefficient and internal recycle in seventh and fourth reactors.

9.1.6.3 Effect of temperature in plant-level (BSM2-P) wastewater treatment process

The effect of temperature on phosphorous, nitrogen, organic matter removal, overall effluent quality, methane, and hydrogen production in an activated sludge system (ASS) is assessed in this research. For the plant-wide model of the ASS, the benchmark Simulation model (BSM2-P) with an ASS (ASM2d) is used and the temperature is selected between 10 to 35°C covering different seasons. A steady-state simulation is carried out to evaluate the effluent compositions by changing kinetic parameters. A total of fourteen kinetic expressions for the maximum growth rate of heterotrophic biomass, autotrophic, phosphate accumulating organisms and their decay rates, oxygen saturation, hydrolysis, fermentation, and oxygen mass transfer coefficients are also considered. Further, the anaerobic digestion model (ADM1) is also used with changing Physico-

chemical parameters which are functions of temperature. The corresponding physico-chemical parameters are analyzed in the range of 25 to 55°C. A total of seven physico-chemical kinetic expressions for the acid-base equilibrium gases are considered which includes Henry's law coefficient for carbon dioxide, methane, hydrogen, and partial pressure of water.

9.2 Conclusions

9.2.1 Design of lower-level control strategies on BSM1-P

Different control frameworks from CLS1 to CLS8 in the BSM1-P plant layout under the ASM3bioP framework are implemented. In comparison, it is observed that the effluent pollutant considerations for CLS1 and CLS2 are better than CLS3–CLS8. In the former case, the operational cost index of CLS2 is far better than CLS1. MPC provides good tracking performance on comparing with PI. MPC shows slightly better than the PI approach and fuzzy shows better removal of phosphorus when compared with PI and MPC. MPC is much favorable for both ammonia and nitrogen removal. MPC gives efficient removal of TN and ammonia when compared with PI and FLC.

9.2.2 Design of supervisory-level control strategies on BSM1-P

Four control combinations (PI-MPC, MPC-MPC, PI-Fuzzy, and MPC-Fuzzy) are evaluated and tested for dry weather, rainy weather, and storm weather conditions. The corresponding performance indexes are compared with the default strategy. EQI is minimized when compared with the existing default PI control approach and in some cases, a tradeoff is observed between OCI and EQI. For all the compared control strategies, MPC-MPC shows better effluent quality and high operating costs. It was noticed that on comparing all control applications, it was found that average effluent concentrations like BOD, COD, TN, and TSS attained stringent regulations except ammonia and phosphorus. Better optimized result for ammonia removal is observed in MPC-MPC whereas better-optimized result for phosphorus removal is noticed in PI-MPC. As for effluent violations are concerned, it was observed that for rain and storm conditions, improved quality is achieved in ammonia and phosphorus.

9.2.3 Design of integrated supervisory and override control strategies on BSM1-P

We propose SOPCA (PI-Fuzzy) and SOPCA (PI-PI) to balance S_{PO4} in tank7 and $S_{NO,4}$ in tank4. Further, S_O control loops for the last three aerobic reactors are added by varying set points (each

consisting of eight combinations). SOPCA (PI-Fuzzy) [I-VIII] and SOPCA (PI-PI) [IX-XVI]. With the proposed control approaches, the effluent phosphorus was decreased notably. All the average compositions of TP, ammonia, and TN in the effluent were under regulatory limits. Further, SOPCA (I) and SOPCA (IX) control schemes showed better EQI and OCI. If the operator requires to achieve efficient TN removal, SOPCA (VIII) and SOPCA (IX) are recommended. On comparing with default PI, all sixteen control strategies showed improved effluent quality and higher operational cost. The simulation outcomes showed that the control applications enhanced the performance of WWTP and the application of SOPCA controllers was more advantageous for the phosphorus removal rate.

9.2.4 Development of control strategies based on plant-wide WWTP models

MPC and Fuzzy are designed at the supervisory level, and PI is designed for lower-level control for BSM2-P in ASM2d as an activated sludge model. Total four control frameworks are implemented to evaluate and test the plant performance, concentrations as well as effluent quality. The resultant performance indices are compared with the PI strategy. In each control application case, there is a trade-off between EQI and OCI. In comparison with PI (one loop). Of all the compared outcomes, PI-Fuzzy shows better EQI and increased OCI. On comparing all the four control strategies, it was reported that average effluent pollutant concentrations like BOD5, COD, TN, ammonia, and TSS attained the regulatory limits except for phosphorus. Optimized ammonia removal is noticed in PI-MPC whereas better optimized phosphorous removal is noticed in PI-Fuzzy. PI-Fuzzy showed high production rates of greenhouse gas emissions and low consumption of aeration energy. The percentage of violations of total phosphorus showed less in the case of PI-Fuzzy.

9.2.5 Analysis of different reactors combinations and configurations for biological WWTP

Comparative analysis on A^2O, R-A^2O, and I-A^2O are tested and it is found that R-A^2O shows the optimized results in OCI with slight high EQI. Hence, R-A^2O is taken as a benchmark and tested with different applications like carbon loading, metal loading, and control approaches to know how it will impact the EQI and OCI. It is noticed that the increase of metal and carbon dosages leads to lower EQI and higher OCI with better removal of nutrients. The combination of both metal and carbon loading simultaneously in the process shows better efficient nutrient removal, DO is directly proportional to the formation of orthophosphates. If DO is high, then the phosphorous

level is also high and it is contradictory with lower DO. Later, the combination of metal and carbon loading with DO control application is also tested which shows the tradeoff between EQI and OCI.

9.2.6 Effect of temperature on WWTPs

9.2.6.1 Model-based analysis of the effect of temperature on ASP (BSM1-P)

A considerable violation in EQ is observed with the variation in kinetic parameters when the temperature is <15°C and >30°C. For Phosphorous removal, at 5 to 10^{o}C, a higher sludge age is needed because of a decrease in the reaction rate.

- On considering 10^{o}C and 35^{o}C as the lower and upper-temperature ranges, at both the temperatures, it is observed that the simulation is stopped when stoichiometric parameters are reached beyond their limit.
- b_{PAO} is estimated with multiple temperature changes within the range of 10°C - 30°C, and finally, it is observed that the appropriate temperature ranges to get the simulation results is 15^{o}C – 28^{o}C.
- Generally, in phosphorous removal, it is noticed that at very low temperatures (5 to 10^{o}C), a higher sludge age is needed because of a decrease in the rate of the kinetic process.

9.2.6.2 Effect of temperature using BSM1-P model with fuzzy control application

On changing kinetic parameters based on temperature ranges, additionally, coupled S_{NO} and DO control loops are designed using fuzzy logic. For 10^{o}C and 35^{o}C, the microbes are inert as there is no response on the EQI and effluent violations; it is always above the limit value range. From 15 to 30^{o}C there is a tradeoff between EQI and OCI. It is observed that if the temperature increases the EQI decreases, but OCI increases. On comparing results with 15^{o}C a good improvement is found at 30^{o}C as the effluent quality is improved 72% with an increasing 17% of operational cost. Moreover, on changing temperature pollutant concentrations like TP, ammonia, and TN are heavily impacted. At 30^{o}C the improved pollutant concentrations are 83.4, 87.5, and 40% on comparing with 15^{o}C. Other pollutants like BOD_5, TSS, and COD are not affected largely by changing temperature.

9.2.6.3 Effect of temperature in plant-level (BSM2-P) wastewater treatment process

WWTP's are largely influenced by operating temperature. Based on the Arrhenius-based temperature equation, in this paper, fourteen kinetic parameters with K_La and are tested with different temperature ranges in a plant-wide biological WWTP. Besides that, ADM1 is also studied

by considering seven physico-chemical kinetic parameters to check the production rates of methane, carbon dioxide, and hydrogen in the range of 25-55^{o}C. Based on the observed results, the temperature has a huge influence on process operations. As a result, it is crucial to understand the performance of WWTP's at various temperatures. This leads to a better understanding of optimal pollutant removal efficiency. The findings of this study distinguish the effects of temperature variations on biological processes over the plant-wide scenario.

9.3 Suggestion for future work

Based on the research carried out in this thesis, one can extend the ideas to solve different other advanced control applications related to BSM1-P and BSM2-P. The suggestions for future work include the following:

- Design of fractional order, artificial neural network, non-linear MPC control strategies for both BSM1-P and BSM2-P simulation platforms can be studied.
- In most of the existing studies, ideal sensors are considered. However, in practice, the sensors performance deteriorate. Hence, design of advanced control strategies with non-ideal sensors can be carried out and performance can be checked.
- By incorporating the life cycle analysis, suitable decision support tools for flexible and optimal operation of activated sludge process can be studied.
- Water-food-energy nexus can be explored from the perspective of biological WWTP using activated sludge process.
- One can carry experimentally implement some of these developed strategies on a lab scale WWTP.

10 References

Agarwal M, Singh K, Dohare RK, Upadhyaya S (2016) Process control and optimization of wastewater treatment plants using simulation softwares: a review. International J of Advanced Techn & Eng Explor, 3(22):145.

Åmand L, Olsson G, Carlsson B (2013) Aeration Control—A Review. Water Sci. Techn 67 (11):2374–2398.

Alex, J., Beteau, J.F., Copp, J.B., Hellinga, C., Jeppsson, U., Marsili-Libelli, S., Pons, M.N., Spanjers, H. and Vanhooren, H., 1999. Benchmark for evaluating control strategies in wastewater treatment plants. In 1999 European Control Conference, IEEE, 3746-3751. DOI: 10.23919/ECC.1999.7099914.

Alisawi, H.A.O., 2020. Performance of wastewater treatment during variable temperature, Applied Water Science, 10(4), 1-6.

Amand, L., Olsson, G., and Carlsson, B., 2013. Aeration control–a review. Water Science and Technology, 67(11), 2374-98. https://doi.org/ 10.2166/wst.2013.139.

Aström KJ, Hägglund T (1995) PID Controllers: Theory, Design and Tuning. Instrument Society of America, Research Triangle Park, NC, USA.

ASCE., A standard for the measurement of oxygen transfer in clan water, ASCE standard committee., 1993, New York, NY, USA.

Azeez, R.A., 2010. A study on the effect of temperature on the treatment of industrial wastewater using chlorella vulgaris alga. Engineering and Technology Journal, 28(4), 785-792.

Barker, P.S. and Dold, P.L., 1996. Denitrification behaviour in biological excess phosphorus removal activated sludge systems, Water Research, 30(4),769-780.

Batstone, D.J., Keller, J., Angelidaki, I., Kalyuzhnyi, S.V., Pavlostathis, S.G., Rozzi, A., Sanders, W.T.M., Siegrist, H. and Vavilin, V.A., 2002. The IWA Anaerobic Digestion Model No. 1 (ADM1). Water Science and Technology,45(10), 65-73.

Baklouti, I., Mansouri, M., Hamida, A.B., Nounou, H. and Nounou, M., 2018. Monitoring of wastewater treatment plants using improved univariate statistical technique. Process Safety and Environmental Protection, 116, 287-300. https://doi.org/10.1016/j.psep.2018.02.006.

Baeza, J.A., Gabriel, D., and Lafuente, F.J., 2002. Improving the nitrogen removal efficiency of an A2/O based WWTP by using an on-line Knowledge Based Expert System. Water Research, 36, 2109–2123. https://doi.org/10.1016/S0043-1354(01)00402-X.

Baeza, J.A., Gabriel, D., and Lafuente, F.J., 1999. An expert supervisory system for a pilot WWTP. Environmental Modelling and Software. 14, 383-390. https://doi.org/10.1016/S1364-8152(98)00101-7

Baetens, D., Vanrolleghem, P.A., Van Loosdrecht, M.C.M. and Hosten, L.H., 1999. Temperature effects in bio-P removal. Water science and technology, 39(1), 215-225. https://doi.org/10.1016/S0273-1223(98)00787-2.

Bekele, Z.A., Delgado Vela, J., Bott, C.B., and Love, N.G., 2020. Sensor-mediated granular sludge reactor for nitrogen removal and reduced aeration demand using a dilute wastewater. Water Environment Research, wer.1296. https://doi.org/10.1002/wer.1296.

Béraud, B., Steyer, J.P., Lemoine, C., Latrille, E., Manic, G. and Printemps-Vacquier, C., 2007. Towards a global multi objective optimization of wastewater treatment plant based on modeling and genetic algorithms. Water science and technology, 56(9), pp.109-116.

Blackall L., G. R. Crocetti, A. M. Saunders, and P. L. Bond., 2002. A review and update of the microbiology of enhanced biological phosphorus removal in wastewater treatment plants. International Jornal of Gen. Mol. Microbiol, 81, 1–4, 681–691.

Bo, BXZ., 2006. The principle and full-scale application of reversed a~ 2/o process for removing nitrogen and phosphorus. Journal of Environmental Engineering, 3. https://doi.org/10.1109/ICBBE.2009.5163643.

Boiocchi R, Gernaey KV, Sin G (2017) A Novel Fuzzy-Logic Control Strategy Minimizing N2O Emissions. Water Res 123:479–494.

Brdys, M.A., Chotkowski, W., Duzinkiewicz, K., Konarczak, K. and Piotrowski, R., 2002. Two-level dissolved oxygen control for activated sludge processes. IFAC Proceedings Volumes, 35(1), 467-472. https://doi.org/10.3182/20020721-6-ES-1901.01387.

Brdjanovic, D., Loosdrecht, M.C.V., Hooijmans, C.M., Alaerts, G.J. and Heijnen, J.J., 1997. Temperature effects on physiology of biological phosphorus removal. Journal of environmental engineering, 123(2), 144-153. DOI:10.1061/(ASCE)0733-9372(1997)123:2(144).

Brdjanovic, D., Loosdrecht, M.C.V., Hooijmans, C.M., Alaerts, G.J. and Heijnen, J.J., 1997. Temperature effects on physiology of biological phosphorus removal. Journal of environmental engineering, 123(2), 144-153. DOI:10.1061/(ASCE)0733-9372(1997)123:2(144)

Brehar, M.A., Varhelyi, M., Cristea, V.M., Cristiu, D. and AGACHI, Ş.P., 2019. Influent temperature effects on the activated sludge process at a municipal wastewater treatment plant. Chemia, 2019, 64(1).

Bunce, J.T., Ndam, E., Ofiteru, I.D., Moore, A., and Graham, D.W., 2018. A review of phosphorus removal technologies and their applicability to small-scale domestic wastewater treatment systems. Frontiers in Environmental Science, 6, 8. http://10.3389/fenvs.2018.00008.

Carrera, J., Sarra, M., Lafuente, F.J., and Vicent, T., 2001. Effect of different operational parameters in the enhanced biological phosphorus removal process. Experimental design and results. Environmental technology, 22(12), 1439-1446. http://10.1080/09593332208618181.

Copp, J.B., 1999. Development of standardised influent files for the evaluation of activated sludge control strategies. IAWQ Scientific and Technical Report Task Group, Respirometry in Control of the Activated Sludge Process–internal report.

Copp, J.B., 2002. The cost simulation benchmark: description and simulator manual (COST Action 624 and Action 682). Luxembourg, Office for Official Publications of the European Union.

Chang, N.B., Chen, W.C. and Shieh, W.K., 2001. Optimal control of wastewater treatment plants via integrated neural network and genetic algorithms. Civil Engineering Systems, 18(1), pp.1-17.

Charef A, Ghauch A, Martin-Bouyer M (2000) An Adaptive and Predictive Control Strategy for an Activated Sludge Process. Bioprocess Eng 23 (5):529–534

Chen, W.C., Chang, N.B. and Chen, J.C., 2002. GA-based fuzzy neural controller design for municipal incinerators. Fuzzy Sets and Systems, 129(3), pp.343-369.

Chen, W.C., Chang, N.B. and Chen, J.C., 2003. Rough set-based hybrid fuzzy-neural controller design for industrial wastewater treatment. Water Research, 37(1), pp.95-107.

Chen, W., Yao, C. and Lu, X., 2014. Optimal design activated sludge process by means of multi-objective optimization: case study in Benchmark Simulation Model 1 (BSM1). Water science and technology, 69(10), pp.2052-2058.

Chen, HB., Tang, XC., He, QB., Qu, JN., and Gao, TY., 2007. Phosphorus uptaking behavior of phosphorus accumulating organisms in reversed AAO Process. China Environmental Science, 27(1), 49-53.

Chen, Z., Chang, Z., Zhang, L., Wang, J., Qiao, L., Song, X., and Li, J., 2020. Effects of carbon source addition on microbial community and water quality in recirculating aquaculture systems for Litopenaeus vannamei. Fisheries Science, 1, 1-1. https://doi.org/10.1007/s12562-020-014233.

Cho, J.H., Sung, S.W. and Lee, I.B., 2002. Cascade control strategy for external carbon dosage in predenitrifying process. Water science and Technology, 45(4-5), 53-60. https://doi.org/10.2166/wst.2002.0550.

Cristea, V.M., Pop, C., and Agachi, P.S., 2008. Model Predictive Control of the waste water treatment plant based on the Benchmark Simulation Model No. 1-BSM1. In Computer Aided Chemical Engineering, 25, 441-446. DOI: 10.1016/S1570-7946(04)80170-6.

Crisan, R., Harja, G., Nascu, I. and Nicoara, I., 2018. Hierarchical control system for energy savings in wastewater treatment plant. In 2018 IEEE International Conference on Automation, Quality and Testing, Robotics (AQTR), IEEE, 1-6. DOI: 10.1109/AQTR.2018.8402741.

De Kreuk, M.K., Pronk, M., and Van Loosdrecht., M.C.M., 2005. Formation of aerobic granules and conversion processes in an aerobic granular sludge reactor at moderate and low temperatures. Water research, 39(18), 4476-4484. DOI: 10.1016/j.watres.2005.08.031.

Do, H.T., Van Bach, N., Van Nguyen, L., Tran, H.T. and Nguyen, M.T., 2021. A design of higher-level control based genetic algorithms for wastewater treatment plants. Engineering Science and Technology, an International Journal, 24(4), pp.872-878.

Doyle JC, Francis BA, Tannenbaum AR (2013) Feedback Control Theory. Courier Corporation 41.

Ekama, G.A., 2009. Using bioprocess stoichiometry to build a plant-wide mass balance based steady-state WWTP model. Water research, 43(8), pp.2101-2120.

Ersu, CB., Ong, SK., Arslankaya, E., and Lee, YW., 2010 Impact of solids residence time on biological nutrient removal performance of membrane bioreactor. Water research, 44(10), 3192-202. https://doi.org/10.1016/j.watres.2010.02.036.

Fang, F., Ni, B., Li, W., Sheng, G., and Yu, H., 2011. A simulation-based integrated approach to optimize the biological nutrient removal process in a full-scale wastewater treatment plant. Chemical Engineering Journal, 174(2-3), 635-43. https://doi.org/10.1016/j.cej.2011.09.079.

Fang, F., Qiao, LL., Cao, JS., Li, Y., Xie, WM., Sheng, GP., and Yu, HQ., 2016. Quantitative evaluation of A2O and reversed A2O processes for biological municipal wastewater treatment

using a projection pursuit method. Separation & Purification Technology, 166, 164-70. https://doi.org/10.1016/j.seppur.2016.04.036.

Fiter M, Güell D, Comas J, Colprim J, Poch M, Rodríguez-Roda I (2005) Energy Saving in a Wastewater Treatment Process: An Application of Fuzzy Logic Control. Environ. Techn 26 (11):1263–1270.74.

Flores-Alsina, X., Ikumi, D., Batstone, D., Gernaey, K.V., Brouckaert, C., Ekama, G.A. and Jeppsson, U., 2012. Towards a plant-wide Benchmark Simulation Model with simultaneous nitrogen and phosphorus removal wastewater treatment processes, IWA World Water Congress and Exhibition.

Flores-Alsina, X., Gernaey, K.V., and Jeppsson, U., 2012. Benchmarking biological nutrient removal in wastewater treatment plants: Influence of mathematical model assumptions. Water Science and Technology, 65(8), 1496-1505.

Flores-Alsina, X., Solon, K., Kazadi Mbamba, C., Tait, S., Jeppsson, U., Gernaey, K.V., and Batstone, D.J., 2016. Modelling phosphorus, sulphur and iron interactions during the dynamic simulation of anaerobic digestion processes. Water Research, 95, 370e382.

Flores-Alsina, X., Comas, J., Rodríguez Roda, I., Poch, M., Gernaey, K. V., and Jeppsson, U., 2009. Evaluation of plant-wide WWTP control strategies including the effects of filamentous bulking sludge. Water Science and Technology, 60, 2093–2103. https://doi.org/10.2166/wst.2009.523.

Flores-Alsina, X., Solon, K., Kazadi Mbamba, C., Tait, S., Jeppsson, U., Gernaey, K.V., and Batstone, D.J., 2016. Modelling phosphorus, sulphur and iron interactions during the dynamic simulation of anaerobic digestion processes. Water Research, 95, 370e382.

Flores-Alsina, X., Ramin, E., Ikumi, D., Harding, T., Batstone, D., Brouckaert, C., Sotemann, S. and Gernaey, K.V., 2021. Assessment of sludge management strategies in wastewater treatment systems using a plant-wide approach. Water Research, 190, 116714.

Flores-Alsina, X., Arnell, M., Amerlinck, Y., Corominas, L., Gernaey, K.V., Guo, L., Lindblom, E., Nopens, I., Porro, J., Shaw, A., and Snip, L., 2014. Balancing effluent quality, economic cost and greenhouse gas emissions during the evaluation of (plant-wide) control/operational strategies in WWTPs. Science of the Total Environmnet, 466, 616-624.

Garikiparthy, P.S.N., Lee, S.C., Liu, H., Kolluri, S.S., Esfahani, I.J., Yoo, and C.K., 2016. Evaluation of multiloop chemical dosage control strategies for total phosphorus removal of

enhanced biological nutrient removal process. Korean Journal of Chemical Engineering, 33(1), 14-24. http://10.1007/s11814-015-0132-9.

Grau, P., Vanrolleghem, P. and Ayesa, E., 2007. BSM2 Plant-Wide Model construction and comparative analysis with other methodologies for integrated modelling, Water Science and Technology, 56(8), 57-65.

Gernaey, K., Jeppsson, U., Batstone, D.J., and Ingildsen, P., 2006. Impact of reactive settler models on simulated WWTP performance. Water Science and Technology, 53(1), 159-167.

Gernaey, K.V., Jeppsson, U., Vanrolleghem, P.A., and Copp, J.B., 2014. Benchmarking of Control Strategies for Wastewater Treatment Plants. IWA Publishing, London, UK, IWA Scientific and Technical Report No. 23.

Gernaey, K.V. and Jørgensen, S.B., 2004. Benchmarking combined biological phosphorus and nitrogen removal wastewater treatment processes. Control Engineering Practice, 12(3), 357-373. https://doi.org/10.1016/S0967-0661(03)00080-7.

Guerrero, J., Guisasola, A., and Baeza, J.A., 2014. A novel control strategy for efficient biological phosphorus removal with carbon-limited wastewaters. Water Science and Technology, 70, 691. https://doi.org/10.2166/wst.2014.280.

Grimholt, C. and Skogestad, S., 2018. Optimal PI and PID control of first-order plus delay processes and evaluation of the original and improved SIMC rules. Journal of Process Control, 70, 36-46.

Gujer, W., Henze, M., Min, T., and van Loosdrecht, M.C.M., 2000. Activated sludge model no. 3. Water Science and Technology, 39(1), 183–193. https://doi.org/10.1016/S0273-1223(98)00785-9.

Guerrero, J., Flores-Alsina, X., Guisasola, A., Baeza, J.A., and Gernaey, K.V., 2013. Effect of nitrite, limited reactive settler and plant design configuration on the predicted performance of simultaneous C/N/P removal WWTPs. Bioresource Technology, 136, 680-688.

Guerrero, J., Guisasola, A., Comas, J., Rodríguez-Roda, I., and Baeza, J.A., 2012. Multi-criteria selection of optimum WWTP control setpoints based on microbiology-related failures, effluent quality and operating costs. Journal of Chemical Engineering, 188, 23–29. https://doi.org/10.1016/j.envsoft.2010.10.012

Guerrero, J., Guisasola, A., Vilanova, R., and Baeza, J.A., 2011. Improving the performance of a WWTP control system by model-based setpoint optimisation. Environmental Modelling Software, 26, 492-497. https://doi.org/10.1016/j.cej.2012.01.115

Gujer, W., Henze, M., Mino, T., Matsuo, T., Wentzel, M.C., and Marais, G.V.R., 1995. The activated sludge model No. 2: biological phosphorus removal. Water science and technology, 31(2), 1-11. https://doi.org/10.1016/0273-1223(95)00175-M.

Guerrero, J., Guisasola, A., and Baeza, J.A., 2011. The nature of the carbon source rules the competition between PAO and denitrifiers in systems for simultaneous biological nitrogen and phosphorus removal. Water Research, 45(16), 4793-4802.

Görgün, E., Insel, G., Artan, N, and Orhon., D., 2007. Model evaluation of temperature dependency for carbon and nitrogen removal in a full-scale activated sludge plant treating leather-tanning wastewater. Journal of Environmental Science and Health, 42(6), 747-756. DOI:10.1080/10934520701304427.

Ghanizadeh, G., Sarafpour, R., 2001. The effects of temperature and pH on settlability of activated sludge flocs. Iranian journal of public health, 30(3-4), 139-142. http://10.1016/j.watres.2011.06.019.

Hamdani, A., Amrane, A., Yettefti, I.K., Mountadar, M. and Assobhei, O., 2020. Carbon and nitrogen removal from a synthetic dairy effluent in a vertical-flow fixed bed bioreactor. Bioresource Technology Reports, 12, 100581.

Henze, M., Gujer, W., Mino, T., and van Loosdrecht, M.C., 2000. Activated sludge models ASM1, ASM2, ASM2d and ASM3. IWA publishing in its Scientific and Technical report, London.

Han, H.G., Qiao, J.F. and Chen, Q.L., 2012. Model predictive control of dissolved oxygen concentration based on a self-organizing RBF neural network. Control Engineering Practice, 20(4), pp.465-476.

Hakanen, J., Sahlstedt, K. and Miettinen, K., 2013. Wastewater treatment plant design and operation under multiple conflicting objective functions. Environmental modelling & software, 46, pp.240-249.

Holenda, B., Domokos, E., Redey, A. and Fazakas, J., 2008. Dissolved oxygen control of the activated sludge wastewater treatment process using model predictive control. Computers and Chemical Engineering, 32(6), 1270-1278. DOI: 10.1016/j.compchemeng.2007.06.008.

Hongyang, X., Pedret, C., Santin, I. and Vilanova, R., 2018. Decentralized Model Predictive Control for N and P removal in wastewater treatment plants. In 2018 22nd International Conference on System Theory, Control and Computing (ICSTCC), IEEE, 224-230.

Henze, M., Gujer, W., Mino, T., Matsuo, T., Wentzel, M.C., Marais, G.V.R., and van Loosdrecht, M.C.M., 1999. Activated Sludge Model No. 2d, ASM2d. Water Science and Technology, 39(1), 165-182.

Hu, X., Wisniewski, K., Czerwionka, K., Zhou, Q., Xie, L., and Makinia, J., 2016. Modeling the effect of external carbon source addition under different electron acceptor conditions in biological nutrient removal activated sludge systems. Environmental Science and Technology, 50(4), 1887-96. https://doi.org/10.1021/acs.est.5b04849.

Hu, Z.R., Wentzel, M.C. and Ekama, G.A., 2007. A general kinetic model for biological nutrient removal activated sludge systems: model development. Biotechnology and bioengineering, 98(6), pp.1242-1258.

Henze, M., Grady Jr, C.L., Gujer, W., Marais, G.V.R., and Matsuo, T., 1987. A general model for single-sludge wastewater treatment systems. Water research, 21(5), 505-515.

Jeppsson U., 1996. Modelling Aspects of Wastewater Treatment Processes. Lund Institute of Technology (LTH), Reports.

Jeppsson, U., Pons, M.N., Nopens, I., Alex, J., Copp, J.B., Gernaey, K.V., Rosén, C., Steyer, J.P. and Vanrolleghem, P.A., 2007. Benchmark simulation model no 2: general protocol and exploratory case studies. Water Science and Technology, 56(8), 67-78.

Jeppsson, U., and Pons, M.N., 2004. The COST benchmark simulation model—current state and future perspective.

Kalker TJJ, van Goor CP, Roeleveld PJ, Ruland MF, Babuška R (1999) Fuzzy Control of Aeration in an Activated Sludge Wastewater Treatment Plant: Design, Simulation and Evaluation. Water Sci. Techn 39 (4):71–78.73.

Kazadi Mbamba, C., Flores-Alsina, X., Batstone, D.J., and Tait, S., 2016. Validation of a plant-wide phosphorus modelling approach with minerals precipitation in a full-scale WWTP. Water Research, 100, 169-183.

Kazadi Mbamba, C., Tait, S., and Flores-Alsina, X., and Batstone, D.J. (2015). A systematic study of multiple minerals precipitation modelling in wastewater treatment. Water Research, 85, 359-370.

Kang, XS., Liu, CQ., Zhang, B., Bi, XJ., Zhang, F., and Cheng, LH., 2011. Application of reversed A2/O process on removing nitrogen and phosphorus from municipal wastewater in China. Water Science and Technology. 63(10):2138-42. https://doi.org/10.2166/wst.2011.340.

Kouvaritakis B, Cannon M (2016) Model predictive control. Switzerland: Springer International Publishing 38.

Klaus, S., and Bott, C.B., 2020. Comparison of sensor driven aeration control strategies for improved understanding of simultaneous nitrification/denitrification. Water Environment Research, wer.1359. https://doi.org/10.1002/wer.1359.

Lema JM, Martinez SS (2017) Innovative wastewater treatment & resource recovery technologies: impacts on energy, economy and environment. IWA publishing.

Ledakowicz, S.M. Solecka, and Zylla R., 2001. Biodegradation, decolourisation and detoxification of textile wastewater enhanced by advanced oxidation processes. Journal Biotechnology, 89, (2–3), 175–184, 2001.

Liu, CQ., Zhang, F., Bi, XJ., and Zhang, B., 2008. Contrast between Inverted A2/O process and Improved A2/O process in full-scale test. Technology of Water Treatment. 34(5), 53-6.

Liu, H., Chang, K.H. and Yoo, C., 2012. Multi-objective optimization of cascade controller in combined biological nitrogen and phosphorus removal wastewater treatment plant. Desalination and Water Treatment, 43(1-3), pp.138-148.

Li, P., Bi, X.J., Wang, J., and Ru, S.G., 2017. Microbial diversity in activated sludges of conventional and reversed A2/O processes. China Environmental Science. 2017(37), 1137-45.

Lippi, S., Rosso, D., Lubello, C., Canziani, R. and Stenstrom, M.K., 2009. Temperature modelling and prediction for activated sludge systems. Water Science and Technology, 59(1), 125-131. DOI: 10.2166/wst.2009.587.

López-Vázquez, C.M., Hooijmans, C.M., Brdjanovic, D., Gijzen, H.J. and van Loosdrecht, M.C., (2008). Factors affecting the microbial populations at full-scale enhanced biological phosphorus removal (EBPR) wastewater treatment plants in The Netherlands. Water research, 42(10-11), 2349-2360. https://doi.org/10.1016/j.watres.2008.01.001.

Lopez-Vazquez, C.M., Oehmen, A., Hooijmans, C.M., Brdjanovic, D., Gijzen, H.J., Yuan, Z. and van Loosdrecht, M.C., 2009. Modeling the PAO–GAO competition: effects of carbon source, pH and temperature. Water Research, 43(2), pp.450-462.

Luca, L., Pricopie, A., Barbu, M., Ifrim, G. and Caraman, S., 2019. Control Strategies of Phosphorus Removal in Wastewater Treatment Plants. In 2019 23rd International Conference on System Theory, Control and Computing (ICSTCC), IEEE, 236-241. https://doi.org/10.1109/ICSTCC.2019.8886023.

Lumley D (2002) On-line instrument confirmation: how can we check that our instruments are working? Water Sci and Techn 45(4–5):469–476.

Maciejowski, J.M., 2002. Predictive Control with Constraints. Pearson Education, Harlow, England, 1st edition.

Machado, V.C., Gabriel, D., Lafuente, J., and Baeza, J.A., 2009. Cost and effluent quality controllers design based on the relative gain array for a nutrient removal WWTP. Water Research, 43, 5129–41. https://doi.org/10.1016/j.watres.2009.08.011.

Maheswari, P., Sheik, A.G., Tejaswini, E.S.S., and Ambati, S.R., 2020. Nested control loop configuration for a three stage biological wastewater treatment process. Chemical Product and Process Modeling. 1(ahead-of-print). http://10.1515/cppm-2020-0035.

Machado, VC., Gabriel, D., Lafuente, J., and Baeza, JA., 2009. Cost and effluent quality controllers design based on the relative gain array for a nutrient removal WWTP. Water Research. 43(20), 5129-41. https://doi.org/10.1016/j.watres.2009.08.011.

Massara, TM., Solís, B., Guisasola, A., Katsou, E., and Baeza, JA., 2018. Development of an ASM2d-N2O model to describe nitrous oxide emissions in municipal WWTPs under dynamic conditions. Chemical Engineering Journal., 335, 185-96. https://doi.org/10.1016/j.cej.2017.10.119.

Mareda, T., Gaudard, L. and Romerio, F., 2017. A parametric genetic algorithm approach to assess complementary options of large scale windsolar coupling. IEEE/CAA Journal of Automatica Sinica, 4(2), pp.260-272.

Metcalf and Eddy., Burton, F.L., Stensel, H.D., and Tchobanoglous, G., 2003. Wastewater engineering: treatment and reuse, McGraw Hill, New York.

Meijer, S.C.F., 2004. Theoretical and practical aspects of modelling activated sludge processes. (PhD Thesis). Delft university of technology, The Netherlands.

Meng, J., Li, J., Li, J., Nan, J., Deng, K., and Antwi, P., 2019. Effect of temperature on nitrogen removal and biological mechanism in an up-flow microaerobic sludge reactor treating wastewater rich in ammonium and lack in carbon source, Chemosphere, 216, 186-194.

Murat, S., Insel, G., Artan, N., and Orhon, D., 2004. Effect of temperature on the nitrogen removal performance of a sEQIuencing batch reactor treating tannery wastewater. Water science and technology, 48(11-12), 319-326. DOI:10.2166/wst.2004.0870.

Nopens, I., Benedetti, L., Jeppsson, U., Pons, M. N., Alex, J., Copp, J. B., 2010. Benchmark Simulation model no. 2: Finalization of plant layout and default control strategy. Water Science and Technology, 62, 1967–1974. https://doi.org/10.2166/wst.2010.044.

Nopens, I., Batstone, D.J., Copp, J.B., Jeppsson, U., Volcke, E., Alex, J. and Vanrolleghem, P.A., 2009. An ASM/ADM model interface for dynamic plant-wide simulation, water res,43(7), 1913-1923.

Oehmen, A., Carvalho, G., Lopez-Vazquez, C.M., Van Loosdrecht, M.C.M. and Reis, M.A.M., 2010. Incorporating microbial ecology into the metabolic modelling of polyphosphate accumulating organisms and glycogen accumulating organisms. Water research, 44(17), pp.4992-5004.

Olsson, G., Nielsen, M.K., Yuan, Z., Lynggaard-Jensen, A., Steyer, J.-P., 2005. Instrumentation, control and automation in wastewater systems. IWA Publishing.

Otterpohl, R., 1995. Dynamische Simulation zur Unterstützung der Planung und des Betriebes von kommunalen Kläranlagen [Dynamic Simulation to Support the Design and Operation of Municipal Wastewater Treatment Plants]. Ph.D. Thesis, Technical University of Aachen, Aachen, Germany.

Ostace, G.S., Baeza, J.A., Guerrero, J., Guisasola, A., Cristea, V.M., Agachi, P.Ş., and Lafuente, F.J., 2013. Development and economic assessment of different WWTP control strategies for optimal simultaneous removal of carbon, nitrogen and phosphorus. Computers and Chemical Engineering, 53, 164–177. https://doi.org/10.1016/j.compchemeng.2013.03.007

Ostace, G.S., Cristea, V.M., Agachi, P.Ş., 2011. Cost reduction of the wastewater treatment plant operation by MPC based on modified ASM1 with two-step nitrification/denitrification model. Computers and Chemical Engineering, 35, 2469 - 2479. https://doi.org/10.1016/j.compchemeng.2011.03.031

Puyol, D., Batstone, D.J., Hülsen, T., Astals, S., Peces, M. and Krömer, J.O., 2017. Resource recovery from wastewater by biological technologies: opportunities, challenges, and prospects. Frontiers in microbiology, 7(1-23)-2106.

Piotrowski, R., 2020. Supervisory fuzzy control system for biological processes in sequencing wastewater batch reactor. Urban Water Journal, 1-8. https://doi.org/10.1080/1573062X.2020.1778744.

Rieger, L., Koch, G., Kühni, M., Gujer, W. and Siegrist, H., 2001. The EAWAG Bio-P module for activated sludge model No. 3. Water research, 35(16), pp.3887-3903. DOI: 10.1016/S0043-1354(01)00110-5.

Rieger L, Alex J, Winkler S, Boehler M, Thomann M, Siegrist H (2003). Progress in sensor technology – Progress in process control? Part I: Sensor property investigation and classification. Wat. Sci. Techn 47(2):103-112.

Rojas, J.D., Baeza, J.A., and Vilanova, R., 2011. Effect of the controller tuning on the performance of the BSM1 using a data driven approach, in: Watermatex 2011. 8th IWA Symposium on Systems Analysis and Integrated Assessment. pp. 785–792.

Rosen C, Jeppsson U, Rieger L, Vanrolleghem PA (2008). Adding realism to simulated sensors and actuators. Wat. Sci. Tech 57(3):337-344.

Takács, I., Patry, G.G. and Nolasco, D., 1991. A dynamic model of the clarification-thickening process. Water research, 25(10), 1263-1271. https://doi.org/10.1016/0043-1354(91)90066-Y.

Tejaswini, E.S.S., Panjwani, S. and Rao, A.S., 2020. Design of Hierarchical Control Strategies for Biological Wastewater Treatment Plants to Reduce Operational Costs. Chemical Engineering Research and Design. https://doi.org/10.1016/j.cherd.2020.07.003.

Tejaswini, E., Babu, G.U.B. and Rao, A.S., Effect of temperature on effluent quality in a biological wastewater treatment process, Chemical Product and Process Modeling., 2019, 15(1).

Tejaswini, E.S.S., Panjwani, S., Gara, U.B.B. and Ambati, S.R., 2021. Multi-objective optimization based controller design for improved wastewater treatment plant operation. Environmental Technology & Innovation, 23, p.101591.

Sadeghassadi, M., Macnab, C.J.B., Gopaluni, B., Westwick, D., 2018. Application of neural networks for optimal-setpoint design and MPC control in biological wastewater treatment. Comput. Chem. Eng. 115, 150–160. https://doi.org/10.1016/j.compchemeng.2018.04.007.

Santin, I., Pedret, C. and Vilanova, R., 2015. Applying variable dissolved oxygen set point in a two level hierarchical control structure to a wastewater treatment process. Journal of Process Control, 28, 40-55. https://doi.org/10.1016/j.jprocont.2015.02.005.

Santín, I., Pedret, C., Vilanova, R. and Meneses, M., 2016. Advanced decision control system for effluent violations removal in wastewater treatment plants. Control Engineering Practice, 49, 60-75. https://doi.org/10.1016/j.conengprac.2016.01.005

Santín, I., Vilanova, R., Pedret, C. and Barbu, M., 2019, October. Dissolved oxygen control in wastewater treatment plants considering sensor noise and actuator delays. In 2019 23rd International Conference on System Theory, Control and Computing (ICSTCC), IEEE, 230-235. https://doi.org/10.1109/ICSTCC.2019.8885677.

Santín, I., Pedret, C. and Vilanova, R., 2015, June. Control strategies for ammonia violations removal in BSM1 for dry, rain and storm weather conditions. In 2015 23rd Mediterranean Conference on Control and Automation (MED), IEEE, 577-582. DOI:10.1109/MED.2015.7158809.

Schraa, O., Rieger, L., Alex, J., Miletić, I., 2019. Ammonia-based aeration control with optimal SRT control: improved performance and lower energy consumption. Water Science and Technology, 79, 63–72. https://doi.org/10.2166/wst.2019.032.

Seborg DE, Mellichamp DA, Edgar TF, Doyle FJ (2010) III Process Dynamics and Control. John Wiley & Sons: New York.

Sousa, J., Ribeiro, A., da Conceição Cunha, M. and Antunes, A., 2002. An optimization approach to wastewater systems planning at regional level. Journal of Hydroinformatics, 4(2), pp.115-123.

Solon, K. Extending Wastewater Treatment Process Models for Phosphorus Removal and Recovery: A Framework for Plant-Wide approach of Phosphorus, Sulfur and Iron, 2017, Doctoral dissertation, Lund University.

Solon, K., Flores-Alsina, X., Mbamba, C.K., Ikumi, D., Volcke, E.I.P., Vaneeckhaute, C., Ekama, G., Vanrolleghem, P.A., Batstone, D.J., Gernaey, K.V. and Jeppsson, U., 2017. Plant-wide modelling of phosphorus transformations in wastewater treatment systems: Impacts of control and operational strategies, Water Research, 113, 97-110.

Solon, K., 2015. Activated sludge model no. 3 with bioP module (ASM3bioP) implemented within the benchmark simulation model no.1, Technical Report. Division of Industrial Electrical Engineering and Automation Faculty of Engineering, Lund University, Sweden.

Sotomayor OA, Park SW, Garcia C (2002) MPC Control of a Predenitrification Plant Using Linear Subspace Models. In Computer Aided Chemical Engineering, Elsevier: Hague, The Netherlands. 10: 553–558.

Singh, K.S., and Viraraghavan, T., (2002). Effect of temperature on bio-kinetic co-efficients in UASB treatment of municipal wastewater. Water, Air, and Soil Pollution, 136(1-4), 243-254. DOI: 10.1023/A:1015212524720.

Shen, W., Chen, X., Corriou, J.P., 2008. Application of model predictive control to the BSM1 benchmark of wastewater treatment process. Computers and Chemical Engineering, 32, 2849–2856. https://doi.org/10.1016/j.compchemeng.2008.01.009.

Shen, W., Chen, X., Pons, M.N. and Corriou, J.P., 2009. Model predictive control for wastewater treatment process with feedforward compensation. Chemical Engineering Journal, 155(1-2), 161-174. DOI: 10.1016/j.cej.2009.07.039.

Shahzad, M., Khan, S.J. and Paul, P., 2015. Influence of temperature on the performance of a full-scale activated sludge process operated at varying solids retention times whilst treating municipal sewage, Water, 7(3), 855-867.

Snip, L.J.P.; Flores-Alsina, X.; Aymerich, I.; Rodríguez-Mozaz, S.; Barcelo, D.; Plosz, B.G.; Corominas, L.; Rodriguez-Roda, I.; Jeppsson, U.; Gernaey, K.V. Generation of synthetic data to perform (micro) pollutant wastewater treatment modelling studies. Sci. of Total Environ. 2016, 569(570), 278-290.

Stare, A., Vrečko, D., Hvala, N., Strmčnik, S., 2007. Comparison of control strategies for nitrogen removal in an activated sludge process in terms of operating costs: A simulation study. Water Reseach, 41, 2004–2014. https://doi.org/10.1016/j.watres.2007.01.029.

Steffens M, Lant P (1999) Multivariable Control of Nutrient-Removing Activated Sludge Systems. Water Res 33(12):2864–2878.

United Nations World Water Assessment Programme (WWAP) (2016). The United Nations World Water Development Report 2016: Water and Jobs. Paris, France: UNESCO.

Von Sperling, M., and de Lemos Chernicharo, C.A., 2005. Biological wastewater treatment in warm climate regions, IWA publishing., London, UK, 1.

Valverde-Pérez, B., Fuentes-Martínez, J.M., Flores-Alsina, X., Gernaey, K. V, Huusom, J.K., Plósz, B.G., 2016. Control structure design for resource recovery using the enhanced biological phosphorus removal and recovery (EBP2R) activated sludge process. Chemical engineering journal, 296, 447–457. https://doi.org/10.1016/j.cej.2016.03.021.

Van Der Hoek, J. P., De Fooij, H., and Struker, A., 2016. Wastewater as a resource: Strategies to recover resources from Amsterdam's wastewater. Resouce. Conservation Recycle,113, 53–64.

Xu, H., Vilanova, R., 2013. Comparison of control strategies on combined biological phosphorus and nitrogen removal wastewater treatment process. In 2013 17th International Conference on System Theory, Control and Computing (ICSTCC), IEEE, 595-600. https://doi.org/10.1109/ICSTCC.2013.6689024.

Xu H, Vilanova, R., 2015. PI and fuzzy control for P-removal in wastewater treatment plant. International Journal of Computers Communications and Control, 10(6), 176-191. https://doi.org/10.15837/ijccc.2015.6.2081.

Xu, S., Bernards, M., Hu, Z., 2014. Evaluation of anaerobic/anoxic/oxic (A2/O) and reverse A2/O processes in biological nutrient removal., Water Environment Research 86(11), 2186-93. https://doi.org/10.2175/106143014X14062131178394.

Xie, WM., Zeng, RJ., Li, WW., Wang, GX., Zhang, LM., 2018. A modeling understanding on the phosphorous removal performances of A 2 O and reversed A 2 O processes in a full-scale wastewater treatment plant. Environmental Science and Pollution Research, 25(23), 22810-7. https://doi.org/10.1007/s11356-018-2317-3.

Wang, Q., Chen, Q., and Chen, J., 2017. Optimizing external carbon source addition in domestics wastewater treatment based on online sensoring data and a numerical model. Water Science and Technology, 75(11), 2716-25. https://doi.org/10.2166/wst.2017.128.

Zhang, B., Gao, T., 2000. An anoxic/anaerobic/aerobic process for the removal of nitrogen and phosphorus from wastewater. Journal of Environ Science and Health, 35(10), 1797-801. https://doi.org/10.1080/10934520009377075.

Zhou, Z., Wu, Z., Wang, Z., Tang, S., Gu, G., Wang, L., Wang, Y., and Xin, Z., 2011. Simulation and performance evaluation of the anoxic/anaerobic/aerobic process for biological nutrient removal., Korean Journal of Chemical Engineering, 28(5), 1233. https://doi.org/10.1007/s11814-010-0502-2.

Zhou, Z., Shen, X., Jiang, LM., Wu, Z., Wang, Z., Ren, W., and Hu, D., 2015. Modeling of multimode anaerobic/anoxic/aerobic wastewater treatment process at low temperature for process optimization. Chemical Engineering Journal, 281, 644-50. https://doi.org/10.1016/j.cej.2015.07.017.

Zhang, M., Peng, Y., Wang, C., Wang, C., Zhao, W., Zeng, W., 2016. Optimization denitrifying phosphorus removal at different hydraulic retention times in a novel anaerobic anoxic oxic-biological contact oxidation process. Biochemical Engineering Journal, 106, 26-36. https://doi.org/10.1016/j.bej.2015.10.027.

APPENDIX A

Table A1 Stoichiometric parameters matrix for the soluble components of ASM3 (Henze et al. (2000))

	Model components (i)	1	2	3	4	5	6	7	8
j	Process	S_O ($gO2\ m^{-3}$)	S_S ($gCOD/m^3$)	S_I ($gCOD/m^3$)	S_{NH} ($gN\ m^{-3}$)	S_{NO} ($gN\ m^{-3}$)	S_{N2} ($gN\ m^{-3}$)	S_{PO4} ($gP\ m^{-3}$)	S_{HCO} ($mol\ m^{-3}$)
1	Hydrolysis		$1-f_{SI}$		$i_{N,XS}+i_{N,SS}(f_{SI}-1)-i_{N,SI}.f_{SI}$			$i_{P,XS}-i_{P,SS}$	$V_{1,HCO}$
Heterotrophic organisms X_H									
2	Aer. Storage of X_{STO}	Y_{STO,O_2}^{-1}	-1		$i_{N,SS}$			$i_{P,SS}$	$V_{2,HCO}$
3	Anox. Storage of X_{STO}		-1		$i_{N,SS}$	$-(1-Y_{STO,NO})/2.86$	$(1-Y_{STO,NO})/2.86$	$i_{P,SS}$	$V_{3,HCO}$
4	Aerobic growth	$1-1/Y_{H,O_2}$			$-i_{N,BM}$			$-i_{P,BM}$	$V_{4,HCO}$
5	Anoxic growth				$-i_{N,BM}$	$-(1-Y_{H,NO}^{-1})/2.86$	$(1-Y_{H,NO}^{-1})/2.86$	$-i_{P,BM}$	$V_{5,HCO}$
6	Aer. endog. Respiration	$-(1-f_{XI})$			$i_{N,BM}-f_{XI}i_{N,XI}$			$i_{P,BM}-f_{XI}i_{P,XI}$	$V_{6,HCO}$
7	Anox. endog. respiration				$i_{N,BM}-f_{XI}i_{N,XI}$	$-(1-f_{XI})/2.86$	$(1-f_{XI})/2.86$	$i_{P,BM}-f_{XI}i_{P,XI}$	$V_{7,HCO}$
8	Aer. respiration of X_{STO}	-1							

9	Anox. resp. of X_{STO}					-1/2.86	1/2.86		$V_{9,HCO}$
	Autotrophic organisms X_A								
10	Growth	1-4.57/Y_A			-1/Y_A-$i_{N,BM}$	1/Y_A		-$i_{P,BM}$	$V_{10,HCO}$
11	Aer. endog. Respiration	-(1-f_{XI})			$i_{N,BM}$-$f_{XI}i_{N,XI}$			$i_{P,BM}$-$f_{XI}i_{P,XI}$	$V_{11,HCO}$
12	Anox. endog. respiration				$i_{N,BM}$-$f_{XI}i_{N,XI}$	-(1-f_{XI})/2.86	(1-f_{XI})/2.86	$i_{P,BM}$-$f_{XI}i_{P,XI}$	$V_{12,HCO}$
Phosphorus accumulating organisms X_{PAO}									
P1	Storage of X_{PHA}		-1		$i_{N,SS}$			Y_{PO4}+$i_{P,SS}$	$V_{P1,HCO}$
P2	Aerobic storage of X_{PP}	-Y_{PHA}						-1	$V_{P2,HCO}$
P3	Anox. storage X_{PP}					-Y_{PHA}/2.86	Y_{PHA}/2.86	-1	$V_{P3,HCO}$
P4	Aerobic growth	$1 - (1/Y_{PAO,O_2}$			-$i_{N,BM}$			-$i_{P,BM}$	$V_{P4,HCO}$
P5	Anox. growth				-$i_{N,BM}$	(1-(1/$Y_{PAO,NO}$))/2.86	-(1-(1/$Y_{PAO,NO}$))/2.86	-$i_{P,BM}$	$V_{P5,HCO}$
P6	Aer. endog. Respiration	-(1-f_{XI})			$i_{N,BM}$-$f_{XI}i_{N,XI}$			$i_{P,BM}$-$f_{XI}i_{P,XI}$	$V_{P6,HCO}$
P7	Anox. endog. Respiration				$i_{N,BM}$-$f_{XI}i_{N,XI}$			$i_{P,BM}$-$f_{XI}i_{P,XI}$	$V_{P7,HCO}$

P8	Aerobic lysis of X_{PP}							1	$V_{P8,HCO}$
P9	Anox. lysis of X_{PP}							1	$V_{P9,HCO}$
P 10	Aer. respiration of X_{PHA}	-1							
P 11	Anox. resp. of X_{PHA}					-1/2.86	1/2.86		$V_{P11,HCO}$
Composition matrix Conservatives									
1	ThOD[a] g ThOD	-1	1	1		-64/14	-24/14		
2	Nitrogen g N		$i_{N,SS}$	$i_{N,SI}$	1	1	1		
3	Phosphorus g P		$i_{P,SS}$	$i_{P,SI}$				1	
4	Ionic charge Mole+				1/4	-1/4		-1.5/31	-1
	Observables								
5	SS g SS								

* In this model, it is assumed that ThOD is identical to the measured COD. Definition: 1 g SO=-1 g ThOD, 1 g SNH=0 g ThOD, 1 g SNO=-64/14 g ThOD and 1 g SN2=-24/14 g ThOD.

V: stoich. coeff., j: process, i: components, $V_{j,HCO}$ and $V_{j,TSS}$ from charge and mass conservation (Gujer and Larsen, 1995)

Table A2 Stoichiometric parameters matrix for the particulate components of ASM3 (Henze et al. (2000)) and the EAWAG Bio-P module (Rieger et al. (2001))

	Model components (i)	9	10	11	12	13	14	15	16	17
j	Process	X_I ($gCOD/m^3$)	X_S ($gCOD/m^3$)	X_H ($gCOD/m^3$)	X_{STO} ($gCOD/m^3$)	X_{PAO} ($gCOD/m^3$)	X_{PP} (($gCOD/m^3$)	X_{PHA} ($gCOD/m^3$)	X_A ($gCOD/m^3$)	X_{TSS} ($gTSS/m^3$)
1	Hydrolysis		-1							$V_{1,TSS}$
Heterotrophic organisms X_H										
2	Aer. Storage of X_{STO}				$Y_{STO,O2}$					$V_{2,TSS}$
3	Anox. Storage of X_{STO}				$Y_{STO,NO}$					$V_{3,TSS}$
4	Aerobic growth			1	$-1/Y_{H,O2}$					$V_{4,TSS}$
5	Anoxic growth			1	$-1/Y_{H,NO}$					$V_{5,TSS}$
6	Aer. endog. Respiration	f_{XI}		-1						$V_{6,TSS}$
7	Anox. endog. respiration	f_{XI}		-1						$V_{7,TSS}$
8	Aer. respiration of X_{STO}				-1					$V_{8,TSS}$

9	Anox. resp. of X_{STO}				-1					$V_{9,TSS}$
	Autotrophic organisms X_A									
10	Growth								1	$V_{10,TSS}$
11	Aer. endog. Respiration	f_{XI}							-1	$V_{11,TSS}$
12	Anox. endog. respiration	f_{XI}							-1	$V_{12,TSS}$
Phosphorus accumulating organisms X_{PAO}										
P1	Storage of X_{PHA}						$-Y_{PO4}$	1		$V_{P1,TSS}$
P2	Aerobic storage of X_{PP}						1	$-Y_{PHA}$		$V_{P2,TSS}$
P3	Anox. storage X_{PP}						1	$-Y_{PHA}$		$V_{P3,TSS}$
P4	Aerobic growth					1		$-1/Y_{PAO,O2}$		$V_{P4,TSS}$
P5	Anox. growth					1		$-1/Y_{PAO,NO}$		$V_{P5,TSS}$
P6	Aer. endog. Respiration	f_{XI}				-1				$V_{P6,TSS}$
P7	Anox. endog. Respiration	f_{XI}				-1				$V_{P7,TSS}$

P8	Aerobic lysis of X_{PP}									$V_{P8,TSS}$
P9	Anox. lysis of X_{PP}									$V_{P9,TSS}$
P10	Aer. respiration of X_{PHA}							-1		$V_{P10,TSS}$
P11	Anox. resp. of X_{PHA}							-1		$V_{P11,TSS}$
Composition matrix Conservatives										
1	ThOD[a] g Th OD	1	1	1	1	1	1	1	1	
2	Nitrogen g N	$i_{N,XI}$	$i_{N,XS}$	$i_{N,BM}$		$i_{N,BM}$			$i_{N,BM}$	
3	Phosphorus g P	$i_{P,XI}$	$i_{P,XS}$	$i_{P,BM}$		$i_{P,BM}$	1		$i_{P,BM}$	
4	Ionic charge Mole+						-1/31			
	Observables									
5	SS g SS	$i_{TSS,XI}$	$i_{TSS,XS}$	$i_{TSS,BM}$	$i_{TSS,STO}$	$i_{TSS,BM}$	3.23	$i_{TSS,STO}$	$i_{TSS,BM}$	-1

Table A3 Kinetic rate expressions for ASM3 (Henze et al. (2000))

No.	Process	Process rate equation
Hydrolysis		
P1	Hydrolysis	$k_h \frac{X_S/X_H}{K_X + X_S/X_H} X_H$

Heterotrophic organisms		
P2	Aerobic storage of COD	$k_{STO}\frac{S_O}{K_{O,H}+S_O}\frac{S_S}{K_{SS,H}+S_S}X_H$
P3	Anoxic storage of COD	$k_{STO}\eta_{NO,H}\frac{K_{O,H}}{K_{O,H}+S_O}\frac{S_{NO}}{K_{NO,H}+S_{NO}}\frac{S_S}{K_{SS,H}+S_S}X_H$
P4	Aerobic growth	$\mu_H\frac{S_O}{K_{O,H}+S_O}\frac{S_{NH}}{K_{NH,H}+S_{NH}}\frac{S_{PO4}}{K_{PO4,H}+S_{PO4}}\frac{S_{HCO}}{K_{HCO,H}+S_{HCO}}\frac{X_{STO}/X_H}{K_{STO}+X_{STO}/X_H}X_H$
P5	Anoxic growth(deni)	$\mu_H\eta_{NO,H}\frac{K_{O,H}}{K_{O,H}+S_O}\frac{S_{NO}}{K_{NO,H}+S_{NO}}\frac{S_{NH}}{K_{NH,H}+S_{NH}}\frac{S_{PO4}}{K_{PO4,H}+S_{PO4}}\frac{S_{HCO}}{K_{HCO,H}+S_{HCO}}\frac{X_{STO}/X_H}{K_{STO}+X_{STO}/X_H}X_H$
P6	Aerobic endog. Resp	$b_H\frac{S_O}{K_{O,H}+S_O}X_H$
P7	Anoxic endog. Resp	$b_H\eta_{NO,end,H}\frac{K_{O,H}}{K_{O,H}+S_O}\frac{S_{NO}}{K_{NO,H}+S_{NO}}X_H$
P8	Aerobic resp. of X_{STO}	$b_H\frac{S_O}{K_{O,H}+S_O}X_{STO}$
P9	Anoxic resp. of X_{STO}	$b_H\eta_{NO,end,H}\frac{K_{O,H}}{K_{O,H}+S_O}\frac{S_{NO}}{K_{NO,H}+S_{NO}}X_{STO}$
Autotrophic organisms		
P10	Nitrification	$\mu_A\frac{S_O}{K_{O,H}+S_O}\frac{S_{NH}}{K_{NH,H}+S_{NH}}\frac{S_{PO4}}{K_{PO4,H}+S_{PO4}}\frac{S_{HCO}}{K_{HCO,H}+S_{HCO}}X_A$
P11	Aerobic endog. resp.	$b_A\frac{S_O}{K_{O,H}+S_O}X_A$
P12	Anoxic endog. resp.	$b_A\eta_{NO,A}\frac{K_{O,H}}{K_{O,H}+S_O}\frac{S_{NO}}{K_{NO,H}+S_{NO}}X_A$

Table A4 Kinetic rate expressions for the EAWAG Bio-P module (Rieger et al. (2001))

No.	Process	Process rate equations
Phosphorus accumulating organisms		
P13	Storage of X_{PHA}	$q_{PHA}\frac{S_S}{K_{SS,PAO}+S_S}\frac{S_{HCO}}{K_{HCO,PAO}+S_{HCO}}\frac{X_{PP}/X_{PAO}}{K_{PP,PAO}+X_{PP}/X_{PAO}}X_{PAO}$
P14	Aer. storage of X_{PP}	$q_{PP}\frac{S_O}{K_{O,PAO}+S_O}\frac{S_{PO4}}{K_{PO4,PP}+S_{PO4}}\frac{S_{HCO}}{K_{HCO,PAO}+S_{HCO}}\frac{X_{PHA}/X_{PAO}}{K_{PHA}+X_{PHA}/X_{PAO}}\frac{K_{max,PAO}-(X_{PHA}/X_{PAO})}{K_{iPP,PAO}+K_{max,PAO}-(X_{PP}/X_{PAO})}X_{PAO}$
P15	Anox. storage of X_{PP}	$q_{PP}\eta_{NO,PAO}\frac{K_{O,PAO}}{K_{O,PAO}+S_O}\frac{S_{NO}}{K_{NO,PAO}+S_{NO}}\frac{S_{PO4}}{K_{PO4,PP}+S_{PO4}}\frac{S_{HCO}}{K_{HCO,PAO}+S_{HCO}}\frac{X_{PHA}/X_{PAO}}{K_{PHA}+X_{PHA}/X_{PAO}}\frac{K_{max,PAO}-(X_{PHA}}{K_{iPP,PAO}+K_{max,PAO}-}$
P16	Aer. growth of X_{PAO}	$\mu_{PAO}\frac{S_O}{K_{O,PAO}+S_O}\frac{S_{NH}}{K_{NH,PAO}+S_{NH}}\frac{S_{PO4}}{K_{PO4,PP}+S_{PO4}}\frac{S_{HCO}}{K_{HCO,PAO}+S_{HCO}}\frac{X_{PHA}/X_{PAO}}{K_{PHA}+X_{PHA}/X_{PAO}}X_{PAO}$
P17	Anox. growth of X_{PAO}	$\mu_{PAO}\eta_{NO,PAO}\frac{K_{O,PAO}}{K_{O,PAO}+S_O}\frac{S_{NO}}{K_{NO,PAO}+S_{NO}}\frac{S_{NH}}{K_{NH,PAO}+S_{NH}}\frac{S_{PO4}}{K_{PO4,PP}+S_{PO4}}\frac{S_{HCO}}{K_{HCO,PAO}+S_{HCO}}\frac{X_{PHA}/X_{PAO}}{K_{PHA}+X_{PHA}/X_{PAO}}X_{PAO}$
P18	Aerobic endog. respiration	$b_{PAO}\frac{S_O}{K_{O,PAO}+S_O}X_{PAO}$
P19	Anoxic endog. respiration	$b_{PAO}\eta_{NO,end,PAO}\frac{K_{O,PAO}}{K_{O,PAO}+S_O}\frac{S_{NO}}{K_{NO,PAO}+S_{NO}}X_{PAO}$
P20	Aerobic lysis of X_{PP}	$b_{PP}\frac{S_O}{K_{O,PAO}+S_O}X_{PP}$
P21	Anoxic lysis of X_{PP}	$b_{PAO}\eta_{NO,lysis,PP}\frac{K_{O,PAO}}{K_{O,PAO}+S_O}\frac{S_{NO}}{K_{NO,PAO}}X_{PP}$
P22	Aerobic resp. of X_{PHA}	$b_{PHA}\frac{S_O}{K_{O,PAO}+S_O}X_{PHA}$
P23	Anoxic resp. of X_{PHA}	$b_{PHA}\eta_{NO,resp,PHA}\frac{K_{O,PAO}}{K_{O,PAO}+S_O}\frac{S_{NO}}{K_{NO,PAO}}X_{PHA}$

Procedure for Identification of Different Models used in this work Identification of FOPTD/State Space (SS) Model for Lower Level

System Identification process is used to identify the plant models to be used for control of BSM1-P/BSM2-P in FOPTD/SS form.

Step 1. Decide the control loops and corresponding manipulated and controlled variables.

Step 2. Run the Plant simulation model to reach steady state. It may be achieved after 100- 150 days for BSM1 and approximately after 200 days for BSM2. (Steady state should be the point around which identification is desired to be performed).

Important Tip: Make sure that steady state achieved for the controlled variable should be approximately the value near the set-points wished to be maintained in closed loop. Thus, a set of manipulated variables needed to maintain the controlled variables at their set-points with define an operating point. Here, for PI configuration the operating point used is $S_{O,7}$*=2 mg* (O_2)*/l,* $S_{NO,4}$*=1 mg N/l,* K_La_7*=252 1/d and* Q_{intr}*=34500* m^3*/d.*

Step 3. Now run the identification file which varies all the manipulated variables (here, K_La_7 and Q_{intr}) ±10% around their operating point simultaneously and record this input. If there is a need, include the disturbance variable as an additional input (here Q_{intr}) and give only the +5% to +10% of step change to it.

Step 4. Collect the data for variations respective controlled variables (here $S_{O,7}$ and $S_{NO,4}$) due to input supplied.

Step 5. Create a "*iddata*" object with recorded controlled and manipulated variables including disturbance variable and use a proper sampling time (here, 1/96).

Step 6. Go to System Identification tool box and import the data object created in previous step.

Step 7. Use only the portion with consistent oscillations in output around operating point. (Use select range option provided in toolbox).

Step 8. Preprocess the data if needed (i.e. remove means and trends).

Step 9. Create the estimation and validation parts of data (generally 2/3 part is used for estimation and 1/3 part for validation) and import estimation data in "working data" and rest in "validation data" in toolbox.

Step 10. For estimating FOPTD model, chose the option of "Process Model" form estimation options and provide any of the initial details (like gain) if available and estimate the model. For estimating State space model, chose the option of "State Space Models"

from estimation option and specify the order and type of model (continuous or discrete) to be estimated. There are several methods available for estimation like Subspace N4SID algorithm or prediction error method but the later one is generally used. There is an option available to choose the

input which have immediate effect on output (i.e. values in D matrix). Usually, matrix D=0. Chose all the desired options and estimate the model.

Step 11. Check the fit to estimation data and validation data, if it is within acceptable limits (generally above 70%) then model is fit to use otherwise repeat steps 2 -10 again.

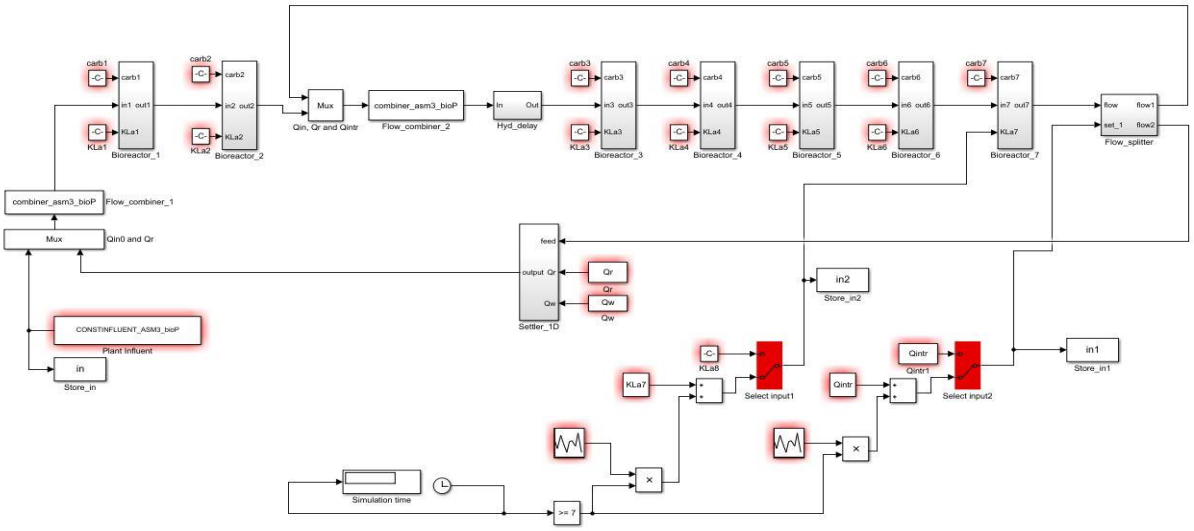

Figure A1. Lower Level Identification File

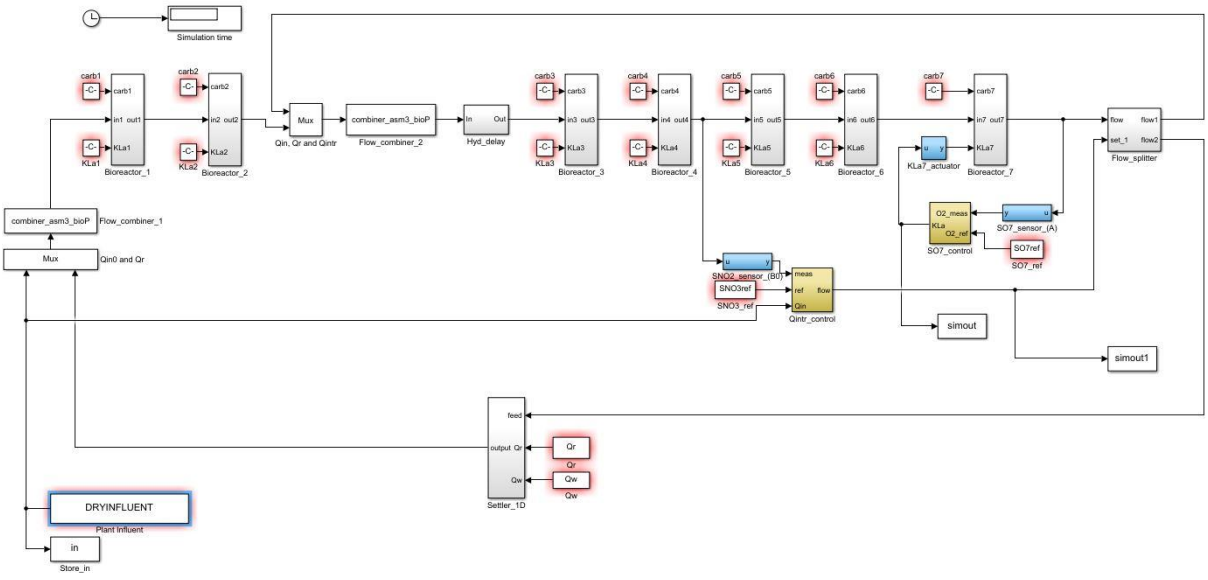

Figure A2. BSM1 Simulink Diagram with Default Controllers

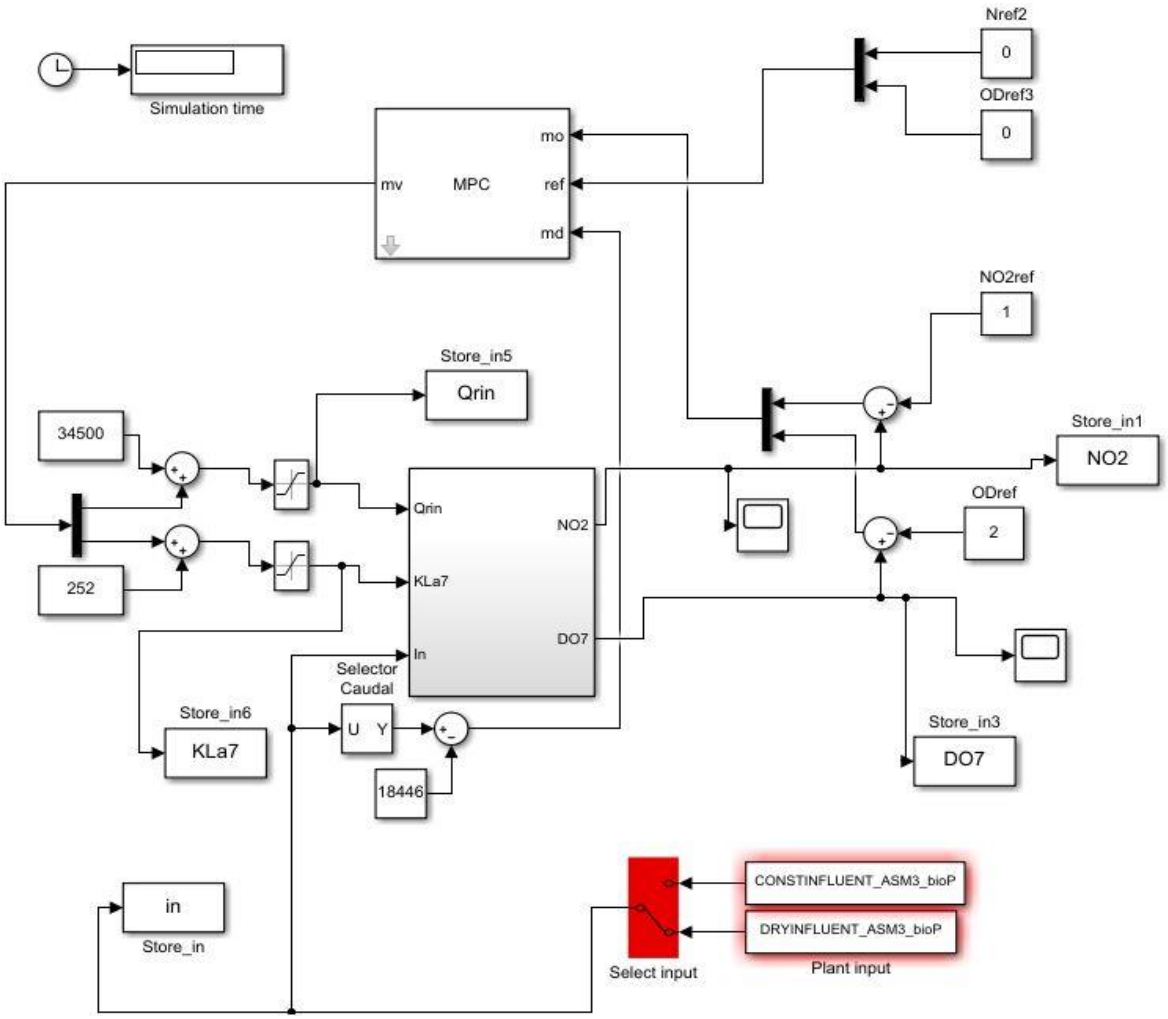

Figure A3. BSM1 with Lower Level MPC

Deciding Membership Function Ranges and Rules for Lower Level Fuzzy Controller

Step 1. Generally, MFs and rules for fuzzy controller are decided using expert knowledge of the operator (the fact that fuzzy controller is known as expert system is reflected here) or by using past data. Here as we have simulation file available for the plant, we can generate the steady data from which the rules can be deduced.

Step 2. Run the code given for generating the data.

Step 3. Table below shows the data used for deducing rules.

Step 4. The trend followed by data is captured in the graphs below. And the respective regions are used in fuzzification are marked in the graph. These are used in the division of variable in fuzzy sets and can also be used to determine the overlapping between them.

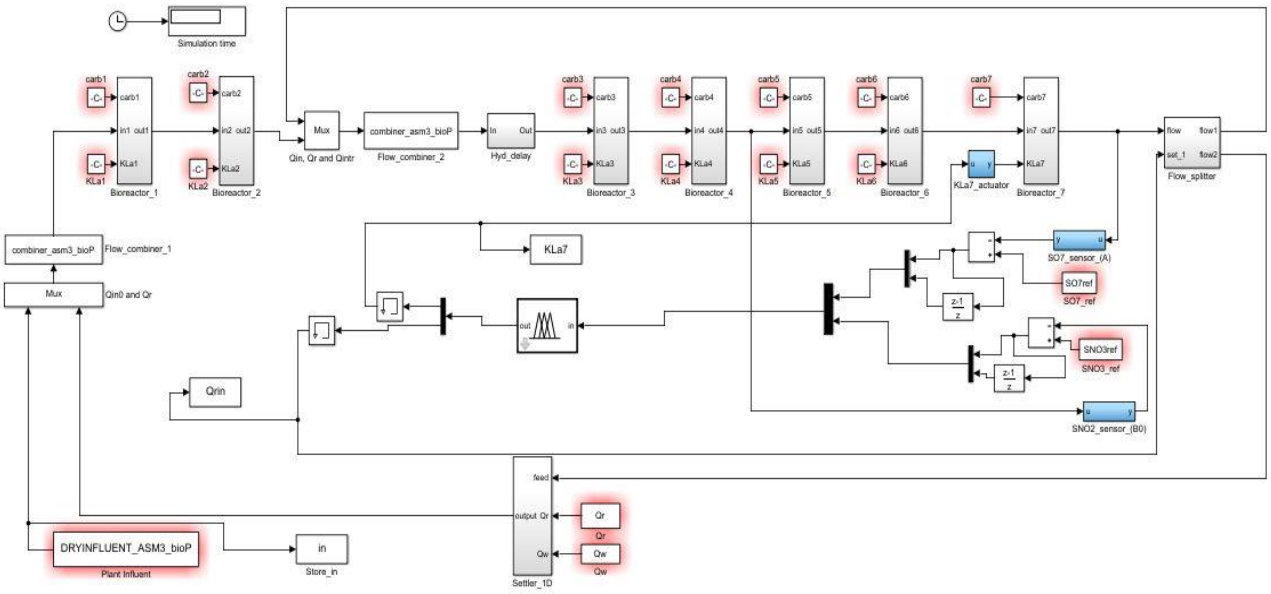

Figure A4. BSM1 with Lower Level Fuzzy logic controller (FLC)

APPENDIX B

Identification of State Space Model for Higher Level

Step 1. Fix the lower level controller to be used along with higher level control. Decide the control loops and corresponding manipulated and controlled variables for higher level.

Step 2. Run the Plant simulation model to reach steady state. It may be achieved after 100- 150 days for BSM1 and approximately after 200 days for BSM2. (steady state should be the point around which identification is desired to be performed).

Important Tip: For higher level control, the value of ammonia concentration and DO concentration in tank 5. Make sure that the steady state reached for ammonia concentration should be the value of set-point of ammonia you plan to achieve. The DO value needed to achieve the desired set-point of ammonia and the steady state value of ammonia concentration itself make a set of operating point. For example, if $S_{NH,7}$ ref =3.45 for PI-MPC configuration then the steady state value of DO set-point needed is $S_{O,7}$ ref=3.00.

Step 3. Now run the identification file (close lower level loop and open higher level loop) which varies all the manipulated variable (here $S_{O,7}$ ref) ±10% around their operating point simultaneously and record this input.

Step 4. Collect the data for variations in respective controlled variable (here $S_{NH,7}$) due to input supplied.

Step 5. Create a "iddata" object with recorded controlled and manipulated variable and use a proper sampling time (here, 1/96).

Step 6. Go to System Identification tool box and import the data object created in previous step.

Step 7. Use only the portion with consistent oscillations in output around operating point. (Use select range option provided in toolbox).

Step 8. Preprocess the data if needed (i.e. remove means and trends).

Step 9. Create the estimation and validation parts of data (generally 2/3 part is used for estimation and 1/3 part for validation) and import estimation data in "working data" and rest in "validation data" in toolbox.

Step 10. For estimating State space model, chose the option of "State Space Models" from estimation option and specify the order and type of model (continuous or discrete) to be estimated. There are several methods available for estimation like Subspace or prediction error method but the later one is generally used. There is an option available to choose the input which have immediate effect on output (i.e. values in D matrix). Usually, matrix D=0. Chose all the desired options and estimate the

model.

Step 11. Check the fit to estimation data and validation data, if it is within acceptable limits (generally above 70%) then model is fit to use otherwise repeat steps 2 -10 again.

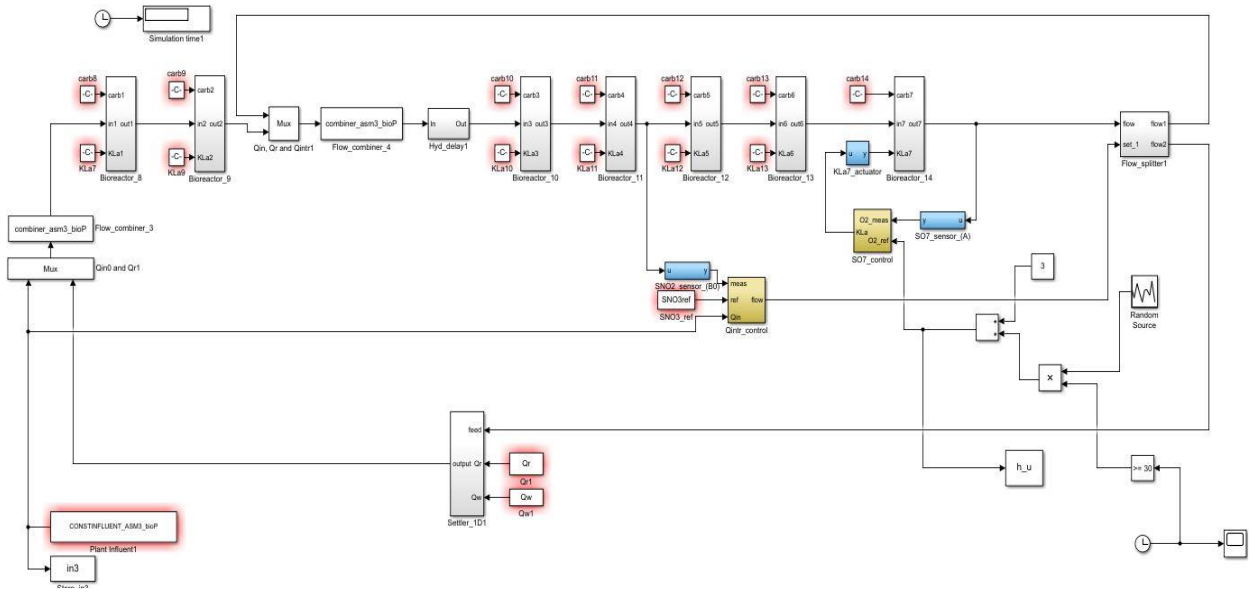

Figure B1. An Example of Higher Level Identification File

Designing of MPC Controller

Step 1. Determine the state space model of the plant to be controlled with MPC controller. And save the model in workspace.

Step 2. Import the model in MPC designer app and give the nominal values for controlled and manipulated variables.

Step 3. After the model is imported, a default controller is created in controller section. Tune the controller parameters and export the designed controller to workspace.

Note: The response of the controller to test signals (step, ramp, etc) in controlled as well as manipulated variables, assuming that the model of the plant describes the exact dynamics as real plant can be checked simulating a scenario in designer app.

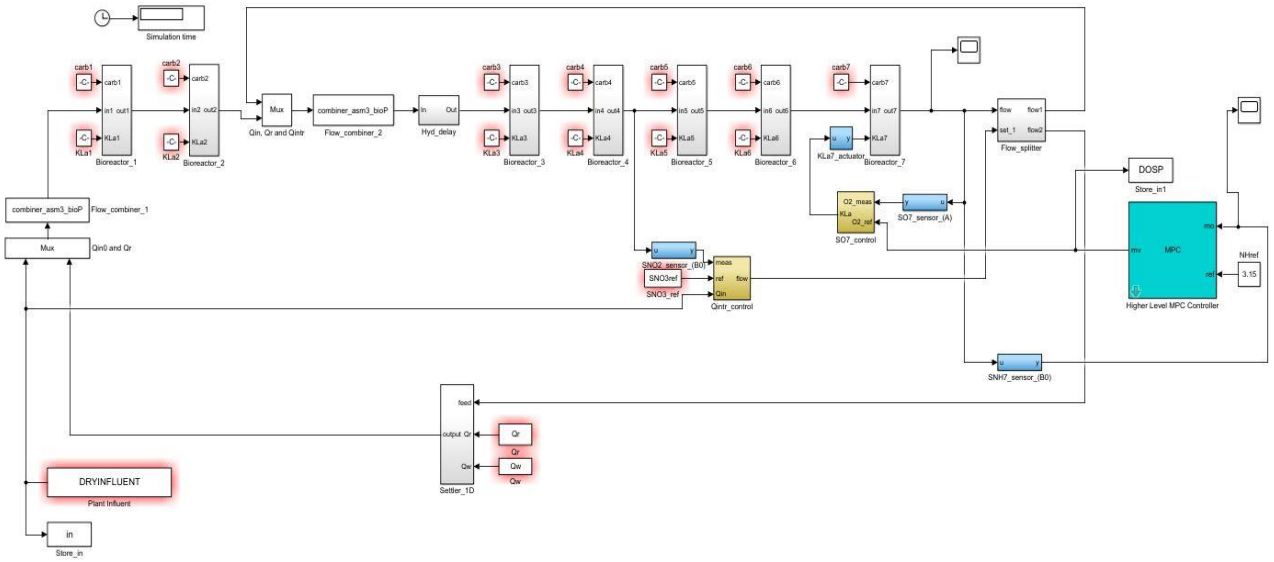

Figure B2. BSM1-P with PI-MPC Configuration

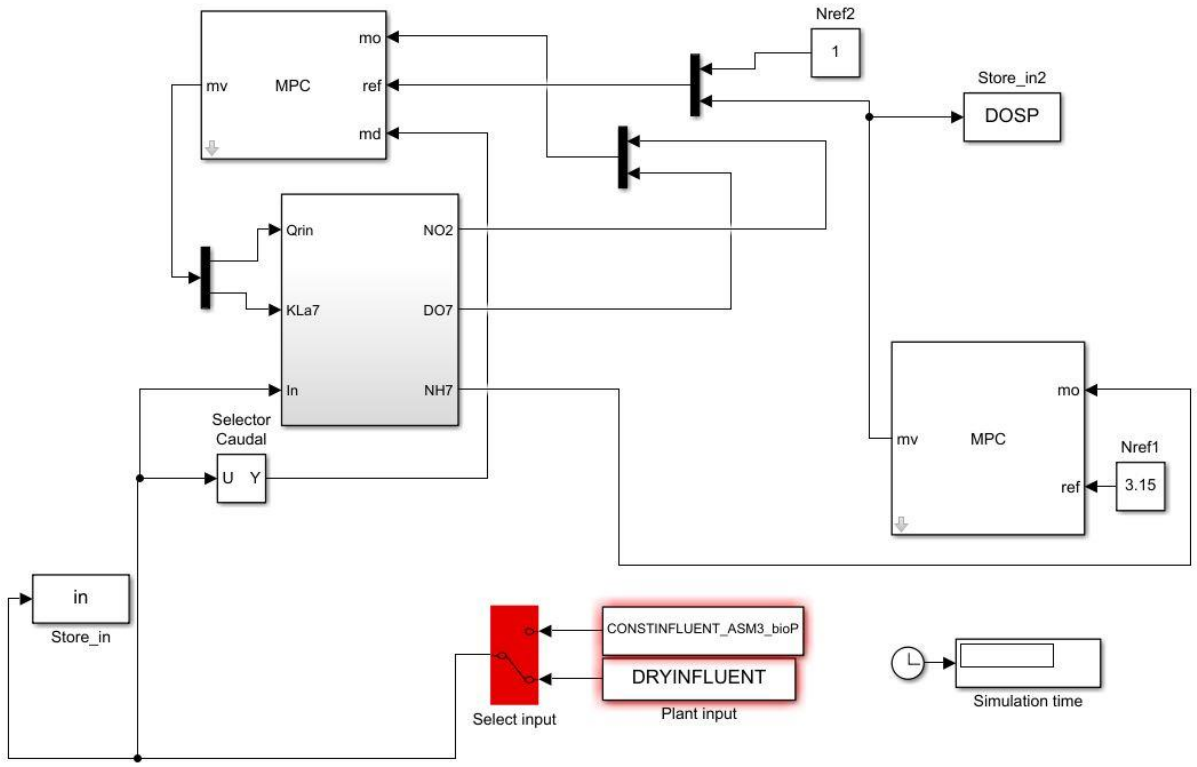

Figure B3. BSM1-P with MPC-MPC Configuration

Deciding Rules for Higher Level Fuzzy Controller

As the procedure is described for deducing the membership functions and rules for lower level fuzzy controller, similar approach is followed for higher level fuzzy controller also. Here, data is collected for ammonia concentration in tank 7 and respective DO set-point needed to be maintained by lower level control in tank 7 and a graph is generated between both variables. this graph then can be used

for diving the variables into fuzzy sets.

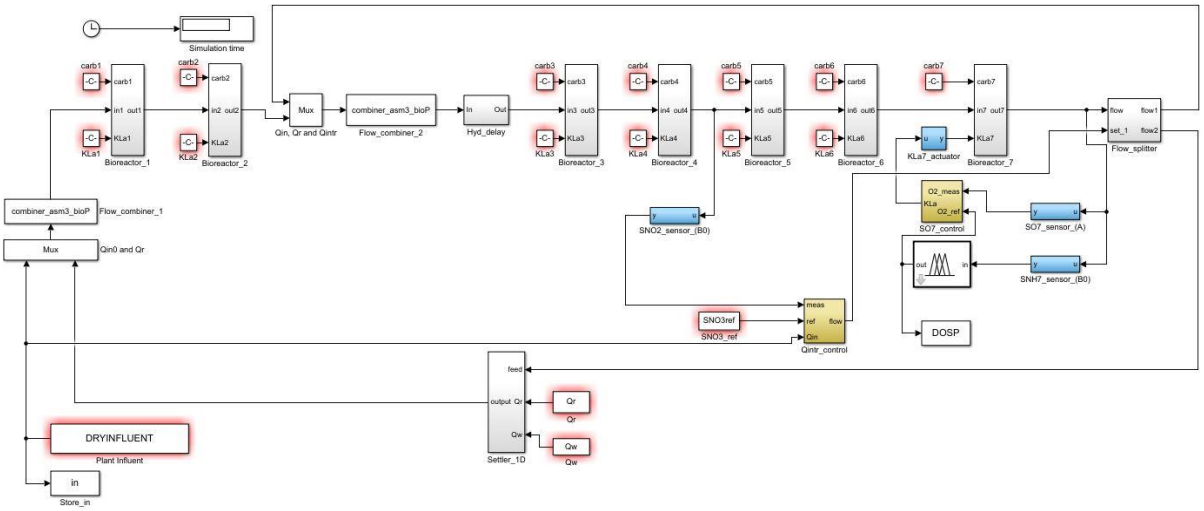

Figure B4. BSM1-P with PI-Fuzzy Configuration

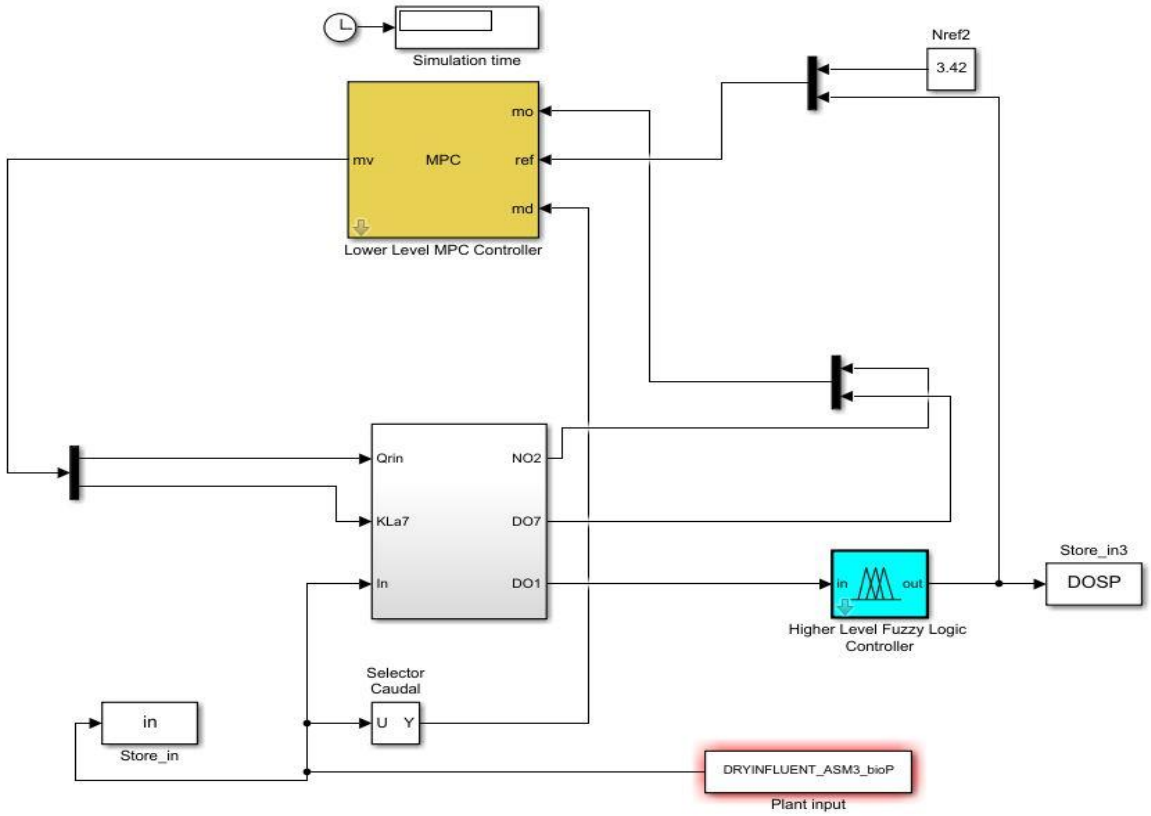

Figure B5. BSM1-P with MPC-Fuzzy Configuration

Table B1 Comparison PI-MPC, MPC-MPC, PI-Fuzzy, and MPC-Fuzzy schemes for rain season

Average effluent		Default PI	PI-MPC	MPC-MPC	PI-Fuzzy	MPC-Fuzzy
Components	Limit			`		

NH	4	4.45	3.95	3.77	3.78	3.622
TSS	30	16.41	16.71	17.54	16.68	16.80
TN	18	10.93	10.05	10.10	10.46	10.10
TP	2	5.32	4.87	5.48	5.16	5.35
COD	100	41.08	41.16	40.58	41.19	41.11
BOD_5	10	2.21	2.23	2.34	2.22	2.24
Percentage of violations (%)						
NH		58.63	38.09	27.77	43.30	38.98
TP		73.06	68.60	82.14	82.14	74.70
Plant performance						
IQI		71981	71981	71981	71981	71981
EQI		19829	18320	18601	18949	18863
OCI		17255	17486	18044	17174	17440

Table B2 Comparison of PI-MPC, MPC-MPC, PI-Fuzzy, and MPC-Fuzzy schemes for storm season

Average effluent concentration		Default PI	PI-MPC	MPC-MPC	PI-Fuzzy	MPC-Fuzzy
Components	Limit	`				
NH	4	4.30	3.95	3.63	3.72	3.85
TSS	30	15.57	15.78	15.54	15.75	15.78
TN	18	11.35	10.42	10.62	10.52	10.52
TP	2	4.53	3.96	4.37	4.30	3.39
COD	100	43.68	43.66	43.58	43.66	43.64
BOD_5	10	2.05	2.09	2.05	2.08	2.08
Percentage of violations (%)						
NH		54.61	37.94	37.35	42.26	40.77
TP		66.22	62.94	65.05	65.77	67.11
TSS		1.19	1.33	1.19	1.90	1.33
Plant performance						
IQI		71006	71006	71006	71006	71006
EQI		15592	14086	14920	14721	14063
OCI		18490	18806	18746	18789	18824

APPENDIX C

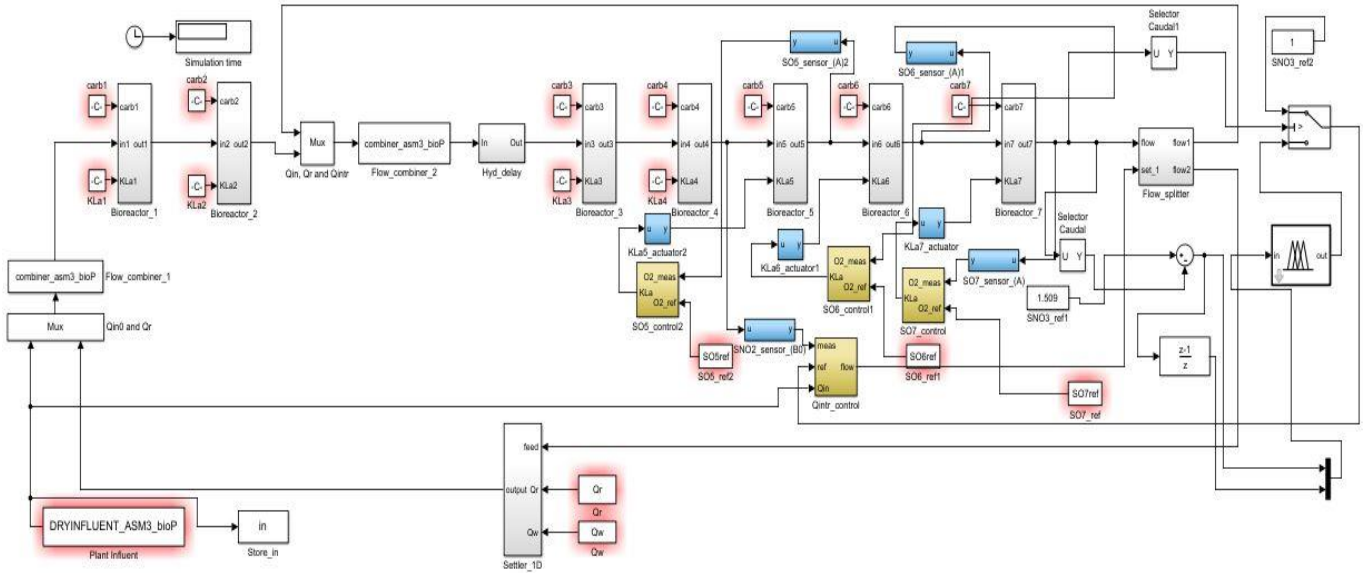

Figure C1. BSM1-P with SOPCA (PI-Fuzzy) Configurations

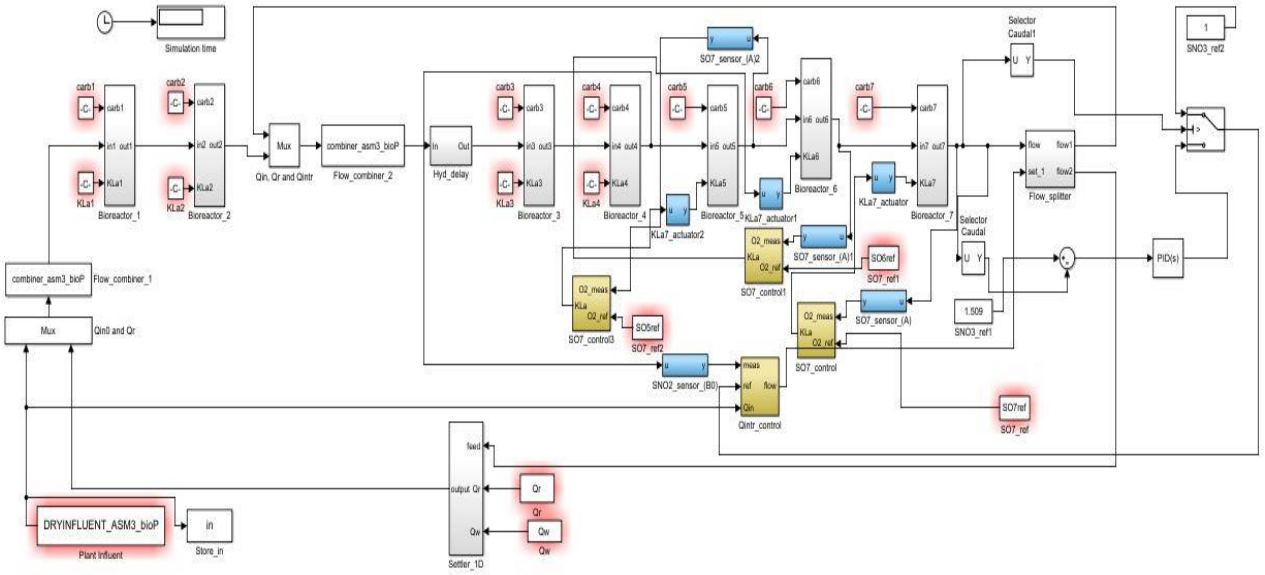

Figure C2. BSM1-P with SOPCA (PI-PI) Configurations

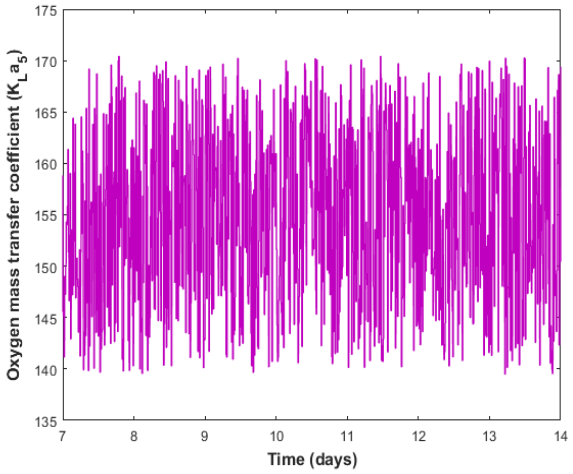

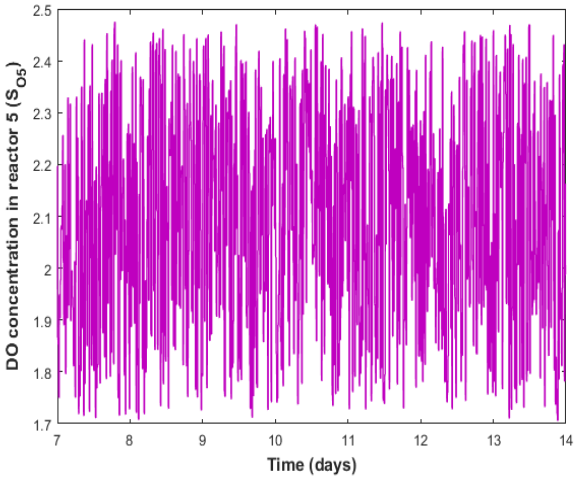

(a) Input and output data for S_{O5} loop

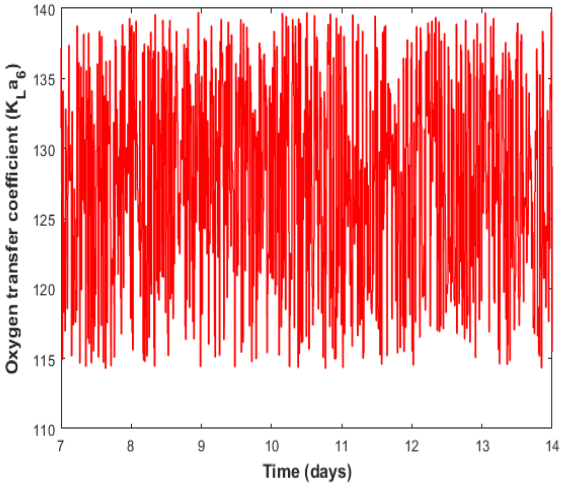

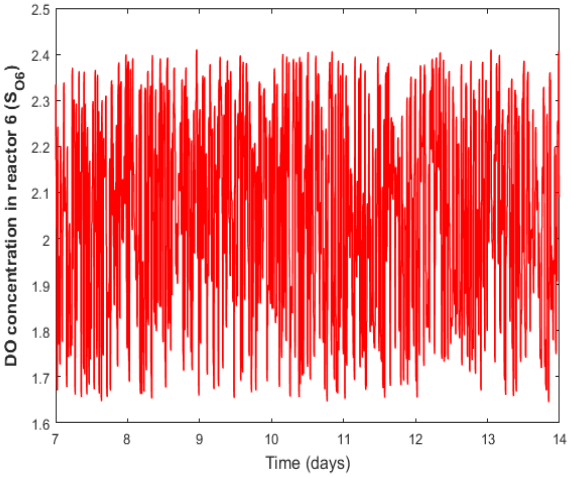

(b) Input and output data S_{O6} loop

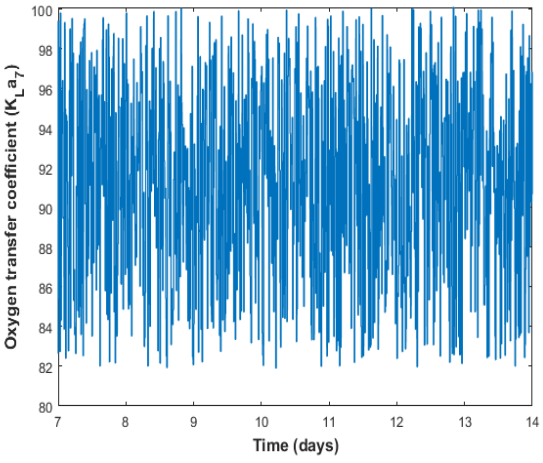

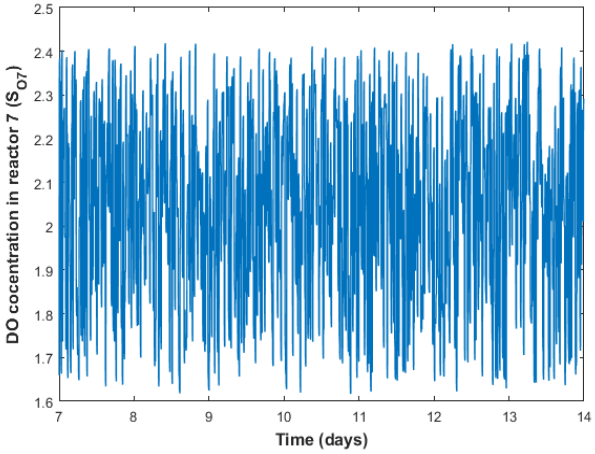

(c) Input and output data for S_{O7} loop

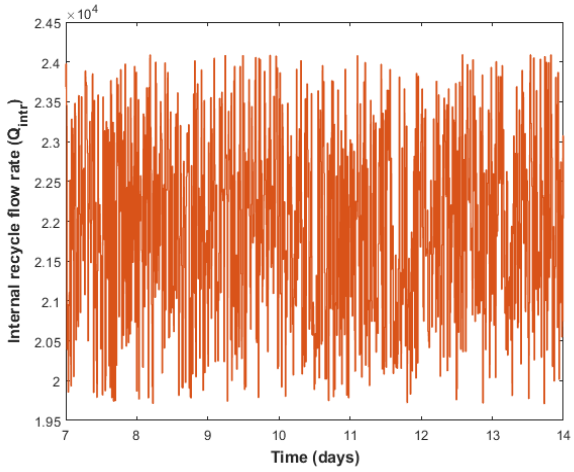

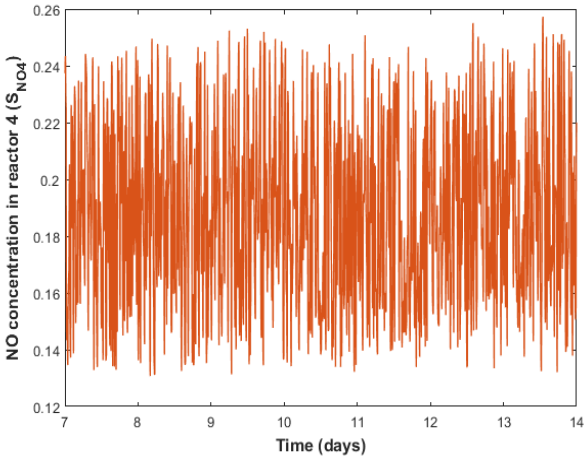

(d) Input and output data $S_{NO,4}$ loop

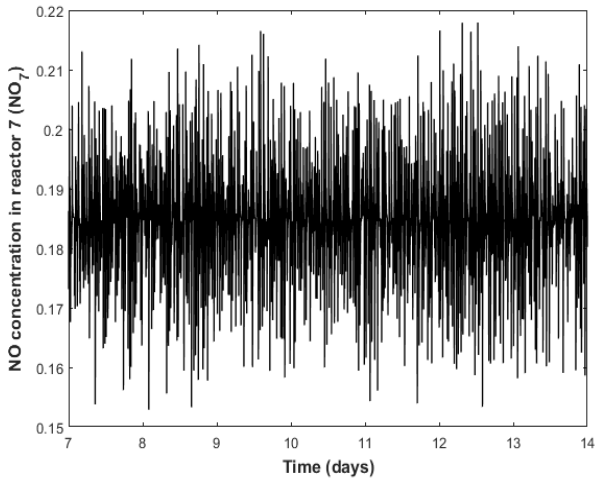

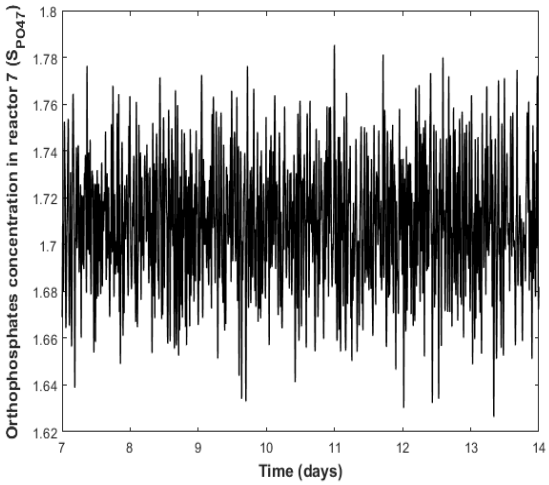

(e) Input and output data for $S_{PO,7}$ loop

Figure C3. Input and Output data for system identification

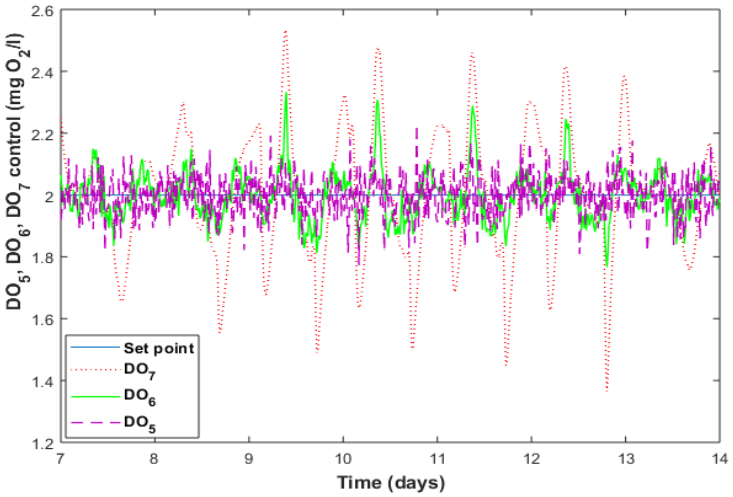

Figure C4. DO control tracking performance in the aerobic reactors

Identified Models for Controller Design

The design of PI controllers is based on the identified first order plus time order delay (FOPTD) models in all control loops. FOPTD model is represented as:

$$G(S) = \frac{K_P}{1+T_i*S} * exp^{-T_d*S}$$

Controls of S_{O5}, S_{O6}, S_{O7} in last three reactors, $S_{NO,4}$ in fourth reactor and $S_{PO4,7}$ in last reactor, all the respective obtained FOPTD model parameters are given below:

Model for S_{O5} loop: $K_P = 0.04152$, $T_i = 0.010586$ and $T_d = 0$

Model for S_{O6} loop: $K_P = 0.028491$, $T_i = 0.0055903$ and $T_d = 0$

Model for S_{O7} loop: $K_P = 0.023392$, $T_i = 0.0014262$ and $T_d = 0.0073752$

Model for $S_{NO,4}$ loop: $K_P = 0.0000334$, $T_i = 0.031488$ and $T_d = 0.0015521$

Model for $S_{PO4,7}$ loop: $K_P = -7.0063$, $T_i = 0.07213$ and $T_d = 0.0254$

Based on these models, PI controllers are designed using SIMC method and the obtained controller parameters are:

S_{O5} loop: $K_c = 12.042$ and $T_i = 0.010586$

S_{O6} loop: $K_c = 17.549$ and $T_i = 0.0055903$

S_{O7} loop: $K_c = 6.9256$ and $T_i = 0.0014262$

$S_{NO,4}$ loop: $K_c = 28533.61$ and $T_i = 0.031488$

$S_{PO4,7}$ loop: $K_c = -0.1055$ and $T_i = 0.07213$

APPENDIX D

Table D.1 State variables of ASM2d, units with notations, and average influent data

Notation	Parameters	Units	Average influent data
S_O	Dissolved oxygen	gO_2/ m^3	0
S_F	Fermentable substrate	g/m^3	69.9
S_A	Acetate	g/m^3	57.4
S_I	Soluble inerts	kg/m^3	26.5
S_{NH4}	Ammonium	g/m^3	25.1
S_{N2}	Dinitrogen	g/m^3	0
S_{NOX}	Nitrate plus nitrite	g/m^3	0
S_{PO4}	Phosphate	g/m^3	5.6
S_I	Saturation index	kg COD $/m^3$	84
X_i	Inert particulate organics	g COD $/m^3$	94.09
X_S	Sulfate reducing bacteria	kg COD $/m^3$	369.9
X_H	Heterotrophic biomass	g COD $/m^3$	51.5
X_{PAO}	Poly accumulating organisms	g COD $/m^3$	0
X_{PP}	Polyphosphates	(g $/m^3$) (kmol $/m^3$)	0
X_{PHA}	Polyhydroxy alkanoates	(g COD $/m^3$) (kg COD $/m^3$)	0
X_A	Autotrophic biomass	g COD $/m^3$	0
X_{TSS}	Total suspended solids	g SS/m^3	374.6
S_K	Potassium	(g m/m^3) (kmol $/m^3$)	20
S_{Mg}	Magnesium	(g m/m^3) (kmol m/m^3)	30
Q_{in}	Flow	m^3/d	20648
Temp	Temperature	^oC	15
S_{Na}	Sodium	(g $/m^3$) (kmol $/m^3$)	175
S_{Cl}	Chloride	(g $/m^3$) (kmol $/m^3$)	300
S_{Ca}	Calcium	(g $/m^3$) (kmol $/m^3$)	60
S_{SO4}	Sulfate	(g $/m^3$) (kmol $/m^3$)	0
S_{Fe2}	Iron (II)	(g $/m^3$) (kmol $/m^3$)	0
S_{Fe3}	Iron (III)	(g $/m^3$) (kmol $/m^3$)	0
S_{Al}	Alkalinity	$kmol/m^3$	0
S_{IS}	Inorganic total sulfides	kg COD $/m^3$	0

X_{HFOL}	Hydrous ferric oxide with low number of active sites	(g /m^3) (kmol /m^3)	0
X_{HFOH}	Hydrous ferric oxide with high number of active sites	(g /m^3) (kmol /m^3)	0
X_{HFOLP}	XHFO_L with bounded adsorption sites	g/m^3	0
X_{HFOHP}	XHFO_H with bounded adsorption sites	g/m^3	0
X_{S0}	Elemental sulfur	(g/m^3) (kg/m^3)	0
X_{SRB}	Sulfate-reducing bacteria	kg/m^3	0
X_{ISS}	Inorganic suspended soilds	g SS/m^3	33.5

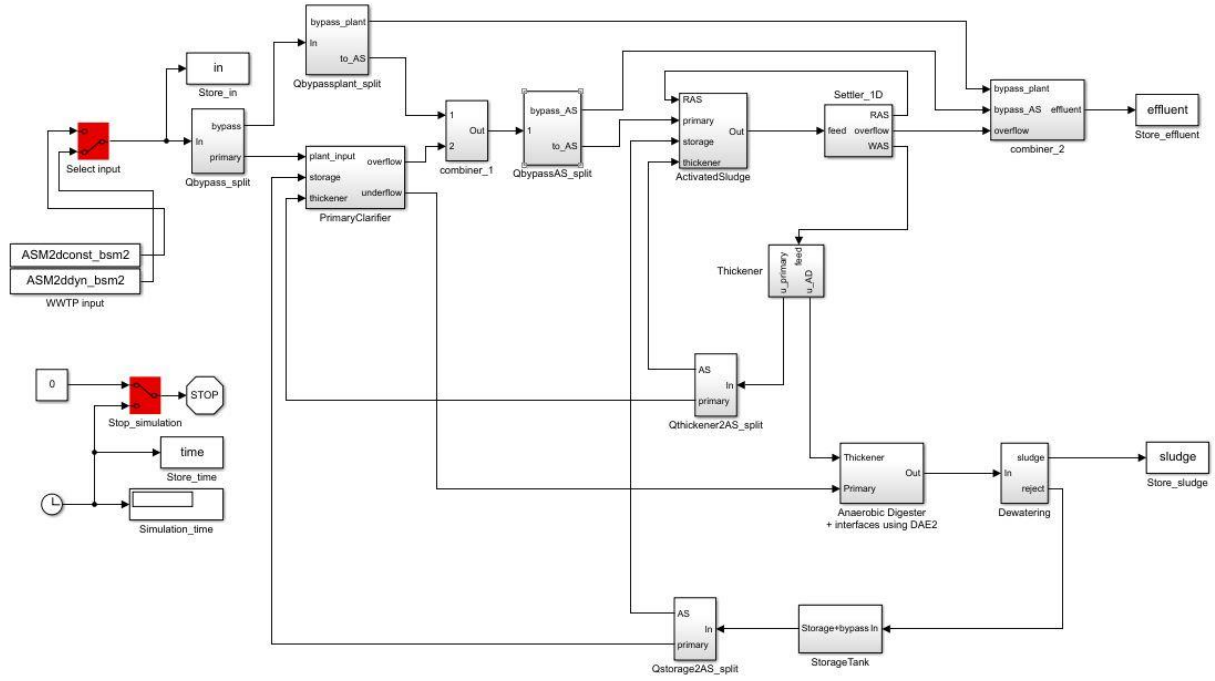

Figure D1. Open-loop for BSM2-P

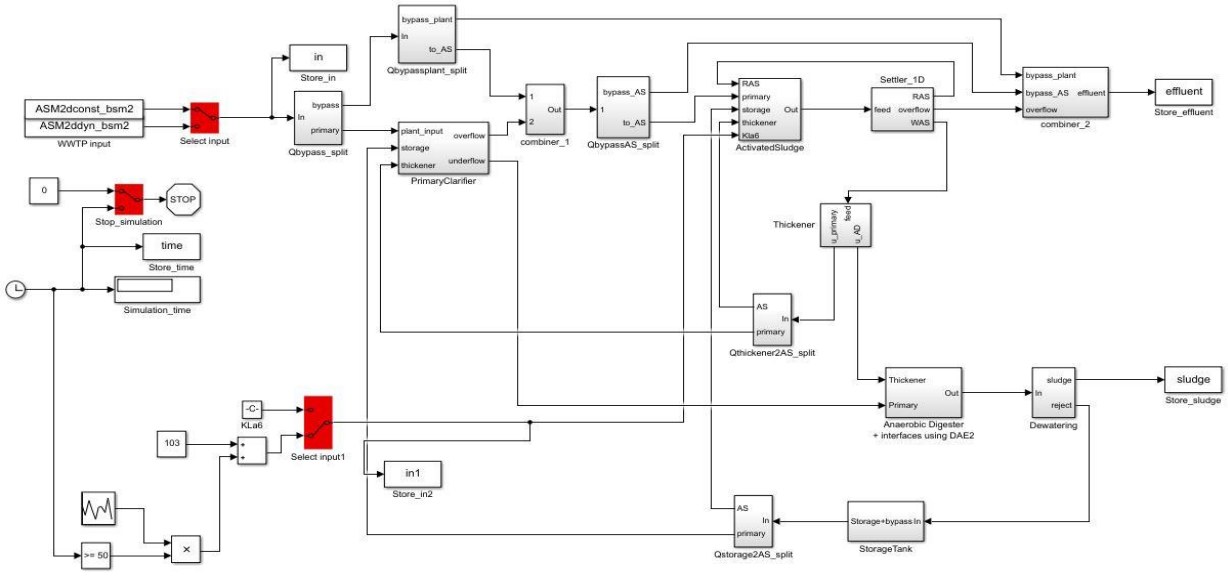

Figure D.2 Identification file for BSM2-P

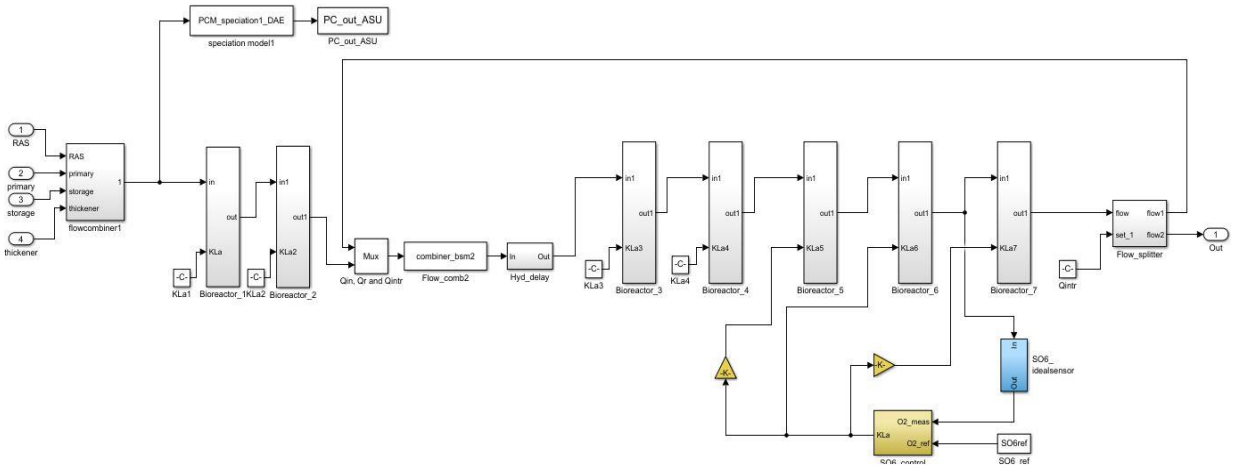

Figure D.3 BSM2-P with lower-level PI Configuration

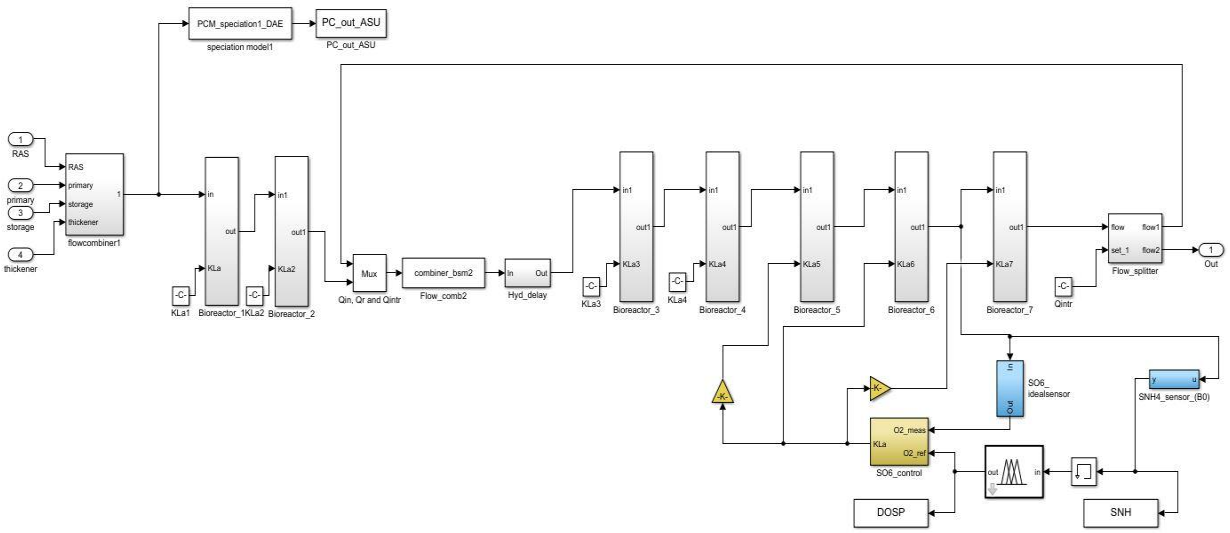

Figure D.4 BSM2-P with lower-level PI-Fuzzy Configuration

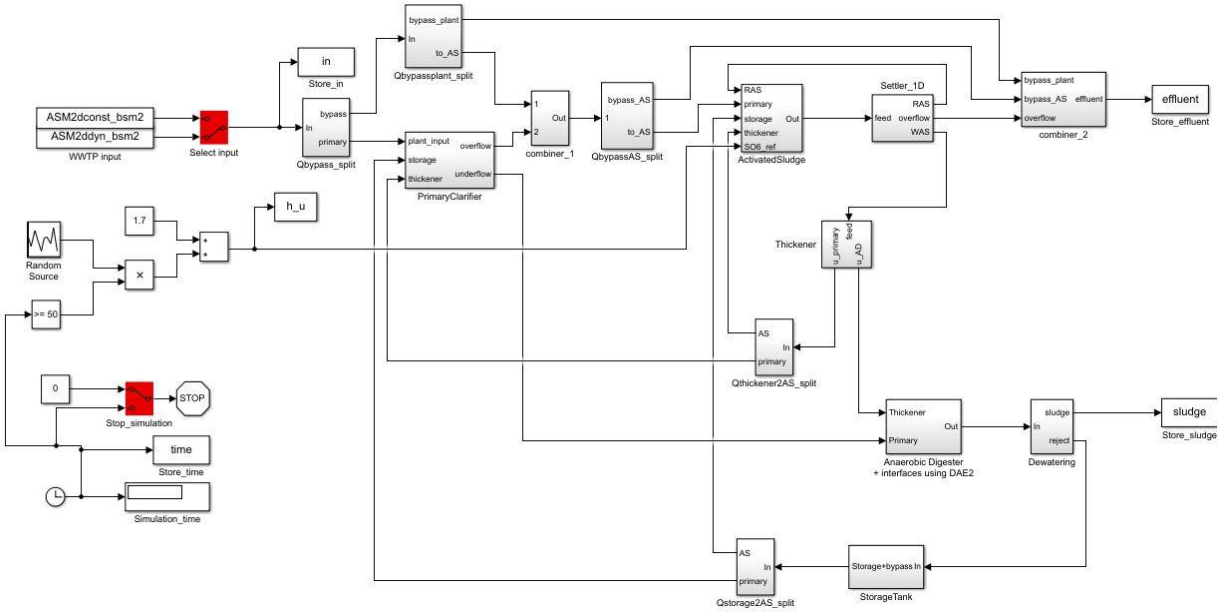

Figure D.5 Identification file for BSM2-P for supervisory controller

APPENDIX E

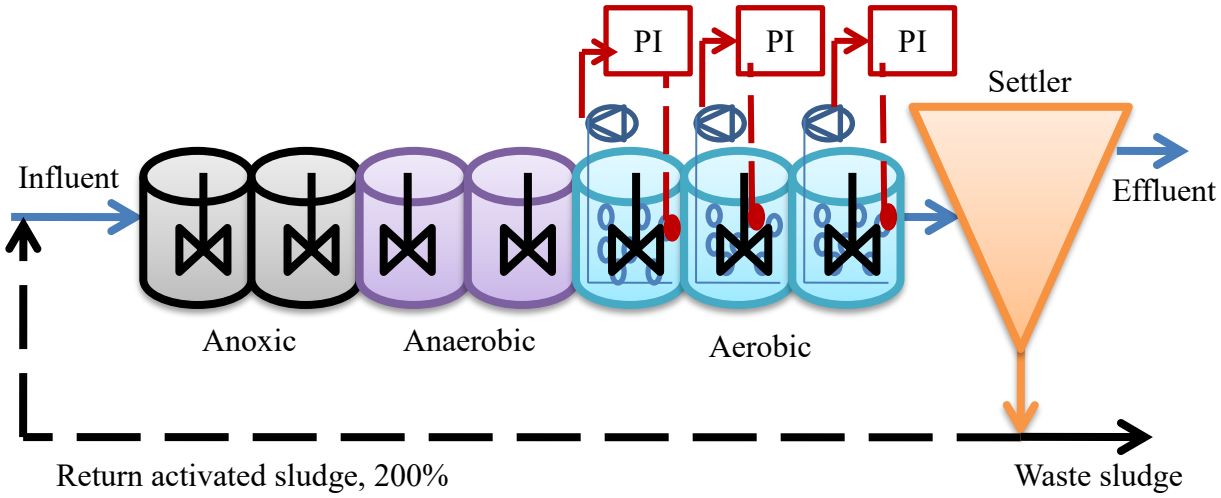

Figure E.1 Three DO control application in R-A^2/O process

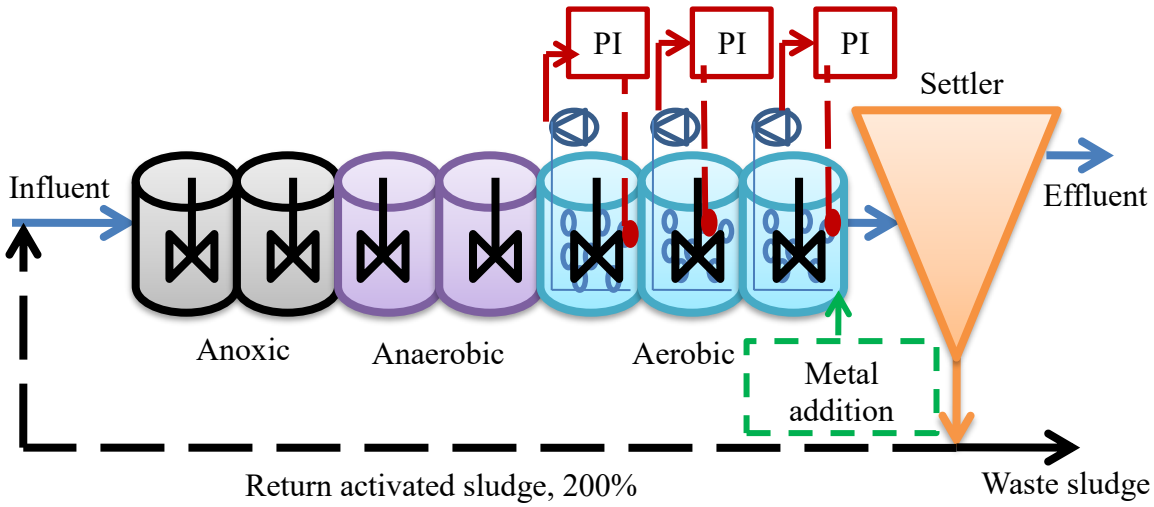

Figure E.2 Three DO control application with metal addition in R-A^2/O process

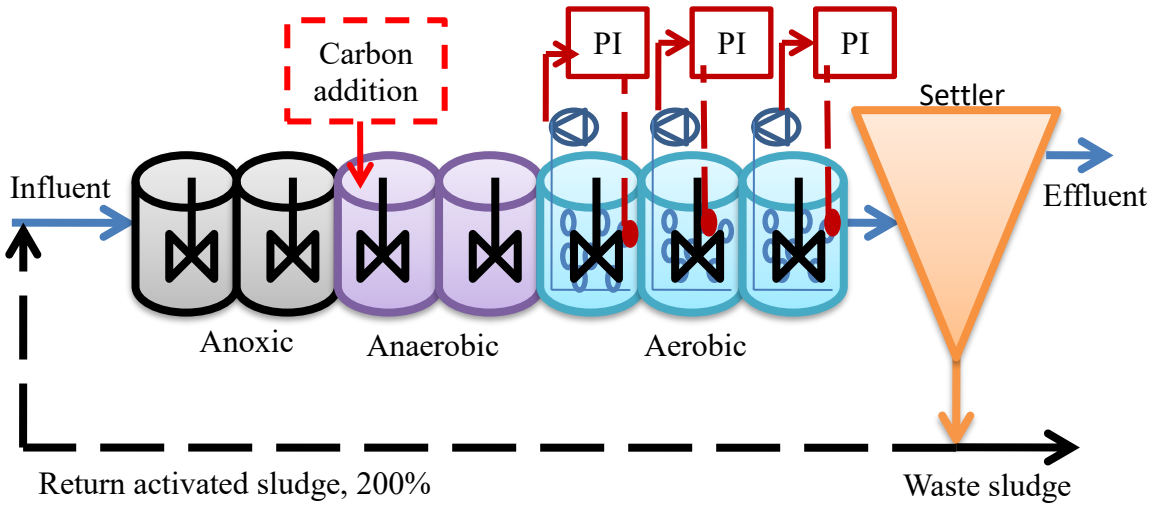

Figure E.3 Three DO control application with carbon addition in R-A^2/O process

Identified Models for Controller Design:

A first order plus time order delay (FOPTD) model as given is identified for design of PI controllers for each loop.

$$G(S) = \frac{K_P}{1+T_i*S} * exp^{-T_d*S}$$

Control of last three aerobic reactors of 5, 6 and 7 are maintaining 2gCOD/m^3 in DO, the respective obtained FOPTD model parameters are:

K_P = 0.012152, T_i = 0.001247 and T_d = 0.0070523 (DO_5).

K_P = 0.00726, T_i = 0.001280 and T_d = 0.00726 (DO_6).

K_P = 0.02938, T_i = 0.00142 and T_d = 0.007250(DO_7).

Based these models, PI controllers are designed using SIMC method and are obtained as K_c = 82.64, T_i= 0.001247 (DO_5), K_c = 8.841, T_i= 0.001280 (DO_6) and K_c = 5.61, T_i= 0.00142 (DO_7).

Table E1 Average effluent data with increased carbon addition in R-A^2/O

Average concentration	Open loop (R-A2/O)	CA anaerobic 0.25(m3/d)	CA anaerobic 0.5(m3/d)	CA anaerobic 0.75(m3/d)	CA anaerobic 1(m3/d)
S_{NH}	4.73	4.87	5.01	5.19	5.40
TSS	17.13	17.52	18.28	19.60	21.59
TN	15.68	15.58	15.52	15.53	15.62
TP	3.88	3.12	2.48	2.03	1.82
COD	48.51	48.69	49.30	50.52	52.47
BOD_5	2.74	2.79	2.90	3.10	3.42
Carbon add	0	100	200	300	400
IQI	56766.9	56766.9	56766.9	56766.9	56766.9
EQI	5220.01	4926.16	4685.67	4520.79	4459.64
Plant performance assessment					
SP	3518.43	3610.51	3696.01	3773.71	3839.19
OCI	19695.1	20419.87	21078.98	21648.50	22096.03
Percentage of violations (%)					
TP	62.20	54.31	50	30.20	23.36
TN	10.26	9.37	9.52	10.26	11.60
S_{NH}	58.48	59.07	60.11	60.56	61.54
TSS	---	---	---	0.59	8.48

Table E2 Average effluent data with increased metal addition in R-A^2/O

Average concentration	(R-A^2/O)	MA 0.25(m3/d)	MA 0.5(m3/d)	MA 0.75(m3/d)	MA 1(m3/d)	MA and CA 0.25 (m3/d)	MA and CA 1 (m3/d)
S_{NH}	4.73	4.73	4.76	4.799	4.82	4.88	2.30
TSS	17.13	17.28	17.28	17.23	17.18	17.64	18.57
TN	15.68	15.66	15.69	15.73	15.76	15.56	15.33
TP	3.88	2.06	1.69	1.55	1.47	1.89	1.47
COD	48.51	48.487	48.54	48.59	48.64	48.78	50.21
BOD_5	2.74	2.73	2.74	2.75	2.76	2.80	3.08
Carbon add	0	0	0	0	0	100	400
Metal add	0	250	500	750	1000	250	1000
IQI	56766.9	56766.9	56766.9	56766.9	56766.9	56766.9	56766.9
EQI	5220.01	4496.82	4349.26	4290.6	4260.20	4433.96	4289.83
Plant performance assessment							
SP	3518.43	3549.70	3528.75	3508.69	3490.33	3609.14	3675.67
OCI	19695.1	20212.30	20483.12	20762.21	21049.85	20777.02	22051.29
Percentage of violations (%)							
TP	62.20	44.19	7.44	0.29	----	38.39	0.744
TN	10.26	10.26	10.71	11.30	11.75	9.97	7.73
S_{NH}	58.48	58.33	58.63	58.63	58.69	59.07	61.30

Table E.3 Average effluent data with the control of three DO applications with metal and carbon addition in R-A^2/O

Average concentration	(RA^2/O)	$DO_{2,2,2}$	$DO_{1,1,2}$	$DO_{1,1,2}$ + CA (1m3/d)	$DO_{1,1,2}$ + MA (1m3/d)	$DO_{1,1,2}$ + MA and CA
S_{NH}	4.73	1.04	1.48	1.51	1.51	1.64
TSS	17.13	15.81	15.91	17.14	16.57	17.42
TN	15.68	15.79	15.26	14.62	15.23	14.68
TP	3.88	4.35	4.15	3.55	1.96	1.51
COD	48.51	49.07	49.13	49.60	48.60	49.03
BOD_5	2.74	2.70	2.73	2.80	2.65	2.79
Carbon add	0	0	0	----	400	400
Metal add	0	0	0	1000	----	1000
IQI	56766	56766	56766	56766	56766	56766
EQI	5220.01	8071.3	8010.96	6702.2	4979.23	4066.39
Plant performance assessment						
SP	3518.43	3034.7	3068.12	3472.42	3283.08	3548.74
AE	2843.73	3659.7	2851.35	2905.64	2850.11	2870.17
OCI	19695.1	18211	17660.75	20725.44	20084.80	22546.10
Percentage of violations (%)						
TP	62.20	91.25	88.45	68.5	26.33	11.01
TN	10.26	14.13	12.20	10.71	12.20	11.60
S_{NH}	58.48	4.46	9.67	10.56	10.11	-----

APPENDIX F

Table F.1 Effect of z on EQI when b_H *is determined at* 25°C

TemCo-eff →	0.05	0.08	0.1	0.2	0.3	0.4	0.5	0.6	0.8	1
Variables ↓	State variables									
S_O	**1.8364**	**1.7089**	**1.6568**	**1.73**	**1.99**	**2.2346**	**2.44**	**2.63**	**2.93**	**3.1167**
S_S	**0.563**	**0.389**	**0.32**	**0.178**	**0.1339**	**0.1125**	**0.0994**	**0.092**	**0.082**	**0.077**
S_I	30	30	30	30	30	30	30	30	30	30
S_{nh}	**0.4196**	**0.4299**	**0.43769**	**0.412**	**0.3723**	**0.333**	**0.3047**	**0.274**	**0.243**	**0.22**
S_{NO}	**10.3**	**9.9376**	**9.79**	**9.615**	**9.69**	**9.7621**	**9.812**	**9.83**	**9.89**	**9.92**
S_{N2}	**35.38**	**36.055**	**36.32**	**36.38**	**35.79**	**35.25**	**34.77**	**34.37**	**33.66**	**33.21**
S_{PO4}	**2.48**	**3.3758**	**3.766**	**4.91**	**5.4**	**5.67**	**5.82**	**5.92**	**6.03**	**6.08**
S_{alk}	3.5722	3.5832	3.58	3.58	3.56	3.55	3.55	3.55	3.54	3.544
X_I	**6.88**	**6.88**	**6.88**	**6.79**	**6.47**	**6.31**	**6.109**	**5.98**	**5.72**	**5.55**
X_S	**0.225**	**0.12911**	**0.1121**	**0.0926**	**0.0866**	**0.0841**	**0.08143**	**0.0808**	**0.0793**	**0.077**
X_H	**0.3222**	**0.69**	**0.988**	**2.34**	**3.28**	**3.941**	**4.45**	**4.83**	**5.72**	**5.66**
X_{STO}	**0.006532**	**0.010187**	**0.0122**	**0.017067**	**0.0183**	**0.0188**	**0.0188**	**0.019**	**0.0191**	**0.0189**
X_{PAO}	**4.365**	**4.0301**	**3.76**	**3.1141**	**2.7131**	**2.534**	**2.366**	**2.3**	**2.17**	**2.099**
X_{PP}	**0.5126**	**0.48281**	**0.4533**	**0.3809**	**0.335**	**0.3152**	**0.29**	**0.28**	**0.27**	**0.2671**
X_{PHA}	**0.1562**	**0.14259**	**0.133**	**0.1067**	**0.0907**	**0.08199**	**0.075**	**0.072**	**0.066**	**0.063**
X_A	**0.3987**	**0.41243**	**0.4155**	**0.416**	**0.3939**	**0.3814**	**0.366**	**0.36319**	**0.34**	**0.337**
X_{TSS}	**11.984**	**11.93**	**11.95**	**11.98**	**12.216**	**12.34**	**12.56**	**12.592**	**12.7**	**12.88**
Composite variables										
TKN	1.307	1.3123	1.31	1.33	1.321	1.3108	1.2968	1.2842	1.27	1.26
TN	11.61	11.24	11.11	10.95	11.01	11.072	11.109	11.12	11.17	11.18
TP	**3.136**	**4**	**4.36**	**5.44**	**5.892**	**6.15**	**6.2797**	**6.37**	**6.48**	**6.517**
COD	**42.19**	**42.68**	**42.61**	**43.04**	**43.18**	**43.47**	**43.54**	**43.73**	**43.91**	**43.88**
BOD_5	1.24	1.185	1.16	1.26	1.3514	1.442	1.49	1.55	1.64	1.67
EQI	16369.02	15827.25	15599.99	15465.89	15795.62	16126.5	17214.95	17027.61	17626.15	17939.09

Table F.2 Effect of z on EQI when μ_{mA} is determined at 25°C

Tem co-eff →	**0.6**	**0.7**	**0.8**	**0.9**	**1**	**1.2**	**1.4**	**1.6**	**1.8**	**2**
Variables ↓	**State variables**									
S_O	2.6	2.43	2.29	2.12	1.99	1.718	1.522	1.4	1.42	1.544

S_S	0.132	0.13	0.13	0.132	0.13	0.134	0.13	0.13	0.13	0.13
S_I	30	30	30	30	30	30	30	30	30	30
S_{nh}	**0.0946**	**0.13**	**0.19**	**0.273**	**0.37**	**0.69**	**1.26**	**2.45**	**4.59**	**7.69**
S_{NO}	8.55	8.9	9.2	9.47	9.71	9.98	10.08	9.92	9.43	8.66
S_{N2}	36.99	36.6	36.36	36.09	35.75	35.27	34.62	33.63	31.96	29.6
S_{PO4}	**4.44**	**4.8**	**5.04**	**5.252**	**5.39**	**5.61**	**5.69**	**5.69**	**5.522**	**5.25**
S_{alk}	3.64	3.617	3.59	3.57	3.5	3.56	3.59	3.69	3.88	4.16
X_I	6.31	6.35	6.35	6.388	6.469	6.58	6.49	6.6	6.6021	6.55
X_S	0.085708	0.085	0.085	0.0859	0.08741	0.0875	0.0875	0.0877	0.088138	0.0872
X_H	3.199	3.21	3.22	3.26	3.3	3.33	3.3081	3.26	3.24	3.13
X_{STO}	0.0184	0.0182	0.0182	0.0182	0.0185	0.0185	0.01843	0.01828	0.01835	0.0179
X_{PAO}	2.92	2.88	2.79	2.7471	2.7261	2.6813	2.65	2.7101	2.74	2.806
X_{PP}	0.38	0.37	0.35	0.343	0.33	0.32	0.32	0.32	0.32	0.33
X_{PHA}	0.125	0.111	0.1	0.0952	0.0911	0.0849	0.082	0.082	0.086	0.0916
X_A	0.4	0.4	0.39	0.3946	0.394	0.39	0.384	0.375	0.36	0.33
X_{TSS}	**12.33**	**12.31**	**12.32**	**12.29**	**12.13**	**12.11**	**12.12**	**12.11**	**12.08**	**12.19**
Composite variables										
TKN	1.0481	1.09	1.141	1.22	1.3284	1.64	2.211	3.4035	5.54	8.639
TN	**9.6**	**10**	**10.34**	**10.69**	**11.04**	**11.63**	**12.29**	**13.32**	**14.98**	**17.3**
TP	**4.99**	**5.33**	**5.55**	**5.74**	**5.89**	**6.09**	**6.16**	**6.17**	**6.007**	**5.74**
COD	43.18	43.19	43.09	43.1	43.2	43.3	43.14	43.26	43.26	43.15
BOD5	**1.38**	**1.37**	**1.35**	**1.35**	**1.35**	**1.35**	**1.34**	**1.34**	**1.34**	**1.33**
EQI	**16183.67**	**16096.3**	**15874.06**	**15788.65**	**15816.35**	**15714.5**	**15630.6**	**15655.5**	**15715.5**	**15828.6**

Table F.3 Effect of z on EQI when b_A *is determined at* 25°C

Tem co eff →	**0.14**	**0.16**	**0.18**	**0.19**	**0.2**	**0.22**	**0.24**	**0.26**	**0.28**	**0.3**
variables ↓	**State variables**									
S_O	**1.643**	**1.74**	**1.89**	**1.94**	**1.98**	**2.067**	**2.111**	**2.186**	**2.22**	**2.27**
S_S	0.1350	0.1348	0.1344	0.1345	0.131	0.133	0.133	0.132	0.132	0.132
S_I	30	30	30	30	30	30	30	30	30	30
S_{nh}	**0.7919**	**0.594**	**0.457**	**0.407**	**0.38**	**0.320**	**0.30**	**0.250**	**0.23**	**0.2110**
S_{NO}	9.99	9.87	9.807	9.75	9.68	9.60	9.52	9.439	9.37	9.32
S_{N2}	32.23	33.98	35.64	35.719	35.99	35.88	35.95	36.09	36.15	36.19
S_{PO4}	5.66	5.55	5.48	5.44	5.40	5.32	5.27	5.19	5.14	5.080
S_{alk}	3.57	3.568	3.564	3.561	3.568	3.571	3.57	3.58	3.85	3.58

X_I	6.48	6.49	6.518	6.50	6.48	6.44	6.42	6.40	6.43	6.451
X_S	0.0868	0.0869	0.08700	0.086711	0.0869	0.0867	0.08674	0.0866	0.0863	0.08615
X_H	3.27	3.274	3.288	3.26	3.282	3.28	3.29	3.3001	3.25	3.27
X_{STO}	0.0182	0.01830	0.01836	0.01828	0.01831	0.01838	0.01840	0.01843	0.01838	0.01834
X_{PAO}	2.69	2.70	2.714	2.72	2.728	2.73	2.75	2.76	2.77	2.77
X_{PP}	0.327	0.30	0.333	0.335	0.3365	0.338	0.340	0.346	0.348	0.349
X_{PHA}	0.0841	0.0864	0.08854	0.08955	0.09021	0.0927	0.0955	0.0969	0.0978	0.0995
X_A	0.3124	0.334	0.369	0.3817	0.4011	0.415	0.434	0.454	0.465	0.480
X_{TSS}	12.196	12.19	12.18	12.217	12.218	12.211	12.21	12.21	12.24	12.27
Composite variables										
TKN	1.734	1.543	1.405	1.355	1.31	1.217	1.19	1.20	1.18	1.168
TN	**11.72**	**11.545**	**11.21**	**11.10**	**11.01**	**10.71**	**10.68**	**10.64**	**10.55**	**10.49**
TP	**6.14**	**6.04**	**5.97**	**5.93**	**5.88**	**5.7**	**5.88**	**5.69**	**5.62**	**5.58**
COD	43.07	43.14	43.19	43.18	43.12	43.21	43.22	43.23	43.27	43.29
BOD5	1.32	1.33	1.34	1.34	1.34	1.36	1.37	1.37	1.37	1.37
EQI	**15108.9**	**14597.5**	**14521.0**	**14492.8**	**14367.6**	**14207.3**	**14115.6**	**13917.4**	**13726.5**	**13681.6**

Table F.4 Effect of z on EQI when mu_{PAO} is determined at 25°C

Tem co-eff →	**0.7**	**0.9**	**1**	**1.2**	**1**	**1.4**	**1.6**	**1.8**	**2**	**2.2**
variables		**State variables**								
S_O ↓	2.0965	2.042	2.0132	1.99	1.99	1.964	1.12	1.91	1.92	1.91
S_S	0.12	0.13	0.13	0.13	0.1343	0.133	0.133	0.13	0.133	0.132
S_I	30	30	30	30	30	30	30	30	30	30
S_{nh}	0.35	0.36	0.36	0.36	0.37	0.374	0.38	0.379	0.37	0.37
S_{NO}	9.4	9.56	9.63	9.65	9.712	9.77	9.85	9.88	9.95	9.982
S_{N2}	35.9	35.86	35.83	35.79	35.76	35.76	35.74	35.76	35.73	35.78
S_{PO4}	**8.9**	**7.2**	**6.12**	**5.98**	**5.399**	**4.64**	**4.22**	**4.12**	**4.15**	**4.34**
S_{alk}	3.53	3.54	3.55	3.55	3.566	3.57	3.57	3.57	3.56	3.562
X_I	6.7	6.58	6.58	6.57	6.53	6.42	6.39	3.344	6.4	6.411
X_S	0.0893	0.0877	0.0879	0.0876	0.0873	0.864	0.08596	0.08494	0.0855	0.0856
X_H	3.9	3.43	3.3714	3.32	3.299	3.23	3.23	3.23	3.269	3.3
X_{STO}	0.0254	0.0201	0.0191	0.0188	0.01849	0.0178	0.01765	0.0175	0.01787	0.01809
X_{PAO}	2.45	2.705	2.74	2.726	2.728	2.7	2.633	2.53	2.43	2.3422
X_{PP}	**0.0971**	**0.2**	**0.285**	**0.303**	**0.336**	**0.399**	**0.436**	**0.43**	**0.43**	**0.4263**

X_{PHA}	**0.0364**	**0.057**	**0.0745**	**0.0845**	**0.09111**	**0.128**	**0.198**	**0.266**	**0.387**	**0.519**
X_A	0.415	0.402	0.4	0.398	0.394	0.3917	0.388	0.38	0.387	0.39
X_{TSS}	11.84	12.079	12.07	12.11	12.14	12.25	12.3	12.4	12.33	12.32
	Composite variables									
TKN	1.33	1.327	1.327	1.329	1.33	1.3171	1.317	1.3079	1.3047	1.2984
TN	**10.74**	**10.89**	**10.96**	**11.01**	**11.04**	**11.081**	**11.17**	**11.19**	**11.25**	**11.28**
TP	**9.15**	**7.365**	**6.56**	**6.11**	**5.89**	**5.19**	**4.81**	**4.71**	**4.74**	**4.91**
COD	43.73	43.41	43.39	43.27	43.27	43.1	43.07	42.98	43.1	43.19
BOD5	1.41	1.37	1.37	1.36	1.35	1.34	1.34	1.33	1.35	1.36
EQI	20236.02	17507.07	15594.40	14920	14385.7	13132.79	12457.96	12283.37	12345.26	12665.66

Table F.5 Effect of z on EQI at b_{PAO} is determined at 25°C

Tem co-eff →	**0.085**	**0.09**	**0.095**	**0.1**	**0.15**	**0.2**	**0.3**	**0.4**	**0.5**	**0.6**
variables ↓		**State variables**								
S_O	**1.646**	**1.649**	**1.65**	**1.66**	**1.67**	**1.97**	**2.23**	**2.39**	**2.51**	**2.6**
S_S	0.12	0.133	0.133	0.134	0.134	0.133	0.132	0.13	0.13	0.12
S_I	30	30	30	30	30	30	30	30	30	30
S_{nh}	0.36	0.414	0.412	0.4178	0.39	0.377	0.33	0.3	0.29	0.28
S_{NO}	9.27	9.37	9.38	9.54	9.60	9.69	9.82	9.87	9.93	9.96
S_{N2}	36.84	36.91	36.6	36.72	36.02	35.82	35.18	34.82	34.5	34.29
S_{PO4}	**7.24**	**7.85**	**8.02**	**7.56**	**6.45**	**5.41**	**4.32**	**3.71**	**3.3**	**3.05**
S_{alk}	3.52	3.53	3.55	3.548	3.55	3.56	3.57	3.58	3.58	3.58
X_I	**7.01**	**6.98**	**6.89**	**6.79**	**6.64**	**6.43**	**6.24**	**6.15**	**5.99**	**5.91**
X_S	0.0933	0.0908	0.0842	0.0893	0.084	0.08649	0.0852	0.0842	0.08362	0.083
X_H	4.49	3.92	3.7484	3.67	3.34	3.3003	3.1176	3.0484	2.975	2.95
X_{STO}	0.0313	0.0246	0.02612	0.022	0.021	0.01832	0.01688	0.01612	0.015616	0.01539
X_{PAO}	0.737	1.33	1.55	1.749	1.94	2.7165	3.208	3.5	3.69	3.76
X_{PP}	0.1107	0.19067	0.1949	0.239	0.28	0.33	0.374	0.3949	0.40662	0.4073
X_{PHA}	0.176	0.1342	0.1205	0.1149	0.104	0.0904	0.0836	0.0805	0.0782	0.076
X_A	0.462	0.44	0.4102	0.426	0.401	0.3929	0.3744	0.3702	0.362	0.35
X_{TSS}	**11.7**	**11.74**	**11.78**	**11.83**	**11.88**	**12.23**	**12.41**	**12.543**	**12.63**	**12.71**
	Composite variables									
TKN	1.288	1.33	1.33	1.33	1.32	1.32	1.3002	1.28	1.27	1.26
TN	**10.56**	**10.707**	**10.75**	**10.79**	**10.89**	**11.01**	**11.122**	**11.16**	**11.2**	**11.23**
TP	**8.88**	**8.45**	**8.33**	**7.985**	**6.45**	**5.9**	**4.85**	**4.27**	**3.87**	**3.61**

COD	43.39	43.14	43.01	42.98	43.05	43.15	43.24	43.36	43.31	43.28
BOD5	1.22	1.22	1.22	1.2	1.22	1.35	1.41	1.45	1.47	1.48
EQI	**19473.58**	**19845.17**	**19945.6**	**18052.4**	**16124.4**	**14400.37**	**12526.6**	**11485.91**	**10774.74**	**10312.28**

List of Publications

International Journals

1. **Abdul Gaffar Sheik**, MVS Raghu Kumar, Murali Mohan Seepana and Seshagiri Rao Ambati, Design of control strategies for nutrient removal in biological wastewater treatment plants, ***Environmental Science and Pollution Research***, 28-12092–12106, 2021 (SCI, Impact Factor: 4.3)
2. **Abdul Gaffar Sheik,** Murali Mohan Seepana and Seshagiri Rao Ambati, Supervisory control configurations design for nitrogen and phosphorus removal in wastewater treatment plants, ***Water Environment Research***, Published, https://doi.org/10.1002/ WER. 512, 2021. (SCI, Impact Factor: 1.9).
3. **Abdul Gaffar Sheik**, MVS Raghu Kumar, Murali Mohan Seepana and Seshagiri Rao Ambati, An integrated supervisory and override control strategies for effective biological phosphorous removal and reduced operational costs in wastewater treatment processes, ***Chemosphere***, 287 (2022) 132346, Published, https://doi.org/10.1016/j.chemosphere. 2021.132 346, 2021s (SCI, Impact Factor: 7.1).
4. **Abdul Gaffar Sheik,** E.S.S. Tejaswini, Murali Mohan Seepana, Montse Meneses, Ramon Vilanova and Seshagiri Rao Ambati, Design of Feedback Control Strategies in a Plant-Wide Wastewater Treatment Plant for Simultaneous Evaluation of Economics, Energy Usage, and Removal of Nutrients, ***Energies***, 14, 6386, 2021, https://doi.org/10.3390/en14196386. (SCIE, Impact Factor: 3.004).
5. **Abdul Gaffar Sheik,** Murali Mohan Seepana, and Seshagiri Rao Ambati, Model-based approach to study the effect of temperature in plant-wide biological wastewater treatment plants, ***Journal of Water Chemistry and Technology***. Accepted, 2021 (SCIE, Impact Factor: 0.67).
6. **Abdul Gaffar Sheik**, Murali Mohan Seepana and Seshagiri Rao Ambati, Application of R-A^2/O with carbon and metal dosages and do control approaches for improved nutrient removal in WWTP, submitted to ***Journal of Environmental Chemical Engineering***.
7. **Abdul Gaffar Sheik**, Murali Mohan Seepana, and Seshagiri Rao Ambati, On the effect of temperature for nutrient removal in biological waste water treatment plants: A model-based analysis, Submitted to ***Indian Journal of Chemical Technology***, (SCIE-Under

review).

8. **Abdul Gaffar Sheik**, Murali Mohan Seepana, and Seshagiri Rao Ambati, Control of A^2O processes - a review, submitted to ***Critical Reviews on Environmental Science and Technology***.

Book Chapter

1. **Abdul Gaffar Sheik,** Murali Mohan Seepana and Seshagiri Rao Ambati, Fuzzy logic control of biological wastewater treatment processes, in the book titled Soft Computing Techniques in Wastewater Treatment Plants, Elsevier, 2021.

Conference Proceedings

1. **Sheik Abdul Gaffar,** Seepana Murali Mohan, Ambati Seshagiri Rao. Simulation of different biological nutrient removal processes using GPS-X, First International Conference on Energy and Environment, Global Challenges (ICEE 2018), NIT Calicut. "Best paper award".
2. **Sheik Abdul Gaffar,** Seepana Murali Mohan, Ambati Seshagiri Rao. Studies on aeration systems in biological waste water treatment plants, 2nd International Conference on New Frontiers in Chemical, Energy and Environmental Engineering (INCEE 2019), NIT Warangal, 2019.
3. **Sheik Abdul Gaffar,** Seepana Murali Mohan, Ambati Seshagiri Rao. Simulation studies on biological wastewater treatment plants, 11th International Exergy, Energy and Environment Symposium (IEEES-11), SRM University, Chennai, 2019.
4. **Sheik Abdul Gaffar,** Seepana Murali Mohan, Ambati Seshagiri Rao. Evaluation of effluent quality and operating cost in biological wastewater treatment plants with non-ideal sensors in the feedback control, International Conference on Innovative Trends in Hydrological and Environmental systems (ITHES), April 28-30, 2021, NIT Warangal.